Cover Page

Universiteit Leiden

Leiden University Repository

Author: Wiekmeijer A.S.
Title: In vivo modelling of normal and pathological human T-cell development
Issue Date: 2016-09-08

In vivo modelling of normal and pathological human T-cell development

Anna-Sophia Wiekmeijer

In vivo modelling of normal and pathological
human T-cell development

Proefschrift

ter verkrijging van
de graad van Doctor aan de Universiteit Leiden,
op gezag van Rector Magnificus prof.mr. C.J.J.M. Stolker,
volgens besluit van het College voor Promoties
te verdedigen op donderdag
8 september 2016 klokke 15.00 uur

door

Anna-Sophia Wiekmeijer

geboren te Haarlem

in 1986

Development of human T-cell progenitors after transplantation of human hematopoietic stem cells in severe immunodeficient mice mirrors human T-cell development, which is difficult to study *in vivo*. Studying human T-cell development in these transplanted mice, represented by the reflection of the mountain in the lake, provides insight (by looking over the bushes) into the real situation (the mountain itself).

Promotor: Prof. dr. F.J.T. Staal

Co-promotor: Dr. K. Pike-Overzet

Promotiecommissie: Prof. dr. F. Koning
                    Prof. dr. A. Thrasher (University College London)
                    Dr. M. van der Burg (Erasmus Universiteit Rotterdam)

Table of Contents

Chapter 1

General Introduction

"As part of a normal day, most people will flush a toilet, open a door, or drink from a water fountain without even thinking about it – or about the lurking pathogens poised to infect us. We are afforded this luxury, because of our immune system, which responds rapidly and specifically to just about anything thrown at it." (from: Editor's Summary of Gaspar *et al.* 2011, Sci Transl Med)[1]

As illustrated by the quote above, our immune system protects us every day from pathogens that are present in the environment. When the immune system is compromised, infections cannot be cleared which can lead to severe illness. Development of the different cells from the immune system is tightly regulated by expression of many genes. Deficiencies or deregulation of these genes can have severe consequences that heavily impact on normal life. In this thesis, the effect of lower or absent expression of genes and overexpression of genes on the development of the human immune system is described using severe combined immunodeficiency (SCID) and T-cell acute lymphoblastic leukemia (T-ALL) as examples. Therefore, the development of lymphoid cells from hematopoietic stem cells (HSCs) is discussed in this introduction together with the consequences of genetic aberrancies affecting these processes.

Hematopoiesis

The blood in our body consists of many different cell types. HSCs, which reside in the bone marrow (BM), are able to produce all the different cells present in our blood system, including platelets, red blood cells and white blood cells. This involves a highly controlled process of both self-renewal, to maintain the pool of HSCs, and differentiation. The process of both self-renewal and differentiation is coordinated by many signaling pathways, such as Notch[2], Wnt[3, 4], BMP[5] and several others. Aberrancies in genes and their expression, either congenital or acquired, can influence these processes, eventually leading to arrests in development or to the development of hematological malignancies.

Under normal circumstances, HSCs give rise to all white blood cells, including both innate and adaptive immune cells. The innate immune system is already present at birth and is a non-specific defense against pathogens and therefore is able to respond quickly. It is comprised of different cells types, including mast cells, macrophages, neutrophils, eosinophils, dendritic cells and natural killer (NK) cells. The cells of the adaptive immune system, comprised of B cells and T cells, are also present at birth as the cells from the innate immune system. However, cells from the adaptive immune system respond in an antigen-specific manner. These cells express receptors specific for antigens and upon antigen encounter they will proliferate but also form memory cells. These memory cells are able to respond quicker upon a second encounter with the same antigen; a regimen that is made use of by vaccination, thereby providing protection against the pathogen. The adaptive immune system is only found in vertebrates.

The regenerative capacity of HSC is of great use in the clinic for the treatment of many diseases affecting the blood system; leukemia, lymphoma, SCID and hemoglobinopathies, encompassing thalassemia and sickle cell disease. Either autologous or allogeneic stem cells are used for transplantation, often depending on the availability of the donor material. As a first step in the transplantation procedure, the cells of the immune system in the patient are often depleted by chemotherapy, which is called conditioning, and then the patient will receive donor-derived HSC that can engraft and develop a new healthy immune system. HSCs can be isolated from different sources; BM, mobilized peripheral blood and umbilical cord blood, all of which are used in the clinic for transplantation.

HSCs are rare cells that are difficult to characterize precisely by marker expression alone. The most robust criterion to determine true stem cell potential is the ability to provide long-term repopulation of an entire host with all hematopoietic lineages. In mice, this is often assessed by performing transplantations in secondary recipients to determine self-renewal capacity. For human HSCs this is, of course, not feasible in a clinical setting.

When an HSC is transplanted it can migrate to the BM of the recipient, which in most but not all patients had been depleted of autologous cells before transplantation by irradiation or chemotherapeutics. The BM niche contains many different stromal cells providing a favorable milieu for the HSC, which in turn will undergo the process of both self-renewal and differentiation[6]. Long-term repopulating (LT)-HSCs give rise to short-term repopulating (ST)-HSCs giving rise to multi-potent progenitors (MPPs), each being more restricted in their potential to self-renew and their multi-lineage differentiation potential[7]. A lot of studies have been performed to determine the phenotype of the LT-HSC, most of which have been performed in mice. The field of human HSC knowledge lags behind compared to that of mice due to absence of appropriate models to study both self-renewal and multi-lineage differentiation.

In a clinical setting, the $CD34^+$ fraction is used for transplantation as these cells can be isolated in a good laboratory practice (GLP) setting. However, already in 1997 it was described that the phenotype of HSCs could be further refined to $CD34^+CD38^-$ containing a frequency of 1 in 617 cells with true HSC potential, defined by the capacity to repopulate a NOD/Scid mouse[8]. Thereafter, it was shown that this cell fraction can be divided in 3 groups based on the expression of both CD90 and CD45RA. The $Lin^-CD34^+CD38^-CD90^+CD45RA^-$ cell population isolated from umbilical cord blood was demonstrated to have multi-lineage BM engraftment potential when 10 cells were transplanted[9]. This cell population could be further subdivided by CD49f discrimination of which the $CD49f^+$ population contained a frequency of LT-HSC of 1 in 10.5 cells[10]. This illustrates that currently we are not yet able to identify the one cell phenotype that is most primitive and contains the highest long term repopulating capacity. Currently, the human HSC is described to be most enriched within the $Lin^-CD34^+CD38^-CD45RA^-CD90^+CD49f^+$ population followed by the MPP that has lost expression of both CD90 and CD49f[11] (Fig. 1). From the MPP two cell types branch off; the $CD34^+CD38^-CD45RA^+CD90^-$ MLP (multi-lymphoid progenitor) that can give rise to NK-, B- and T cells, and the $Lin^-CD34^+CD38^+CD45RA^-CD135^+$ CMP (common myeloid progenitor) that can give rise to the megakaryocytic-erythroid progenitor (MEP) and granulocyte-monocyte progenitor (GMP)[12]. The MLP has also been named common lymphoid progenitor (CLP), which comes from many studies on hematopoiesis in the mouse. In humans this has been studied less extensively. Cells from the myeloid lineage, erythrocytes and granulocytes are progeny from the last two progenitor types. Also on the gene expression

level there is a separation between lymphoid fate and a myeloid fate at the MLP stage[13]. Many of the transcription factors that are important in HSCs are known to be causative of leukemia when deregulated, for example RUNX1, MLL, SCL/TAL1 and LMO2[7, 14]. From the progenitors onwards, most of the lineages develop within the BM, except for the T cells that need the specialized environment provided by the thymus. Hereafter, the focus will be on lymphocytes that have developed from the MLP.
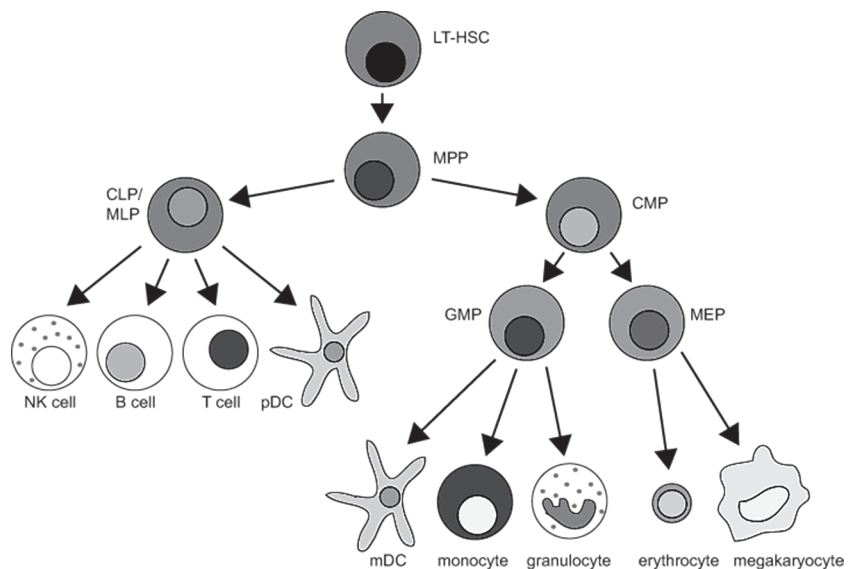

Figure 1: Overview of hematopoiesis. Schematic depiction of hematopoiesis starting from the long-term reconstituting hematopoietic stem cell (LT-HSC) that gives rise to the multi-potent progenitor (MPP). From the MPP onwards two branches diverge; the common myeloid progenitor (CMP) and the common lymphoid progenitor (CLP)/multi-lymphoid progenitor (MLP). The CMP gives rise to both the megakaryocytic-erythroid progenitor (MEP) and granulocyte-monocyte progenitor (GMP). Myeloid dendritic cells (mDC), monocytes and granulocytes develop from the GMP, while erythrocytes and megakaryocytes develop from the MEP. The MLP gives rise to natural killer (NK) cells, B cells, T cells and plasmacytoid dendritic cells (pDC). This is according to the classical model of hematopoiesis as studied extensively in the mouse, the alternative model suggests a less strict separation of lineages but more a loss of potential during development.

NK cells

NK cells are part of the innate immune system and develop in the BM but can further mature in other lymphoid organs. They need interleukin (IL)-15 for their survival and proliferation. In addition, NK cells can be found in the thymus[15] and they share a common progenitor with the developing T cells[16]. Mature NK cells in humans are characterized by the expression of CD56 and absence of the T cell marker CD3. NK cells are cytolytic cells that release granules or secrete cytokines upon activation to kill tumor cells or virus infected cells. It recognizes these cells with both activating and inhibitory molecules that are expressed on the surface of the NK cell (reviewed in [17]). When, for instance a cell has downregulated MCH class I expression, inhibitory

receptors cannot bind and therefore the NK cell will be activated. Activating receptors are able to recognize infected cells and often activation needs to occur via recognition with more than one activating receptors except for CD16.

Rearrangement of antigen specific receptors

Unlike NK cells that express both activating and inhibitory receptors for recognition of pathogens or allogeneic cells, B cells and T cells have antigen-specific receptors. A high degree of diversity is created by V(D)J recombination of the receptor loci. Both the T-cell receptor (TCR) and immunoglobulin (Ig) loci contain variable (V) and joining (J) segments, some also contain diversity (D) segments, and through recombination of these segments a high diversity is generated to be able to recognize many different antigens. The Ig heavy chain contains V, D and J segments, while the Ig kappa and Ig lambda chain only contain V and J segments. An Ig molecule, also known as B-cell receptor (BCR) contains 2 heavy chains together with 2 light chains, either kappa or lambda. For the TCR, the loci encoding the delta (*TRD*) and beta (*TRB*) chain contain V, D and J segments and the alpha (*TRA*) and gamma (*TRG*) loci contain only V and J segments. A TCR is either composed of a TCRγ chain paired with TCRδ or of a TCRα chain paired with TCRβ.

Rearrangements of Ig and TCR loci take place in a highly ordered fashion. First, a D segment rearranges to a J segment which is then followed by rearrangement of a V segment to DJ. When D segments are not present within the locus, V rearranges directly to a J segment. Recombination activating gene (RAG) proteins (RAG1 and RAG2) make double strand breaks (DSB) at the recombination signal sequences (RSSs) between the V (D) and J segments. These DSBs are recognized by a complex of DNA-dependent protein kinase catalytic subunit (DNAPKcs) together with KU70 and KU80, which can phosphorylate Artemis which then opens the coding joints that are left after RAG mediated enzymatic DNA cleavage[18]. Another complex involving X-ray repair cross-complementing protein 4 (XRCC4), DNA ligase IV (LIG4) and XRCC4-like factor (XLF) is needed for ligation in order to complete recombination.

B cells

As NK cells, B cells develop in the BM up to an immature stage after which they migrate to peripheral lymphoid organs, such as spleen and lymph nodes, to further mature. In BM aspirates the different stages of development can be characterized using flow cytometry[19]. Using this approach, patients suffering from B-cell deficiencies, for instance SCID, can be identified by determining arrests in B-cell development. During development the Ig heavy chain and the kappa and lambda light chain loci are rearranged to generate a functional and diverse repertoire. Rearrangement of *IGH* starts in the pro-B cell stage and in the small pre-B-II stage the *IGK* and *IGL* loci are rearranged[20] (Fig. 2). In *Pax5* deficient mice, it was demonstrated that expression of *Pax5* is needed for rearrangement of the *IGH* locus and is considered as a B-cell

commitment factor as it is required for B-cell development and suppresses the development of other lineages[21]. B cells that have in-frame rearrangement of the heavy chain and one of the light chains, either κ or λ, are able to express a BCR and will be positively selected. Naïve B cells in the periphery can be recognized by expression of both IgM and IgD. First the immature B cell expresses the IgM chain but by alternative splicing of the heavy chain transcript it will also express IgD when becoming a naïve B cell. Immunoglobulins can be either membrane bound to serve as BCR or can be secreted as antibodies. When a B cell recognizes antigen through the BCR it can either become a natural effector B cell or it will migrate to a germinal center. Here it can encounter a T cell recognizing the same antigen which will than provide the T cell help needed for class switch recombination of the heavy chain to change isotype to IgG, IgA or IgE[22]. Different isotypes confer different effector functions while still recognizing the same antigen. During this process the naïve B cell will become a memory B cell characterized by upregulation of CD27[23], which in its turn can give rise to plasma cells that can produce large amounts of antibody.
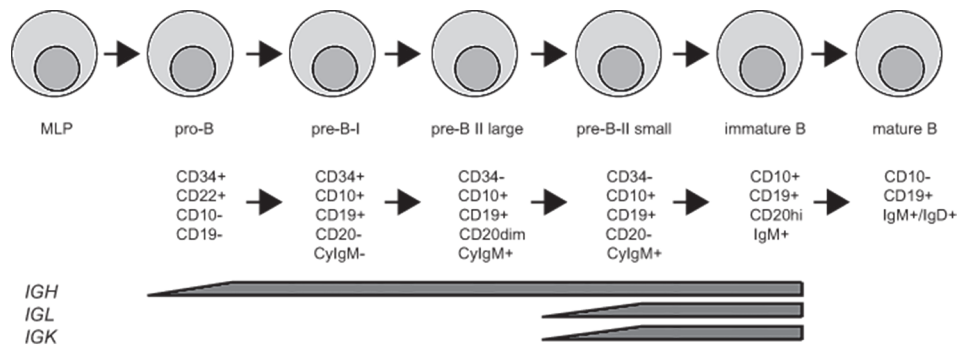

Figure 2: Human B cell development. B cells develop in the bone marrow from the multi-lymphoid progenitor (MLP). Indicated are the different stages of B cell development, the markers that can be used to identify these stages and the stages at which recombination of immunoglobulin (Ig) loci is ongoing. Adapted from thesis of H. IJspeert and thesis of K. Pike-Overzet.

T cells

T cells develop within the thymus providing a specialized environment consisting of the appropriate cytokines and specialized stromal cells[24]. Thymus seeding progenitors (TSP) that have developed from the HSC in the BM, migrate via the peripheral blood to the thymus. Both the precise phenotype of this cell and the signals that drive its migration to the thymus are still controversial. It has been estimated that there are only 10-50 cells migrating to the thymus each day[25], which makes it hard to detect and isolate these cells. In mice, studies have been performed to identify the early thymic progenitor (ETP) by careful flow cytometric analysis and isolation of murine thymi. It was found that the fetal thymus is seeded in two waves by distinct progenitors, first by a T-lineage restricted progenitor and later by a more multipotent progenitor[26]. Also in the setting of HSC transplantations it has been proposed that administration of T-cell progenitors might improve the outgrowth of T cells from the HSCs,

as it has been postulated that developing T cells "prime" the thymic environment making it more receptive[27]. The first wave of thymus seeding cells, as described in mice, might have this same function allowing for better seeding and differentiation of the second wave comprised of more multipotent cells. Robust and rapid outgrowth of T cells after HSC transplantations can still be problematic[28] and ways to improve this might benefit clinical outcome.

In humans, three phenotypes of TSPs have been proposed; a CD34^{hi}CD45RA^{hi}CD7$^+$ phenotype[29, 30], Lin$^-$CD34$^+$CD10$^+$CD24$^-$ [31] and cells characterized as Lin$^-$CD34$^+$CD10$^-$CD45RA$^+$CD62L^{hi} [32]. Haddad et al. did show that the CD34^{hi}CD45RA^{hi}CD7$^+$ cells they identified were able to migrate into thymic lobes in an ex vivo culture system. These cells could be differentiated from CD34$^+$ cells isolated from cordblood using the in vitro OP9-DL1 coculture system and were able to engraft thymi of immunodeficient mice[33]. The TSP phenotype identified by Six et al., however, do not express CD7 and have capacity to develop into B cells, NK cells and T cells using in vitro coculture systems[31]. Furthermore, in the human thymus cells positive for the expression of CD34 but negative for the expression of CD7 can be found, and it was demonstrated that CD34$^+$ cells upregulate CD7 only after 4 days of coculture on OP9-DL1[33]. This argues against CD7$^+$ cells as being the most immature cells in present in the thymus; however, it might be that the thymus can also be seeded by multiple populations. The cells identified by Kohn et al. are negative for the expression of CD7 but they did not succeed in transplanting these cells in immunodeficient mice to monitor for thymus seeding and engraftment. Therefore, the nature of the TSP in humans remains controversial.

The subsequent steps of T-cell development and commitment and the phenotypes associated with these processes have been extensively described in the mouse[26, 34]. There are many similarities between T-cell development in mice and men, as in both species it starts in de CD4$^-$CD8$^-$ double negative (DN) compartment and also the CD4$^+$CD8$^+$ double positive (DP) stage is comparable after which cells become either CD4$^+$ single positive (SP) or CD8$^+$ SP (Fig. 3). The SP cells have undergone positive selection, to select for thymocytes of which their TCR can bind major histocompatibility complex (MHC, in humans also called human leukocyte antigen - HLA), and negative selection, to eliminate cells that recognize self-antigens. These mature T cells are now ready to emigrate to the peripheral blood.

However, differences also exist between T-cell development in mice and men. Between the DN and DP stage lies the immature single positive (ISP) stage that is CD8$^+$ in mice and CD4$^+$ in humans, but in both species there is no expression of CD3 or a TCR[35]. In mice, the DN compartment can be further subdivided in DN1-4 based on the expression of CD44 and CD25[36] and further subdivision of these DN compartments has been described too[26, 34]. The DN compartment of human developing T-cell progenitors can also be subdivided, but different markers have been described to do so; such as CD34 in combination with CD38 and CD1a[37], CD1a and CD5[38] and CD7[33, 39]. During T-cell development the TCR loci are rearranged, most cells will eventually become a TCRαβ$^+$ T cell, and in mice the point of β-selection is at the DN3 stage. At this point the progenitor needs to have rearranged the *TRB* locus in a way that it produces a functional β-chain, otherwise the progenitor cannot progress in its development and will eventually die[38]. In humans, it has been debated where the point of β-selection exactly resides;

it has been ascribed to the DP stage[40], the ISP stage[41-43] and to the CD1a+ DN3 stage[35]. The current opinion is that, as in mice, it resides in the DN3 population[35, 37].
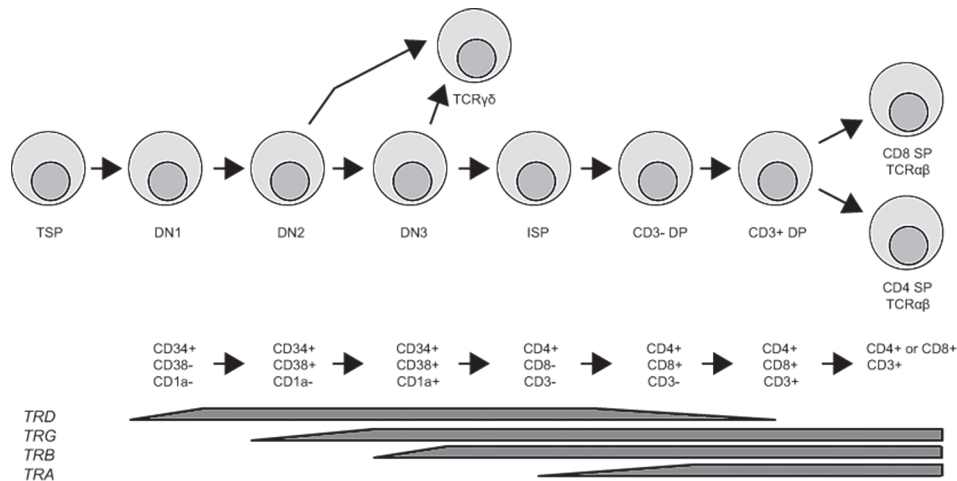

Figure 3: Human T cell development. T cells develop within the specialized environment provided by the thymus. The thymus seeding progenitor (TSP) seeds the thymus and develops into the immature thymocytes. Indicated are the stages of rearrangement of T cell receptor (TR) loci and markers to identify different stages. DN; double negative (CD4-CD8-), ISP; immature single positive, DP; double positive (CD4+CD8+), SP; single positive. Adapted from thesis of K. Pike-Overzet and Dik et al.[37].

After successful development and selection of the progenitors in the thymus they emigrate as mature T cells to the peripheral lymphoid organs and help protect us against pathogens. These mature CD4+ and CD8+ T cells have a TCR comprised of an α and a β chain. CD8+ T cells are also called cytotoxic T cells and recognize antigens that are presented by MHC class-I to fight virus infected cells and it has been demonstrated that they can be reactive towards tumor cells[44]. CD4+ T cells recognize MHC class-II restricted antigens and are also called T helper cells. These cells help other white blood cells to fight pathogens, for example they are needed for class switching of B cells. The different subtypes of T helper cells secrete different cytokines after antigen recognition to aid in distinct immune responses. Another type of CD4+ T cells is the regulatory T cell that has a high expression of CD25[45]. Regulatory T cells, which can develop in the thymus during the DP stage[46], help to dampen the immune response and play important roles in autoimmunity and cancer; with autoimmunity they do not respond adequate enough to dampen immune responses and T cells attack autologous cells, in the case of cancer the cancer cells induce regulatory T cells to dampen the T cell response against the tumor[47].

There are also T cells that have a TCR comprised of a γ and a δ chain (γδ T cells). Less is known about the development and function of these cells especially when compared to TCRαβ+ T cells. During T-cell development γδ T cells split of before the point of β-selection, as the TRD and TRG loci are rearranged before the TRB locus and productive rearrangement of TRB cannot be detected in TCRγδ+ T cells[37, 48, 49]. When rearrangement of TRD and TRG is non-functional,

the TRB locus will start rearranging and the precursor will develop along the TCRαβ lineage. γδ T cells do not recognize MHC-restricted antigens but do recognize CD1, which can present lipids[50] and are frequently found in gut and skin[51].

Severe Combined Immunodeficiency

SCID is a subset of primary immunodeficiency (PID) that is characterized by a deficiency in (functional) T cells with an incidence ranging from 1-2 per 100,000 live births[52-55]. Patients often present within their first year of life with a failure to thrive and recurrent infections[52, 56]. Different forms of SCID exist in which the deficiency in T cells can be accompanied by a deficiency in B cells or NK cells or both[57, 58]. As SCID patients lack an adaptive immune response they present with opportunistic infections and a failure to thrive, which is often diagnosed within their first year of life. The different phenotypes of SCID are caused by the differences in mutations and affected genes that are causative of SCID (Table 1). Currently, around 16 genes have been identified[59] but there are still cases remaining of affected children without a known genetic cause. In a cohort studied by Gaspar et al.[60] there were 20 out of 117 patients (17%) without a molecular diagnosis, this percentage might be different in other cohorts as presence of certain types of SCID can vary between geographic regions. The different types of SCID are categorized in two different groups based on the presence or absence of B cells: T-B- SCID and T-B+ SCID[61]. Both groups encompass patients with presence or absence of circulating NK cells, depending on the genetic aberrancy.

Table 1: Overview of SCID-causing genes.

T-B-	ADA, AK2
	RAG1, RAG2, Artemis (DCLRE1C), DNA-PKcs (PRKDC), LIG4, XLF
T-B+	IL2RG, JAK3
	IL7RA, CD45 (PTPRC), CD3D, CD3E, CD3Z (CD247), CORO1A

Severe combined immunodeficiency (SCID) is characterized by a deficiency of (functional) T cells that can be accompanied by a deficiency in B cells or NK cells or both. Indicated are the different phenotypes of SCID and the genes, when mutated, can cause this type of deficiency. Included genes were based on criteria described by Bousfiha et al.[59].

T-B- SCID

T-B-NK- SCID is caused by genes that are involved in cell metabolism, such as ADA[62], PNP[63, 64] or AK2[65], the latter leading to a disease also called reticular dysgenesis. As the phenotype caused by PNP deficiency is less profound these patients are often classified as combined immunodeficiency (CID) instead of SCID[66]. Deficiency in ADA, encoding adenosine deaminase, results in the accumulation of 2'-deoxyadenosine, which will be converted to deoxyadenosinetriphosphate (dATP). The dATP is the primary cause of lymphotoxicity as demonstrated in mice[67]. Using FTOC, it was demonstrated that inhibition of ADA in human thymocytes does results in accumulation of intracellular dATP which leads to apoptosis[68]. ADA-SCID patients can be treated by BM

transplantation, enzyme replacement therapy (ERT) using bovine PEG-ADA or gene therapy[69]. Mutations in purine nucleoside phosphatase (PNP) that affect the enzymatic activity can cause the same phenotype as ADA-deficiency[70]. However, they can have variable B-cell function. PNP catalyzes the conversion of both inosine and deoxyinosine to hypoxanthine and of both guanosine and deoxyguanosine to guanine. The intracellular accumulation of deoxyguanosine triphosphate is believed to be toxic for lymphocytes and blocks cell division[63]. Patients suffering from reticular dysgenesis have one of the most severe forms of SCID as they, in addition to the absence of lymphocytes, also do not have granulocytes. AK2 (adenylate kinase 2) is involved in mitochondrial oxidative phosphorylation and its deficiency can be compensated for in many cells types by AK1. In the mononuclear cell fraction from the BM, no expression of AK1 was detected whereby this could not compensate the AK2 deficiency and the disease manifests so profound in the immune system[65]. Furthermore, it was demonstrated that restoration of AK2 expression in bone marrow cells restores development towards neutrophils, thereby, showing the causative effect of AK2 deficiency[71].

Mutations in genes involved in V(D)J recombination of TCR and immunoglobulins lead to SCID characterized as T-B-NK+. Genes that have been identified include: RAG1 or RAG2[72], Artemis (encoded by DCLRE1C)[73], LIG4[74], XLF (also known as Cernunnos and Non-homologous end-joining factor 1, NHEJ1)[75] and DNA-PKcs (encoded by PRKDC)[76]. As with PNP deficiency, mutations in LIG4 and XLF can also be classified as CID instead of SCID[66]. As described, these genes are needed during V(D)J recombination of TCR and immunoglobulin loci. When one of all these genes is mutated this can lead to defective recombination, which leads to absence of expression of a functional TCR in T cells or immunoglobulins in B cells and because these receptors are needed to proceed during T-cell and B-cell development, defects in recombination will result in immunodeficiency.

T-B+ SCID

Mutations in the interleukin-2 receptor gamma chain (IL2RG)[77] and Janus kinase 3 (JAK3)[78, 79] can be causative of T-B+NK- SCID, which is the most prevalent form of SCID[80]. IL2RG encodes the common gamma chain (γ_c), which is involved in IL-2, -4, -7, -9,-15 and -21 signaling[81]. The gene is located on the X chromosome, thereby mainly affecting boys and also known as X-linked SCID or X-SCID. JAK3 is downstream of IL2RG on the cytoplasmic part of the receptor complex and thereby deficiencies in both these genes result in a comparable phenotype. As humans that only lack IL-2 had normal T-cell and NK-cell development[82], it is thought that the absence of signaling through IL -7 and IL-15 are causative for the deficiency in both T cells and NK cells, respectively, as these cytokines are known to be important early in development of these lymphocytes. Furthermore, it has been observed that in T-B+NK- SCID patients also the B cells do not function completely normal; they are present in normal or sometimes elevated numbers but their production of immunoglobulins is often impaired. This can be caused by the lack of T cells of which the helper T cells are needed for class switching of immunoglobulins, but it has also been demonstrated that the lack of IL-21 signaling is partially causative[83]. The

effects on B cells are difficult to study in knockout mice for Il2rg or Il7ra as these mice also suffer from a B-cell deficiency which is opposed to the phenotype observed in patients[84, 85]. Furthermore, this demonstrates differences in lymphoid development between mice and men.

Another type of SCID only involves deficiency specific for T cells resulting in a T-B+NK+ phenotype. Most often this is caused by a mutation in the IL-7 receptor α chain (IL7RA), which, together with IL-2Rγ, makes up the receptor for IL-7 that is needed early in T-cell development[86, 87]. Furthermore, mutations in CD45 (encoded by PTPRC)[88, 89], the molecule that marks lymphocytes and in Coronin 1a (CORO1A), which is important in thymic egress[90] have been found in SCID patients only deficient in T cells. Mutations in the kinase ZAP-70 lead to a deficiency in peripheral CD8+ T cells, while CD4+ T cells are present but fail to respond to TCR stimulation, do not produce IL-2 and have reduced tyrosine phosphorylation[91]. Of most SCID patients it is unknown at which stage the arrest in T-cell development resides as thymic biopsies are not routinely performed. For the ZAP-70 deficiency it has been demonstrated using immunohistochemistry of thymic biopsies that DP cells were present in the cortex but no CD8+ SP cells were present, showing a CD8 specific block at the DP stage[91]. For SCID caused by mutations in the CD3 δ chain (CD3D) the developmental arrest has been described and assigned to the ISP to DP transition[92] although by a different group ascribed to the DN stage, but in that study the presence of ISP cells was not determined[93]. The CD3 complex, which associates with the TCR, exists of different subunits next to the δ chain; the γ chain (CD3G), ε chain (CD3E) and ζ chain (CD3Z). Mutations in all of these different CD3 chains have been described in T-B+NK+ SCID patients[92, 94, 95]. Patients with mutations in CD3G, CORO1A and ZAP70 have also been classified as CID[66].

For SCID caused by various mutations it is known where the arrest in B-cell development reside as this can be determined by flow cytometric analyses and repertoire analysis of the immunoglobulin loci in bone marrow aspirates [19, 74, 76]. On the T cell side the arrests are only known for mutations in ZAP70 and CD3D[91-93]; for other mutations this remains unknown as thymus biopsies are not routinely taken. To further study the effects of mutations causing SCID different knockout mouse models have been made and studied[84, 85, 96-100]. As already mentioned, murine and human T-cell development show similarities but also many discrepancies. This is also illustrated in many of these mouse models, as for instance, Il7r-/- mice are deficient in both T cells and B cells[85] while in humans only T cells are absent[86] and in Il2rg-/- mice the arrest in T-cell development is less strict[84]. This underscores the need for better models to study T-cell arrests for human SCID.

Gene therapy for SCID

SCID is fatal if left untreated. For a long time, the only treatment for SCID was a BM transplant, although ADA-SCID patients can benefit from ERT using bovine PEG-ADA. However, ERT is very costly as it involves lifelong administration and requires appropriate monitoring[69]. Depending on the donor, the extent of human leukocyte antigen (HLA) matching and type of SCID can lead

to differences in outcome. Transplantation of HSC from a related genetically matched donor results in a 10-year survival of 84%[101]. For a related phenotypically identical and an unrelated donor the survival is 64% and 66% respectively, and for a related HLA-mismatched this is only 54%[101]. For monogenic disease, such as SCID, gene therapy might be a successful treatment option, especially when an HLA-matched donor is not available.

The advantage is that autologous HSCs are used and therefore the risk of graft rejection or graft-versus-host-disease is very low. Furthermore, gene corrected cells will, most likely, have a selective growth advantage over their non-transduced counterparts that suffer from a developmental arrest[102]. Several gene therapy trials have been conducted for different types of SCID, starting in the early 2000s[103-105]. In short, blood stem cells are harvested from the BM of the patient, in which a correct copy of the affected gene is introduced *ex vivo* using a crippled virus for gene delivery after which the cells are given back to the patient. These initial studies used a mouse leukemia virus (MLV)-based γ-retroviral vector to drive expression of the transgene by the long terminal repeat (LTR). A retrovirus reverse transcribes its RNA into DNA which then uses the enzyme integrase to integrate the DNA into the host genome. Due to this integration, the gene will be passed on to every daughter cell. Initially, there was restoration of functionality and patients demonstrated presence of cells from different lymphoid cell lineages in their peripheral blood together with improved immune functionality. Patients were able to go home and live in a normal environment and had normal growth and development. Unfortunately, thereafter it was reported that 4 patients in the X-linked SCID trial conducted in Paris and 1 patient in the London X-linked SCID trial out of the 20 total treated patients developed T-ALL[106-108]. In the trial for ADA-SCID, that had used a similar vector, no T-ALL development was observed[109] and also not in another ADA-SCID gene therapy trial conducted in London[110]. The T-ALLs in the X-linked SCID trials did result from insertional mutagenesis leading to ectopic expression of oncogenes. Insertional mutagenesis was also detected in gene therapy trials for X-linked chronic granulatomous disease (CGD)[111] and Wiskott-Aldrich Syndrome (WAS)[112] leading to development of myelodysplasia and leukemia, respectively. Below, the mechanisms of insertional mutagenesis and T-ALL development will be described in more detail. Due to the occurrence of these adverse side effects, new viral vectors were designed for delivery of the transgene (reviewed in [113, 114]).

The 5 patients that developed a T-ALL due to insertional mutagenesis were treated with chemotherapy, which cured the leukemia in 4 patients. Unfortunately, one patient did not survive[106]. No insertional mutagenesis related T-ALL developed in both gene therapy trials for ADA-SCID although integrations near LMO2 were detected, which lead to T-ALL development in the X-linked SCID trials[109]. In 2010, it was reported that for gene therapy trials using a MLV-based γ-retroviral vector 18 out of 20 X-linked SCID patients treated with gene therapy and all 27 treated ADA-SCID patients are alive[115]. In addition, 17 X-linked SCID patients and 19 ADA-SCID patients have correction of their immunodeficiency and are now able to have a normal life, although some patients still need some immunoglobulin substitution, indicating incomplete B cell recovery or function[1, 115, 116].

SIN lentiviral vectors

After the occurrence of severe adverse events in the gene therapy trials based on the γ-retroviral vector, new vectors have been studied that do not rely on the strong viral LTR for expression of the transgene. These new vectors were based on human immunodeficiency virus type 1 (HIV-1), which is a lentivirus also belonging to the family of *retroviridae*. Effectiveness of this system, encompassing a split-genome packaging design using 3 plasmids, was shown by Naldini *et al.*[117]. Furthermore, they demonstrated that lentivirus is far more effective in transducing non-dividing cells than the MLV-based counterpart. This is especially of use for transduction of HSCs, as the otherwise needed proliferation might affect their pluripotency. Thereafter this system was modified to the so-called third generation lentivirus vector system. A split-genome packaging design of 4 plasmids was used to increase safety and viral genes that are important for virus replication were removed[118]. Furthermore, an additional modification was made that removes the U3 region from the 3' LTR, thereby decreasing the transactivational activity it can have on nearby genes[119]. These self-inactivating (SIN) lentiviruses have been used widely for preclinical[120-126] and clinical[127-130] gene therapy studies. Besides being able to transduce non-proliferating cells, lentiviruses also have a favorable integration pattern when compared to γ-retroviruses. Gamma retroviruses have a tendency to integrate more frequently around the transcription start site of a gene and thereby the risk of dysregulation is higher[109, 131]. The more random integration pattern, together with the removal of the U3 region from the LTR region, make these third generation SIN lentiviruses safer than the MLV-based γ-retroviral vectors. Indeed, no development of leukemia has been observed using the lentiviral vectors[127, 128, 132], which have now been widely implemented. Only one clonal dominance with integration near *HMG2A* has been observed in a trial for β-thallasemia, but no leukemia development has been documented[130]. Furthermore, when integration sites of both vectors were compared it was observed that integrations detected for lentiviral vectors have a safer integration profile[133, 134]. So far, SIN lentiviral vectors have been proven safe in clinical trials.

SIN γ-retroviral vectors

Next to SIN lentiviruses, SIN γ-retroviral vectors have been created. These also have a deletion of the U3 region in the LTR and need an internal promoter to drive expression of the transgene[135]. The SIN design eliminates, as with the lentiviral vectors, the enhancer activities on neighboring genes. However, a concern might be that their integration pattern is comparable to the MLV-based γ-retroviral vectors[136]. These vectors have been developed and tested in preclinical models for CGD, WAS and X-linked SCID, which demonstrated efficacy[135, 137, 138]. Trials using SIN γ-retroviral vectors for X-linked SCID using the elongation factor 1α short (EFS) promoter are currently ongoing[139-141]. Recently, it was reported that gene therapy using a SIN γ-retroviral vector in which *IL2RG* expression is driven by the EFS promoter was effective in 7 out of 9 treated patients[142]. One patient died of an adenoviral infection before T-cell reconstitution. This study demonstrated initial safety of the SIN γ-retroviral vector, as no leukemias were observed, and the efficacy of gene therapy using a γ-retroviral vector expressing *IL2RG*. It

1

needs to be noted that the follow-up time in this report was too short to conclusively say that the SIN retroviral vector was safer than the full LTR homolog.

Insertional mutagenesis

During the gene therapy trials performed for X-linked SCID using the MLV-based γ-retroviral vectors T-ALL was observed in 5 out of 20 patients[106-108]. The same phenomenon was observed in a gene therapy trial for CGD[111] and in a WAS gene therapy trial[112] using comparable vectors. In the CGD trial this led to the development of myelodysplasia in 2 out of 2 treated patients and in the WAS trial 1 patient developed AML, 4 patients developed T-ALL and 2 patients developed T-ALL with secondary AML. The development of these leukemias was caused by integration of the therapeutic vector in the DNA, resulting in dysregulation of surrounding genes, which is called insertional mutagenesis. The γ-retroviral vector preferentially integrates in transcription start sites (TSS) and transcriptionally active regions[143]. Indeed, in 5 patients that were treated with gene therapy for X-linked SCID in London, which did not have T-ALL, it was found that a high percentage of integrations was located around the TSS and a higher percentage than expected was located in common integrations sites (CIS)[131]. In addition, many integration sites were found near genes that are transcriptionally active in CD34+ cells, which is the cell type used for transduction in these trials. There are several mechanisms that can underlie insertional mutagenesis; a long read-through transcript could be generated from the viral gene including a nearby gene, the LTR could have enhancer effects on the promoter from nearby genes, integration of the vector could potentially disrupt a negative regulatory element and integration of the vector within a gene could generate a truncated constitutively active form of the gene (Fig. 4)[114].

In the X-linked SCID trials in London an integration upstream of LIM-domain only 2 (*LMO2*) was found[108], while in Paris two patients had integrations near the TSS of *LMO2*[107], one patient near the TSS of cyclin D2 (*CCND2*) and one patient harbored integrations in both *LMO2* and BMI1 polycomb ring finger oncogene (*BMI1*)[106]. Furthermore, it was demonstrated that these genes were highly expressed in the T-ALLs. In the CGD trial the two treated patients developed myelodysplasia due to insertional mutagenesis in the *MDS1-EVI1* locus, which led to higher expression of ecotropic viral integration site 1 (*EVI1*)[111]. Insertions within or near *LMO2* were found in all 6 T-ALL cases which in 2 patients was combined with an integration upstream of *TAL1* (T-cell acute lymphocytic leukemia 1) and in another patient combined with an integration near the TSS of *LYL1* (lymphoblastic leukemia derived sequence 1) in the WAS trial (Table 2)[112]. Four of the patients had overexpression of *LMO2*, *TAL1* was found to be overexpressed in 2 patients but *LYL1* was not found to be overexpressed. The secondary AMLs were caused by a meningioma (disrupted in balance) 1 (*MN1*) dominant clone and by a *MDS1* clone, an integration in the *MDS1* locus was also found in the patient that only developed AML in this trial. The developed leukemias all had a long latency, suggesting that additional mutations were needed besides the insertional mutagenesis. These were indeed found in leukemic cells from patients and were comprised of *NOTCH1* mutations, a *STIL-TAL1* fusion, *CDKN2A* deletion[106, 108] or monosomy 7 (Table 2)[111].
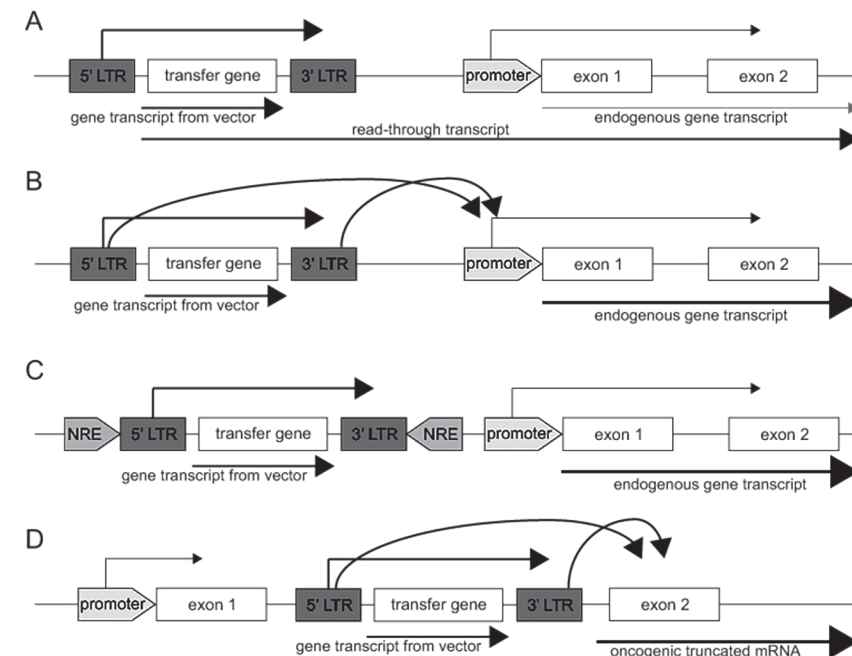

Figure 4: Different mechanisms of insertional mutagenesis leading to aberrant expression of endogenous genes. It is needed to have integration of the vector in the DNA in order to have expression of the therapeutic gene in all offspring from a cell. This can, however, lead to overexpression of genes which might lead to the development of leukemia. Different mechanisms leading to aberrant expression are: **A)** integration of the vector in front of an oncogene leading to a long read-through transcript, **B)** enhancer effects of the viral long terminal repeat (LTR) on an oncogene, **C)** disruption of a negative regulatory element (NRE) thereby leading to aberrant expression of an oncogene and **D)** integration within a gene thereby generating a truncated constitutively active form. Adapted from Staal *et al.*[114].

It has been demonstrated that the expression of *LMO2*, *TAL1* and *LYL1* is high in human CD34+ cells and increases when stimulated with cytokines used in the X-linked SCID gene therapy trials[144]. This was confirmed by the data from Schwarzwaelder *et al.*[131] that postulated that many of the integrations that they found in X-linked SCID patients were in genes that are active in CD34+ cells. Indeed *LMO2*, *TAL1* and *LYL1* were frequently hit by insertional mutagenesis in the patients that developed T-ALL as outlined above. However, it has been suggested that the constitutive expression of *IL2RG* might be causative of the observed T-ALLs, as it was observed that overexpression of *IL2RG* in a murine X-linked SCID model led to the development of thymomas[145]. In response to this, it was demonstrated that the overexpression of *IL2RG* in human CD34+ cells did not lead to aberrant T-cell development *in vitro* culture systems, while overexpression of *LMO2* did[144, 146]. Furthermore, *LMO2*, *TAL1* and *LYL1* are known oncogenes associated with human T-ALL[147], while *IL2RG* is not. Intriguingly, integrations near *LMO2* were also found in patients in the ADA-SCID gene therapy trial, but here it did not lead to development of T-ALL[148].

Table 2: Overview of leukemias that developed from insertional mutagenesis in different gene therapy trials.

Trial	Patient	Leukemia	Reported insertions	Other aberrancies	Reference
X-SCID (London)[1]	P8	T-ALL	LMO2	NOTCH1, CDKN2A, TCRB-SIL/TAL1	3 (106)
X-SCID (Paris)[2,3]	P4	T-ALL	LMO2	t(6;13), CDKN2A	4, 5 (104,105)
X-SCID (Paris)[2,3]	P5	T-ALL	LMO2	SIL-TAL1, trisomy 10, NOTCH1	4, 5 ()
X-SCID (Paris)[3]	P7	T-ALL	CCND2	CDKN2A	5 (95)
X-SCID (Paris)[3]	P10	T-ALL	LMO2, BMI1	NOTCH1	5 (95)
CGD[4]	Subject 1	MDS	MDS1-EVI1	monosomy 7, CDKN2B methylation, increased genomic instability, centrosomal aberrations	1 (100)
CGD[4]	Subject 2	MDS	MDS1-EVI1	monosomy 7, CDKN2B methylation, increased genomic instability, centrosomal aberrations	1 (100)
WAS[5]	WAS1	T-ALL / +AML	LMO2, MRPS28, IQSEC2 MN1	TCRB-TAL2[¥]	2 (101)
WAS[5]	WAS5	T-ALL	LMO2, TAL1,TMEM217, UBB, ST8SIA6,CPSF6, CD46, RIN3 C11orf74	t(1;8)(q31;q23)[¥]	2 (101)
WAS[5]	WAS6	T-ALL	LMO2	TCRA/D-MYC-C[¥]	2 (101)
WAS[5]	WAS7	T-ALL	LMO2, TAL1	TCRB-CCND2[¥]	2 (101)
WAS[5]	WAS8	T-ALL / +AML	LMO2,TRMT1 (LYL1) CYTIP, IMMP2L, GSDMC MDS1	TCRA/D-CEBPB[¥]	2 (101)
WAS[5]	WAS9	AML	MDS1		2 (101)
WAS[5]	WAS10	T-ALL	LMO2, TRMT1 (LYL1)*		2 (101)

The columns of the table indicate the trial (the type of immunodeficiency for which the trial was performed), the number of the patient that did develop leukemia, the type of leukemia, the genes in which insertions were found and other aberrancies that were detected in leukemic cells. X-SCID; X-linked SCID, CGD; X-linked chronic granulatomous disease, WAS; Wiskott-Aldrich Syndrome, T-ALL; T-cell acute lymphoblastic leukemia, AML; acute myeloid leukemia. * analysis of WAS10 was still ongoing at time of publication of manuscript by Braun et al.[112], [¥] detailed data obtained from karyotyping can be found in manuscript of Braun et al.[112], [1] patient has been described by Howe et al.[108], [2] patients have been described by Hacein-Bey-Abina et al.[107], [3] patients have been described by Hacein-Bey-Abina et al.[106], [4] patients have been described by Stein et al.[111], [5] patients have been described by Braun et al.[112].

T-cell acute lymphoblastic leukemia (T-ALL)

Overexpression of oncogenes or deletions in tumor suppressor genes can lead to the development of cancer. Often more consecutive mutations are needed for a cell to become cancerous as described in the multiple-hit model[149, 150] and as also has been observed for the T-ALLs that developed in the gene therapy trials. Overexpression of proto-oncogenes or loss of tumor-suppressor genes can lead to aberrant T-cell development and if more genetic lesions are acquired this can lead to T-ALL. The leukemic cells will then migrate to lymphoid organs such as peripheral blood, BM and spleen. The symptoms associated with T-ALL are a result of the increase in white blood cells in the blood of the patient, which decreases the number of red blood cells per mm^3 and can lead to anemia, dizziness and fever.

T-ALL can present with different phenotypes mirroring different stages of T-cell development, which is caused by the genes that are affected or aberrantly expressed. Different clusters have been described using these expression profiles and phenotypes, which demonstrated that T-ALLs from different clusters have different prognoses and sometimes need different treatment regimens. NOTCH1 has a prominent role in T-cell development and activating mutations in this gene have been found in more than 50% of T-ALL cases[151]. Activation of NOTCH1 can also be caused by genomic rearrangements. Rearrangements are often detected in T-ALL cells and they mostly involve translocation of one of the TCR loci to an oncogene, which, in addition to NOTCH1, has been described for LYL1, LMO1, LMO2, TAL1 (SCL), TAL2, HOX11 (TLX1), HOX11L2 (TLX3), LCK, CCND2, and BHLHB1[152]. The promoter or enhancer sequences from the TCR loci will then drive the expression of the oncogenes. Most of these genes are expressed in HSC and in the early stages of T-cell development and are downregulated thereafter. The translocations keep these genes constitutively active whereby thymocytes retain a high proliferative potential and arrest in development until they acquire additional mutations that can lead to T-ALL.

Two types of mutations can be distinguished in T-ALL; type A, which are also called driver mutations, and type B mutations, which are also known as helper mutations. Type A mutations can be grouped in 7 different clusters; TAL/LMO, TLX1, TLX3, LYL1[147, 153], HOXA[42], NKX2.1/NKX2.2 and MEF2C[154]. The TAL/LMO cluster is phenotypically characterized as late cortical by the expression of TCRαβ and CD3[147]. NKX2.1/NKX2.2 is biologically related with TLX1 T-ALL, both having an arrest at the cortical stage characterized by CD1 expression[147, 154] while the TLX3 cluster is more mature compared to TLX1[42]. The T-ALLs characterized by high MEF2C expression have a very immature phenotype with expression of CD34 and the myeloid markers CD13 and/or CD33 and are also called ETP T-ALL[154]. The T-ALLs in the MEF2C cluster also have high expression of LYL1 and LMO2. High expression of LMO2 was also found in the LYL1 cluster in other studies while the latter cluster is characterized as immature[42, 147, 155]. Type B mutations include, amongst others, mutations in NOTCH1, CDKN2A, CDKN2B, FBWX7, IL7R and RAS[153, 156]. To determine overexpression of genes in T-ALL it is necessary to have the right control samples from the corresponding developmental stage as some of the oncogenes have a high expression level during early stages of normal T-cell development[157]. Otherwise overexpression can be falsely claimed and T-ALLs will be assigned to a different cluster with different prognosis and treatment.

Humanized mouse model

It is difficult to study human T-cell development, especially in an *in vivo* system. Many studies on T-cell development have been performed in mice, where the thymus can be removed and studied and furthermore transgenic mice can be created to study the effects of genes on T-cell development. However, human and mouse T-cell development are quite similar but also differ in many aspects[35, 37, 48, 158]. As mentioned, markers to describe the DN compartments and ISP stage differ between mice and men. Ways to study human T-cell development are largely descriptive, including gene expression analysis and phenotyping by flow cytometry. The only models to study functionality and differentiation of human T-cell progenitors is the OP9-DL1 model[159, 160] and fetal thymic organ cultures (FTOC)[161]. Advantages of these models are the ability to study kinetics and follow differentiation over time, which cannot be done on *ex vivo* thymi. The disadvantage of these models is that it is an *in vitro* situation with supplemented cytokines and therefore might be different from the physiological situation. Furthermore, in OP9-DL1 cocultures the 3D architectural structure is lost, which is still present in FTOC cultures.

Humanized mice are a better alternative for studies on human T-cell development, as this offers the possibility to study the development in an *in vivo* setting. Development of humanized mice started with the description of the spontaneous *Prkdc^scid* mutation in CB17 mice in 1983[162] and the observation that these mice could be engrafted with different types of human hematopoietic cells although no functional human immune system was generated (reviewed by Shultz *et al.*[163]). These CB17-*scid* mice were then crossed with the non-obese diabetic (NOD) mice to create NOD/Scid mice; mice that allowed a higher level of engraftment of human cells. For a long period these NOD/Scid mice have been used extensively to study human HSCs and their differentiation towards different lineages[164]. These mice do not have endogenous B cells and T cells due to the mutation in *Prkdc* and therefore human HSC are less frequently rejected and able to engraft. These mice have been used widely for e.g. HSC expansion protocols[165] and gene therapy approaches[166]. Unfortunately, these mice do not allow for development of human T cells. In 2004, human CD34$^+$ cells that were derived from cordblood were intrahepatically injected into newborn Rag2$^{-/-}$ $\gamma_c^{-/-}$ mice[167]. These mice developed a human immune system, which was demonstrated to be functional too. In 2002 and 2005, new mouse models have been described that were an adaptation of the earlier NOD/Scid model; by crossing it with an *Il2rg^{-/-}* (*Il2rg* encodes the γ_c chain) mouse to generate NOD/Shi-*scidIl2rg^{-/-}* (NOG)[168] or NOD/LtSz-*scidIl2rg^{-/-}* (NSG)[169] mice, respectively. These mice do not have NK-, B- and T cells whereby they are not able to reject human cells and these can engraft with higher efficiency than in the NOD/Scid model. The difference between both mouse strains is a small difference in the NOD background and in the type of *Il2rg* mutation, the NOG mice have a truncated form, which might be able to bind and capture cytokine, while the NSG mice carry a null mutation. Both mice have been compared side by side with the NOD/Scid model; both demonstrated higher engraftment of human lymphoid cells[170]. In addition, the NSG mice showed a higher engraftment in their BM especially when transplanting limiting cell doses. This might either be caused by the type of mutation in *Il2rg* or the difference in the NOD background. It has been described that mice on the NOD background have a different polymorphism of signal regulatory protein alpha (SIRPα)[171]. This polymorphism has enhanced binding to human CD47,

a ubiquitously expressed protein, and interaction of both molecules inhibits phagocytosis. NSG mice show increased repopulation levels as compared to other humanized mouse models probably due to this polymorphism of SIRPα.

Besides allowing higher engraftment of human cells, the NOG and NSG mice also sustain human T-cell development in their thymus[172, 173]. It was shown that the developed lymphocytes were functional too, as demonstrated by production of cytokines, antibodies and HLA-restricted immune responses[173-175]. Engraftment capacity and lineage differentiation of expanded HSC have been studied in the NSG model[176] and the model can even be used to study the phenotype and functionality of human LT-HSC by performing single cell transplantations in NSG mice[10]. Because the NSG mice allow for the development of different cell types of the human immune system after transplantation of human HSC, even at limiting, doses, this model offers a great potential for the studies of normal and pathological human T-cell development. Furthermore, the NSG mice are useful in testing preclinical gene therapy approaches[120], since the viral doses needed and efficacy might be different between murine and human cells.

Outline of this thesis

Both in SCID and in the T-ALLs that developed due to LMO2 insertional mutagenesis there are problems in T-cell development. In this thesis the results of studying human T-cell development are described. The overall aim of the research described in this thesis is to study normal and pathological forms of human T-cell development in an *in vivo* setting to obtain insight into the regulation of human T-cell development. First, we have optimized the NSG humanized mouse model to allow for robust T-cell development from cryopreserved BM derived human HSCs. This model has been used for the other studies and is described in **chapter 2**. In **chapter 3** we describe the results obtained after transplantation of SCID-patient derived HSC in the NSG xenograft model in order to study the stages of developmental arrest for different types of SCID. Furthermore, the results gave new insights in human T-cell development. There are still patients suffering from SCID with an unknown genetic cause. One of these we have studied in **chapter 4** to determine whether this patient suffered from a cell intrinsic defect or a niche problem. Here, we could identify the block in T-cell development and identify this patient as being a true SCID. With exome sequencing we identified a potential underlying genetic cause. By the use of cellular barcoding, we have studied the number of clones that seed the thymus and the restriction during T-cell development as described in **chapter 5**. With SCID, the absent expression of a gene causes the problem in T-cell development, however, overexpression of a gene can also results in arrests in development. In **chapter 6** we have studied the effects of LMO2 overexpression, as was observed in the T-ALLs that developed in several gene therapy trials, and to determine the mechanisms that underlie the T-ALL development caused by LMO2. The data from the different chapters are put in perspective to each other and existing literature in **chapter 7** together with suggestions for further research.

References

1. Gaspar, H.B., *et al.* Long-term persistence of a polyclonal T cell repertoire after gene therapy for X-linked severe combined immunodeficiency. *Sci Transl Med* 2011, **3**(97): 97ra79.

2. Bigas, A., Espinosa, L. Hematopoietic stem cells: to be or Notch to be. *Blood* 2012, **119**(14): 3226-3235.

3. Luis, T.C., Ichii, M., Brugman, M.H., Kincade, P., Staal, F.J. Wnt signaling strength regulates normal hematopoiesis and its deregulation is involved in leukemia development. *Leukemia* 2012, **26**(3): 414-421.

4. Luis, T.C., *et al.* Canonical wnt signaling regulates hematopoiesis in a dosage-dependent fashion. *Cell Stem Cell* 2011, **9**(4): 345-356.

5. Soderberg, S.S., Karlsson, G., Karlsson, S. Complex and context dependent regulation of hematopoiesis by TGF-beta superfamily signaling. *Ann N Y Acad Sci* 2009, **1176**: 55-69.

6. Trumpp, A., Essers, M., Wilson, A. Awakening dormant haematopoietic stem cells. *Nat Rev Immunol* 2010, **10**(3): 201-209.

7. Orkin, S.H., Zon, L.I. Hematopoiesis: an evolving paradigm for stem cell biology. *Cell* 2008, **132**(4): 631-644.

8. Bhatia, M., Wang, J.C., Kapp, U., Bonnet, D., Dick, J.E. Purification of primitive human hematopoietic cells capable of repopulating immune-deficient mice. *Proc Natl Acad Sci U S A* 1997, **94**(10): 5320-5325.

9. Majeti, R., Park, C.Y., Weissman, I.L. Identification of a hierarchy of multipotent hematopoietic progenitors in human cord blood. *Cell Stem Cell* 2007, **1**(6): 635-645.

10. Notta, F., *et al.* Isolation of single human hematopoietic stem cells capable of long-term multilineage engraftment. *Science* 2011, **333**(6039): 218-221.

11. van Galen, P., *et al.* Reduced lymphoid lineage priming promotes human hematopoietic stem cell expansion. *Cell Stem Cell* 2014, **14**(1): 94-106.

12. Doulatov, S., *et al.* Revised map of the human progenitor hierarchy shows the origin of macrophages and dendritic cells in early lymphoid development. *Nat Immunol* 2010, **11**(7): 585-593.

13. Laurenti, E., *et al.* The transcriptional architecture of early human hematopoiesis identifies multilevel control of lymphoid commitment. *Nat Immunol* 2013, **14**(7): 756-763.

14. Sive, J.I., Gottgens, B. Transcriptional network control of normal and leukaemic haematopoiesis. *Exp Cell Res* 2014.

15. Spits, H., *et al.* Early stages in the development of human T, natural killer and thymic dendritic cells. *Immunol Rev* 1998, **165**: 75-86.

16. Vargas, C.L., Poursine-Laurent, J., Yang, L., Yokoyama, W.M. Development of thymic NK cells from double negative 1 thymocyte precursors. *Blood* 2011, **118**(13): 3570-3578.

17. Lanier, L.L. Up on the tightrope: natural killer cell activation and inhibition. *Nat Immunol* 2008, **9**(5): 495-502.

18. Ma, Y., Pannicke, U., Schwarz, K., Lieber, M.R. Hairpin opening and overhang processing by an Artemis/DNA-dependent protein kinase complex in nonhomologous end joining and V(D)J recombination. *Cell* 2002, **108**(6): 781-794.

19. Noordzij, J.G., *et al.* The immunophenotypic and immunogenotypic B-cell differentiation arrest in bone marrow of RAG-deficient SCID patients corresponds to residual recombination activities of mutated RAG proteins. *Blood* 2002, **100**(6): 2145-2152.

20. van Zelm, M.C., *et al.* Ig gene rearrangement steps are initiated in early human precursor B cell subsets and correlate with specific transcription factor expression. *J Immunol* 2005, **175**(9): 5912-5922.

21. Nutt, S.L., Thevenin, C., Busslinger, M. Essential functions of Pax-5 (BSAP) in pro-B cell development. *Immunobiology* 1997, **198**(1-3): 227-235.

22. Klein, U., *et al.* Transcriptional analysis of the B cell germinal center reaction. *Proc Natl Acad Sci U S A* 2003, **100**(5): 2639-2644.

23. van Zelm, M.C., Szczepanski, T., van der Burg, M., van Dongen, J.J. Replication history of B lymphocytes reveals homeostatic proliferation and extensive antigen-induced B cell expansion. *J Exp Med* 2007, **204**(3): 645-655.

24. Rothenberg, E.V. Transcriptional control of early T and B cell developmental choices. *Annu Rev Immunol* 2014, **32**: 283-321.

25. Zlotoff, D.A., Bhandoola, A. Hematopoietic progenitor migration to the adult thymus. *Ann N Y Acad Sci* 2011, **1217**: 122-138.

26. Ramond, C., *et al.* Two waves of distinct hematopoietic progenitor cells colonize the fetal thymus. *Nat Immunol* 2014, **15**(1): 27-35.

27. Reimann, C., *et al.* Human T-lymphoid progenitors generated in a feeder-cell-free Delta-like-4 culture system promote T-cell reconstitution in NOD/SCID/gammac(-/-) mice. *Stem Cells* 2012, **30**(8): 1771-1780.

28. Danby, R., Rocha, V. Improving engraftment and immune reconstitution in umbilical cord blood transplantation. *Front Immunol* 2014, **5**: 68.

29. Haddad, R., *et al.* Molecular characterization of early human T/NK and B-lymphoid progenitor cells in umbilical cord blood. *Blood* 2004, **104**(13): 3918-3926.

30. Haddad, R., *et al.* Dynamics of thymus-colonizing cells during human development. *Immunity* 2006, **24**(2): 217-230.

31. Six, E.M., *et al.* A human postnatal lymphoid progenitor capable of circulating and seeding the thymus. *J Exp Med* 2007, **204**(13): 3085-3093.

32. Kohn, L.A., *et al.* Lymphoid priming in human bone marrow begins before expression of CD10 with upregulation of L-selectin. *Nat Immunol* 2012, **13**(10): 963-971.

33. Awong, G., *et al.* Characterization in vitro and engraftment potential in vivo of human progenitor T cells generated from hematopoietic stem cells. *Blood* 2009, **114**(5): 972-982.

34. Tan, C., *et al.* Ten-color flow cytometry reveals distinct patterns of expression of CD124 and CD126 by developing thymocytes. *BMC Immunol* 2011, **12**: 36.

35. Weerkamp, F., Pike-Overzet, K., Staal, F.J. T-sing progenitors to commit. *Trends Immunol* 2006, **27**(3): 125-131.

36. Godfrey, D.I., Kennedy, J., Suda, T., Zlotnik, A. A developmental pathway involving four phenotypically and functionally distinct subsets of CD3-CD4-CD8- triple-negative adult mouse thymocytes defined by CD44 and CD25 expression. *J Immunol* 1993, **150**(10): 4244-4252.

37. Dik, W.A., *et al.* New insights on human T cell development by quantitative T cell receptor gene rearrangement studies and gene expression profiling. *J Exp Med* 2005, **201**(11): 1715-1723.

38. Blom, B., *et al.* TCR gene rearrangements and expression of the pre-T cell receptor complex during human T-cell differentiation. *Blood* 1999, **93**(9): 3033-3043.

1

39. Hao, Q.L., *et al.* Human intrathymic lineage commitment is marked by differential CD7 expression: identification of CD7- lympho-myeloid thymic progenitors. *Blood* 2008, **111**(3)**:** 1318-1326.

40. Carrasco, Y.R., Trigueros, C., Ramiro, A.R., de Yebenes, V.G., Toribio, M.L. Beta-selection is associated with the onset of CD8beta chain expression on CD4(+)CD8alphaalpha(+) pre-T cells during human intrathymic development. *Blood* 1999, **94**(10)**:** 3491-3498.

41. Blom, B., Spits, H. Development of human lymphoid cells. *Annu Rev Immunol* 2006, **24:** 287-320.

42. Soulier, J., *et al.* HOXA genes are included in genetic and biologic networks defining human acute T-cell leukemia (T-ALL). *Blood* 2005, **106**(1)**:** 274-286.

43. Taghon, T., *et al.* Notch signaling is required for proliferation but not for differentiation at a well-defined beta-selection checkpoint during human T-cell development. *Blood* 2009, **113**(14)**:** 3254-3263.

44. Gros, A., *et al.* PD-1 identifies the patient-specific CD8(+) tumor-reactive repertoire infiltrating human tumors. *J Clin Invest* 2014, **124**(5)**:** 2246-2259.

45. Shevach, E.M. CD4+ CD25+ suppressor T cells: more questions than answers. *Nat Rev Immunol* 2002, **2**(6)**:** 389-400.

46. Nunes-Cabaco, H., Caramalho, I., Sepulveda, N., Sousa, A.E. Differentiation of human thymic regulatory T cells at the double positive stage. *Eur J Immunol* 2011, **41**(12)**:** 3604-3614.

47. Taams, L.S., *et al.* Regulatory T cells in human disease and their potential for therapeutic manipulation. *Immunology* 2006, **118**(1)**:** 1-9.

48. Joachims, M.L., Chain, J.L., Hooker, S.W., Knott-Craig, C.J., Thompson, L.F. Human alpha beta and gamma delta thymocyte development: TCR gene rearrangements, intracellular TCR beta expression, and gamma delta developmental potential--differences between men and mice. *J Immunol* 2006, **176**(3)**:** 1543-1552.

49. Sherwood, A.M., *et al.* Deep sequencing of the human TCRgamma and TCRbeta repertoires suggests that TCRbeta rearranges after alphabeta and gammadelta T cell commitment. *Sci Transl Med* 2011, **3**(90)**:** 90ra61.

50. Spada, F.M., *et al.* Self-recognition of CD1 by gamma/delta T cells: implications for innate immunity. *J Exp Med* 2000, **191**(6)**:** 937-948.

51. Vantourout, P., Hayday, A. Six-of-the-best: unique contributions of gammadelta T cells to immunology. *Nat Rev Immunol* 2013, **13**(2)**:** 88-100.

52. Yee, A., De Ravin, S.S., Elliott, E., Ziegler, J.B., Contributors to the Australian Paediatric Surveillance, U. Severe combined immunodeficiency: a national surveillance study. *Pediatr Allergy Immunol* 2008, **19**(4)**:** 298-302.

53. Kwan, A., *et al.* Newborn screening for severe combined immunodeficiency in 11 screening programs in the United States. *JAMA* 2014, **312**(7)**:** 729-738.

54. Kwan, A., *et al.* Newborn screening for severe combined immunodeficiency and T-cell lymphopenia in California: results of the first 2 years. *J Allergy Clin Immunol* 2013, **132**(1)**:** 140-150.

55. Stephan, J.L., *et al.* Severe combined immunodeficiency: a retrospective single-center study of clinical presentation and outcome in 117 patients. *J Pediatr* 1993, **123**(4)**:** 564-572.

56. Buckley, R.H., *et al.* Human severe combined immunodeficiency: genetic, phenotypic, and functional diversity in one hundred eight infants. *J Pediatr* 1997, **130**(3)**:** 378-387.

57. Dvorak, C.C., *et al.* The natural history of children with severe combined immunodeficiency: baseline features of the first fifty patients of the primary immune deficiency treatment consortium prospective study 6901. *J Clin Immunol* 2013, **33**(7)**:** 1156-1164.

58. Shearer, W.T., *et al.* Establishing diagnostic criteria for severe combined immunodeficiency disease (SCID), leaky SCID, and Omenn syndrome: the Primary Immune Deficiency Treatment Consortium experience. *J Allergy Clin Immunol* 2014, **133**(4)**:** 1092-1098.

59. Bousfiha, A., *et al.* The 2015 IUIS Phenotypic Classification for Primary Immunodeficiencies. *J Clin Immunol* 2015, **35**(8)**:** 727-738.

60. Gaspar, H.B., *et al.* How I treat severe combined immunodeficiency. *Blood* 2013, **122**(23)**:** 3749-3758.

61. Al-Herz, W., *et al.* Primary immunodeficiency diseases: an update on the classification from the international union of immunological societies expert committee for primary immunodeficiency. *Front Immunol* 2011, **2:** 54.

62. Giblett, E.R., Anderson, J.E., Cohen, F., Pollara, B., Meuwissen, H.J. Adenosine-deaminase deficiency in two patients with severely impaired cellular immunity. *Lancet* 1972, **2**(7786)**:** 1067-1069.

63. Dalal, I., Grunebaum, E., Cohen, A., Roifman, C.M. Two novel mutations in a purine nucleoside phosphorylase (PNP)-deficient patient. *Clin Genet* 2001, **59**(6)**:** 430-437.

64. Pannicke, U., Tuchschmid, P., Friedrich, W., Bartram, C.R., Schwarz, K. Two novel missense and frameshift mutations in exons 5 and 6 of the purine nucleoside phosphorylase (PNP) gene in a severe combined immunodeficiency (SCID) patient. *Hum Genet* 1996, **98**(6)**:** 706-709.

65. Pannicke, U., *et al.* Reticular dysgenesis (aleukocytosis) is caused by mutations in the gene encoding mitochondrial adenylate kinase 2. *Nat Genet* 2009, **41**(1)**:** 101-105.

66. Al-Herz, W., *et al.* Primary immunodeficiency diseases: an update on the classification from the international union of immunological societies expert committee for primary immunodeficiency. *Front Immunol* 2014, **5:** 162.

67. Apasov, S.G., Blackburn, M.R., Kellems, R.E., Smith, P.T., Sitkovsky, M.V. Adenosine deaminase deficiency increases thymic apoptosis and causes defective T cell receptor signaling. *J Clin Invest* 2001, **108**(1)**:** 131-141.

68. Joachims, M.L., *et al.* Restoration of adenosine deaminase-deficient human thymocyte development in vitro by inhibition of deoxynucleoside kinases. *J Immunol* 2008, **181**(11)**:** 8153-8161.

69. Gaspar, H.B., *et al.* How I treat ADA deficiency. *Blood* 2009, **114**(17)**:** 3524-3532.

70. Giblett, E.R., Ammann, A.J., Wara, D.W., Sandman, R., Diamond, L.K. Nucleoside-phosphorylase deficiency in a child with severely defective T-cell immunity and normal B-cell immunity. *Lancet* 1975, **1**(7914)**:** 1010-1013.

71. Lagresle-Peyrou, C., *et al.* Human adenylate kinase 2 deficiency causes a profound hematopoietic defect associated with sensorineural deafness. *Nat Genet* 2009, **41**(1)**:** 106-111.

72. Schwarz, K., *et al.* RAG mutations in human B cell-negative SCID. *Science* 1996, **274**(5284)**:** 97-99.

73. Moshous, D., *et al.* Artemis, a novel DNA double-strand break repair/V(D)J recombination protein, is mutated in human severe combined immune deficiency. *Cell* 2001, **105**(2)**:** 177-186.

74. van der Burg, M., *et al.* A new type of radiosensitive T-B-NK+ severe combined immunodeficiency caused by a LIG4 mutation. *J Clin Invest* 2006, **116**(1)**:** 137-145.

1

75. Buck, D., *et al.* Cernunnos, a novel nonhomologous end-joining factor, is mutated in human immunodeficiency with microcephaly. *Cell* 2006, **124**(2): 287-299.

76. van der Burg, M., *et al.* A DNA-PKcs mutation in a radiosensitive T-B- SCID patient inhibits Artemis activation and nonhomologous end-joining. *J Clin Invest* 2009, **119**(1): 91-98.

77. Noguchi, M., *et al.* Interleukin-2 receptor gamma chain mutation results in X-linked severe combined immunodeficiency in humans. *Cell* 1993, **73**(1): 147-157.

78. Macchi, P., *et al.* Mutations of Jak-3 gene in patients with autosomal severe combined immune deficiency (SCID). *Nature* 1995, **377**(6544): 65-68.

79. Russell, S.M., *et al.* Mutation of Jak3 in a patient with SCID: essential role of Jak3 in lymphoid development. *Science* 1995, **270**(5237): 797-800.

80. Fischer, A. Have we seen the last variant of severe combined immunodeficiency? *N Engl J Med* 2003, **349**(19): 1789-1792.

81. Rochman, Y., Spolski, R., Leonard, W.J. New insights into the regulation of T cells by gamma(c) family cytokines. *Nat Rev Immunol* 2009, **9**(7): 480-490.

82. Leonard, W.J. Cytokines and immunodeficiency diseases. *Nat Rev Immunol* 2001, **1**(3): 200-208.

83. Recher, M., *et al.* IL-21 is the primary common gamma chain-binding cytokine required for human B-cell differentiation in vivo. *Blood* 2011, **118**(26): 6824-6835.

84. DiSanto, J.P., Muller, W., Guy-Grand, D., Fischer, A., Rajewsky, K. Lymphoid development in mice with a targeted deletion of the interleukin 2 receptor gamma chain. *Proc Natl Acad Sci U S A* 1995, **92**(2): 377-381.

85. Peschon, J.J., *et al.* Early lymphocyte expansion is severely impaired in interleukin 7 receptor-deficient mice. *J Exp Med* 1994, **180**(5): 1955-1960.

86. Puel, A., Ziegler, S.F., Buckley, R.H., Leonard, W.J. Defective IL7R expression in T(-)B(+)NK(+) severe combined immunodeficiency. *Nat Genet* 1998, **20**(4): 394-397.

87. Roifman, C.M., Zhang, J., Chitayat, D., Sharfe, N. A partial deficiency of interleukin-7R alpha is sufficient to abrogate T-cell development and cause severe combined immunodeficiency. *Blood* 2000, **96**(8): 2803-2807.

88. Kung, C., *et al.* Mutations in the tyrosine phosphatase CD45 gene in a child with severe combined immunodeficiency disease. *Nat Med* 2000, **6**(3): 343-345.

89. Tchilian, E.Z., *et al.* A deletion in the gene encoding the CD45 antigen in a patient with SCID. *J Immunol* 2001, **166**(2): 1308-1313.

90. Shiow, L.R., *et al.* The actin regulator coronin 1A is mutant in a thymic egress-deficient mouse strain and in a patient with severe combined immunodeficiency. *Nat Immunol* 2008, **9**(11): 1307-1315.

91. Arpaia, E., Shahar, M., Dadi, H., Cohen, A., Roifman, C.M. Defective T cell receptor signaling and CD8+ thymic selection in humans lacking zap-70 kinase. *Cell* 1994, **76**(5): 947-958.

92. de Saint Basile, G., *et al.* Severe combined immunodeficiency caused by deficiency in either the delta or the epsilon subunit of CD3. *J Clin Invest* 2004, **114**(10): 1512-1517.

93. Dadi, H.K., Simon, A.J., Roifman, C.M. Effect of CD3delta deficiency on maturation of alpha/beta and gamma/delta T-cell lineages in severe combined immunodeficiency. *N Engl J Med* 2003, **349**(19): 1821-1828.

94. Arnaiz-Villena, A., *et al.* T lymphocyte signalling defects and immunodeficiency due to the lack of CD3 gamma. *Immunodeficiency* 1993, **4**(1-4): 121-129.

95. Roberts, J.L., *et al.* T-B+NK+ severe combined immunodeficiency caused by complete deficiency of the CD3zeta subunit of the T-cell antigen receptor complex. *Blood* 2007, **109**(8): 3198-3206.

96. Mombaerts, P., *et al.* RAG-1-deficient mice have no mature B and T lymphocytes. *Cell* 1992, **68**(5): 869-877.

97. Ohbo, K., *et al.* Modulation of hematopoiesis in mice with a truncated mutant of the interleukin-2 receptor gamma chain. *Blood* 1996, **87**(3): 956-967.

98. Rooney, S., *et al.* Leaky Scid phenotype associated with defective V(D)J coding end processing in Artemis-deficient mice. *Mol Cell* 2002, **10**(6): 1379-1390.

99. Shinkai, Y., *et al.* RAG-2-deficient mice lack mature lymphocytes owing to inability to initiate V(D)J rearrangement. *Cell* 1992, **68**(5): 855-867.

100. Wakamiya, M., *et al.* Disruption of the adenosine deaminase gene causes hepatocellular impairment and perinatal lethality in mice. *Proc Natl Acad Sci U S A* 1995, **92**(9): 3673-3677.

101. Gennery, A.R., *et al.* Transplantation of hematopoietic stem cells and long-term survival for primary immunodeficiencies in Europe: entering a new century, do we do better? *J Allergy Clin Immunol* 2010, **126**(3): 602-610 e601-611.

102. Cavazzana-Calvo, M., Fischer, A. Gene therapy for severe combined immunodeficiency: are we there yet? *J Clin Invest* 2007, **117**(6): 1456-1465.

103. Aiuti, A., *et al.* Correction of ADA-SCID by stem cell gene therapy combined with nonmyeloablative conditioning. *Science* 2002, **296**(5577): 2410-2413.

104. Gaspar, H.B., *et al.* Gene therapy of X-linked severe combined immunodeficiency by use of a pseudotyped gammaretroviral vector. *Lancet* 2004, **364**(9452): 2181-2187.

105. Hacein-Bey-Abina, S., *et al.* Sustained correction of X-linked severe combined immunodeficiency by ex vivo gene therapy. *N Engl J Med* 2002, **346**(16): 1185-1193.

106. Hacein-Bey-Abina, S., *et al.* Insertional oncogenesis in 4 patients after retrovirus-mediated gene therapy of SCID-X1. *J Clin Invest* 2008, **118**(9): 3132-3142.

107. Hacein-Bey-Abina, S., *et al.* LMO2-associated clonal T cell proliferation in two patients after gene therapy for SCID-X1. *Science* 2003, **302**(5644): 415-419.

108. Howe, S.J., *et al.* Insertional mutagenesis combined with acquired somatic mutations causes leukemogenesis following gene therapy of SCID-X1 patients. *J Clin Invest* 2008, **118**(9): 3143-3150.

109. Aiuti, A., *et al.* Multilineage hematopoietic reconstitution without clonal selection in ADA-SCID patients treated with stem cell gene therapy. *J Clin Invest* 2007, **117**(8): 2233-2240.

110. Gaspar, H.B., *et al.* Successful reconstitution of immunity in ADA-SCID by stem cell gene therapy following cessation of PEG-ADA and use of mild preconditioning. *Mol Ther* 2006, **14**(4): 505-513.

111. Stein, S., *et al.* Genomic instability and myelodysplasia with monosomy 7 consequent to EVI1 activation after gene therapy for chronic granulomatous disease. *Nat Med* 2010, **16**(2): 198-204.

112. Braun, C.J., *et al.* Gene therapy for Wiskott-Aldrich syndrome--long-term efficacy and genotoxicity. *Sci Transl Med* 2014, **6**(227): 227ra233.

113. Maetzig, T., Galla, M., Baum, C., Schambach, A. Gammaretroviral vectors: biology, technology and application. *Viruses* 2011, **3**(6): 677-713.

114. Staal, F.J., Pike-Overzet, K., Ng, Y.Y., van Dongen, J.J. Sola dosis facit venenum. Leukemia in gene therapy trials: a question of vectors, inserts and dosage? *Leukemia* 2008, **22**(10): 1849-1852.

1

115. Fischer, A., Hacein-Bey-Abina, S., Cavazzana-Calvo, M. 20 years of gene therapy for SCID. *Nat Immunol* 2010, **11**(6)**:** 457-460.

116. Hacein-Bey-Abina, S., *et al.* Efficacy of gene therapy for X-linked severe combined immunodeficiency. *N Engl J Med* 2010, **363**(4)**:** 355-364.

117. Naldini, L., *et al.* In vivo gene delivery and stable transduction of nondividing cells by a lentiviral vector. *Science* 1996, **272**(5259)**:** 263-267.

118. Dull, T., *et al.* A third-generation lentivirus vector with a conditional packaging system. *J Virol* 1998, **72**(11)**:** 8463-8471.

119. Zufferey, R., *et al.* Self-inactivating lentivirus vector for safe and efficient in vivo gene delivery. *J Virol* 1998, **72**(12)**:** 9873-9880.

120. Carbonaro, D.A., *et al.* Preclinical demonstration of lentiviral vector-mediated correction of immunological and metabolic abnormalities in models of adenosine deaminase deficiency. *Mol Ther* 2014, **22**(3)**:** 607-622.

121. Chiriaco, M., *et al.* Dual-regulated lentiviral vector for gene therapy of X-linked chronic granulomatosis. *Mol Ther* 2014, **22**(8)**:** 1472-1483.

122. Huston, M.W., *et al.* Correction of murine SCID-X1 by lentiviral gene therapy using a codon-optimized IL2RG gene and minimal pretransplant conditioning. *Mol Ther* 2011, **19**(10)**:** 1867-1877.

123. Ng, Y.Y., *et al.* Correction of B-cell development in Btk-deficient mice using lentiviral vectors with codon-optimized human BTK. *Leukemia* 2010, **24**(9)**:** 1617-1630.

124. Pike-Overzet, K., *et al.* Correction of murine Rag1 deficiency by self-inactivating lentiviral vector-mediated gene transfer. *Leukemia* 2011, **25**(9)**:** 1471-1483.

125. Scaramuzza, S., *et al.* Preclinical safety and efficacy of human CD34(+) cells transduced with lentiviral vector for the treatment of Wiskott-Aldrich syndrome. *Mol Ther* 2013, **21**(1)**:** 175-184.

126. van Til, N.P., *et al.* Correction of murine Rag2 severe combined immunodeficiency by lentiviral gene therapy using a codon-optimized RAG2 therapeutic transgene. *Mol Ther* 2012, **20**(10)**:** 1968-1980.

127. Aiuti, A., *et al.* Lentiviral hematopoietic stem cell gene therapy in patients with Wiskott-Aldrich syndrome. *Science* 2013, **341**(6148)**:** 1233151.

128. Biffi, A., *et al.* Lentiviral hematopoietic stem cell gene therapy benefits metachromatic leukodystrophy. *Science* 2013, **341**(6148)**:** 1233158.

129. Cartier, N., *et al.* Hematopoietic stem cell gene therapy with a lentiviral vector in X-linked adrenoleukodystrophy. *Science* 2009, **326**(5954)**:** 818-823.

130. Cavazzana-Calvo, M., *et al.* Transfusion independence and HMGA2 activation after gene therapy of human beta-thalassaemia. *Nature* 2010, **467**(7313)**:** 318-322.

131. Schwarzwaelder, K., *et al.* Gammaretrovirus-mediated correction of SCID-X1 is associated with skewed vector integration site distribution in vivo. *J Clin Invest* 2007, **117**(8)**:** 2241-2249.

132. Cartier, N., *et al.* Lentiviral hematopoietic cell gene therapy for X-linked adrenoleukodystrophy. *Methods Enzymol* 2012, **507:** 187-198.

133. Cornils, K., *et al.* Comparative clonal analysis of reconstitution kinetics after transplantation of hematopoietic stem cells gene marked with a lentiviral SIN or a gamma-retroviral LTR vector. *Exp Hematol* 2013, **41**(1)**:** 28-38 e23.

134. Gabriel, R., Schmidt, M., von Kalle, C. Integration of retroviral vectors. *Curr Opin Immunol* 2012, **24**(5)**:** 592-597.

135. Thornhill, S.I., *et al.* Self-inactivating gammaretroviral vectors for gene therapy of X-linked severe combined immunodeficiency. *Mol Ther* 2008, **16**(3)**:** 590-598.

136. Moiani, A., *et al.* Deletion of the LTR enhancer/promoter has no impact on the integration profile of MLV vectors in human hematopoietic progenitors. *PLoS One* 2013, **8**(1)**:** e55721.

137. Avedillo Diez, I., *et al.* Development of novel efficient SIN vectors with improved safety features for Wiskott-Aldrich syndrome stem cell based gene therapy. *Mol Pharm* 2011, **8**(5)**:** 1525-1537.

138. Stein, S., *et al.* From bench to bedside: preclinical evaluation of a self-inactivating gammaretroviral vector for the gene therapy of X-linked chronic granulomatous disease. *Hum Gene Ther Clin Dev* 2013, **24**(2)**:** 86-98.

139. Persons, D.A. Lentiviral vector gene therapy: effective and safe? *Mol Ther* 2010, **18**(5)**:** 861-862.

140. Persons, D.A., Baum, C. Solving the problem of gamma-retroviral vectors containing long terminal repeats. *Mol Ther* 2011, **19**(2)**:** 229-231.

141. Wu, C., Dunbar, C.E. Stem cell gene therapy: the risks of insertional mutagenesis and approaches to minimize genotoxicity. *Front Med* 2011, **5**(4)**:** 356-371.

142. Hacein-Bey-Abina, S., *et al.* A modified gamma-retrovirus vector for X-linked severe combined immunodeficiency. *N Engl J Med* 2014, **371**(15)**:** 1407-1417.

143. Baum, C., *et al.* Chance or necessity? Insertional mutagenesis in gene therapy and its consequences. *Mol Ther* 2004, **9**(1)**:** 5-13.

144. Pike-Overzet, K., *et al.* Ectopic retroviral expression of LMO2, but not IL2Rgamma, blocks human T-cell development from CD34+ cells: implications for leukemogenesis in gene therapy. *Leukemia* 2007, **21**(4)**:** 754-763.

145. Woods, N.B., Bottero, V., Schmidt, M., von Kalle, C., Verma, I.M. Gene therapy: therapeutic gene causing lymphoma. *Nature* 2006, **440**(7088)**:** 1123.

146. Pike-Overzet, K., *et al.* Gene therapy: is IL2RG oncogenic in T-cell development? *Nature* 2006, **443**(7109)**:** E5; discussion E6-7.

147. Ferrando, A.A., *et al.* Gene expression signatures define novel oncogenic pathways in T cell acute lymphoblastic leukemia. *Cancer Cell* 2002, **1**(1)**:** 75-87.

148. Candotti, F., *et al.* Gene therapy for adenosine deaminase-deficient severe combined immune deficiency: clinical comparison of retroviral vectors and treatment plans. *Blood* 2012, **120**(18)**:** 3635-3646.

149. Fearon, E.R., Vogelstein, B. A genetic model for colorectal tumorigenesis. *Cell* 1990, **61**(5)**:** 759-767.

150. Hanahan, D., Weinberg, R.A. The hallmarks of cancer. *Cell* 2000, **100**(1)**:** 57-70.

151. Weng, A.P., *et al.* Activating mutations of NOTCH1 in human T cell acute lymphoblastic leukemia. *Science* 2004, **306**(5694)**:** 269-271.

152. Aifantis, I., Raetz, E., Buonamici, S. Molecular pathogenesis of T-cell leukaemia and lymphoma. *Nat Rev Immunol* 2008, **8**(5)**:** 380-390.

153. Van Vlierberghe, P., Pieters, R., Beverloo, H.B., Meijerink, J.P. Molecular-genetic insights in paediatric T-cell acute lymphoblastic leukaemia. *Br J Haematol* 2008, **143**(2)**:** 153-168.

1

154. Homminga, I., *et al.* Integrated transcript and genome analyses reveal NKX2-1 and MEF2C as potential oncogenes in T cell acute lymphoblastic leukemia. *Cancer Cell* 2011, **19**(4): 484-497.

155. Asnafi, V., *et al.* Age-related phenotypic and oncogenic differences in T-cell acute lymphoblastic leukemias may reflect thymic atrophy. *Blood* 2004, **104**(13): 4173-4180.

156. Zenatti, P.P., *et al.* Oncogenic IL7R gain-of-function mutations in childhood T-cell acute lymphoblastic leukemia. *Nat Genet* 2011, **43**(10): 932-939.

157. Larmonie, N.S., *et al.* Correct interpretation of T-ALL oncogene expression relies on normal human thymocyte subsets as reference material. *Br J Haematol* 2012, **157**(1): 142-146.

158. Spits, H. Development of alphabeta T cells in the human thymus. *Nat Rev Immunol* 2002, **2**(10): 760-772.

159. De Smedt, M., *et al.* T-lymphoid differentiation potential measured in vitro is higher in CD34+CD38-/lo hematopoietic stem cells from umbilical cord blood than from bone marrow and is an intrinsic property of the cells. *Haematologica* 2011, **96**(5): 646-654.

160. La Motte-Mohs, R.N., Herer, E., Zuniga-Pflucker, J.C. Induction of T-cell development from human cord blood hematopoietic stem cells by Delta-like 1 in vitro. *Blood* 2005, **105**(4): 1431-1439.

161. Fisher, A.G., *et al.* Human thymocyte development in mouse organ cultures. *Int Immunol* 1990, **2**(6): 571-578.

162. Bosma, G.C., Custer, R.P., Bosma, M.J. A severe combined immunodeficiency mutation in the mouse. *Nature* 1983, **301**(5900): 527-530.

163. Shultz, L.D., Ishikawa, F., Greiner, D.L. Humanized mice in translational biomedical research. *Nat Rev Immunol* 2007, **7**(2): 118-130.

164. Lapidot, T., *et al.* Cytokine stimulation of multilineage hematopoiesis from immature human cells engrafted in SCID mice. *Science* 1992, **255**(5048): 1137-1141.

165. Yao, C.L., *et al.* Characterization of serum-free ex vivo-expanded hematopoietic stem cells derived from human umbilical cord blood CD133(+) cells. *Stem Cells Dev* 2006, **15**(1): 70-78.

166. Lagresle-Peyrou, C., *et al.* Restoration of human B-cell differentiation into NOD-SCID mice engrafted with gene-corrected CD34+ cells isolated from Artemis or RAG1-deficient patients. *Mol Ther* 2008, **16**(2): 396-403.

167. Traggiai, E., *et al.* Development of a human adaptive immune system in cord blood cell-transplanted mice. *Science* 2004, **304**(5667): 104-107.

168. Ito, M., *et al.* NOD/SCID/gamma(c)(null) mouse: an excellent recipient mouse model for engraftment of human cells. *Blood* 2002, **100**(9): 3175-3182.

169. Shultz, L.D., *et al.* Human lymphoid and myeloid cell development in NOD/LtSz-scid IL2R gamma null mice engrafted with mobilized human hemopoietic stem cells. *J Immunol* 2005, **174**(10): 6477-6489.

170. McDermott, S.P., Eppert, K., Lechman, E.R., Doedens, M., Dick, J.E. Comparison of human cord blood engraftment between immunocompromised mouse strains. *Blood* 2010, **116**(2): 193-200.

171. Takenaka, K., *et al.* Polymorphism in Sirpa modulates engraftment of human hematopoietic stem cells. *Nat Immunol* 2007, **8**(12): 1313-1323.

172. Ishikawa, F., *et al.* Development of functional human blood and immune systems in NOD/SCID/IL2 receptor {gamma} chain(null) mice. *Blood* 2005, **106**(5): 1565-1573.

173. Marodon, G., *et al.* High diversity of the immune repertoire in humanized NOD.SCID.gamma c-/- mice. *Eur J Immunol* 2009, **39**(8): 2136-2145.

174. Choi, B., *et al.* Human B cell development and antibody production in humanized NOD/SCID/IL-2Rgamma(null) (NSG) mice conditioned by busulfan. *J Clin Immunol* 2011, **31**(2): 253-264.

175. Unsinger, J., McDonough, J.S., Shultz, L.D., Ferguson, T.A., Hotchkiss, R.S. Sepsis-induced human lymphocyte apoptosis and cytokine production in "humanized" mice. *J Leukoc Biol* 2009, **86**(2): 219-227.

176. Drake, A.C., *et al.* Human CD34+ CD133+ hematopoietic stem cells cultured with growth factors including Angptl5 efficiently engraft adult NOD-SCID Il2rgamma-/- (NSG) mice. *PLoS One* 2011, **6**(4): e18382.

1

Chapter 2

Sustained engraftment of cryopreserved human bone marrow CD34+ cells in young adult NSG mice

Anna-Sophia Wiekmeijer[1], Karin Pike-Overzet[1], Martijn H. Brugman[1], Daniela C.F. Salvatori[2], R. Maarten Egeler[3,4], Robbert G.M. Bredius[3], Willem E. Fibbe[1] and Frank J.T. Staal[1]

[1]Department of Immunohematology and Blood Transfusion,
Leiden University Medical Center, Leiden, The Netherlands

[2]Central Laboratory Animal Facility,
Leiden University Medical Center, Leiden, The Netherlands

[3]Department of Pediatrics,
Leiden University Medical Center, Leiden, The Netherlands

[4]Division of Hematology/Oncology,
Hospital for Sick Children/University of Toronto, Toronto, Canada

Abstract

Hematopoietic stem cells (HSC) are defined by their ability to repopulate the bone marrow of myeloablative conditioned and/or (lethally)-irradiated recipients. To study the repopulating potential of human HSC, murine models have been developed that rely on the use of immunodeficient mice that allow engraftment of human cells. The NSG xenograft model has emerged as the current standard for this purpose allowing for engraftment and study of human T cells. Here, we describe adaptations to the original NSG xenograft model that can be readily implemented. These encompass use of adult mice instead of newborns and a short *ex vivo* culture. This protocol results in robust and reproducible high levels of lympho-myeloid engraftment. Immunization of recipient mice with relevant antigen resulted in specific antibody formation, showing that both T cells and B cells were functional. In addition, bone marrow cells from primary recipients exhibited repopulating ability following transplantation into secondary recipients. Similar results were obtained with cryopreserved human bone marrow samples thus circumventing the need for fresh cells and allowing the use of patient derived bio-bank samples. Our findings have implications for use of this model in fundamental stem cell research, immunological studies *in vivo* and pre-clinical evaluations for HSC transplantation, expansion and genetic modification.

Introduction

Transplantation of hematopoietic stem and progenitor cells (HSPC) is applied for a variety of diseases, including for patients with malignant diseases or congenital immune deficiencies. In spite of major improvements, HSPC transplantation is still associated with high morbidity and mortality.[1-3] Gene therapy has emerged as an alternative for treatment of severe combined immunodeficiency (SCID).[4]

Repopulation of human HSPC is difficult to study experimentally in humans; therefore studies rely primarily on the use of xenotransplantation in mice. The most widely used mouse model for this purpose was the NOD-*scid* mouse strain, which can be engrafted with human HSPC.[5] This mouse is deficient in B cells and T cells but develops functional NK cells. However, this model gives low levels of human blood cell chimerism and lacks proper human T cell development. Another disadvantage was the relatively short life-span of the mice due to development of thymic lymphomas.[6] With the development of mouse strains with more severe immune deficiency it became possible to transplant human HSPC with higher efficiency. The first such mouse strain that became available was the Rag2$^{-/-}$γc$^{-/-}$ mouse that is on a mixed background, in which both peripheral blood lymphocytes[7] and CD34$^+$ cells isolated from cord blood[8] could be engrafted. This was followed by a report in which CD34$^+$ HSPC were transplanted in newborn BALB/c-*Rag2*$^{-/-}$*Il2rg*$^{-/-}$.[9] In these mice both human myeloid and lymphoid cells developed and it was demonstrated that the human adaptive immune system was functional.

Further improvement was obtained by crossing the NOD-*scid* mouse to an *Il2rg*$^{-/-}$ mouse (NOG mouse, NOD/Shi-*scidIl2rg*$^{-/-}$)[10] and later on by development of the NSG mice (NOD/LtSz-*scidIl2rg*$^{-/-}$)[11, 12] These mice differ from the NOG mice[10] in the substrain of NOD-*scid* that was used and their mutation in *Il2rg*. While the NOG mouse has a truncated non-signalling form of Il2rg, the NSG mouse has a null mutant of Il2rg and therefore is lacking the ability to bind cytokines. Both mouse strains were compared side by side, which demonstrated higher engraftment of human cells in the bone marrow of NSG mice, especially at limiting cell doses.[13] This can either be caused by the difference in background or the different mutation in Il2rg.

In this study, we show the feasibility of using cryopreserved human BM following a short *ex vivo* culture in NSG mice. Engrafted cells differentiate into different cell lineages and are also functional. Furthermore, we introduced a short culture that would allow for genetic modification of HSPC. Thus, we provide an adaptation of the original NSG protocol that can be readily implemented and allows for wider and more robust use of this promising xenograft model.

Material and Methods

Isolation of human CD34+cells

Umbilical cord blood was obtained from the Diaconessenhuis Hospital Leiden (Leiden, the Netherlands) after informed consent of the parents. Human BM was obtained from healthy paediatric bone marrow donors at the Leiden University Medical Center (Leiden, The Netherlands). Informed consent was obtained from the parents for use of leftover samples for research purposes. The mononuclear cell fraction was isolated using Ficoll gradient centrifugation, frozen in FCS/10% DMSO (Greiner Bio-One B.V., Alphen aan den Rijn, The Netherlands and Sigma-Aldrich, St. Louis, MO, USA, respectively) and stored in liquid nitrogen until use. CD34+ progenitors were isolated using the CD34 Microbead Kit (Miltenyi Biotec GmbH, Bergisch Gladbach, Germany). Isolated cells were cultured overnight (o/n, unless indicated differently) in StemSpan serum-free expansion medium (StemSpan-SFEM, StemCell Technologies Inc., Vancouver, BC, Canada) in the presence of 10 ng/mL stem cell factor (SCF, a gift from Amgen, Thousand Oaks, CS, USA), 20 ng/mL recombinant human thrombopoietin (rhTPO, R&D Systems, Abingdon, UK), 20 ng/mL recombinant mouse insulin-like growth factor 2 (rmIGF-2, R&D Systems) and 10 ng/mL recombinant human fibroblast growth factor-acidic (rhFGF-1, Peprotech, Rocky Hill, NJ, USA). After overnight culture, cells were washed and resuspended in Iscove's Modified Dulbecco's Medium (IMDM) without phenol red (Gibco, Life Technologies, Bleiswijk, The Netherlands).

Mice

NOD.Cg-Prkdc[scid] Il2rg[tm1Wjl]/SzJ (NSG) mice were obtained from Charles River Laboratories (UK) and bred in the animal facility at the Leiden University Medical Center. Experimental procedures were approved by the Ethical Committee on Animal Experiments of the Leiden University Medical Center. Mice aged 5-6 weeks were sublethally irradiated with 1.91 Gy using orthovoltage X-rays. Within 24 hours after irradiation, CD34+ cells were transplanted by intravenous (i.v.) injection (200 µL) in the tail vein. The first four weeks, mice were maintained on water containing 0.07 mg/mL polymixin B (Bupha, Uitgeest, The Netherlands), 0.0875 mg/mL ciprofloxacin (Bayer, Mijdrecht, The Netherlands) and 0.1 mg/mL amphotericin B (Bristol-Myers Squibb, Woerden, The Netherlands) with *ad libitum* food pellets and DietGel Recovery (Clear H_2O, Portland, ME, USA). After 4 weeks, mice were maintained on *ad libitum* water and regular chow. Peripheral blood was drawn from the tail vein every 4 weeks. At the end of experiments, mice were sacrificed by CO_2 inhalation and thymus, spleen, peripheral blood, femurs and tibiae were obtained. Single cell suspensions were made from thymus and spleen using a 70 µm nylon cell strainer (BD Falcon, Franklin Lakes, NJ, USA). Bone marrow was obtained by flushing femurs and tibiae with IMDM (Gibco, Life Technologies, Bleiswijk, The Netherlands) 2.5% FCS (Greiner Bio-One B.V., Alphen aan den Rijn, The Netherlands) supplemented with 100 U/mL penicillin and 100 µg/mL streptomycin (Gibco, Life Technologies).

For secondary transplantations, half of the bone marrow from a donor was thawed and transplanted via i.v. injection in the lateral tail vein of irradiated NSG recipients.

Flow cytometry

Erythrocytes from spleen and peripheral blood samples were lysed using NH_4Cl (8.4 g/L)/ $KHCO_3$ (1 g/L) solution. Mononuclear cells were stained in fluorescence-activated cell sorter (FACS) buffer (PBS/0.2% bovine serum albumin/0.1% sodium azide). Staining was performed for 30 minutes at 4°C. The following anti-human antibodies were used: CD3-PECy5 (UCHT1), CD4-APCCy7 (RPA-T4), CD8-PECy7 (SK1), CD13-APC (WM15), CD14-PE (M5E2), CD16-PE (B73.1), CD19-APCCy7 (SJ25C1), CD33-APC (WM53), CD34-PE (8G12), CD45-V450, CD45RA-FITC (L48), CD56-PE (MY31) (all from BD Biosciences, San Jose, CA), CD38-PECy7 (HIT2), CD49f PerCP-efluor710 (eBioG0H3) and CD90-APC (eBio5e10) (all from eBioscience, San Diego, CA). Data were acquired on a Canto II (BD Biosciences) and analyzed using FlowJo software (Treestar, Ashland, OR, USA).

Immunization

Mice were immunized by intraperitoneal injection of 100 µg TNP-KLH (Biosearch Technologies Inc., Novato, CA, USA) in 50% Imject Alum (Thermo Scientific, Rockford, IL, USA). The animals were boosted with 100 µg TNP-KLH in PBS by intraperitoneal injection 3 weeks after the first injection. Serum was collected one week after the last injection. TNP-specific IgG antibodies were determined by sandwich enzyme-linked immunosorbent assay (ELISA). Plates coated with TNP-KLH were incubated for 3 hours at room temperature with serial dilutions of the obtained sera. After washing with PBS/0.05% Tween 20 (Sigma Aldrich, St. Louis, MO, USA), plates were incubated with goat-anti-human-IgG conjugated to biotin (Biosource, Life Technologies, Bleiswijk, The Netherlands, kindly provided by dr. A. Mulder, Leiden University Medical Center, Leiden, The Netherlands) for 30 minutes at room temperature. After washing, plates were incubated with streptavidin conjugated to horseradish peroxidase (Jackson ImmunoResearch, Newmarket, Suffolk, UK) for 30 minutes at room temperature. Azino-bis-ethylbenzthiazoline sulfonic acid (ABTS, Sigma Aldrich, St. Louis, MO, USA) was used as a substrate for detection using a Bio-Rad Model 680 microplate reader (Bio-Rad Laboratories B.V., Veenendaal, The Netherlands) at a wavelength of 415 nm.

Immunohistochemistry

Paraffin sections of spleens obtained from NSG mice transplanted with human CD34+ cells were stained with Hematoxylin & Eosin. Final magnifications of images were 100x.

Results

Similar engraftment levels of cultured HSPC and fresh HSPC

For genetic modification, e.g. gene therapy, HSPC need to be cultured for a short period. To test whether this is feasible for the NSG model, we cultured HSPC isolated from UCB o/n to determine the effect on engraftment potential. NSG mice were transplanted with 0.5×10^5 or 1.5×10^5 HSPC directly after isolation or after o/n culture in StemSpan supplemented with cytokines. The transplanted cells were analyzed for expression of surface markers that define human HSC subsets.[14] An increase in the percentage of CD90+CD45RA- cells and, within

this population, CD49f⁺ cells was observed after o/n culture (Fig. 1A). This increase of more primitive HSC subsets was associated with similar engraftment of human cells in lymphoid organs (Fig. 1B) and similar contribution of cell lineages to engraftment in peripheral blood between recipients of fresh or cultured HSPC (Fig. 1C and 1D). Engraftment of human cells and lineage contribution were both unaffected by the number of transplanted cells. No differences in numbers of cells belonging to the most primitive human HSC subset were found in the BM of recipients of fresh and cultured HSPC, although there was a trend at lower transplanted cell numbers (0.5x10⁵, 50k) for more primitive stem cells to be detected in the BM of recipients of cultured HSPC (Fig. 1E). This led us to conclude that the short o/n culture, as needed for genetic modification, does not compromise engraftment potential and lineage contribution of human HSPC in primary recipients. Furthermore, the described protocol allows for a high level of engraftment in different organs (Fig. 1B).
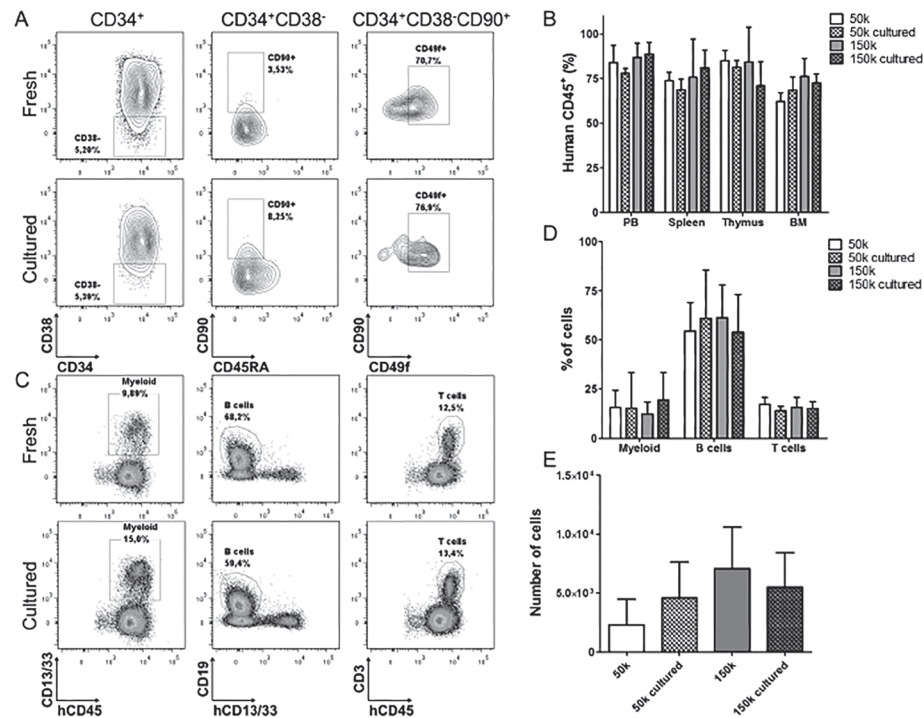

Figure 1: Engraftment capacity of HSPC is not affected by a short in vitro culture. A) Phenotype of transplanted cells. Plots are gated on the population indicated on top. **B)** Engraftment as measured by percentage of human CD45 expressing cells in peripheral blood of humanized NSG mice transplanted with different cell doses of either fresh or cultured HSPC isolated from UCB. **C)** Different cell lineages in peripheral blood of mice transplanted with 150k non-cultured HSPC isolated from UCB (top) or 150k cultured HSPC (bottom). Myeloid cells (left), B cells (middle) and T cells (right) were gated within human CD45⁺ cells **D)** Contribution of different cell lineages in peripheral blood at 18 weeks after transplantation. Percentages are gated within human CD45⁺ cells. **E)** Numbers of LT-HSC (hCD45⁺CD34⁺CD38⁻CD90⁺CD45RA⁻CD49f⁺) present in BM of NSG recipients transplanted with different cell doses of either fresh or cultured HSPC isolated from UCB. Data are represented as mean ± standard deviation (SD) in **(B, D, E)**. 50k, 0.5x10⁵ cells; 150k, 1.5x10⁵cells. HSPC were isolated from a pool of 7 UCB donors, 3 mice per group.

Specific antibodies are produced after immunization

To test the functionality of both T and B cells, we immunized the mice that were transplanted with cultured human HSPC with TNP-KLH, a T-cell-dependent-B-cell-antigen. One week after the last challenge an increase in the number of T cells in the peripheral blood of immunized mice was observed as compared to non-immunized mice (Fig. 2A). This increase in number of T cells was caused by an expansion of CD4⁺ T helper cells, which are the cells to provide crosstalk to B cells (p<0.05, Fig. 2B). To determine the functionality of the B cells, an ELISA for TNP-specific antibodies was performed. An increase of TNP-specific IgG was only measured in the serum of immunized animals (Fig. 2C). In addition, more plasma cells were observed in the spleens, but not in the BM, of immunized animals as compared to non-immunized mice (Fig. 2D). Germinal centers could also be detected by H&E staining of sections of the spleen of immunized mice (Fig. 2E). In conclusion, immunization of young NSG mice transplanted with o/n cultured human HSC showed that both T cells and B cells are functional.
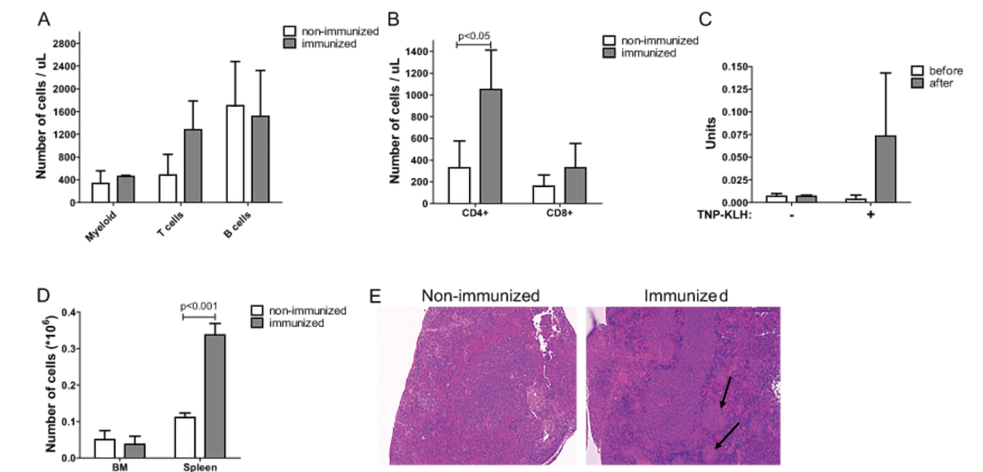

Figure 2: Immunization of humanized NSG mice shows the functionality of both T cells and B cells. A) Expansion of T cells in peripheral blood after immunization. **B)** Number of CD4⁺ and CD8⁺ T cells in peripheral blood. **C)** Quantification of TNP-specific IgG in serum of immunized mice. **D)** Number of human plasma cells that were present in spleens after immunization. **E)** Detection of germinal centers in spleens of immunized mice by hematoxylin & eosin staining (100x final magnification). Data are represented as mean ± SD in **A-D**. HSPC were isolated from a pool of 5 UCB donors, 3 mice per group.

Secondary transplantation results in high multilineage engraftment

To determine the long-term repopulating ability of stem cells residing in the BM of humanized mice, we performed a secondary transplantation in a total of five mice. Half of the BM of primary recipients that had received cultured HSPC, was thawed and transplanted via i.v. injection in 1 (donor 9) or 2 recipients (donor 2 and 15) depending on the number of cells that was recovered. Yet the recipient of donor 9 received half of the number of HSC as compared to recipients from cells of the other 2 donors (Fig. 3D). Good engraftment was observed in the peripheral blood of all secondary recipients (Fig. 3A). The effect of cell number was reflected

in the level of engraftment as measured in peripheral blood. Also in all secondary recipients normal development of T cells was present (Fig. 3B, for gating strategy see Supplementary Fig. S1) and all major cell lineages were present in the BM (Fig. 3C). These data show that with this protocol engraftment can be observed in secondary recipients, indicating that there was no stem cell exhaustion in the primary recipients that were transplanted with cultured HSPC.

We compared the number of HSC that was transplanted with the number of HSC that was obtained 17 weeks after secondary transplantation. Cells were analyzed for different phenotypes that have been described to stage human hematopoietic stem and progenitor cells.[14] Using this method, the $CD34^+CD38^-CD90^+CD45RA^-CD49f^+$ population contains the highest frequency of long-term reconstituting HSC. For all different phenotypes we observed an expansion in the bone marrow obtained from both hind legs of the secondary recipient as compared to the number of cells that was transplanted (Fig. 3D-F, for gating strategy see Supplementary Fig. S2). This was observed for 2 out of 3 donors.
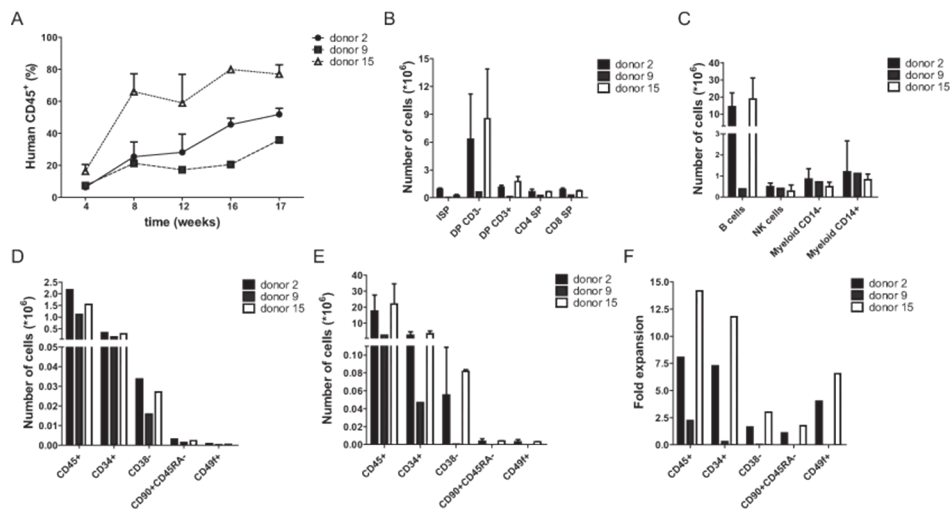
Transplantation of HSC from both UCB and BM results in high engraftment and development of all lineages

We tested whether our optimized protocol gave good engraftment of HSPC from cryopreserved BM and development of different lymphoid lineages. Different cell doses of o/n cultured HSPC from UCB and BM were transplanted in NSG mice. For both HSPC sources it was observed that there was a higher engraftment when more cells were transplanted (Fig. 4A). Although engraftment was consistently higher in mice transplanted with cryopreserved UCB, we observed good repopulation in mice transplanted with cells obtained from cryopreserved BM but higher cell doses are needed for robust engraftment compared to UCB. There was no difference observed in lineage contribution in peripheral blood between the two cell sources (Fig. 4B and 4C). This data shows that with our optimized protocol it is possible to get good engraftment and development of all lineages in NSG mice transplanted with HSPC isolated from cryopreserved human BM samples.

Figure 3: Secondary transplantation results in high engraftment and development of all lineages. A) Engraftment over time as measured by human CD45 expressing cells in peripheral blood of secondary recipients. **B)** Development of human T cells in the thymus of secondary recipients. Gated on human CD45$^+$ cells, ISP; immature single positive, DP; double positive, SP; single positive. **C)** Development of lineages in the bone marrow of secondary recipients. Gated on human CD45$^+$ cells. **D)** The number of cells that was transplanted into secondary recipients and **E)** the number of cells that was obtained from both hind legs of secondary recipients. Gated on human CD45$^+$ cells. Data are represented as mean ± standard deviation (SD). **F)** When the numbers in D and E are divided, this results in the fold expansion of HSC in both hind legs of secondary recipients. Data are represented as mean ± SD in **A-E**. Half of total BM of 3 primary recipients was transplanted in 2 secondary recipients (donor 2 and 15) or 1 recipient (donor 9).
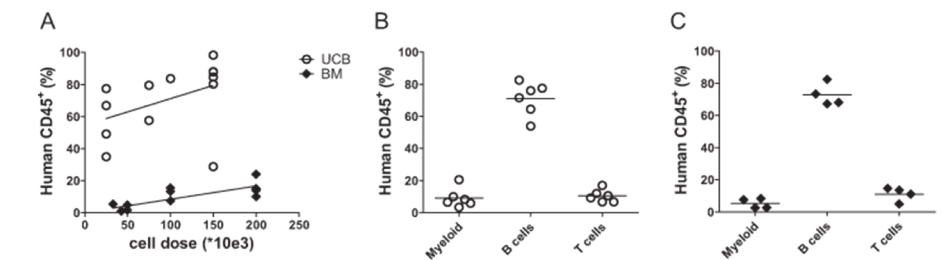

Figure 4: Transplantation of o/n cultured HSC from both cryopreserved UCB and cryopreserved BM results in development of all lymphoid lineages and high human chimerism. A) Engraftment in peripheral blood of hCD45$^+$ cells in mice transplanted with different cell doses of HSC isolated from umbilical cord blood (UCB) or human bone marrow (BM). Contribution of different lineages in peripheral blood of NSG mice transplanted with 150,000 HSC obtained from UCB **B)** or 200,000 HSC obtained from BM **C)**. Gated on human CD45$^+$ cells. UCB: 3 different pools of at least 2 donors in a total of 13 recipients, BM: 3 different donors in a total of 13 recipients.

Discussion

Here we report on adaptations to the NSG mouse model to achieve high and robust engraftment even with HSPC isolated from cryopreserved human BM samples. An overnight culture of HSPC was introduced as this is needed to allow for genetic modification of HSPC. Using the described protocol, cryopreserved patient BM material could be used to test the efficacy of gene therapy in an *in vivo* setting. With culturing of HSPC for longer periods, the repopulation capacity can be lost.[15] However, reports have shown that culturing in defined serum-free medium supplemented with different cytokines can enhance engraftment,[16] even of HSPC in an allogeneic setting.[17]

We demonstrate reproducibly high engraftment in the NSG mouse model using a simple protocol of i.v. transplantation in the tail vein of young NSG mice. Here we obtained high engraftment of cultured HSPC transplanted in young adult NSG mice even when low cell numbers (25,000 cells) were transplanted. Using this protocol we observed T cell development similar to fresh human thymi,[18] successful immunization leading to human antibody production, and successful engraftment into secondary recipients.

The humanized mouse model is frequently used when the immune system, HIV biology or stem cell expansion protocols are studied. Although myeloid and lymphoid cell lineages do develop and specific immune responses can be measured, it remains unclear how T cell progenitors are selected in the thymus of humanized mice due to MHC differences between species. However, it has been reported that a diverse repertoire is generated in NSG mice, and HLA-specific immune responses can be detected, although weak.[19] Furthermore, it has been demonstrated that cryopreservation of UCB does not compromise the production of immunoglobulins in the NSG mouse model.[20] Here, we have demonstrated that both T cells and B cells were functional by immunization with a T-cell-dependent-B-cell-antigen. Plasma cells and germinal centers were found in the spleen of immunized mice, as also shown by others.[21, 22] Therefore, we think the NSG mouse is a good model to study human lymphoid cell development in an *in vivo* setting. Furthermore, LT-HSC were found in the BM of primary recipients and these were able to repopulate secondary recipients with development of myeloid and lymphoid lineages. This shows that the transplanted stem cells were not exhausted in the primary recipient and even expansion of HSC was observed. The number of primitive HSC tended to be increased in BM of primary recipients that were transplanted with 0.5×10^5 CD34^{+} cells. This is in line with work by Zheng *et al.*,[17] who have shown using a similar cytokine cocktail that murine HSC can be transplanted over major MHC barriers because of up regulation of the CD47 molecule that gives an anti-endocytosis signal to macrophages. Extrapolating these findings to the current xenotransplantation data, we also found CD47 up regulation on human CD34^{+} cells after culturing (Supplementary Fig. S3). No increase in number of primitive HSC was observed when a higher dose of 1.5×10^5 CD34^{+} cells were transplanted, probably due to the already high engraftment observed with 0.5×10^5 CD34^{+} cells.

CD34^{+} cells can be readily isolated from mobilized peripheral blood, UCB or BM. It has been demonstrated using the NOD-*scid* model that there are differences in engraftment efficiency between the different sources, with HSPC from UCB being superior to HSPC obtained from mobilized peripheral blood and BM.[23, 24] Furthermore, HSPC isolated from UCB have a higher cloning efficiency[25] and UCB contains more primitive HSC.[26] As NOD-*scid* mice do not allow proper T cell development and still have residual NK cell activity, causing much lower engraftment, it is not easy to compare this strain to the NSG mouse side by side. However, anecdotal information from various researchers also indicated that engraftment and T cell development from cryopreserved BM material was highly problematic in NSG mice. Here, we show that using the described protocol good engraftment was achieved when HSPC from cryopreserved human BM samples were transplanted. As we did not transplant uncultured BM derived HSPC it is hard to determine the effect of culturing on their engraftment potential. On the other

hand, for HSPC isolated from UCB we do not observe a difference in repopulation between fresh and cultured HSPC. Furthermore, we do not know what the effect of cryopreservation is on engraftment potential of BM derived HSPC. It has been described that HSPC isolated from cryopreserved and fresh UCB perform equally well in engrafting NSG mice.[20] Therefore, it seems that HSPC quality is not affected by cryopreservation.

In conclusion, the optimization of the NSG humanized mouse model as described here, facilitates the use of human HSC obtained from different sources with robust engraftment The described protocol does allow transplantation of HSPC derived from cryopreserved BM with good engraftment and robust T cell development. This might be very relevant for material present in bio-banks that could now be used for fundamental studies or pre-clinical evaluations of transplantation protocols regarding stem cell expansion and gene therapy approaches.

Acknowledgments

Author Disclosure Statement

The authors declare no competing financial interests.

2

References

1. Eapen M, Rocha V, Sanz G, et al. Effect of graft source on unrelated donor haemopoietic stem-cell transplantation in adults with acute leukaemia: A retrospective analysis. Lancet Oncol 2010; 11: 653-660.

2. Gennery AR, Slatter MA, Grandin L, et al. Transplantation of hematopoietic stem cells and long-term survival for primary immunodeficiencies in europe: Entering a new century, do we do better? J Allergy Clin Immunol 2010; 126: 602-610 e601-611.

3. Servais S, Porcher R, Xhaard A, et al. Pre-transplant prognostic factors of long-term survival after allogeneic peripheral blood stem cell transplantation with matched related/unrelated donors. Haematologica 2013.

4. Gaspar HB, Qasim W, Davies EG, et al. How i treat severe combined immunodeficiency. Blood 2013; 122: 3749-3758.

5. Lapidot T, Pflumio F, Doedens M, et al. Cytokine stimulation of multilineage hematopoiesis from immature human cells engrafted in scid mice. Science 1992; 255: 1137-1141.

6. Prochazka M, Gaskins HR, Shultz LD, et al. The nonobese diabetic scid mouse: Model for spontaneous thymomagenesis associated with immunodeficiency. Proc Natl Acad Sci U S A 1992; 89: 3290-3294.

7. Goldman JP, Blundell MP, Lopes L, et al. Enhanced human cell engraftment in mice deficient in rag2 and the common cytokine receptor gamma chain. Br J Haematol 1998; 103: 335-342.

8. Mazurier F, Fontanellas A, Salesse S, et al. A novel immunodeficient mouse model--rag2 x common cytokine receptor gamma chain double mutants--requiring exogenous cytokine administration for human hematopoietic stem cell engraftment. J Interferon Cytokine Res 1999; 19: 533-541.

9. Traggiai E, Chicha L, Mazzucchelli L, et al. Development of a human adaptive immune system in cord blood cell-transplanted mice. Science 2004; 304: 104-107.

10. Ito M, Hiramatsu H, Kobayashi K, et al. Nod/scid/gamma(c)(null) mouse: An excellent recipient mouse model for engraftment of human cells. Blood 2002; 100: 3175-3182.

11. Ishikawa F, Yasukawa M, Lyons B, et al. Development of functional human blood and immune systems in nod/scid/il2 receptor {gamma} chain(null) mice. Blood 2005; 106: 1565-1573.

12. Shultz LD, Lyons BL, Burzenski LM, et al. Human lymphoid and myeloid cell development in nod/ltsz-scid il2r gamma null mice engrafted with mobilized human hemopoietic stem cells. J Immunol 2005; 174: 6477-6489.

13. McDermott SP, Eppert K, Lechman ER, et al. Comparison of human cord blood engraftment between immunocompromised mouse strains. Blood 2010; 116: 193-200.

14. Notta F, Doulatov S, Laurenti E, et al. Isolation of single human hematopoietic stem cells capable of long-term multilineage engraftment. Science 2011; 333: 218-221.

15. Bhatia M, Bonnet D, Kapp U, et al. Quantitative analysis reveals expansion of human hematopoietic repopulating cells after short-term ex vivo culture. J Exp Med 1997; 186: 619-624.

16. Zhang CC, Lodish HF. Murine hematopoietic stem cells change their surface phenotype during ex vivo expansion. Blood 2005; 105: 4314-4320.

17. Zheng J, Umikawa M, Zhang S, et al. Ex vivo expanded hematopoietic stem cells overcome the mhc barrier in allogeneic transplantation. Cell Stem Cell 2011; 9: 119-130.

18. Weerkamp F, de Haas EF, Naber BA, et al. Age-related changes in the cellular composition of the thymus in children. J Allergy Clin Immunol 2005; 115: 834-840.

19. Marodon G, Desjardins D, Mercey L, et al. High diversity of the immune repertoire in humanized nod. Scid.Gamma c-/- mice. Eur J Immunol 2009; 39: 2136-2145.

20. Scholbach J, Schulz A, Westphal F, et al. Comparison of hematopoietic stem cells derived from fresh and cryopreserved whole cord blood in the generation of humanized mice. PLoS One 2012; 7: e46772.

21. Becker PD, Legrand N, van Geelen CM, et al. Generation of human antigen-specific monoclonal igm antibodies using vaccinated "human immune system" mice. PLoS One 2010; 5.

22. Choi B, Chun E, Kim M, et al. Human b cell development and antibody production in humanized nod/scid/il-2rgamma(null) (nsg) mice conditioned by busulfan. J Clin Immunol 2011; 31: 253-264.

23. Ng YY, van Kessel B, Lokhorst HM, et al. Gene-expression profiling of cd34+ cells from various hematopoietic stem-cell sources reveals functional differences in stem-cell activity. J Leukoc Biol 2004; 75: 314-323.

24. Noort WA, Wilpshaar J, Hertogh CD, et al. Similar myeloid recovery despite superior overall engraftment in nod/scid mice after transplantation of human cd34(+) cells from umbilical cord blood as compared to adult sources. Bone Marrow Transplant 2001; 28: 163-171.

25. Hao QL, Shah AJ, Thiemann FT, et al. A functional comparison of cd34 + cd38- cells in cord blood and bone marrow. Blood 1995; 86: 3745-3753.

26. Wang JC, Doedens M, Dick JE. Primitive human hematopoietic cells are enriched in cord blood compared with adult bone marrow or mobilized peripheral blood as measured by the quantitative in vivo scid-repopulating cell assay. Blood 1997; 89: 3919-3924.

2
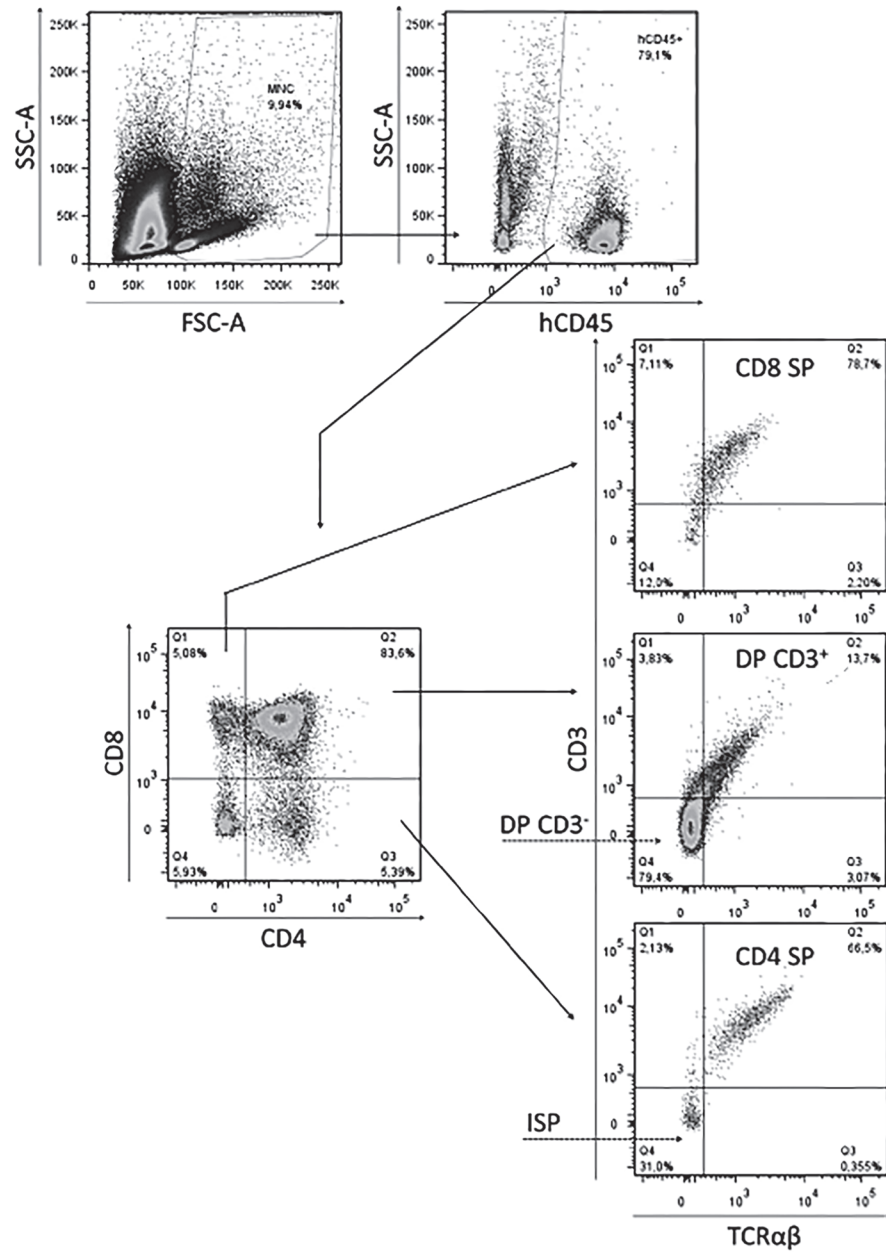
Supplementary figure S1: Gating strategy for T cell developmental stages in thymus of secondary recipient. Thymocytes were gated based on side scatter (SSC-A) and forward scatter (FSC-A) and thereafter on expression of human CD45 (hCD45). Four populations can be discriminated based on expression of CD4 and CD8, within these we gated on CD3⁻TCRαβ⁻ and CD3⁺TCRαβ⁺. ISP, immature single positive, CD4⁺CD3⁻ TCRαβ⁻; DP CD3⁻, double positive CD3⁻, CD4⁺CD8⁺CD3⁻ TCRαβ⁻; DP CD3⁺, double positive CD3⁺, CD4⁺CD8⁺CD3⁺ TCRαβ⁺; CD4 SP, CD4⁺ single positive, CD4⁺CD3⁺ TCRαβ⁺; CD8 SP, CD8⁺ single positive, CD8⁺CD3⁺ TCRαβ⁺.
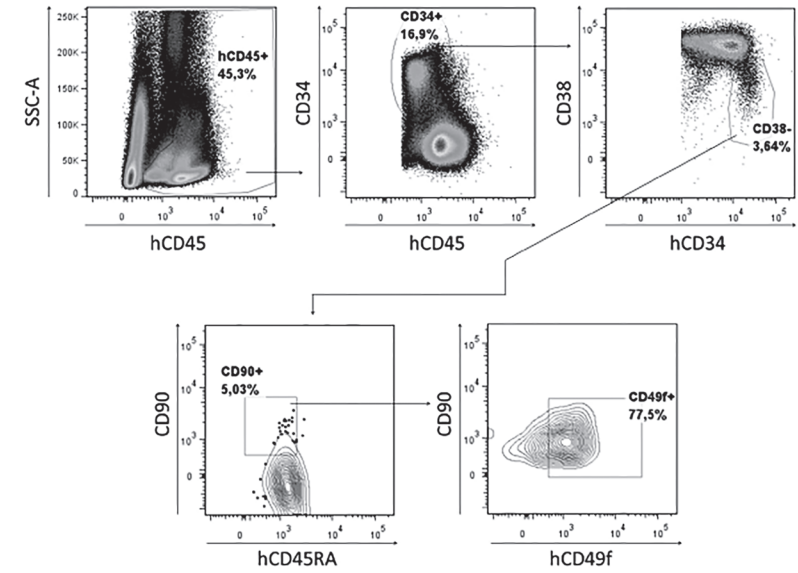
Supplementary figure S2: Gating strategy for human HSC in bone marrow of secondary recipient. CD34⁺ HSPC were gated within human CD45⁺ cells. Within the CD34⁺ a sequential gating was performed on CD38⁻ cells, followed by CD90⁺CD45RA⁻ cells and CD49f⁺ cells as described by Notta *et al.* in 2011 [14].
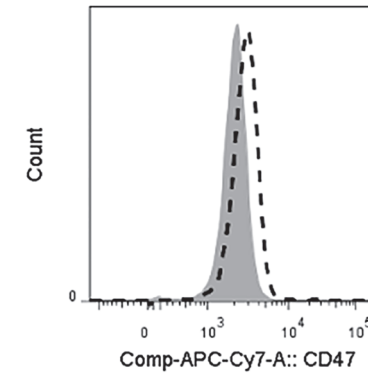
Supplementary figure S3: Upregulation of CD47 on CD34⁺ cells after overnight culture. Expression of CD47 on human CD34⁺ UCB cells before (filled grey) and after (dashed black) overnight culture in StemSpan supplemented with SCF, TPO, IGF-2 and FGF-1. Representative figure of 3 independent experiments.

Chapter 3

Identification of checkpoints in human T-cell development using severe combined immunodeficiency stem cells

Anna-Sophia Wiekmeijer[1], Karin Pike-Overzet[1], Hanna IJspeert[2], Martijn H. Brugman[1], Ingrid L.M. Wolvers-Tettero[2], Arjan C. Lankester[3], Robbert G.M. Bredius[3], Jacques J.M. van Dongen[2], Willem E. Fibbe[1], Anton W. Langerak[2], Mirjam van der Burg[2], Frank J.T. Staal[1]

[1]Department of Immunohematology and Blood Transfusion, Leiden University Medical Center, Leiden, The Netherlands

[2]Department of Immunology, Erasmus MC, University Medical Center Rotterdam, Rotterdam, The Netherlands

[3]Department of Pediatrics, Leiden University Medical Center, Leiden, The Netherlands

Abstract

Background: Severe combined immunodeficiency (SCID) represents congenital disorders characterized by a deficiency of T cells due to arrested development in the thymus. Yet, the nature of these developmental blocks has remained elusive due to the difficulty of taking thymic biopsies from affected children.

Objective: Identify the stages of developmental arrest in human T-cell development caused by various major types of SCID.

Methods: Transplantation of SCID CD34^{+} bone marrow stem/progenitor cells into an optimized NSG xenograft mouse model, followed by detailed phenotypic and molecular characterization using flow cytometry, Ig and TCR spectratyping and deep sequencing of *IGH* and *TRD* loci.

Results: Arrests in T-cell development caused by mutations in *IL7RA* and *IL2RG* were observed at the most immature thymocytes, much earlier than expected based on gene expression profiling of human thymocyte subsets and studies with corresponding mouse mutants. TCR rearrangements were functionally required at the CD4^{-}CD8^{-}CD7^{+}CD5^{+} stage, given the developmental block and extent of rearrangements in mice transplanted with Artemis-SCID. The xenograft model used is not informative for ADA-SCID, while hypomorphic mutations lead to less severe arrests in development

Conclusion: Transplanting CD34^{+} stem cells from SCID patients into a xenograft mouse model provides previously unattainable insight into human T-cell development and functionally identifies the arrests in thymic development caused by several SCID mutations.

Key messages:
- The arrests in thymic development have been unknown for most types of human SCID
- Using a xenograft model, IL2RG- and IL7RA-SCID showed very early arrests in the thymus, followed by recombination defective SCID (Artemis), all blocking in the CD4^{-}CD8^{-} DN stages.
- This approach can be used for other types of SCID and help in unraveling unknown SCID cases

Capsule summary: The nature of the blocks in T-cell development for SCID has remained elusive. Using a xenograft model, we show that different SCID-causing mutations lead to severe defects at different early developmental stages in the thymus.

Key Words: SCID, thymus, NSG, IL2Rg, IL7Ra, ADA, Artemis, T-cell development, B-cell development

Abbreviations:
ADA; adenosine deaminase, BM; bone marrow, DN; double negative, FTOC; fetal thymic organ culture, HSC; hematopoietic stem cells, HSPCs; hematopoietic stem and progenitor cells, Ig; immunoglobulin, IGH; immunoglobulin heavy chain, IL2RG; interleukin-2 receptor gamma, IL7RA; interleukin-7 receptor alpha, ISP; immature single positive, NK cell; natural killer cell, NSG; NOD-*Scid-Il2rg*^{-/-} mice, PB; peripheral blood, SCID; severe combined immunodeficiency, TCR; T-cell receptor, UCB; umbilical cord blood

Introduction

Severe combined immunodeficiency (SCID) comprises a series of congenital disorders characterized by a deficiency of (functional) T cells. This can be accompanied by deficiencies in either NK or B cells or both. These different phenotypes are caused by mutations in several genes[1]. It remains unknown where the blocks in human T-cell development reside for these different deficiencies, except for mutations in *CD3D*[2, 3] and *ZAP70*[4]. For the three major types of human SCID that represent >80% of known SCID mutations, the stage of arrest in T-cell development is unknown. These three types are: 1, receptor signaling defects reflecting for instance mutations in *IL2RG, IL7RA and JAK3*, 2, recombination defects (*Artemis (DCLRE1C), RAG1, RAG2, LIG4, XLF, DNA-PKcs*) and 3, metabolic enzyme deficiencies (*ADA, PNP*).

One approach to obtain insight into human T-cell development is the careful analysis of gene expression and T-cell receptor (TCR) rearrangement of *ex vivo* isolated developmental subsets[5]. While such studies have shown that murine and human T-cell development are overall very comparable, important differences in for instance the early double negative (DN) compartment and the thymus seeding progenitor have been described[5, 6, 7, 8, 9].

Mice with targeted mutations in key genes, including SCID-causing genes, have provided important insights in T-cell development[10, 11, 12, 13, 14, 15, 16]. However, not all of these mice resemble the phenotype of SCID patients. For instance, *Il7r*^{-/-} mice have a deficiency in both B and T cells[12], while in humans only T cells are affected[17]. Whether genetic mouse models for SCID demonstrate comparable blocks in T-cell development to humans remains largely unanswered. Furthermore, gene expression analysis of known SCID genes in different stages of human T-cell development showed that there are differences in expression as compared to blocks observed in mice[5]. Recent advances in xenotransplantation models[18] now allow for better definition of human T-cell development *in vivo*. Importantly, these models can also be used for transplantation of human stem cells isolated from cryopreserved bone marrow (BM) samples stored in bio-banks[19], e.g. from SCID patients.

Using transplantation of CD34^{+} cells isolated from patients with proven functional null mutations in genes characteristic for each of the three major types of SCID, we aimed to study the functional roles of these genes for human T-cell development *in vivo*. This study provides for the first time a description of the arrests in T-cell development in SCID patients and functional insight into two important developmental checkpoints in the human thymus.

3

Methods

Isolation of human CD34⁺cells

Human BM was obtained from healthy pediatric donors at the Leiden University Medical Center (LUMC, Leiden, The Netherlands). Informed consent was obtained from the parents for the use of leftover samples for research purposes. Parents / guardians and donors have consented to the donation procedure, after psychological testing and approval of the Youth Court in case of children. If the genetic research studies show any abnormalities, the parents had the opportunity to be informed. The LUMC medical ethical board (IRB) has approved the use of left over material of normal marrow for research purposes in P01.028 and P08.001. BM samples from children diagnosed with SCID were obtained according to the guidelines of the Erasmus MC. The medical ethical committees of Leiden University Medical Center and of ErasmusMC approved this study and both served as institutional review boards. Informed consent was provided according to the Declaration of Helsinki. Cells were isolated and cultured as described previously [19]. See the Methods section in the Online Repository for further details.

Mice

NOD.Cg-Prkdc[scid] Il2rg[tm1Wjl]/SzJ (NSG) mice were obtained from Charles River Laboratories (UK) and bred in the animal facility at the LUMC. Experimental procedures were approved by the Ethical Committee on Animal Experiments of the LUMC.

In vivo experiments were performed as described [19]. Female mice were transplanted with CD34⁺ cells by intravenous injection within 24 hours after irradiation with 1.91 Gy using orthovoltage X-rays.

Flow cytometry

Labelling of mononuclear cells has been described [19]. Data were acquired on a Canto II (BD Biosciences) and analyzed using FlowJo software (Treestar, Ashland, OR, USA). Flow cytometric analysis of different stages of human B-cell development was performed as described elsewhere [20, 21].

Repertoire analysis

DNA was isolated from single cell suspensions made from total thymus, spleen and BM of transplanted NSG mice using the GeneElute™ Mammalian Genomic DNA Miniprep Kit (Sigma Aldrich, St. Louis, MO, USA). Rearrangements were analyzed using the EuroClonality/BIOMED-2 multiplex PCR protocol [22]. Amplification of IGH rearrangements was performed as previously described [23]. PCR products were sequenced on the Illumina Miseq sequencer using 300 base pairs paired-end sequencing (V3 chemistry). The sequence reads containing the IGH rearrangements were uploaded in IMGT HighV-Quest [24]. Subsequently the output files were analyzed using the IGGalaxy tool [25]. The TRDD2-TRDD3 rearrangements were analyzed by matching the constant genomic region outside the TRDD2 and TRDD3 sequence in the amplicons, after which the length of the TRDD2-TRDD3 regions was determined. Analysis was performed using Bioperl and R.

Statistics

The Wilcoxon rank-sum test was performed when possible. P < 0.05 was considered significant and indicated in figures with *****.

Results

NSG mice transplanted with HSPCs from control samples display low degree of variation

Recently, we have shown that NOD-*Scid-Il2rg*^{-/-} (NSG) mice engrafted with hematopoietic stem and progenitor cells (HSPCs) isolated from umbilical cord blood and, to a lesser degree, from human BM allow robust development of myeloid and lymphoid cells, with functional B cells and T cells [19]. First, we have transplanted NSG mice with HSPCs obtained either from umbilical cord blood (UCB) or human pediatric BM to determine the presence of different stages of human T cell development. We have transplanted 14 mice with CD34⁺ cells isolated from cord blood from different donors and 9 mice with CD34⁺ cells isolated from pediatric bone marrow, with cell doses ranging from 25,000 to 200,000 total cells per mouse. All stages were present in NSG mice transplanted with HSPCs obtained from UCB as well as human BM (Fig. 1A). Different DN subsets could be discriminated based on the expression of CD7 and CD5 within the CD4⁻CD8⁻ DN compartment (Fig. 1B). Moreover, the relative presence of all subsets is highly comparable and showed a low degree of variation (Fig. 1A and B). Together these data demonstrate the reproducible presence of the different stages of human T-cell development. Therefore, the high robustness of the model allows us to study the effect of rare mutations in SCID on human T-cell development. In all the experiments performed hereafter, only BM-derived HSPCs and not UCB-derived HSPCs were used for transplantations as all SCID HSPCs used in this study were also BM-derived and some differences could be observed between mice engrafted with UCB-derived HSPCs compared to BM-derived HSPCs.

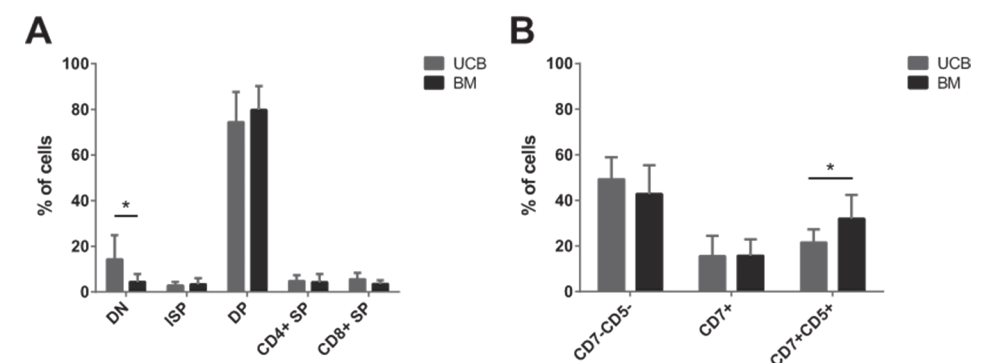**Figure 1: Low variation among stages of human T cell development in NSG mice transplanted with HSPCs from control umbilical cordblood and control human BM. A, B)** Percentage of cells per different stage of human T cell development within thymi of NSG mice transplanted with HSPCs. **A)** Cells were gated within hCD45⁺ cells or **B)** within hCD45⁺CD4⁻CD8⁻ (DN). Depicted is the mean and standard deviation (sd), ***** p < 0.05.

SCID humanized mice display SCID-specific phenotypes

We have engrafted NSG mice with HSPCs isolated from BM of SCID patients with mutations in different genes, including ADA-SCID, Artemis-SCID, IL7RA-SCID and IL2RG-SCID (Table 1). No T cells were detected in peripheral blood (PB) when Artemis-, IL7RA- or IL2RG-SCID HSPCs were transplanted (Fig. 2A), as expected based on the disease-defining absence of T cells. However, for ADA-SCID T, B and NK cells were readily observed (Fig. 2A-C), likely caused by complementation by secreted murine ADA, comparable to the recovery seen in ADA-SCID patients treated with PEG-ADA enzyme replacement therapy. Therefore, we focused our further study on T- and B-cell development in Artemis-, IL7RA- and IL2RG-SCID compared to controls. The results from HSPCs transplanted into NSG mice copied the phenotype found in different types of SCID patients; for Artemis-SCID we observed a deficiency of T and B cells, for IL7RA-SCID an absence of T cells, and for IL2RG-SCID a deficiency of both T and NK cells (Fig. 2A-C, Table 1). In mice transplanted with IL7RA-SCID derived HSPCs the number of NK cells is somewhat lower as compared to controls. Unfortunately clinical data on NK cells in the IL7RA-SCID patient were not available and therefore it is hard to draw conclusions from this observation, but the transplantation data are consistent with a $T^-B^+NK^+$ phenotype. Human myeloid cells developed in all mice, although in a higher percentage and number in mice transplanted with Artemis-SCID HSPCs (Fig. 2D). Besides myeloid cells, also NK cells were present both in higher percentages and numbers, probably due to the severe T- and B-cell deficiency observed with Artemis-SCID resulting in increased development of other cell lineages. B cells were present in higher numbers in mice transplanted with ADA-SCID derived HSPCs (Fig. 2B). Since the model used is B cell-prone, this most likely reflects the higher engraftment compared to controls. The same phenotypes as observed in peripheral blood of transplanted mice were observed in the spleen and BM (Fig. 2E and F). Some CD3 expression was observed within the spleens of NSG mice transplanted with Artemis-, IL7RA- and IL2RG-SCID, however, these cells did not express TCR, CD4 or CD8 on their surface (data not shown) and likely represent staining artefacts.

Table I: Characteristics of SCID patients

SCID	Mutation	T cells (x10⁹/L)	B cells (x10⁹/L)	NK cells (x10⁹/L)
ADA	c.736C>T, p.Gln246Stp	<0.01	<0.01	<0.01
Artemis	c.220C>T, p.Arg74Stp	0.4[a]	<0.01	0.5
IL7RA	c.876+1G>A / c.898_902delCCTGA, p.Pro300LysfsX9	na[b]	na[a]	na[a]
IL2RG	c.209T>G, p.Met70Arg	8.2[c]	4	0.06
IL2RG hypomorphic	c.655T>A, p.Tyr219Asn	3.4	1.4	0.9

Counts of cells from different lineages from peripheral blood of patients as determined by flow cytometry and their mutation as determined by PCR. [a] all T cells were determined to be of maternal origin by their memory phenotype, [b] na = not available, [c] all T cells were of maternal origin (proven with STR analysis on sorted cells).
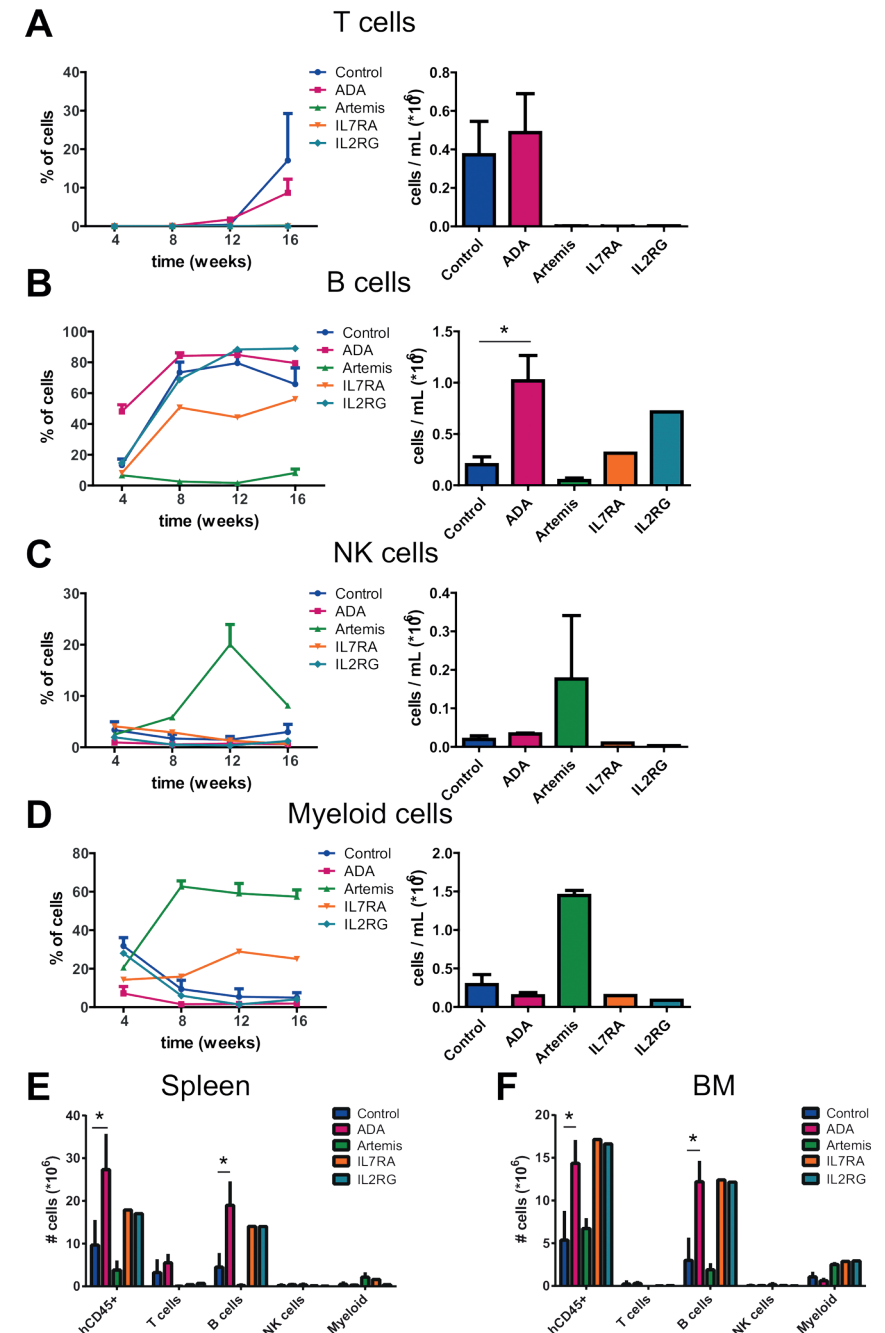
Figure 2: NSG mice transplanted with SCID HSPCs show same phenotype as patients in their peripheral blood. A-D) Cells present in PB in percentage of human CD45⁺ cells over time after transplantation (left panel) or in absolute numbers at the end of the experiment (right panel); **A)** T cells, **B)** B cells, **C)** NK cells and **D)** myeloid cells. **E)** Absolute numbers of different cell types within spleen or **F,** BM. Depicted is the mean and standard deviation (sd), * $p<0.05$.

Artemis-SCID demonstrates a block in B-cell development before the cytoplasmic Igμ⁺ pre-B-II stage

To further validate the NSG xenograft model, we first investigated B cell development in NSG mice transplanted with CD34⁺ SCID cells and compared this to the *ex vivo* composition of the B-cell precursor compartment in patients. In BM of NSG mice transplanted with Artemis-SCID derived HSPCs, we observed a decrease in percentage and number of CD19⁺ B cells when compared to BM from control mice (Fig. 3A and B). This was not observed for the other types of SCID, which were highly comparable to mice transplanted with HSPCs obtained from healthy pediatric donors. Different stages of B-cell development were determined within the B-cell compartment[20]. B-cell precursors derived from Artemis-SCID HSPCs blocked at the CD10⁺ stage of B-cell development in the BM (Fig. 3C). Furthermore, almost no surface expression of IgM was detected and the percentage of B-cell precursors that expressed IgM in the cytoplasm was decreased more than 18-fold in NSG mice transplanted with Artemis HSPCs when compared to controls (Fig. 3D). There was barely any expression of cytoplasmic Igμ present in the B-cell precursors, therefore precursor B-cell differentiation blocks before the cytoplasmic Igμ⁺ pre-B-II stage. This block in B-cell development was identical to the phenotype observed in a BM aspirate of the Artemis-SCID patient (Fig. 3E). The block at the pre-B-II stage in Artemis-SCID leads to an absence of immature and mature B cells expressing IgM or IgD (Fig. 3F). We also observed a much lower percentage of B cells in spleens of NSG mice transplanted with Artemis-SCID HSPC and no mature CD20⁺, IgM⁺ or IgD⁺ B cells were found (Fig. 3G).

Together these data confirm a block in B-cell development for Artemis-SCID, and not for IL7RA-SCID and IL2RG-SCID. This is highly similar to the observations in the BM aspirates of the corresponding SCID patients, demonstrating that HSPCs transplantation into the NSG model faithfully recapitulates human B-cell development, thereby validating the use of this model for studies of human lymphoid development.

Artemis-SCID cells do not generate a polyclonal IGH repertoire

We performed analysis of the immunoglobulin heavy chain (IGH) repertoire that was generated in the BM of transplanted NSG mice. Both for incomplete D-J (Fig. 4A) and complete V-DJ (Fig. 4B) rearrangements, merely a few incidental rearrangements were observed for Artemis-SCID. For IL7RA- and IL2RG-SCID a polyclonal repertoire, comparable to that observed in controls, was generated (Fig. 4A and B). To determine the repertoire diversity of IGH, we performed deep sequencing using the Illumina Miseq platform. Analysis of D to J recombination showed that a less diverse repertoire was generated in the BM of mice transplanted with Artemis-SCID derived HSPCs while this was not observed for IL7RA- and IL2RG-SCID and controls (Fig. 4C). Thus, only for a recombination defect, as exemplified by Artemis-SCID, both phenotypic and *IGH* rearrangement analysis indicate an arrest in B-cell development at the pre-B-II stage, which in addition led to development of a less diverse repertoire.
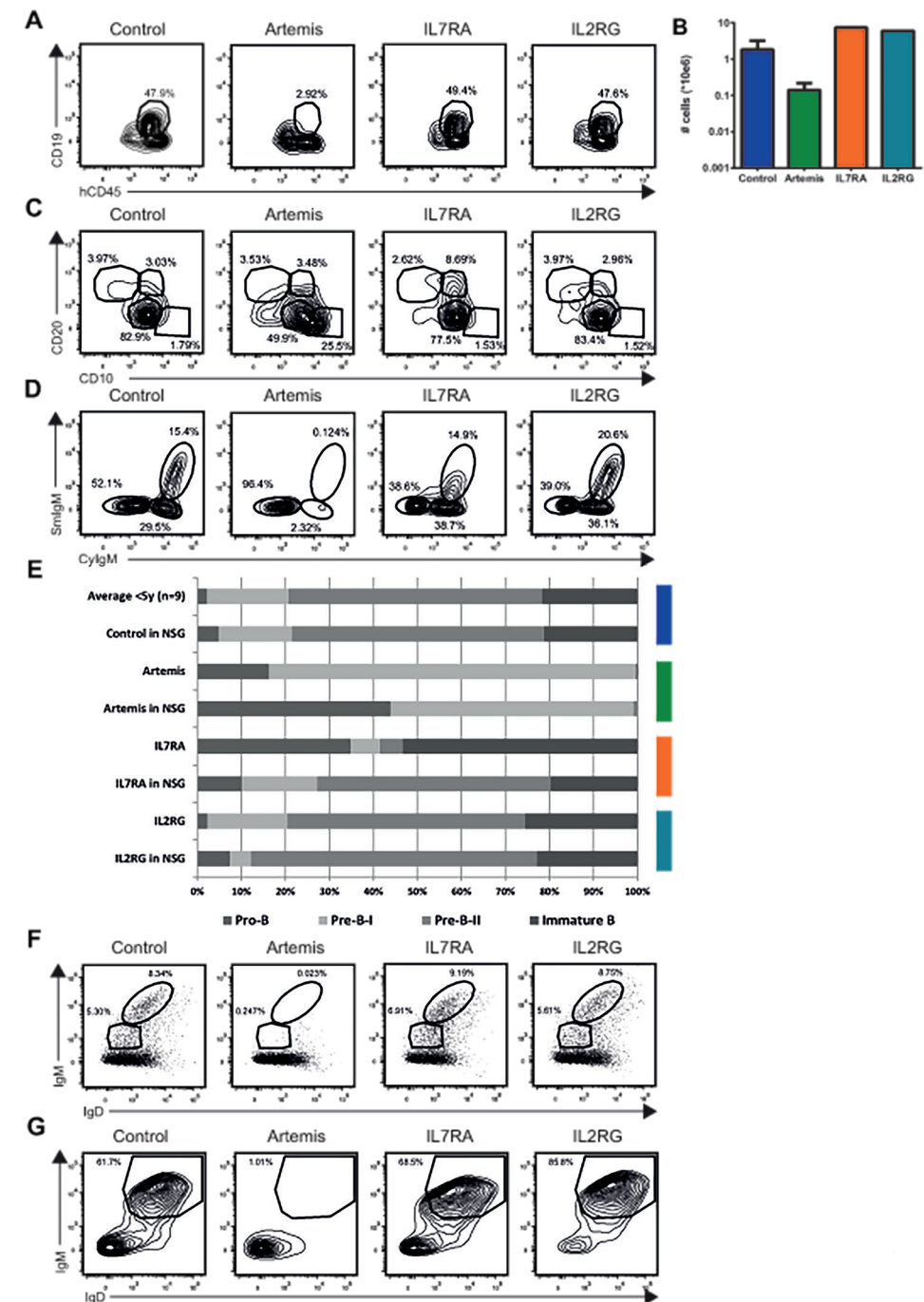
Figure 3: Developmental block at the CD10⁺ stage for B cells in Artemis-SCID. A) Percentage and **B)** number of B cells in transplanted NSG mice BM. **C, D)** Maturational stages of B-cell development in BM of transplanted NSG mice. **E)** Comparison of B-cell precursors in *ex vivo* BM aspirates to BM of transplanted NSG mice. **F)** IgM and IgD expression on non-myeloid hCD45⁺ cells in BM and **G)** spleen of transplanted NSG mice.
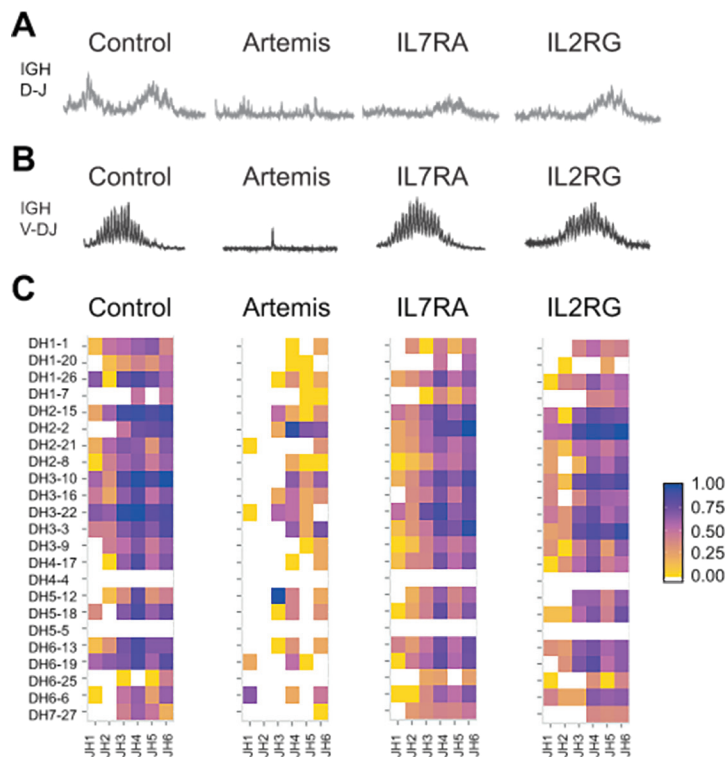
Figure 4: No polyclonal IGH repertoire was generated in developing B cells from Artemis-SCID. A) D-J and **B)** V-DJ rearrangement of IGH locus in total BM cells of NSG mice transplanted with SCID or control HSPCs. **C)** Heatmap depicting the unique junctions of D to J segments for the IGH locus in total BM cells of NSG mice transplanted with SCID or control HSPCs. Colors depict the relative length of CDR3.

Novel early blocks in T-cell development for SCID

For the vast majority of SCID patients, the blocks in T-cell development are only known by extrapolation from mouse models. Here, we directly determined the arrests in T-cell development for different types of human SCID by investigating thymi of NSG mice engrafted with SCID HSPCs. To discriminate different populations within the DN compartment, we measured expression of CD7 and CD5 within this population. Based on the observed developmental arrests at the CD4-CD8- DN stage, all types of SCID block much earlier than observed in corresponding mouse mutants (Fig. 5A). T-cell development in IL2RG-SCID was inhibited at the CD7-CD5- stage followed by IL7RA-SCID where one-third of the cells reached the subsequent CD7+CD5- DN stage (Fig. 5B), although these blocks are somewhat comparable. For Artemis-SCID the block in T-cell development was found at the DN CD7+CD5+ stage without expression of CD1a (Fig. 5B and C). As expected from these early blocks in T-cell development, there was no expression of either TCRαβ or TCRγδ on total thymocytes in mice transplanted with SCID-derived HSPCs, but readily detectable in control mice (see Fig. E1 in the Online Repository). These data demonstrate the stages of arrest in T-cell development for different types of SCID and show an absolute requirement for common-gamma type cytokine signaling

at the most immature thymic stages as also illustrated by the decrease in total hCD45+ cells within thymi of these mice (Fig. 5D). We observed a high percentage of CD19+ B cells in thymi from NSG mice transplanted with HSPCs from Artemis-SCID (Fig 5E). Also for IL7RA- and IL2RG-SCID an increase in the percentage of B cells in the thymus was observed, but not as much as for Artemis-SCID. The increase in B cells that was observed was only relative and not in absolute numbers (Fig. 5F).

Importantly, we also transplanted CD34+ cells from a SCID patient with a hypomorphic mutation in IL2RG. This patient had low numbers of peripheral T cells and NSG mice transplanted with HSPCs derived from this patient indeed showed a much milder block, with only a lower percentage of DP thymocytes (Fig 5G). This demonstrates that less severe mutations lead to a less pronounced arrest in development. In addition, T cells also were detected in the peripheral blood mice transplanted with hypomorphic mutant IL2RG HSPCs (data not shown).
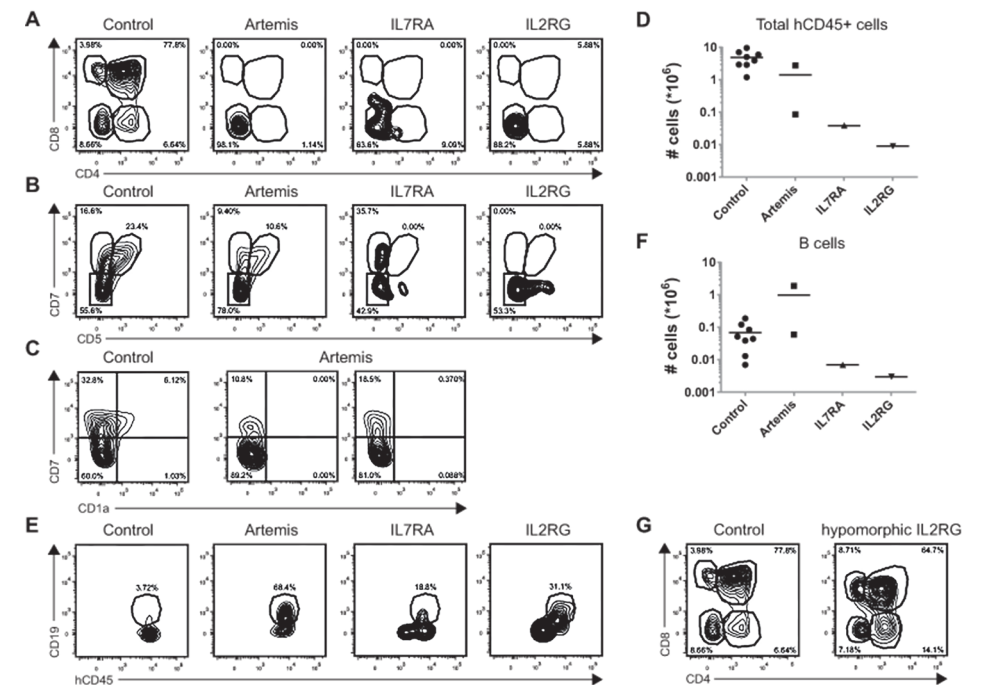
Figure 5: Early blocks in human T-cell development for different types of SCID. A) Phenotype of hCD45+ thymocytes and **B, C)** DN thymocytes in NSG mice transplanted with SCID or control HSPCs. **D)** Quantification of total human CD45+ cells in thymi of NSG mice transplanted with SCID or control HSPCs. **E, F)** Presence of CD19+ B cells in thymi of transplanted NSG mice. **G,** NSG mice transplanted with hypomorphic IL2RG-SCID or control HSPCs.

TCR rearrangement starts very early after thymus entry

TCR rearrangement starts at the *TRD* locus[5]. Since the observed blocks in T-cell development were very early, we focused TCR repertoire analysis on the *TRD* locus, of which Dδ2-Dδ3 is rearranged first. IL7RA- and IL2RG-SCID T-cell progenitors only showed incidental products

of this rearrangement in accordance with the early blocks observed using flow cytometry (Fig. 6A). Using spectratyping of T-cell receptor CDR3 length distribution, Artemis-SCID T-cell progenitors showed a broad repertoire for Dδ2-Dδ3 comparable to NSG mice transplanted with control HSPCs. These spectratyping data were confirmed using next generation sequencing of the TCR Dδ2-Dδ3 locus. Again, we observed a very limited number of reads for IL7RA- and IL2RG-SCID, while the normalized read numbers of Artemis-SCID were similar to those of mice transplanted with wild type cells (Fig. 6B). For the second step of *TRD* rearrangement, Dδ2-Jδ1, the repertoire was more oligoclonal in Artemis-SCID T-cell progenitors, while in IL7RA- and IL2RG-SCID such rearrangements were undetectable (Fig. 6C). However, none of the different types of SCID generated a broad Dδ-Jδ or even Vδ-Jδ repertoire (Fig. 6D). *TRG* is rearranged after *TRD*[5] and for IL2RG-SCID no rearrangement could be observed of *TRG* while for IL7RA-SCID merely a clonal rearrangement was observed, confirming the later block in development of IL7RA-SCID as compared to IL2RG-SCID (Fig 6E). While Artemis-SCID T-cell progenitors were able to perform the first steps of *TRD* rearrangement, they did not rearrange *TRG* and *TRB* loci (Fig. 6E and F). For both loci only a few incidental peaks were detected in Artemis-SCID T-cell progenitors as compared to NSG mice transplanted with control HSPCs. Judging from these clonal peaks, rearrangement of *TRG* is already initiated at the DN CD7^{+} stage and *TRB* at the DN CD7^{+}CD5^{+} stage of T-cell development.
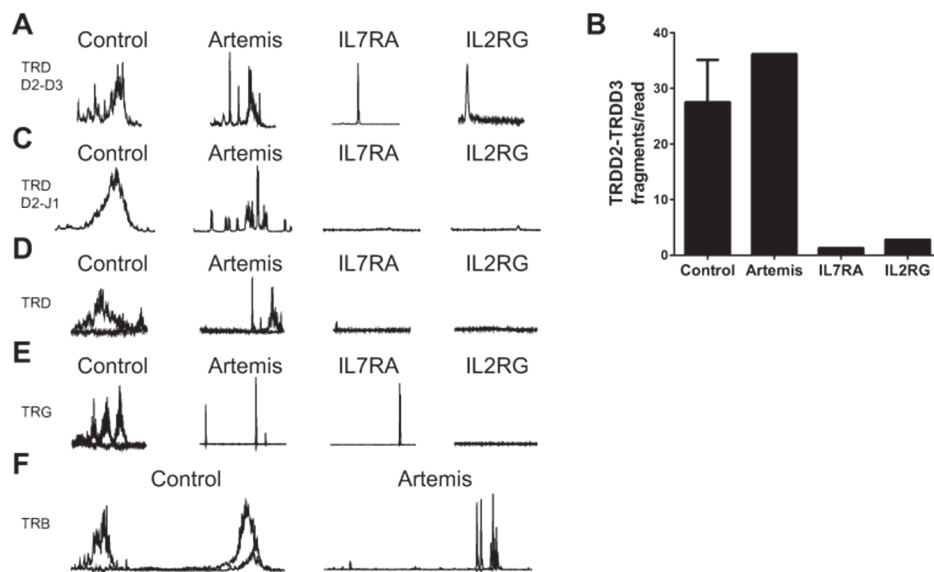

Figure 6: Hierarchical blocks in human T-cell development as demonstrated by TCR repertoire analysis.
A, C-F) Rearrangement of TCR loci in total thymocytes of transplanted NSG mice; **A)** TRD Dδ2-Dδ3, **C)** TRD Dδ2-Jδ1, **D)** TRD Dδ-Jδ (blue) and Dδ-Dδ (green) **E)** TRG and **F)** TRB. **B)** Assigned fragments of TRDD2-TRDD3 were calculated by dividing the number of assigned reads by the number of identified fragments.

Discussion

SCID is a rare disease caused by different genetic defects leading to T cell deficiency that can be accompanied by deficiencies in B and/or NK cells. Here we demonstrate for the first time the arrests in T-cell development for the major types of human SCID using an *in vivo* model; data which typically is not available because thymic biopsies are almost never obtained. Our approach allows for comprehensive loss-of-function insight for two important developmental checkpoints; common-gamma chain cytokine signaling and the initiation of TCR rearrangements.

The arrests in T-cell development observed for the different types of SCID demonstrate a hierarchy in TCR rearrangement and the corresponding phenotypes. The earliest block in T-cell development is observed in IL2RG-SCID, followed by IL7RA-SCID, demonstrating an almost immediate requirement for common-gamma chain cytokine signaling after seeding of the thymus.

Artemis is involved in opening of the hairpin sealed coding ends during recombination[26]. Here, we observed that Artemis-SCID cells are able to initiate rearrangement of the *TRD* locus as demonstrated by polyclonal Dδ2-Dδ3 and oligoclonal Dδ2-Jδ1 rearrangements. However, no complete TCRδ was formed. Apparently, Artemis is not needed for the first steps of *TRD* rearrangement, as confirmed by next generation sequencing, but is needed for complete rearrangement of *TRD*. An explanation would be that in absence of Artemis, the hairpin sealed coding ends are opened by other enzymes[27]. As this process is less efficient, the chance of successful two-step rearrangement is low and only partial rearrangements would be formed, as observed here.

We here demonstrate that rearrangement of *TRG* is initiated at the DN CD7^{+} stage and *TRB* loci is already initiated at the DN CD7^{+}CD5^{+} stage of T-cell development, in contrast to previous models where *TRB* rearrangement was proposed at the immature single positive (ISP)[28, 29] or DN3 stage of development[30]. As these DN CD7^{+}CD5^{+} cells were devoid of CD1a expression that marks human DN3 cells[8] this stage is reminiscent of the DN2 compartment in the mouse. While in the mouse rearrangement of *TRB* starts in the DN3 stage[31], in the human thymus this process seem to start earlier based on our data. In mice, mutations in *Il2rg* lead to reduced thymic cellularity but are permissive for thymocyte development[10, 11], whereas here we observed an absolute and very early requirement for IL2RG signaling. The blocks in IL7RA-SCID and IL2RG-SCID are not completely identical, suggesting that cytokines other than IL-7 may also signal through the common-gamma chain in the early steps after thymus seeding. Cytokines that might be involved in proliferation and development in this very immature stage could be IL-2, IL-4 or IL-15[32, 33, 34]. IL-15 is an important NK cell growth factor and in IL7RA deficiency this cytokine can signal normally via the IL2RG-IL15RA complex. Thus some of the CD7^{+}CD5^{+} DN cells observed may contain mature NK cells, rather than solely uncommitted thymocytes with T/NK cell potential[9, 35]. The increased percentage of B cells observed in thymi of NSG mice transplanted with Artemis-SCID HSPCs is in line with data from the mouse where very early thymic blocks also lead to increased percentages of B cells, which developed from DN

thymocytes underlying the developmental plasticity of these cells that can still develop in non T-lineage cells in mice and men[9, 36].

The point at which in IL2RG deficiency blocks development has sometimes been suggested to occur before thymic seeding. Our data combined with data by Kohn et al., who showed no differences in hematopoietic stem cells (HSC) and pre-thymic progenitors of IL2RG-SCID patients indicates that this is not the case. Rather, very soon after thymic seeding, there is an absolute requirement for gc signaling (see Fig 5). Since Six et al. showed that human thymic progenitors (in contrast to mouse) express IL7Ra and IL2Rg[37], expression and functional requirement for gc are independently regulated.

To the best of our knowledge, only one paper has addressed the effect of human IL2RG deficiency in T cells before. Using an in vitro OP9-DL1 system, an arrest in development was shown at the CD7+CD5+CD1a- stage[38]. As no data are available on the nature of the IL2RG-SCID patient described by Six et al., it is impossible to say if the observed differences are based on differences between an in vitro model system versus in vivo transplantation data or reflect inherent differences based on different mutations with different residual signaling properties. Furthermore, the OP9-DL1 system can only address development until the earliest DP stages and is very sensitive to subtle differences in cytokines and labile contents of culture media[38]. Development proceeds a bit further in fetal thymic organ cultures (FTOC), but fully matured T cells and thymic egress do not occur, limiting the development of human thymocytes. In the NSG model as we describe it, the thymic phenotypes are highly similar to those obtained from human thymi, underscoring the validity of this model to identify the thymic defects in human SCID patients. Another approach to model T-cell developmental blocks in SCID patients, is by measuring rearrangement of TCR loci and TREC levels in peripheral blood T cells[39, 40]. However, many SCID patients do not have peripheral T cells to perform these analyses on and no phenotype of thymocytes is available. The low level of TRD D2-D3 in another IL2RG-SCID patient[39] corroborates our data described here for thymocytes, demonstrating a very early block in T-cell development.

We have chosen SCID patients with mutations that are deleterious for function as this would lead to functional null mutants and included a hypomorphic patient, who had clinically a mild SCID phenotype that was only found because of an affected cousin. This mutation indeed showed a much less severe phenotype and no clear developmental block. This helps explain the divergent findings with IL2RG-SCID thus far and, importantly, validates our approach for genotype-phenotype studies with SCID mutations.

In summary, combining the flow cytometric and molecular data obtained from the engrafted NSG thymi leads to a proposed model for the development of human thymocytes (Fig. 7), in which there is a prominent role for cytokine signaling and initiation of TRB rearrangement marks the presumed b-selection point, as Artemis deficient cells block at this stage. It was shown previously that, indeed, pTα (PTCRA) is abundantly expressed at this point in development[5].
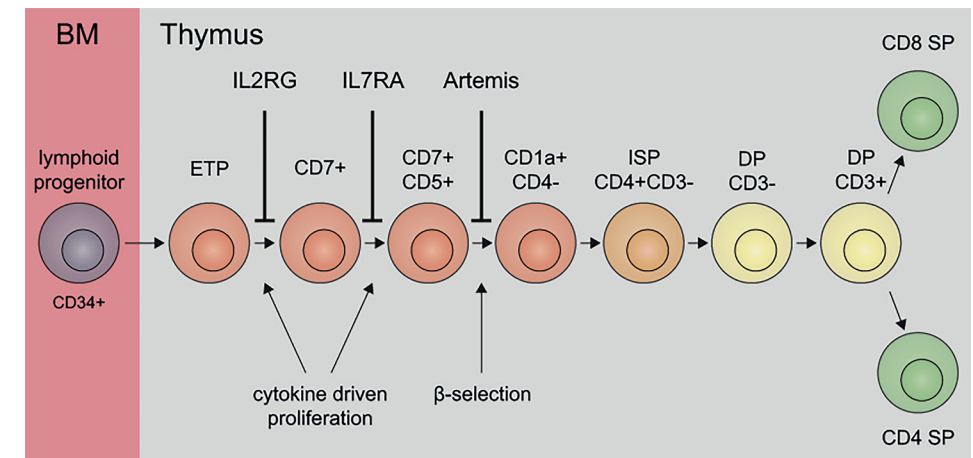

Figure 7: Proposed model for human T-cell development. Indicated are the blocks in human T-cell development for different types of SCID as observed in this study. ETP; early thymic progenitor, ISP; immature single positive, DP; double positive, SP; single positive.

In a xenograft model, it could be argued that the defects observed are not cell-intrinsic but result from incompatibilities between mouse microenvironment and human hematopoietic cells. However, in the NSG model, human T cells develop with all the developmental stages known from ex vivo removed human thymi[41]. In addition, Parietti et al. were able to reproduce the development of human pro-thymocytes in the NSG xenograft model[42] and it was demonstrated that human thymocytes can respond to murine MHC signals and have comparable migration on murine and human thymic slices[43]. Furthermore, for B cells the xenogeneic environment shows a block identical to the block in development directly found in the Artemis-SCID patient and B-cell development in controls was highly comparable to normal human BM. Taken together, this validates the use of xenografted mice for studies of human lymphoid development.

There is much attention for improving thymic output after allogeneic bone marrow transplantation; for acquired immune deficiencies, and during ageing[44]. In particular, strategies targeting the earliest human thymocytes, such as administration of IL-7, growth hormone or TSH or sex hormone ablation[44, 45]. Our results suggest that IL-7 combined with other early acting factors, e.g. Wnt[46], may be promising to restore the early human thymocyte compartment which is expected to sustain thymopoiesis by providing a pool of DN progenitor cells.

In conclusion, we here report loss-of-function data on human T-cell development, demonstrating earlier blocks in T-cell development than proposed before[5, 30]. The obtained insights might give opportunities for treatment of ETP-ALL by interfering with common-gamma signaling which is active in these very early stages of T-cell development. It would be of great interest to study arrests in development for other types of human SCID in this xenograft model. Finally, the xenotransplantation method we here describe may prove useful in unravelling unknown types of human SCID for which the genetic defect has remained elusive and aid diagnosis in cases with blurred phenotypes, e.g. when maternal T cells are present.

Acknowledgements

References

1. Gaspar HB, Qasim W, Davies EG, Rao K, Amrolia PJ, Veys P. How I treat severe combined immunodeficiency. *Blood* 2013, **122**(23)**:** 3749-3758.

2. Dadi HK, Simon AJ, Roifman CM. Effect of CD3delta deficiency on maturation of alpha/beta and gamma/delta T-cell lineages in severe combined immunodeficiency. *The New England journal of medicine* 2003, **349**(19)**:** 1821-1828.

3. de Saint Basile G, Geissmann F, Flori E, Uring-Lambert B, Soudais C, Cavazzana-Calvo M, *et al.* Severe combined immunodeficiency caused by deficiency in either the delta or the epsilon subunit of CD3. *The Journal of clinical investigation* 2004, **114**(10)**:** 1512-1517.

4. Arpaia E, Shahar M, Dadi H, Cohen A, Roifman CM. Defective T cell receptor signaling and CD8+ thymic selection in humans lacking zap-70 kinase. *Cell* 1994, **76**(5)**:** 947-958.

5. Dik WA, Pike-Overzet K, Weerkamp F, de Ridder D, de Haas EF, Baert MR, *et al.* New insights on human T cell development by quantitative T cell receptor gene rearrangement studies and gene expression profiling. *The Journal of experimental medicine* 2005, **201**(11)**:** 1715-1723.

6. Blom B, Verschuren MC, Heemskerk MH, Bakker AQ, van Gastel-Mol EJ, Wolvers-Tettero IL, *et al.* TCR gene rearrangements and expression of the pre-T cell receptor complex during human T-cell differentiation. *Blood* 1999, **93**(9)**:** 3033-3043.

7. Hao QL, George AA, Zhu J, Barsky L, Zielinska E, Wang X, *et al.* Human intrathymic lineage commitment is marked by differential CD7 expression: identification of CD7- lympho-myeloid thymic progenitors. *Blood* 2008, **111**(3)**:** 1318-1326.

8. Pike-Overzet K, van der Burg M, Wagemaker G, van Dongen JJ, Staal FJ. New insights and unresolved issues regarding insertional mutagenesis in X-linked SCID gene therapy. *Molecular therapy : the journal of the American Society of Gene Therapy* 2007, **15**(11)**:** 1910-1916.

9. Weerkamp F, Baert MR, Brugman MH, Dik WA, de Haas EF, Visser TP, *et al.* Human thymus contains multipotent progenitors with T/B lymphoid, myeloid, and erythroid lineage potential. *Blood* 2006, **107**(8)**:** 3131-3137.

10. DiSanto JP, Muller W, Guy-Grand D, Fischer A, Rajewsky K. Lymphoid development in mice with a targeted deletion of the interleukin 2 receptor gamma chain. *Proceedings of the National Academy of Sciences of the United States of America* 1995, **92**(2)**:** 377-381.

11. Ohbo K, Suda T, Hashiyama M, Mantani A, Ikebe M, Miyakawa K, *et al.* Modulation of hematopoiesis in mice with a truncated mutant of the interleukin-2 receptor gamma chain. *Blood* 1996, **87**(3)**:** 956-967.

12. Peschon JJ, Morrissey PJ, Grabstein KH, Ramsdell FJ, Maraskovsky E, Gliniak BC, *et al.* Early lymphocyte expansion is severely impaired in interleukin 7 receptor-deficient mice. *The Journal of experimental medicine* 1994, **180**(5)**:** 1955-1960.

13. Rooney S, Sekiguchi J, Zhu C, Cheng HL, Manis J, Whitlow S, *et al.* Leaky Scid phenotype associated with defective V(D)J coding end processing in Artemis-deficient mice. *Molecular cell* 2002, **10**(6)**:** 1379-1390.

14. Shinkai Y, Rathbun G, Lam KP, Oltz EM, Stewart V, Mendelsohn M, *et al.* RAG-2-deficient mice lack mature lymphocytes owing to inability to initiate V(D)J rearrangement. *Cell* 1992, **68**(5)**:** 855-867.

15. Wakamiya M, Blackburn MR, Jurecic R, McArthur MJ, Geske RS, Cartwright J, Jr., *et al.* Disruption of the adenosine deaminase gene causes hepatocellular impairment and perinatal lethality in mice. *Proceedings of the National Academy of Sciences of the United States of America* 1995, **92**(9)**:** 3673-3677.

3

16. Mombaerts P, Iacomini J, Johnson RS, Herrup K, Tonegawa S, Papaioannou VE. RAG-1-deficient mice have no mature B and T lymphocytes. *Cell* 1992, **68**(5): 869-877.

17. Puel A, Ziegler SF, Buckley RH, Leonard WJ. Defective IL7R expression in T(-)B(+)NK(+) severe combined immunodeficiency. *Nature genetics* 1998, **20**(4): 394-397.

18. Shultz LD, Lyons BL, Burzenski LM, Gott B, Chen X, Chaleff S, *et al.* Human lymphoid and myeloid cell development in NOD/LtSz-scid IL2R gamma null mice engrafted with mobilized human hemopoietic stem cells. *Journal of immunology* 2005, **174**(10): 6477-6489.

19. Wiekmeijer AS, Pike-Overzet K, Brugman MH, Salvatori DC, Egeler RM, Bredius RG, *et al.* Sustained Engraftment of Cryopreserved Human Bone Marrow CD34(+) Cells in Young Adult NSG Mice. *BioResearch open access* 2014, **3**(3): 110-116.

20. Noordzij JG, de Bruin-Versteeg S, Verkaik NS, Vossen JM, de Groot R, Bernatowska E, *et al.* The immunophenotypic and immunogenotypic B-cell differentiation arrest in bone marrow of RAG-deficient SCID patients corresponds to residual recombination activities of mutated RAG proteins. *Blood* 2002, **100**(6): 2145-2152.

21. van der Burg M, van Veelen LR, Verkaik NS, Wiegant WW, Hartwig NG, Barendregt BH, *et al.* A new type of radiosensitive T-B-NK+ severe combined immunodeficiency caused by a LIG4 mutation. *The Journal of clinical investigation* 2006, **116**(1): 137-145.

22. van Dongen JJ, Langerak AW, Bruggemann M, Evans PA, Hummel M, Lavender FL, *et al.* Design and standardization of PCR primers and protocols for detection of clonal immunoglobulin and T-cell receptor gene recombinations in suspect lymphoproliferations: report of the BIOMED-2 Concerted Action BMH4-CT98-3936. *Leukemia* 2003, **17**(12): 2257-2317.

23. Ijspeert H, Driessen GJ, Moorhouse MJ, Hartwig NG, Wolska-Kusnierz B, Kalwak K, *et al.* Similar recombination-activating gene (RAG) mutations result in similar immunobiological effects but in different clinical phenotypes. *The Journal of allergy and clinical immunology* 2014.

24. Li S, Lefranc MP, Miles JJ, Alamyar E, Giudicelli V, Duroux P, *et al.* IMGT/HighV QUEST paradigm for T cell receptor IMGT clonotype diversity and next generation repertoire immunoprofiling. *Nature communications* 2013, **4**: 2333.

25. Moorhouse MJ, van Zessen D, H IJ, Hiltemann S, Horsman S, van der Spek PJ, *et al.* ImmunoGlobulin galaxy (IGGalaxy) for simple determination and quantitation of immunoglobulin heavy chain rearrangements from NGS. *BMC immunology* 2014, **15**(1): 59.

26. Ma Y, Pannicke U, Schwarz K, Lieber MR. Hairpin opening and overhang processing by an Artemis/DNA-dependent protein kinase complex in nonhomologous end joining and V(D)J recombination. *Cell* 2002, **108**(6): 781-794.

27. van der Burg M, Verkaik NS, den Dekker AT, Barendregt BH, Pico-Knijnenburg I, Tezcan I, *et al.* Defective Artemis nuclease is characterized by coding joints with microhomology in long palindromic-nucleotide stretches. *European journal of immunology* 2007, **37**(12): 3522-3528.

28. Blom B, Spits H. Development of human lymphoid cells. *Annual review of immunology* 2006, **24**: 287-320.

29. Soulier J, Clappier E, Cayuela JM, Regnault A, Garcia-Peydro M, Dombret H, *et al.* HOXA genes are included in genetic and biologic networks defining human acute T-cell leukemia (T-ALL). *Blood* 2005, **106**(1): 274-286.

30. Weerkamp F, Pike-Overzet K, Staal FJ. T-sing progenitors to commit. *Trends in immunology* 2006, **27**(3): 125-131.

31. Rothenberg EV, Moore JE, Yui MA. Launching the T-cell-lineage developmental programme. *Nature reviews Immunology* 2008, **8**(1): 9-21.

32. Barcena A, Toribio ML, Pezzi L, Martinez C. A role for interleukin 4 in the differentiation of mature T cell receptor gamma/delta + cells from human intrathymic T cell precursors. *The Journal of experimental medicine* 1990, **172**(2): 439-446.

33. Barcena A, Toribio ML, Gutierrez-Ramos JC, Kroemer G, Martinez C. Interplay between IL-2 and IL-4 in human thymocyte differentiation: antagonism or agonism. *International immunology* 1991, **3**(5): 419-425.

34. Colpitts SL, Stonier SW, Stoklasek TA, Root SH, Aguila HL, Schluns KS, *et al.* Transcriptional regulation of IL-15 expression during hematopoiesis. *Journal of immunology* 2013, **191**(6): 3017-3024.

35. Sanchez MJ, Muench MO, Roncarolo MG, Lanier LL, Phillips JH. Identification of a common T/natural killer cell progenitor in human fetal thymus. *The Journal of experimental medicine* 1994, **180**(2): 569-576.

36. Radtke F, Wilson A, Stark G, Bauer M, van Meerwijk J, MacDonald HR, *et al.* Deficient T cell fate specification in mice with an induced inactivation of Notch1. *Immunity* 1999, **10**(5): 547-558.

37. Six EM, Bonhomme D, Monteiro M, Beldjord K, Jurkowska M, Cordier-Garcia C, *et al.* A human postnatal lymphoid progenitor capable of circulating and seeding the thymus. *The Journal of experimental medicine* 2007, **204**(13): 3085-3093.

38. Six EM, Benjelloun F, Garrigue A, Bonhomme D, Morillon E, Rouiller J, *et al.* Cytokines and culture medium have a major impact on human in vitro T-cell differentiation. *Blood cells, molecules & diseases* 2011, **47**(1): 72-78.

39. Roifman CM, Dadi H, Somech R, Nahum A, Sharfe N. Characterization of zeta-associated protein, 70 kd (ZAP70)-deficient human lymphocytes. *The Journal of allergy and clinical immunology* 2010, **126**(6): 1226-1233 e1221.

40. Roifman CM, Somech R, Kavadas F, Pires L, Nahum A, Dalal I, *et al.* Defining combined immunodeficiency. *The Journal of allergy and clinical immunology* 2012, **130**(1): 177-183.

41. Weerkamp F, de Haas EF, Naber BA, Comans-Bitter WM, Bogers AJ, van Dongen JJ, *et al.* Age-related changes in the cellular composition of the thymus in children. *The Journal of allergy and clinical immunology* 2005, **115**(4): 834-840.

42. Parietti V, Nelson E, Telliam G, Le Noir S, Pla M, Delord M, *et al.* Dynamics of human prothymocytes and xenogeneic thymopoiesis in hematopoietic stem cell-engrafted nonobese diabetic-SCID/IL-2rgammanull mice. *Journal of immunology* 2012, **189**(4): 1648-1660.

43. Halkias J, Melichar HJ, Taylor KT, Ross JO, Yen B, Cooper SB, *et al.* Opposing chemokine gradients control human thymocyte migration in situ. *The Journal of clinical investigation* 2013, **123**(5): 2131-2142.

44. Hollander GA, Krenger W, Blazar BR. Emerging strategies to boost thymic function. *Current opinion in pharmacology* 2010, **10**(4): 443-453.

45. van der Weerd K, van Hagen PM, Schrijver B, Heuvelmans SJ, Hofland LJ, Swagemakers SM, *et al.* Thyrotropin acts as a T-cell developmental factor in mice and humans. *Thyroid : official journal of the American Thyroid Association* 2014, **24**(6): 1051-1061.

46. Khoo ML, Carlin SM, Lutherborrow MA, Jayaswal V, Ma DD, Moore JJ. Gene profiling reveals association between altered Wnt signaling and loss of T-cell potential with age in human hematopoietic stem cells. *Aging cell* 2014.

3

Online repository material

Methods

Cryopreservation of human bone marrow-derived mononuclear cells

Mononuclear cells were isolated using Ficoll gradient separation and washed once with Iscove's Modified Dulbecco's Medium (IMDM) supplemented with supplemented with 100 U/mL penicillin and 100 µg/mL streptomycin (Gibco, Life Technologies) and 2.5% heat-inactivated FCS (Greiner Bio-One B.V., Alphen aan den Rijn, The Netherlands). Cells were resuspended in FCS/10%DMSO (Greiner Bio-One B.V., Alphen aan den Rijn, The Netherlands and Sigma-Aldrich, St. Louis, MO, USA, respectively) or in 50% RPMI/40% FCS/10% DMSO and frozen in 1 ml aliquots with a maximum of $50*10^6$ cells per cryovial. Cryovials were placed in a freezing container in -80°C and relocated to liquid nitrogen storage on the following day.

Isolation of human bone marrow-derived CD34^{+}cells

Cryopreserved vials were thawed in a 37°C waterbath after which the cell suspension was transferred to a 15 mL conical tube. Medium (IMDM supplemented with penicillin/streptomycin and 2.5% heat-inactivated FCS) was added dropwise to the cells. Labelling and isolation of CD34^{+} cells was performed according to the manufacturer's protocol (CD34 Microbead Kit, Miltenyi Biotec GmbH, Bergisch Gladbach, Germany). Cells were centrifuged and resuspended in 300 µL Running Buffer (PBS pH 7.4, 2mM EDTA, 0.5% w/v bovine serum albumin (BSA, Sigma-Aldrich, St. Louis, MO, USA). Add DNAse I (final concentration 5 U/mL, Sigma-Aldrich, St. Louis, MO, USA) together with 100 µL FcR blocking reagent and 100 µL anti-CD34 Microbeads. Cells were not counted before labelling as we never had more then $100*10^6$ mononuclear cells and with counting we would lose cells. Cells were incubated for 30 minutes in the refrigerator while shaking every 10 minutes. Isolation of CD34^{+} cells was performed using 2 times an LS column (Miltenyi Biotec GmbH, Bergisch Gladbach, Germany).

Cells were eluted in 3 mL Running Buffer using the supplied plunger. Eluted cells were centrifuged and resuspended in 500 µL StemSpan serum-free expansion medium (StemSpan-SFEM, StemCell Technologies Inc., Vancouver, BC, Canada) in the presence of 10 ng/mL stem cell factor (SCF, a gift from Amgen, Thousand Oakes, CS, USA), 20 ng/mL recombinant human thrombopoietin (rhTPO R&D Systems, Abingdon, UK), 20 ng/mL recombinant mouse insulin-like growth factor 2 (rmIGF-2, R&D Systems) and 10 ng/mL recombinant human fibroblast growth factor-acidic (rhFGF-1, Peprotech, Rocky Hill, NJ, USA). Cells were counted using a Bürker chamber and trypan blue. Cells concentration was adjusted to $1*10^6$/mL. Cells were cultured overnight in tissue-culture treated 48-well plates (Corning Incorporated, Corning, NY, USA) with 500 µL cell suspension per well. Then, cells were harvested by resuspension and transferred to a 15 mL conical tube. The well was washed by resuspension with 500 µL IMDM without phenol red (Gibco, Life Technologies, Bleiswijk, The Netherlands), which was added to the harvested cells. Cells were counted and an aliquot was taken for flow cytometry analysis to determine purity of CD34^{+} cells.

Transplantation into NSG mice

Cells were centrifuged and resuspended in IMDM without phenol red for intravenous injection into the tail vein of sublethally irradiated female NSG mice (200 µL/mouse). Mice were irradiated with with 1.91 Gy using orthovoltage X-rays one day before injection of the cells. Mice were transplanted within 24 hours after irradiation. Peripheral blood of transplanted mice was analysed every 4 weeks and mice were sacrificed 20-22 weeks after transplantation.

Table E1: Xenograft transplantation details

SCID	Number of mice transplanted	Transplanted number of total cells/mouse	Transplanted number of CD34^{+} cells/mouse
ADA	3	200,000	197,540
Artemis	2	78,000	73,593
IL7RA	1	22,000	19,518
IL2RG	1	47,150	38,559
IL2RG hypomorphic	4	50,000	45,035
Healthy donor	1	33,000	29,555
Healthy donor	4	200,000	167,480
Healthy donor	3	100,000	86,740

Indicated are the numbers of NSG mice in which the sample was transplanted and the total mononuclear cell number and number of CD34^{+} cells transplanted per mouse.
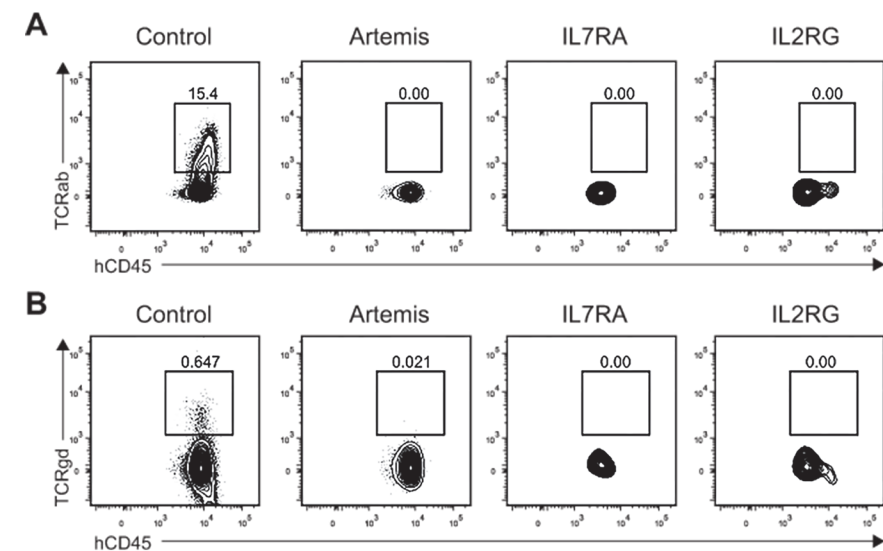
Figure E1: Absence of TCR expression on SCID thymocytes. A) Expression of TCRαβ and **B)** TCR γδ on total hCD45^{+} thymocytes from transplanted NSG mice.

Chapter 4

Identification of a novel type of T⁻B⁺SCID with a late double positive thymic arrest

Anna-Sophia Wiekmeijer[1], Gertjan Driessen[2], Karin Pike-Overzet[1], Martijn H. Brugman[1], Gijs W.E. Santen[3], Sandra A. Vloemans[1], Wibowo Arindrarto[4], Erdogan Taskesen[5,6], Marcel J.T. Reinders[5,6], Rogier Kersseboom[7], Jasper J. Saris[7], Renske Oegema[7], Robbert G.M. Bredius[8], Mirjam van der Burg[2], Frank J.T. Staal[1]

[1]Department of Immunohematology and Blood Transfusion, Leiden University Medical Center, Leiden, The Netherlands

[2]Department of Immunology, Erasmus MC, University Medical Center Rotterdam, Rotterdam, The Netherlands

[3]Department of Clinical Genetics, Leiden University Medical Center, Leiden, The Netherlands

[4]Sequence Analysis Support Core, Leiden University Medical Center, Leiden, The Netherlands

[5]Delft Bioinformatics Lab (DBL), Delft University of Technology, Delft, The Netherlands

[6]Netherlands Bioinformatics Centre (NBIC), The Netherlands

[7]Department of Clinical Genetics, Erasmus MC, University Medical Center Rotterdam, Rotterdam, The Netherlands

[8]Department of Pediatrics, Leiden University Medical Center, Leiden, The Netherlands

Abstract

More than 16 genes have been shown to be causative for severe combined immunodeficiency (SCID). However, around 20% of patients remain without molecular diagnosis. Here, we present data on a female patient with an atypical presentation of SCID whose initial diagnosis was hard to make. By transplantation of patient derived hematopoietic stem and progenitor cells in immunodeficient mice, we could demonstrate that this case was a T⁻B⁺NK⁺-SCID. Phenotypic analysis of the thymocytes of these mice demonstrated an arrest in T-cell development at the CD3⁻ to CD3⁺-CD4⁺CD8⁺ double positive and the subsequent CD4⁺- and CD8⁺-single positive transition. Using whole exome sequencing, we identified a *de novo* heterozygous missense mutation in *VPS4B* that potentially could lead to SCID with atypical presentation.

Introduction

Severe combined immunodeficiency (SCID) is a congenital disorder that is characterized by a deficiency of T cells in peripheral blood (PB). This deficiency in T cells can be accompanied by defects in either B or NK cells or both and can be categorized in 2 groups: T⁻B⁺-SCID and T⁻B⁻-SCID[1, 2]. SCID affects approximately 1 in 100,000 live births and the patients present, mostly within their first year of life, with opportunistic infections and a failure to thrive[3, 4]. Currently, the best treatment option is a hematopoietic stem cell transplantation (HSCT) although clinical trials are ongoing with gene therapy approaches for SCID caused by mutations in either IL2RG or ADA[5, 6, 7, 8, 9]. Patients suffering from SCID caused by a mutation in ADA also benefit from enzyme replacement therapy[10]. Besides IL2RG and ADA, many genes can underlie this disease; up to now more than 16 have been described[2, 10]. However, a substantial fraction of patients without an identified disease-causing mutation is still remaining. Different fractions of SCID patients without a molecular diagnosis have been reported, ranging from 7 to 33%[10, 11, 12, 13, 14].

A new approach to search for disease-causing genes is whole exome sequencing. This can be done by sequencing the coding sequences of the genome of a group of patients, as has been shown for Bartter Syndrome[15] and Miller Syndrome[16]. Due to the rarity of SCID, especially the ones without a molecular diagnosis, it is very difficult to obtain a patient group for exome sequencing with the same molecular defect. In these cases whole exome sequencing of a single patient and both parents can be useful, in which the exome of the patient and both parents are compared to exclude inherited non-damaging single nucleotide variations (SNVs), instead of multiple patients and a control group. This approach has proven successful, for instance, by demonstrating that a mutation in *CARD11* causes SCID[17].

Here, we report on a patient with atypical presentation of SCID. Using the novel approach of transplanting patient derived hematopoietic stem and progenitor cells (HSPCs) in the NOD/Scid-Il2rg⁻/⁻ (NSG) mouse model, we could demonstrate that this patient has a hematopoietic cell-intrinsic defect and identified the stage of arrest in T-cell development. Using exome sequencing combined with whole exome sequencing analysis of patient and both parents we identified a *de novo* mutation in *VPS4B* that might be causative for T⁻B⁺NK⁺-SCID as it is predicted to act as dominant negative molecule.

Materials and methods

Human CD34+ bone marrow derived cells

Human bone marrow (BM) was obtained from healthy pediatric BM donors at the Leiden University Medical Center (LUMC, Leiden, The Netherlands). Informed consent was obtained from the parents for the use of leftover samples for research purposes. BM from the patient was obtained according to the guidelines of the Erasmus MC. The medical ethical committees of LUMC and of Erasmus MC approved this study and both served as institutional review boards. Informed consent was provided according to the Declaration of Helsinki. Mononuclear cells were isolated using Ficoll gradient centrifugation, frozen in fetal calf serum (FCS)/10% DMSO (Greiner Bio-One B.V., Alphen aan den Rijn, The Netherlands and Sigma-Aldrich, St. Louis, MO, USA, respectively) and stored in liquid nitrogen. Cells were isolated and cultured as described previously[18].

Mice

NOD.Cg-*Prkdc*^{scid} *Il2rg*^{tm1Wjl}/SzJ (NSG) mice were obtained from Charles River Laboratories (Kent, United Kingdom) and bred in the animal facility at the Leiden University Medical Center. Experimental procedures were approved by the Ethical Committee on Animal Experiments of the LUMC. Female NSG mice were transplanted with CD34+ cells by intravenous injection within 24 hours after irradiation with 1.91 Gy using orthovoltage X-rays as described previously[18, 19]. Mice transplanted with CD34+ cells derived from healthy pediatric bone marrow are historical controls, due to the rarity of this material, and have been described elsewhere[19].

Flow cytometry

Analysis of lymphocyte populations in peripheral blood and composition of the B-cell precursor compartment in the BM of the patient was performed as previously described[20].

Labeling of mononuclear cells of transplanted NSG mice has been described[18]. The following anti-human antibodies were used: CD3-PECy5 (UCHT1), CD4-APCCy7 (RPA-T4), CD5-FITC (UCHT2), CD7-PECy5 (M-T701), CD8-PECy7 (SK1), CD13-APC (WM15), CD16-PE (B73.1), CD19-APCCy7 (SJ25C1), CD20-PE (L27), CD33-APC (WM53), CD34-PE (8G12), CD45-V450, CD56-PE (MY31), TCRαβ-PE (T10B9.1A-31), streptavidin-PerCPCy5.5 (all from BD Biosciences, San Jose, CA) and CD10-biotin (eBioCB-CALLA) (eBioscience, San Diego, CA). Data were acquired on a Canto II (BD Biosciences) and analyzed using FlowJo software (Treestar, Ashland, OR, USA).

Sequence analysis

DNA was isolated from peripheral blood mononuclear cells from patient and both parents using the GeneElute™ Mammalian Genomic DNA Miniprep Kit (Sigma Aldrich, St. Louis, MO, USA) according to the manufacturer's protocol. Sanger sequencing of known genes causative for SCID (*ADA, RAG1, RAG2, IL2RG, CD3D, CD3E, CD3G, and CD3Z/CD247*) was performed by PCR analysis (primers and amplification protocol are available upon request). The following primers were used for amplification and Sanger sequencing of the *VPS4B* gene: Forward 5'-ATCTGGGAGATTTGATTCAT-3', Reverse 5'-ATGAAAGACAGAAGTGTGTG-3'. Amplification was performed using the following protocol: 2 minutes 94°C, followed by 35 cycles of 94°C 15 seconds, 60°C 30 seconds, 72°C 2 minutes, followed by 10 minutes at 72°C. Products were separated on a 2% gel and fragments were isolated using the Zymoclean Gel DNA Recovery Kit (Zymo Research Corporation, Irvine, CA, USA) for Sanger sequencing.

Whole exome sequencing

Exome sequencing was performed at GATC BioTech (Constance, Germany) using Agilent SureSelect post-capture and enrichment protocols together with Illumina HiSeq 2500 platform. Reads were aligned using an in-house developed GNU Makefile-based pipeline ('Magpie', https://git.lumc.nl/rig-framework/magpie), based on the GATK 2.7 best practices[21]. Briefly, each FASTQ pair was processed using Sickle (version 1.33, https://github.com/najoshi/sickle) with default settings to trim low-quality bases. Remaining reads were mapped to the hg19 human genome sequence using Burrows-Wheeler Aligner (BWA)-MEM (version 0.7.5)[22]. The resulting alignment was then compressed using the Samtools (version 0.1.19) suite[23]. Duplicates were removed using Picard Mark Duplicates (https://broadinstitute.github.io/picard/) and data was subsequently processed through the GATK tools RealignTargetCreator, IndelRealigner, BaseRecalibrator, and PrintReads according to the GATK version 2.7 best practices and using the provided GATK 2.5 data bundle. The resulting alignment file was then used as input for the GATK variant callers HaplotypeCaller and UnifiedGenotyper, followed by variant recalibration. The generated VCF file was annotated using the Seattleseq web service (http://snp.gs.washington.edu/SeattleSeqAnnotation141/) and various other publically available databases (see results).

Results

Clinical presentation of the patient

The patient was a girl born at gestational age of 39 weeks and 5 days with a birth weight of 4120 g. Her parents were non-consanguineous and the pregnancy was without complications. At the age of 5 months she was admitted to the hospital for failure to thrive. An auto-immune thyroiditis with hypothyroidism was detected and levothyroxine treatment was initiated. Nine months later, at the age of one year and two months, she developed a severe bronchiolitis secondary to a bocavirus and adenovirus infection. Because of respiratory failure she was admitted to the intensive care unit and subsequently developed progressive respiratory failure during mechanical ventilation, for which she was treated with extra-corporal membrane oxygenation (ECMO) for 5 days. During ECMO two infusions of high dose methylprednisolon were given. Bronchoscopy showed trachomalacia of the right main bronchus. Immunological examination revealed a severe T-cell cytopenia (Fig. 1A), B-cell cytopenia (Fig. 1B) and a mild hypogammaglobulinemia (IgG: 2.5 g/L, IgA: 0.56 g/L, IgM: < 0.3 g/L). NK cell numbers were low at diagnosis but recovered quickly (Fig. 1C). Initially these abnormalities were thought to result from methylprednisolone treatment, but T-cell lymphopenia persisted, whereas B-cell and NK-cell lymphopenia recovered (Fig. 1A-C). At the time when B-cell numbers were spontaneously recovered, examination of the bone marrow showed no block in precursor B-cell development (Fig. 1D). Response to booster vaccination with tetanus, diphtheria and polio was normal, but no response could be detected to pneumococcal conjugate vaccine.
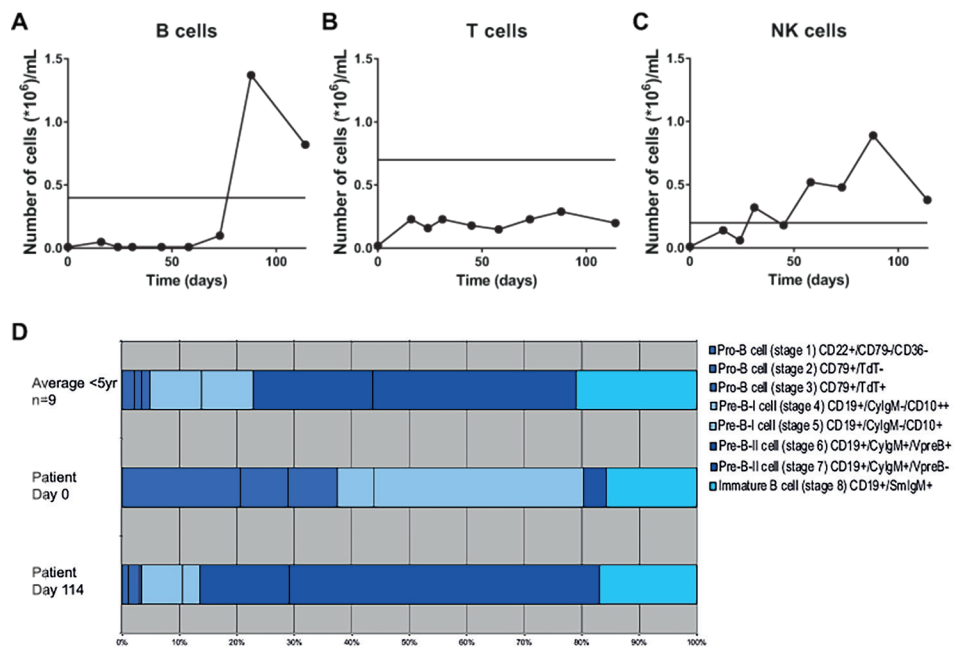
Figure 1: Lymphocyte characteristics in suspected SCID patient. A) B cell counts in peripheral blood of patient over time. **B)** T cell counts in peripheral blood of patient over time. **C)** NK cell counts in peripheral blood of patient over time. **A-C)** Horizontal lines indicate reference values. **D)** Developmental stages of B cell progenitors in BM of patient at two time points and of healthy controls.

Suspicion of SCID

Due to the persisting T-cell lymphopenia there was a suspicion of SCID and therefore genetic and metabolic analysis for ADA and PNP deficiency was initiated, but this showed no abnormalities. Also in the *RAG1* and *RAG2* genes no pathogenic mutations could be detected (data not shown). On karyotyping examination the patient was chromosomally 46,XY. External genital organs had a normal female appearance, except for partial fusion of the labia minora, and abdominal ultrasound revealed the presence of a uterus, but ovaries or testes could not be detected. Diagnostic SNP-array CGH analysis confirmed the chromosomal 46,XY and reported a heterozygous 450kb 4q23 micro-deletion (arr[hg18] ch4:108.60-109.05) of unknown clinical relevance. This variant was also present in her father and therefore presumed unlikely to be pathogenic. Subsequent *IL2RG* analysis was normal (data not shown).

Because of suspected SCID she was treated with (intravenous and later subcutaneous) intravenous immunoglobulin (IVIG) substitution, cotrimoxazol and valaciclovir prophylaxis. For the hypogonadism, treatment with sex hormones was given. Post ECMO she developed recurrent convulsions with multifocal epileptic activity and a delirium, for which she was treated with anti-epileptic drugs (levetiracetam) and haloperidol.

At the age of one year and seven months she underwent a HSCT from her HLA-identical brother. Post transplantation she developed a severe Coombs positive hemolytic anemia for which high dose IVIG, methylprednisolon, rituximab and erythrocyte transfusions were given. Because no donor chimerism was present a second HSCT with the same donor was performed, which resulted in 100% donor chimerism. Post HSCT, ongoing hemolysis was treated with bortezomib and adenovirus reactivation with cidofovir. Later, she developed a progressive severe neurological deterioration; no spontaneous motor activity or tendon reflexes could be detected, and responses to visually evoked potentials were absent. CSF examination revealed no abnormalities. Cerebral MRI showed generalized atrophy and leukoencephalopathy. Next, she developed a severe lower respiratory infection that was fatal. Post mortal examination of the brain showed severe encephalopathy and gliosis, without signs of inflammation or infection.

T-cell deficiency is caused by a cell intrinsic defect

Patient derived hematopoietic stem and progenitor cells (HSPCs) were isolated from a cryopreserved BM aspirate taken at the time when B-cell numbers had recovered. The HSPCs were transplanted in NSG mice to determine whether the immunological defects that were observed in the patient were caused by niche/stromal defects or by a hematopoietic cell intrinsic deficiency. Previously, we have used this approach to determine the arrests in T-cell development for different types of SCID that were caused by different known underlying genetic defects[19]. During follow-up of the mice transplanted with patient-derived HSPCs, there was outgrowth of both myeloid and B cells in peripheral blood, but T cells were not detected at any of the time points, whereas in mice transplanted with normal control HSPCs T cells were readily detected (Fig. 2A). In addition, at the end of the experiment, T cells were hardly detectable in mice transplanted with patient-derived HSPCs while they were present in UCB and BM transplanted control NSG mice (Fig. 2B, C). Taken together, the phenotype observed in mice transplanted with patient-derived HSPCs was consistent with a T⁻B⁺-SCID diagnosis.

Arrest in T-cell development at DP stage

As virtually no T cells could be detected in peripheral blood of both the patient and NSG mice transplanted with patient derived HSPCs, we examined T-cell developmental stages in thymi of transplanted NSG mice. Total thymocyte counts did not differ between mice transplanted with patient derived HSPCs or control HSPCs (Fig. 3A). We then analyzed the thymus of transplanted NSG mice for the presence of the different stages of T-cell development. The percentage of both mature $CD4^+$ single positive (SP) and $CD8^+$ SP was drastically decreased when patient derived HSPCs were transplanted (Fig. 3B, C). Furthermore the percentage of $CD3^+$ $CD4^+CD8^+$ double positive (DP) cells was lower while there was an increase in the percentage of $CD3^-$ DP cells. The level of both CD3 and TCRαβ expression was decreased in the total thymocyte population as compared to mice transplanted with UCB derived HSPCs (Fig. 3D). In addition, no $CD5^{hi}$ expressing cells could be detected (Fig. 3E), a molecule known to be upregulated upon TCR signaling[24]. From these phenotypic data, we could confirm that this patient suffered from SCID. Together these data point to an arrest in development that is most pronounced at the $CD3^+$ DP to SP transition while there might also be problems in TCR expression and signaling, as indicated by the increase in $CD3^-$ DP and decrease of $CD3^+$ DP (Fig. 3C).
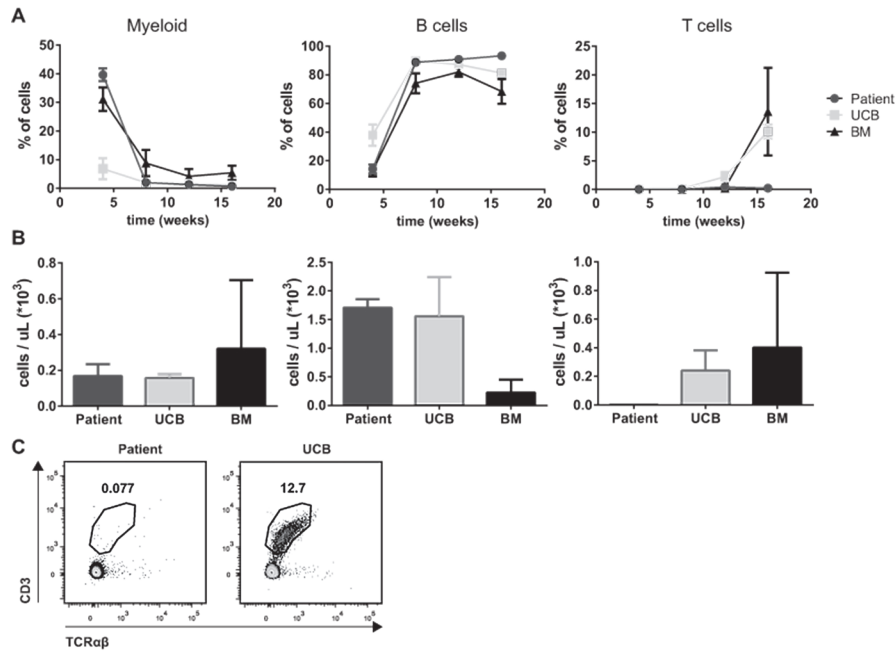
Figure 2: T-cell deficiency is caused by a hematopoietic cell intrinsic defect. A) Percentages of cells from different lineages in peripheral blood of NSG mice transplanted with HSPCs from patient or control UCB and BM. Percentages are within hCD45+ mononuclear cell fraction. **B)** Cell counts of cells from different lineages in peripheral blood of NSG mice at the end of the experiment. **C)** FACS plots showing CD3 and TCRαβ expression in peripheral blood of NSG mice at the end of the experiment. Cells were gated within hCD45+ mononuclear cell fraction.
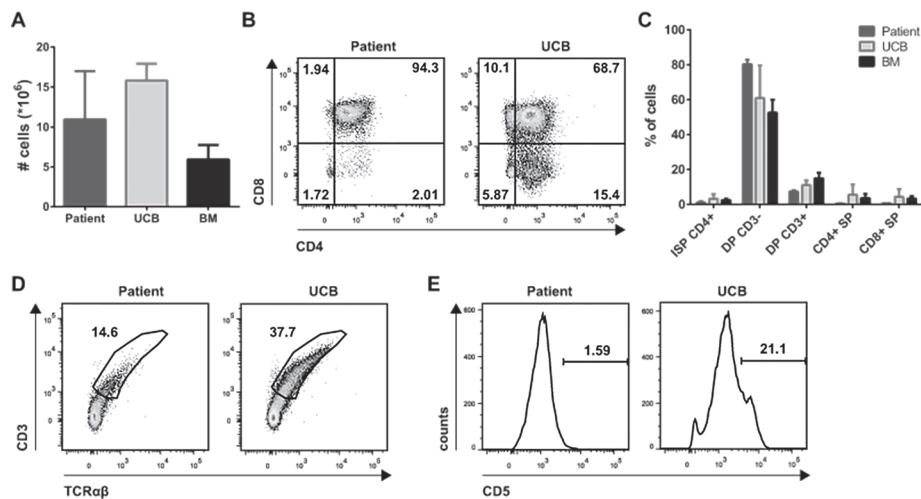

Figure 3: T-cell development is arrested at the transition from CD3+ DP to SP. A) Absolute cell numbers of total thymocytes. **B)** FACS plots depicting CD8 and CD4 expression on mononuclear hCD45+ thymocytes in thymi of transplanted NSG mice. **C)** Frequencies of cells from different T-cell developmental stages within hCD45+ cells in thymi of transplanted NSG mice. **D)** Expression of CD3 and TCRαβ within hCD45+ cells in thymi of transplanted NSG mice. **E)** Expression of CD5 within hCD45+ cells in thymi of transplanted NSG mice.

NK cells were present both in PB and BM (Fig. 4A, B) and no aberrancies were detected within the B-cell compartment in the BM of transplanted NSG mice (Fig. 4C), further supporting that this patient is a T-B+NK+-SCID.
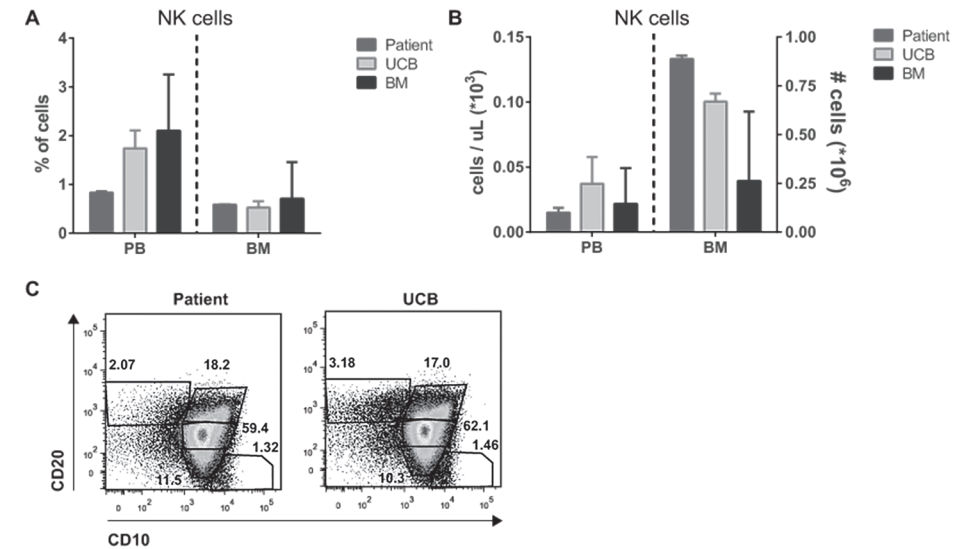
Figure 4: No aberrancies in NK cells and B cells in NSG mice transplanted with patient derived HSPCs. A) Percentages and **B)** numbers of NK cells (CD16/56+CD13/33-) in peripheral blood and bone marrow of NSG mice. Percentages are within hCD45+ mononuclear cell fraction. **C)** B-cell developmental stages characterized by expression of CD20 and CD10 in bone marrow of NSG mice. Fractions are within hCD45+CD19+ mononuclear cell fraction.

Causative genetic defect

Since the arrest in T-cell development was most profound at the DP stage, percentages of CD3 expressing cells were lower and CD5hi expressing thymocytes were absent, mutations in one of the genes encoding the CD3 complex were suspected. Previous analysis had demonstrated that no abnormalities were present in *ADA*, *PNP*, *RAG1*, *RAG2* or *IL2RG*. Therefore, we used Sanger sequencing to determine whether mutations were present in any of the genes encoding the different CD3 chains. No mutations were detected in *CD3D*, *CD3E*, *CD3G* or *CD247* (CD3Z) (data not shown). As other SCID genes had been excluded during diagnosis, exome sequencing was performed on DNA of the patient and both parents. Trio-analysis was performed using the Modular GATK Pipeline (Magpie), which is a variant-calling pipeline based on GATK best practice recommendations to analyze multiple samples simultaneously. More than 177 million raw reads were obtained. Almost 164 million reads (92.5%) were uniquely aligned to hg19 using Burrows-Wheeler Aligner (BWA). Median exome coverage was 61-fold both for the exome of the mother and the patient and 57-fold for the reads obtained from the father. In the patient, 381712 SNVs were identified (Fig. 5A). SNVs were called using both HaplotypeCaller and UnifiedGenotyper from the Genome Analysis Toolkit (GATK). High-quality non-synonymous variants in exons were filtered out and sequentially we only filtered for SNVs that were not

present in either dbSNP (v137) or in the 1000 Genomes Project, leaving 29 variants. Genes that have been previously associated with SCID were checked manually because these could have been filtered out in the previous steps. These genes were also checked for the presence of compound heterozygous mutations, which were not detected. None of these known SCID genes was affected in any of the methods used. Using the trio analysis of patient and both parents, we selected SNVs that were not present in one of the parents as they were both asymptomatic for *de novo* autosomal dominant (AD) modeling. For autosomal recessive (AR) modeling, we filtered SNVs that were homozygous in the patient and heterozygous in at least one parent. X-linked modeling was comparable to AR modeling except that the mother was heterozygous for the SNV and that the SNV was not present in the father. These filtering steps resulted in 13 SNVs (Fig. 5A). Autosomal dominant (AD) *de novo* modeling resulted in a total 3 SNVs, autosomal recessive (AR) in 9 SNVs and X-linked recessive inheritance pattern in 1 SNV. PolyPhen[25] and SIFT[26] databases were used to determine whether variations were predicted as benign and tolerated in which case we did not consider them as being causative of the phenotype observed in the patient. Hereafter, we were left with 1 *de novo* SNV with a possible AD inheritance pattern. This SNV is located in *VPS4B* (vacuolar protein sorting 4 homolog B, NM_004869.3, NP_004860.2) encoding a heterozygous G to A mutation (c.869G>A) resulting in a predicted amino acid change at position 290 from arginine to glutamine (p.Arg290Gln). The variant is located in the AAA-ATPase domain of the protein[27], which is needed for proper function of *VPS4B*. Validation by Sanger sequencing verified the heterozygous genotype of the patient for the mutation in *VPS4B* and the absence of the SNV in both parents (Fig. 5B).

A

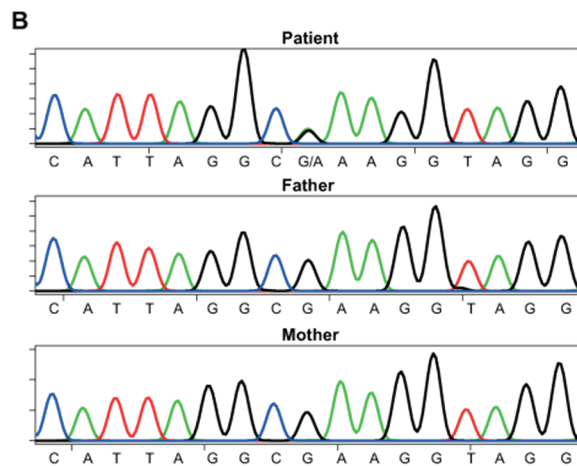| Exome Sequencing Data Filtering	
Aligned SNVs	381712
Nonsynonymous SNVs identified by 2 callers	88
SNVs not present in dbSNP or 100Genomes	29
SNVs not present in parents (AD modeling) or heterozygous (AR modeling)	13
Damaging SNVs (PolyPhen & SIFT)	1

B

Figure 5: Detection of a *de novo* mutation in *VPS4B*. A) Filtering of data derived from exome sequencing of DNA from the patient and both parents. **B)** Sanger sequencing results of *VPS4B* gene in patient and both parents. Top; patient, middle; father, bottom; mother. AD; autosomal dominant, AR; autosomal recessive.

Discussion

Up to now, more than 16 genes have been identified to be causative for SCID that give rise to different phenotypes based on absence and presence of B cells and NK cells besides the T-cell deficiency[2]. However, there remains a large fraction of patients with an unidentified underlying genetic defect and in addition still new SCID causing genes are being identified. Here, we describe a young patient with atypical presentation of SCID for who no mutation could be detected in genes known to be causative for SCID using standard Sanger sequencing protocols.

Previously, we have optimized the NSG humanized mouse model for efficient and robust engraftment of human BM derived HSPCs while maintaining multilineage differentiation and lymphocyte functionality[18]. In addition, we have used this model to determine the arrests in T-cell development for different types of SCID that were caused by a known underlying genetic defect. We also showed that the model faithfully recapitulates the arrests in B-cell development thereby validating this model for studies of human lymphoid development[19]. Here, we demonstrate the use of the NSG humanized mouse model for detection of SCID and determination of the stage of arrest in T-cell development. In addition, we confirmed that the patient with a suspected diagnosis of SCID indeed suffered from this disease with a T⁻B⁺NK⁺ phenotype. When the patient was admitted to the intensive care unit, there was a drop in number of B cells that recovered to normal levels. In line with this, no aberrancies in B-cell development were observed in NSG mice transplanted with patient-derived HSPCs. We demonstrated that solely the T-cell lineage was affected and the arrest in T-cell development was found at the DP to SP transition with an accumulation of CD3⁻ DP at the expense of CD3⁺ DP. Arrests in T-cell development can also be studied using cocultures of HSPCs on OP9-DL1 stromal cells as this model is used to study normal T-cell development *in vitro*[28, 29]. However, it remains difficult to reach the more mature stages, i.e. true DP stages and beyond, using these cultures. Therefore it would have been impossible to identify the late stage of arrest in human T-cell development that was identified here using the humanized mouse model.

A heterozygous microdeletion on chromosome 14 was found using a diagnostic SNP array CGH approach, however, this feature was also present in the father and therefore presumed unlikely to be pathogenic (data not shown). Therefore, we used whole exome sequencing to determine the causative defect using a trio analysis to exclude inherited polymorphisms, which were presumed unlikely to be causative. This approach has been proven successful in studies where they, for instance, identified a mutation in *CARD11* to be causative for SCID[17, 30, 31]. Here, we filtered the data obtained with whole exome sequencing by using 2 different SNV callers, exclusion of SNVs present in either dbSNP or the 1000 Genomes Project and prediction of the possible effect of the SNV by PolyPhen and SIFT prediction tools. Furthermore, we excluded SNVs that were present in the parents. This step is crucial to come to disease-causing SNVs, because the genetic heterogeneity as well as low incidence of SCID make it impossible to analyze large numbers of phenotypically identical patient samples. Furthermore, it allowed us to screen for the presence of compound heterozygous mutations in genes known

4

to be associated with SCID, which were not found. In addition, by reporting single patient studies, other patients suffering from SCID without a known genetic cause can be screened for identified mutations as was also done for Bartter syndrome[15]. The use of whole exome sequencing technology for the use of diagnosis in orphan diseases such as SCID remains challenging and time consuming due to single patient analyses caused by low prevalence, however, we demonstrate here that it is possible.

After filtering of the exome data, we have identified a *de novo* heterozygous missense mutation in *VPS4B* in the patient that most likely has caused the observed immunodeficiency. The heterozygous mutation leads to a change in amino acids from Arginine to Glutamine at codon 290 and was confirmed by Sanger sequencing. We hypothesize that this might translate into a dominant negative form of VPS4B (dnVPS4B) as multiple dnVPS4B sequence variants have indeed been described that interfered with the normal function of VPS4B protein[32, 33]. One described form of dnVPS4B has an amino acid change from the negatively charged glutamic acid to glutamine, which is uncharged and this mutation prevents binding of ATP[30]. The mutation described here leads to a change of the positively charged amino acid arginine to the uncharged glutamine. It is possible that this change leads to a disruption of the function of the AAA-ATPase domain similar to the described dnVPS4B mutant, which had a mutation in the same domain and acts as dominant negative molecule preventing VPS4 function. VPS4B binds to the Endosomal Sorting Complexes Required for Transport (ESCRT)-III complex that is involved in multivesicular endosome (MVE) biogenesis and the final steps of vesicle fission[34]. It has been described that VPS4B mediates scission of microvesicles that contain TCRs from the T-cell plasma membrane at the immunological synapse[32]. Furthermore, expression of a dnVPS4 disrupted the function of endogenous VPS4 resulting in an altered distribution of TCRs at the immunological synapse. In addition, we mined microarray data from sorted human thymus subsets[35] and it was observed that the expression of *VPS4B* increased in the SP stage of human T-cell development (Fig. 6). It is likely that the mutated *VPS4B* identified in the current study functions as a dominant negative mutant that interferes with endogenous VPS4B function, which is normally needed to progress to the SP stage of T-cell development. Moreover, thymocytes from mice that are double knockouts for *Stam1* and *Stam2*, components of the ESCRT-0 complex that initiates the endosomal sorting process[34], have a block in T-cell development at the SP stage and these mice demonstrated defective proliferative responses after TCR stimulation[36]. This demonstrates that processes in which ESCRT-complexes are involved, are needed for the transition from the CD3$^-$ DP to the CD3$^+$ DP and subsequent SP stage and most likely affect TCR signaling as also indicated by the observed decrease in CD5 expression.

The patient also suffered from neurological problems besides SCID, which are not possible to test in the humanized mouse model that was used in this study. However, it has been described that mutations in components of the ESCRT-III complex are involved in neurodegenerative diseases, such as amyotropic lateral sclerosis and frontotemporal dementia (reviewed in[34]). The involvement of the predicted p.Arg290Gln mutation in *VPS4B* in neuronal aberrancies could possibly be tested by generation of patient specific induced pluripotent stem cells

(iPSC) differentiated to the neuronal cell lineage[37]. The same approach could be used together with the CRISPR/Cas9 technology[38] for site-directed repair of the mutation to determine whether this alleviates the phenotype. Unfortunately, it is still a challenge to differentiate repaired iPS cells into HSPCs that can be used for transplantation purposes in e.g. humanized mouse models.
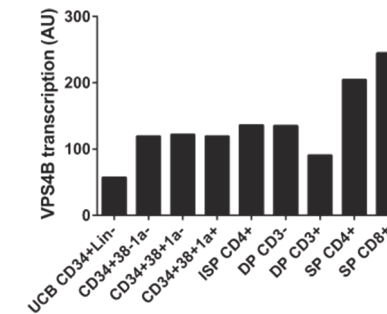
Figure 6: Expression of VPS4B in different stages of human T-cell development. Data was mined from microarray data of sorted populations from human thymus material[35].

To conclude, here we have identified a gene that potentially could be causative for T$^-$B$^+$NK$^+$-SCID. A *de novo* G to A mutation at position c.869 resulting in an amino acid substitution from the negatively charged arginine to the uncharged glutamine that could result in a dnVPS4B protein was identified by exome sequencing of the index patient and both parents. Functional experiments are needed to confirm whether the identified dominant negative mutant indeed leads to an arrest in T-cell development. Furthermore, the NSG humanized mouse model was demonstrated to be useful in the determination whether the patient indeed suffered from SCID. Due to the long duration of the transplantation experiment, this will not be useful to aid in diagnosis. However, by identification of *VPS4B* as a potential candidate gene for SCID and after confirmation by functional experiments, this could be included for screening of other patients suffering from SCID without a known genetic cause[39].

4

References

1. Al-Herz W, Bousfiha A, Casanova JL, Chapel H, Conley ME, Cunningham-Rundles C, *et al.* Primary immunodeficiency diseases: an update on the classification from the international union of immunological societies expert committee for primary immunodeficiency. *Frontiers in immunology* 2011, **2**: 54.

2. Bousfiha A, Jeddane L, Al-Herz W, Ailal F, Casanova JL, Chatila T, *et al.* The 2015 IUIS Phenotypic Classification for Primary Immunodeficiencies. *Journal of clinical immunology* 2015.

3. Buckley RH, Schiff RI, Schiff SE, Markert ML, Williams LW, Harville TO, *et al.* Human severe combined immunodeficiency: genetic, phenotypic, and functional diversity in one hundred eight infants. *The Journal of pediatrics* 1997, **130**(3): 378-387.

4. Yee A, De Ravin SS, Elliott E, Ziegler JB, Contributors to the Australian Paediatric Surveillance U. Severe combined immunodeficiency: a national surveillance study. *Pediatric allergy and immunology : official publication of the European Society of Pediatric Allergy and Immunology* 2008, **19**(4): 298-302.

5. Aiuti A, Cattaneo F, Galimberti S, Benninghoff U, Cassani B, Callegaro L, *et al.* Gene therapy for immunodeficiency due to adenosine deaminase deficiency. *The New England journal of medicine* 2009, **360**(5): 447-458.

6. Gaspar HB, Cooray S, Gilmour KC, Parsley KL, Zhang F, Adams S, *et al.* Hematopoietic stem cell gene therapy for adenosine deaminase-deficient severe combined immunodeficiency leads to long-term immunological recovery and metabolic correction. *Science translational medicine* 2011, **3**(97): 97ra80.

7. Gaspar HB, Parsley KL, Howe S, King D, Gilmour KC, Sinclair J, *et al.* Gene therapy of X-linked severe combined immunodeficiency by use of a pseudotyped gammaretroviral vector. *Lancet* 2004, **364**(9452): 2181-2187.

8. Hacein-Bey-Abina S, Le Deist F, Carlier F, Bouneaud C, Hue C, De Villartay JP, *et al.* Sustained correction of X-linked severe combined immunodeficiency by ex vivo gene therapy. *The New England journal of medicine* 2002, **346**(16): 1185-1193.

9. Hacein-Bey-Abina S, Pai SY, Gaspar HB, Armant M, Berry CC, Blanche S, *et al.* A modified gamma-retrovirus vector for X-linked severe combined immunodeficiency. *The New England journal of medicine* 2014, **371**(15): 1407-1417.

10. Gaspar HB, Qasim W, Davies EG, Rao K, Amrolia PJ, Veys P. How I treat severe combined immunodeficiency. *Blood* 2013, **122**(23): 3749-3758.

11. Alsmadi O, Al-Ghonaium A, Al-Muhsen S, Arnaout R, Al-Dhekri H, Al-Saud B, *et al.* Molecular analysis of T-B-NK+ severe combined immunodeficiency and Omenn syndrome cases in Saudi Arabia. *BMC medical genetics* 2009, **10**: 116.

12. Kwan A, Church JA, Cowan MJ, Agarwal R, Kapoor N, Kohn DB, *et al.* Newborn screening for severe combined immunodeficiency and T-cell lymphopenia in California: results of the first 2 years. *The Journal of allergy and clinical immunology* 2013, **132**(1): 140-150.

13. Pasic S, Vujic D, Veljkovic D, Slavkovic B, Mostarica-Stojkovic M, Minic P, *et al.* Severe combined immunodeficiency in Serbia and Montenegro between years 1986 and 2010: a single-center experience. *Journal of clinical immunology* 2014, **34**(3): 304-308.

14. Yu GP, Nadeau KC, Berk DR, de Saint Basile G, Lambert N, Knapnougel P, *et al.* Genotype, phenotype, and outcomes of nine patients with T-B+NK+ SCID. *Pediatric transplantation* 2011, **15**(7): 733-741.

15. Choi M, Scholl UI, Ji W, Liu T, Tikhonova IR, Zumbo P, *et al.* Genetic diagnosis by whole exome capture and massively parallel DNA sequencing. *Proceedings of the National Academy of Sciences of the United States of America* 2009, **106**(45): 19096-19101.

16. Ng SB, Buckingham KJ, Lee C, Bigham AW, Tabor HK, Dent KM, *et al.* Exome sequencing identifies the cause of a mendelian disorder. *Nature genetics* 2010, **42**(1): 30-35.

17. Greil J, Rausch T, Giese T, Bandapalli OR, Daniel V, Bekeredjian-Ding I, *et al.* Whole-exome sequencing links caspase recruitment domain 11 (CARD11) inactivation to severe combined immunodeficiency. *The Journal of allergy and clinical immunology* 2013, **131**(5): 1376-1383 e1373.

18. Wiekmeijer AS, Pike-Overzet K, Brugman MH, Salvatori DC, Egeler RM, Bredius RG, *et al.* Sustained Engraftment of Cryopreserved Human Bone Marrow CD34(+) Cells in Young Adult NSG Mice. *BioResearch open access* 2014, **3**(3): 110-116.

19. Wiekmeijer AS, Pike-Overzet K, H IJ, Brugman MH, Wolvers-Tettero IL, Lankester AC, *et al.* Identification of checkpoints in human T-cell development using severe combined immunodeficiency stem cells. *The Journal of allergy and clinical immunology* 2015.

20. Noordzij JG, de Bruin-Versteeg S, Verkaik NS, Vossen JM, de Groot R, Bernatowska E, *et al.* The immunophenotypic and immunogenotypic B-cell differentiation arrest in bone marrow of RAG-deficient SCID patients corresponds to residual recombination activities of mutated RAG proteins. *Blood* 2002, **100**(6): 2145-2152.

21. DePristo MA, Banks E, Poplin R, Garimella KV, Maguire JR, Hartl C, *et al.* A framework for variation discovery and genotyping using next-generation DNA sequencing data. *Nature genetics* 2011, **43**(5): 491-498.

22. Li H, Durbin R. Fast and accurate short read alignment with Burrows-Wheeler transform. *Bioinformatics* 2009, **25**(14): 1754-1760.

23. Li H, Handsaker B, Wysoker A, Fennell T, Ruan J, Homer N, *et al.* The Sequence Alignment/Map format and SAMtools. *Bioinformatics* 2009, **25**(16): 2078-2079.

24. Azzam HS, Grinberg A, Lui K, Shen H, Shores EW, Love PE. CD5 expression is developmentally regulated by T cell receptor (TCR) signals and TCR avidity. *The Journal of experimental medicine* 1998, **188**(12): 2301-2311.

25. Adzhubei IA, Schmidt S, Peshkin L, Ramensky VE, Gerasimova A, Bork P, *et al.* A method and server for predicting damaging missense mutations. *Nature methods* 2010, **7**(4): 248-249.

26. Kumar P, Henikoff S, Ng PC. Predicting the effects of coding non-synonymous variants on protein function using the SIFT algorithm. *Nature protocols* 2009, **4**(7): 1073-1081.

27. Takasu H, Jee JG, Ohno A, Goda N, Fujiwara K, Tochio H, *et al.* Structural characterization of the MIT domain from human Vps4b. *Biochemical and biophysical research communications* 2005, **334**(2): 460-465.

28. De Smedt M, Leclercq G, Vandekerckhove B, Kerre T, Taghon T, Plum J. T-lymphoid differentiation potential measured in vitro is higher in CD34+CD38-/lo hematopoietic stem cells from umbilical cord blood than from bone marrow and is an intrinsic property of the cells. *Haematologica* 2011, **96**(5): 646-654.

29. La Motte-Mohs RN, Herer E, Zuniga-Pflucker JC. Induction of T-cell development from human cord blood hematopoietic stem cells by Delta-like 1 in vitro. *Blood* 2005, **105**(4): 1431-1439.

4

30. Bernth-Jensen JM, Holm M, Christiansen M. Neonatal-onset TBNK severe combined immunodeficiency and neutropenia caused by mutated phosphoglucomutase 3. *The Journal of allergy and clinical immunology* 2015.

31. Frugoni F, Dobbs K, Felgentreff K, Aldhekri H, Al Saud BK, Arnaout R, *et al.* A novel mutation in the POLE2 gene causing combined immunodeficiency. *The Journal of allergy and clinical immunology* 2015.

32. Choudhuri K, Llodra J, Roth EW, Tsai J, Gordo S, Wucherpfennig KW, *et al.* Polarized release of T-cell-receptor-enriched microvesicles at the immunological synapse. *Nature* 2014, **507**(7490)**:** 118-123.

33. Garrus JE, von Schwedler UK, Pornillos OW, Morham SG, Zavitz KH, Wang HE, *et al.* Tsg101 and the vacuolar protein sorting pathway are essential for HIV-1 budding. *Cell* 2001, **107**(1)**:** 55-65.

34. Rusten TE, Vaccari T, Stenmark H. Shaping development with ESCRTs. *Nature cell biology* 2012, **14**(1)**:** 38-45.

35. Dik WA, Pike-Overzet K, Weerkamp F, de Ridder D, de Haas EF, Baert MR, *et al.* New insights on human T cell development by quantitative T cell receptor gene rearrangement studies and gene expression profiling. *The Journal of experimental medicine* 2005, **201**(11)**:** 1715-1723.

36. Yamada M, Ishii N, Asao H, Murata K, Kanazawa C, Sasaki H, *et al.* Signal-transducing adaptor molecules STAM1 and STAM2 are required for T-cell development and survival. *Molecular and cellular biology* 2002, **22**(24)**:** 8648-8658.

37. Chamberlain SJ, Li XJ, Lalande M. Induced pluripotent stem (iPS) cells as in vitro models of human neurogenetic disorders. *Neurogenetics* 2008, **9**(4)**:** 227-235.

38. Jinek M, Chylinski K, Fonfara I, Hauer M, Doudna JA, Charpentier E. A programmable dual-RNA-guided DNA endonuclease in adaptive bacterial immunity. *Science* 2012, **337**(6096)**:** 816-821.

39. Casanova JL, Conley ME, Seligman SJ, Abel L, Notarangelo LD. Guidelines for genetic studies in single patients: lessons from primary immunodeficiencies. *The Journal of experimental medicine* 2014, **211**(11)**:** 2137-2149.

4

Chapter 5

Development of a diverse human T cell repertoire despite severe restriction of hematopoietic clonality in the thymus

Martijn H. Brugman[1], Anna-Sophia Wiekmeijer[1], Marja C.J.A van Eggermond[1], Ingrid L.M. Wolvers-Tettero[2], Anton W. Langerak[2], Edwin F.E. de Haas[1], Leonid V. Bystrykh[3], Jon J. van Rood[1], Gerald de Haan[3], Willem E. Fibbe[1], Frank J.T. Staal[1].

[1]Leiden University Medical Center, Department of Immunohematology and Blood Transfusion, Leiden

[2]Erasmus University Medical Center, Department of Immunology, Rotterdam

[3]European Research Institute for the Biology of Ageing, University of Groningen, University Medical Centre Groningen, Laboratory of Ageing Biology and Stem Cells, Groningen.

Abstract

The fate and numbers of hematopoietic stem cells (HSC) and their progeny that seed the thymus constitute a fundamental question with important clinical implications. HSC transplantation is often complicated by limited T-cell reconstitution, especially when HSC from umbilical cord blood are used. Attempts to improve immune reconstitution have until now been unsuccessful, underscoring the need for better insight into thymic reconstitution. Here we made use of the NOD-SCID-IL2Rgamma^{-/-} (NSG) xenograft model and lentiviral cellular barcoding of human HSCs to study T-cell development in the thymus at a clonal level. Barcoded HSCs showed robust (>80% human chimerism) and reproducible myeloid and lymphoid engraftment, with T cells arising 12 weeks after transplantation. A very limited number of HSC clones (<10) repopulated the xenografted thymus, with further restriction of the number of clones during subsequent development. Nevertheless, T-cell receptor rearrangements were polyclonal and showed a diverse repertoire, demonstrating that a multitude of T-lymphocyte clones can develop from a single HSC clone. Our data imply that intra-thymic clonal fitness is important during T-cell development. As a consequence, immune incompetence after HSCT is not related to the transplantation of limited numbers of HSC but to intrathymic events.

Significance statement

The number of hematopoietic stem cell clones contributing to T-cell development is restricted at entry of and during further development inside the thymus. However, despite this severe restriction, a fully diverse T-cell receptor (TCR) repertoire can be generated, indicating that haematological and immunological clonality are independently regulated.

Introduction

Hematopoietic stem cell transplantation (HSCT) has become common clinical practice in the treatment of leukemia, lymphoma and certain inherited immune and metabolic disorders. After transplantation there is an immediate need for *de novo* production of granulocytes, erythrocytes and platelets referred to as hematopoietic reconstitution, later followed by recovery of lymphocyte numbers termed immune reconstitution. While often successful, HSCT is associated with a number of complications arising from poor immune reconstitution, which presents one of the most important causes of morbidity after HSCT[1, 2]. Poor myeloid reconstitution is directly linked to low numbers of HSCs in the transplant, the reasons for poor immune and in particular, T-lymphocyte reconstitution are much less clear.

A study on the application of anti-thymocyte globulin (ATG) in cord blood transplantation showed that ATG administration in pre-transplantation conditioning results in decreased T-cell reconstitution and survival[3], indicating the need for a better understanding of de novo T-cell development after HSCT. As T cells develop in the thymus in contrast to all other blood lineages that develop in the BM, HSC-derived progenitors need to seed the thymus. Earlier work in mice has indicated that relatively few progenitors seed the thymus[4, 5] yet their numbers and the subsequent fate of the progeny derived from a HSC clone has remained elusive. The nature of the thymus seeding cell has been subject of much debate, certainly in humans. CD34+CD38- CD7+ cells[6, 7], CD34+CD38-CD10-CD62L+ cells[8] and others have been proposed as thymus seeding cells in the human situation. In contrast to mice, the earliest human thymocytes show a much broader lineage developmental potential, including low levels of erythroid and megakaryocytic potential[9], and may be therefore be much closer related to HSCs or the proposed myeloid lymphoid precursors (MLP).

In this study, we aimed to address the functional relationship between HSCs and developing T cells by using DNA barcoding. This method allows marking of each stem cells and its progeny by a unique, neutral DNA sequence that can be retrieved by next generation sequencing. Here we used replication deficient lentiviruses to transfer a DNA barcode and the GFP green fluorescent protein into phenotypically defined human HSCs. These marked HSCs were transplanted, using an optimized protocol[10], into NOD/SCID/Il2rgamma^{-/-} (NSG) mice[11] which allowed us to determine the dynamics of clonal reconstitution in the thymus in great detail. We used umbilical cord blood (UCB) as source of human stem cells, because UCB is frequently used as readily available HSC source with less stringent HLA-matching requirements[12]. Yet, T-cell immune reconstitution, a general problem in allogeneic HSCT, is more problematic in UCB. Therefore UCB provides an appropriate HSC source to address questions of lineage tracing and clonality in the blood and immune system. As we demonstrate here only a fraction of HSC clones in UCB contributes to the T cell pool, yet a fully diverse TCR repertoire can be generated in the thymus.

5

Materials and methods

CD34+ and HSC isolations from UCB

Human CD34+ cells were isolated from umbilical cord blood (UCB) samples. Mononuclear cells of UCB were isolated by Ficoll (LUMC apothecary) density centrifugation, washed and stored in liquid nitrogen until further use. Single UCB units (HSC transplantation) or five to ten combined UCB units (CD34+ transplantations) were selected, thawed and selected for CD34+ progenitors using the CD34 Microbead Kit (Miltenyi Biotec GmbH, Bergisch Gladbach, Germany) according to the manufacturers protocol. Purity of the CD34 selection was verified by flowcytometry and exceeded 95% purity. HSCs were isolated by staining with anti-human CD38 (HIT2) PECy7, CD90 (ebio5e10) APC, CD49f (ebioG0H3) PerCP-efluor710 (all eBioscience, San Diego, CA, USA), CD34 (8G12) PE, CD45 (HI30) V450, CD45RA (L48) FITC (BD, Franklin Lakes, NJ, USA) and subsequent sorting of CD34+CD38-CD45RA-CD90+CD49f+ cells using a BD Aria II SORP cell sorter (Beckton-Dickinson). The cells were subsequently cultured in Stemspan (Stem Cell Technologies), in the presence of 10 ng/ml stem cell factor (SCF, a gift from Amgen, Thousand Oakes, CS, USA), 20 ng/ml recombinant human thrombopoietin (rhTHPO, R&D systems, Abington, UK), 20 ng/mL recombinant mouse insulin-like growth factor 2 (rmIGF-2, R&D systems, Abington, UK) and 10 ng/ml recombinant human fibroblast growth factor 1 (rhFGF1, Peprotech GmbH, Hamburg, Germany) and penicillin/streptomycin (Lonza, Basel, Switzerland) on retronectin coated plates (Takara, Otsu, Japan). The cells were incubated for 24 hr at 37°C and 5% CO_2 .

Virus production and transduction procedure

Lentiviral vector pTGZ is derivative of pGIPZ (Thermo, Openbiosystems, USA) where Puromycin-IRES-MCS site locus (BsrGI-MluI) was replaced first by BsrGI-ClaI-BamHI-MluI adapter, then a barcode linker was integrated via BsrGI-BamHI sites between tGFP and the WPRE element as described[13, 14]. The barcode sequence, named B322, was as follows: AGGNNNACNNNGTNNNCGNNNTANNNCANNNTGNNNGAC. Viral particles were generated in 293T cells by transfection of pEnv VSVG, pMD2 GagPol, pREV and the barcoded vector backbone pTGZ-B322. Titers were determined on isolated CD34+ cells to achieve a transduction efficiency of 20% in order to minimize the occurrence of multiple virus integrations per cell, while maintaining a reasonably high marking rate. UCB CD34+ cells were cultured as decribed above at 6500 cells/cm² density. After 24 hr, the cells were spinoculated with virus supernatant at MOI = 1, after which the supernatant was replaced with fresh Stemspan medium with cytokines. The cells were kept for 16 hr at 37°C and 5% CO_2 and then prepared for transplantation. Because lentiviral vectors cause pseudo-transduction (protein expression from the pre-integration complex, PIC) assessment of the transduction rate at the moment of transplantation is not accurate. Instead, a fraction of transduced cells was kept in culture for an additional week until the non-integrated PICs were diluted out and the transduction rate could be determined by flow cytometry.

Animals and transplantation

NSG mice (NOD.Cg-Prkdc[scid] Il2rg[tmWjl]/SzJ, NSG) were obtained from Charles River Laboratories (UK) and bred in individually ventilated cages (IVC) under specific-pathogen free (SPF) conditions. Mice (aged 5-6 weeks) were sublethally irradiated with 1.91 Gy X-rays using orthovoltage irradiation and transplanted 24 hour after irradiation via tail vein injection with the indicated cell numbers. Mice were fed Diet Gel recovery (Clear H_2O, Portland, MA, USA) and kept on antibiotics (560µg/l polymixin B (Bupha, Uitgeest, Netherlands), 700 µg/l ciprofloxacin (Bayer, Mijdrecht, Netherlands) , 800 µg/l amphoteracin B (Bristol-Myers Squibb, Woerden, Netherlands) in autoclaved acidified drinking water until white blood cells counts were recovered at 4 weeks post-transplant. Blood samples were obtained at 4, 8, 12, 16 and 21 weeks by lateral tail vein incision. At 16 or 21 weeks, mice were killed by O_2/CO_2 inhalation and thymus, BM, PB, and spleen were isolated. BM cell suspensions were made by crushing the bones in IMDM (Lonza) and passing the remaining cells through a 70µm filter. Spleen and thymus were homogenized by passing them through a 70 µm filter.

Flowcytometry

Erythrocytes in the PB samples were lysed using an isotonic NH_4Cl buffer (LUMC apothecary), after which the cells were stained with the indicated antibodies in phosphate buffered saline (PBS)/0.2% bovine serum albumin/0.1% sodium azide buffer for 30 minutes on ice. Cells were subsequently sorted using a FACS Aria II SORP (BD)

Spleen and PB cells were stained using anti-human CD45 (HI30) V450, CD19 (SJ25C1) APCCy7, CD3 (SK7) PE, CD4 (RPA-T4) V500, CD8 (SK1) PECy7, CD13 (WM15) APC and CD33 (WM53) APC (all BD). PB cells were sorted into T cells (huCD45+CD3+) B cells (huCD45+CD19+) and myeloid cells (huCD45+CD13/CD33+) and splenocytes into B cell (huCD45+CD19+) and T cell (huCD45+CD3+) populations. Bone marrow cells were stained using anti-human CD45 (HI30) V450, CD34 (8G12) PE, (all BD), CD38 (HIT2) PECy7, CD90 (ebio5e10) APC and CD49f (ebioG0H3) PerCP-efluor710 (all eBioscience). HSC (huCD45+CD34+CD38-CD90+CD49f+) were sorted. Thymus cells were stained using human CD45 (HI30) V450, CD1a (HI149) APC, CD34 (8G12) PE, CD3e (UCHT1) PECy5, CD4 (RPA-T4) APCCy7 and CD8 (SK1) PECy7 (all BD) after which DN1/2 (huCD45+CD3-CD34+CD1a-) and DN3 (huCD45+CD3-CD34+CD1a+), DP (huCD45+CD3+CD4+CD8+) and SP (huCD45+CD3+CD4+ and huCD45+CD3+CD8+) were sorted.

Spike-in experiment

Plasmid DNA with a known barcode was mixed with DNA from polyclonally transduced population of cells at 0, 1, 3, 10, 30 and 100% based on the estimation that one virus was inserted per genome (3.3 x 10⁹ bp). The size of the plasmid was 10201 bp and carried one DNA barcode. The samples were then processed for barcode determination as described below.

DNA preparation and deep sequencing

DNA from the sorted populations was extracted using Sigma GenElute columns (Sigma-Aldrich, Zwijndrecht, The Netherlands), according to the manufacturer's instructions with the addition of 5µg herring sperm DNA as carrier material. The DNA barcode was amplified using LWGFP_pTGZ (CACATGCACTTCAAGAGCGCCAT) and LWPRE_pTGZ (TGAAAGCCATACGGGAAGCA) primers (Sigma-Aldrich), at 0.6 µM, using GoTaq polymerase (Promega) and a temperature profile of 95°C for 5 min, followed by 35 cycles of 95°C for 30 s, 60° for 30 s and 72°C for 30s, with a final extension of product at 72°C for 10 min. The 379 bp resulting product was cleaned using Qiagen PCR cleanup columns according to the manufacturer's instructions (Qiagen, Hilden,

Germany). The cleaned products were then multiplexed by adding an Iontorrent adapter with sample multiplexing barcodes to one side CCATCTCATCCCTGCGTGTCTCCGACTCAG[8 base multiplexing barcode] GCAGATGCCGGTGAAGAATAATGTAC and a common IonTorrent adapter CCTCTCTATGGGCAGTCGGTGATAGTCAATCTTTCACAAATTTTGTA to the other side (95°C for 5 min, followed by 35 cycles of 95°C for 30 s, 60° for 30 s and 72°C for 30s). The resulting 208 bp amplicons were separated on a 2% agarose gel, the products were excised and cleaned using Qiagen gel extraction columns, mixed in equimolar amounts and submitted to the LUMC sequencing core facility (LGTC) where library concentration was determined using a High Sensitivity DNA kit on an Agilent Bioanalyzer (Agilent, Santa Clara, CA, USA). The library was amplified using emulsion PCR using the Ion PGM Template OT2 200 kit (Agilent) and subsequently sequenced using the Ion PGM Sequencing 200 Kit v2 (Agilent) and 314 or 316 chips according to the manufacturer's instructions.

Sequence analysis
FASTQ files were retrieved from the sequencer and underwent overall quality control using FASTQC (Simon Andrews, Babraham Institute,Cambridge, UK available at (http://www. bioinformatics.babraham.ac.uk/projects/fastqc/), after which the sequences were separated by sample multiplexing barcode using a custom BioPerl script(http://www.bioperl.org) that uses regular expressions to determine primer and sample barcode sequences. From the resulting FASTA files, the DNA barcodes were extracted using a custom BioPerl script that determined barcode location based on a regular expression matching the surrounding virus sequences and the invariable doublets within the DNA barcode. Samples with >100 associated reads were considered for analysis. These barcodes were clustered using R (R-3.0.0, www.r-project.org) by calculating dissimilarity between all barcodes for all samples of an animal. Read numbers for barcodes with dissimilarity of less than 2 nt were clustered and added together, thereby correcting for sequencing errors[46]. Simulation of random sets of 485 barcodes showed that the frequency of 1-2 nt distances would occur in less than 1/1000 reads, therefore a dissimilarity threshold of 2 nt seems appropriate to eliminate false barcode reads in sequencing results, caused by PCR and sequencing errors. By applying this strategy to the sequenced library pool this resulted in a set of barcodes that agreed with the expected size of our DNA barcode library (485 barcodes by sequencing with noise removal, compared to the 500 single bacterial clones that were selected for the preparation of the vector library). The contribution of each clone to a particular tissue was normalized by dividing the reads for each clustered clone by the total number of reads per sample. The resulting fraction of contribution was then displayed.

TCR analysis
Rearrangements of *TRB*, *TRG*, and *TRD* loci were analyzed by means of BIOMED-2 multiplex PCR assays[47] and visualized via GeneScan analysis. All assays were performed using the proper clonal, polyclonal and negative controls, and according to the published BIOMED-2 multiplex PCR protocol.

Statistics
To describe the population diversity in the thymus, we calculated the Shannon diversity index using the cell number isolated from a tissue (HSC or thymus DN1/2, DN3, DP and SP or spleen CD3 cells) multiplied by the fraction of each clone as determined by barcode sequencing (shown in Fig. 3A) for all reads making up more than 1% of the reads recovered in these tissues. The Shannon indices obtained in this way were then normalized per animal to allow comparison between animals. Differences in Shannon diversity between subsets were analyzed using a Wilcoxon rank sum test, considering p<0.05 significant.

Study approval
Experimental procedures were approved by the Ethical Committee on Animal Experiments of the Leiden University Medical Center (Leiden, The Netherlands). The umbilical cord blood samples used in this study were collected at the Diakonessenhuis Hospital, Leiden after informed consent was given by the parents. Peripheral blood control samples were obtained with informed consent under guidelines issued by the Medical Ethics Committee of the Leiden University Medical Center.

Results

We set out to better understand the functional relationship between HSCs in the bone marrow and developing T cells in the thymus. Cellular barcoding allows this question to be addressed in a quantitative sense. To do so, human HSC were isolated from umbilical cord blood and were transduced with a lentiviral DNA barcoding vector that carried 485 individual barcodes[13, 14] (Fig. 1A). We aimed to transduce <20% of the target cells to limit the occurrence of multiple lentiviral insertions per cell. A well-defined library with restricted complexity was used to allow full quantification yet also to contain enough diversity to individually track HSC given the number of transduced HSCs per mouse. In three independent experiments, a total of 17 mice were transplanted with either low (26,000; n=4) or high dose (150,000; n=4) of CD34+ cells or ~1000 highly purified HSCs (n=9), defined as $CD34^+CD38^-CD45RA^-CD90^+CD49f^+$ [15].

To ensure that viral DNA barcoding methodology allows quantification of marked clones, calibration experiments were performed. The mixtures of DNA barcodes resulting from the spike-in experiments demonstrate a decrease of the sample from the 100% down to the 1% spike-in sample (Supplementary Fig. 1A). Linear regression analysis showed a Pearson correlation coefficient R^2=0.994 (Supplementary Fig. 1B). In a separate experiment, nine repeat measurements of the polyclonally transduced samples were analyzed for reproducibility. Read fractions below 0.5% of the sample threshold were progressively more difficult to quantify reliably as demonstrated by the increase in coefficient of variation at lower fractions of reads (Supplementary Fig. 1C). Deep sequencing is prone to generate sequence misreads at low frequency, and because our analysis is dependent on the ability to assign and distinguish individual barcodes, we compared all identified DNA barcodes against each other and determined their dissimilarity. We considered barcodes with up to 2 dissimilar bases to originate from the same original barcode (Supplementary Fig. 1D). Repeated measurements on CD19+ cells isolated from PB (Supplementary Fig. 1E) also demonstrated that the method results in limited variation between samples. Thus, the applied barcoding strategy can reliably quantify progeny of individual HSC clones in this setting.

5

Transplantation of human HSC from umbilical cord blood resulted in a robust reconstitution (median 81%, range 53-92% at 16 weeks, Fig. 1B) in all 9 mice. Green fluorescent protein (GFP) marking was initially around 20% and stabilized at 16 weeks at median 8.9% (range 4.5-20%, Fig. 1C), consistent with the intended low transduction rate, which limits the occurrence of multiple integrations per cell. After 12 weeks, CD3⁺ T cells were detectable for the first time (Fig. 1D), which coincides with a concomitant reduction in the percentages CD19⁺ B cells (Fig. 1F), which form the majority of repopulating human cells.
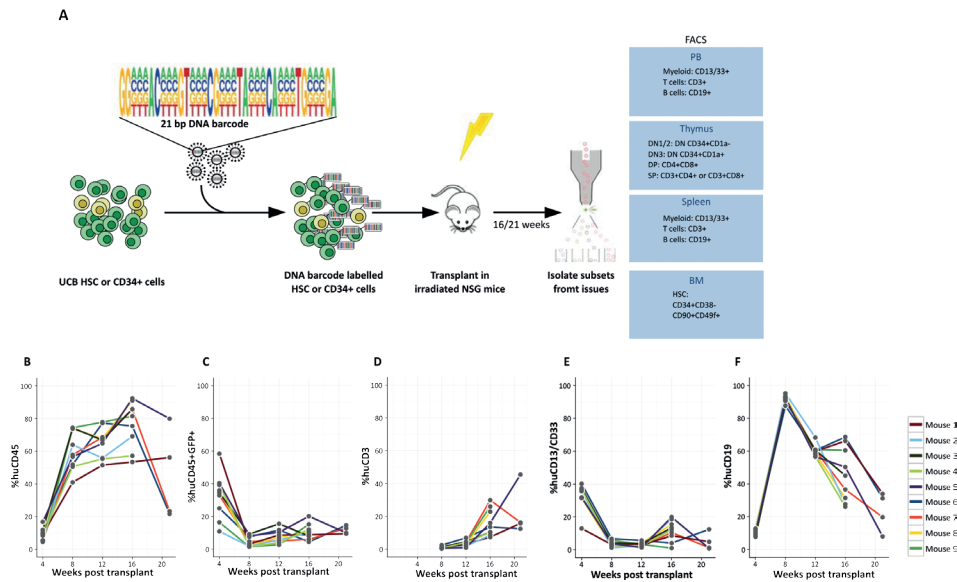

Figure 1: Barcoding human HSC and xenotransplantation. A) Human HSC (CD34⁺CD38⁻CD45RA⁻CD90⁺CD49f⁺) or CD34⁺ cells were isolated and transduced with the PTGZ barcode library carrying 21 variable bases in the barcode with a total complexity of 485 different barcodes. The transduced cells were transplanted in to 5-6 week old sublethally irradiated NSG mice. The mice were bled monthly and myeloid cells, T cells and B cells were isolated from PB. At 16 or 21 weeks, the experiment was terminated and, in addition to PB, cells isolated from thymus, spleen and bone marrow were sorted as indicated and the barcode content of the samples was analyzed. From the thymus, double negative (DN), double positive (DP), and single positive (SP) cells were isolated using the indicated markers. **B)** Chimerism in PB of 9 mice transplanted with 1000 purified human HSCs as determined by human CD45 expression, **C)** GFP marking of human cells. **D)** Development of CD3⁺ T cells, **E)** CD13/CD33⁺ myeloid cells and F) CD19⁺ B cells within the human CD45⁺ population were followed in time after transplantation of the transduced cells.

Analysis of the barcodes present during repopulation demonstrated that a limited repertoire of hematopoietic clones was responsible for the generation of myeloid cells, B cells and T cells. We detected a median number of 70 clones (range 51-88) per mouse in the peripheral blood, rising to a median of 83 (range 57-107) when bone marrow and thymus samples with different barcodes were included. Because the barcodes in purified HSCs are inherited by the daughter cells, we could also investigate the contribution of the marked clones in HSC to the B- and T-cell lineage. We therefore analyzed the extent to which a clone retrieved from the human

HSC isolated from the NSG mice was also detected in CD19⁺ B cells or CD3⁺ T cells in the spleen. The ternary plots (Fig. 2 and Supplementary Fig. 4) showed that a considerable fraction of single clones was shown to be present in two or three of these three cell types, demonstrating contribution to sorted HSC as well as the adaptive lymphoid lineage. This confirms that true HSCs with multi lineage differentiation capacity were marked by lentiviral barcoding. The existence of myeloid, lymphoid or mixed progenitors is in line with previous reports in mice[16] and human cells in the NSG xenograft model[17]. However, none of these studies specifically addressed the thymus or T-cell reconstitution.
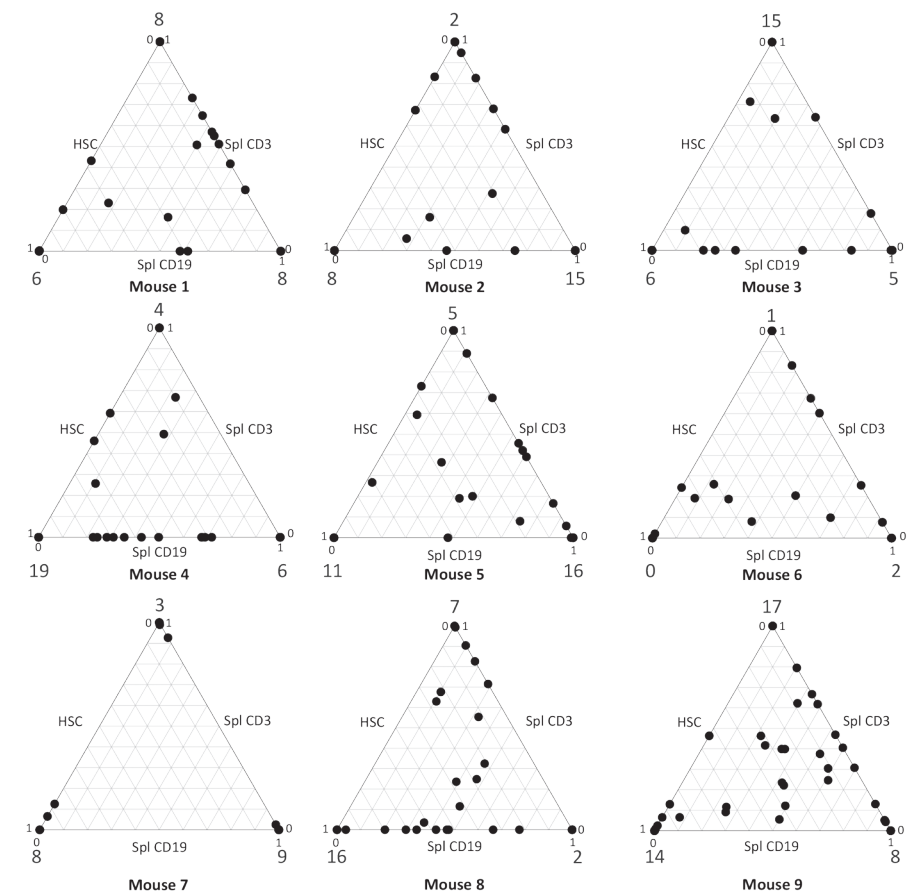
Figure 2: Clonal contribution to HSC and adaptive immune cells. Multilineage engraftment is demonstrated by contribution of barcoded clones to HSC, splenic CD3⁺ T cells and CD19⁺ B cells in 9 NSG mice that were transplanted with purified barcoded human HSCs are shown. The barcode content of these compartments was determined by comparing the normalized contribution of clones. The relative contributions to the total human HSC (BM) and T- and B-lymphoid lineages (spleen) in each mouse are shown as a ternary plot. Each point represents the contribution of a clone to HSC, CD19⁺ B cell and CD3⁺ T cell lineages. The extent of contribution is depicted by the location of the point along the three axes with clones contributing equally to all lineages being closer to the center of the triangle. In most mice, but especially in mouse 8 and 9 true multilineage contribution of HSC clones can be observed. The numbers at the points of the triangle indicate the number of detected clones for which contribution to only one lineage was detected.
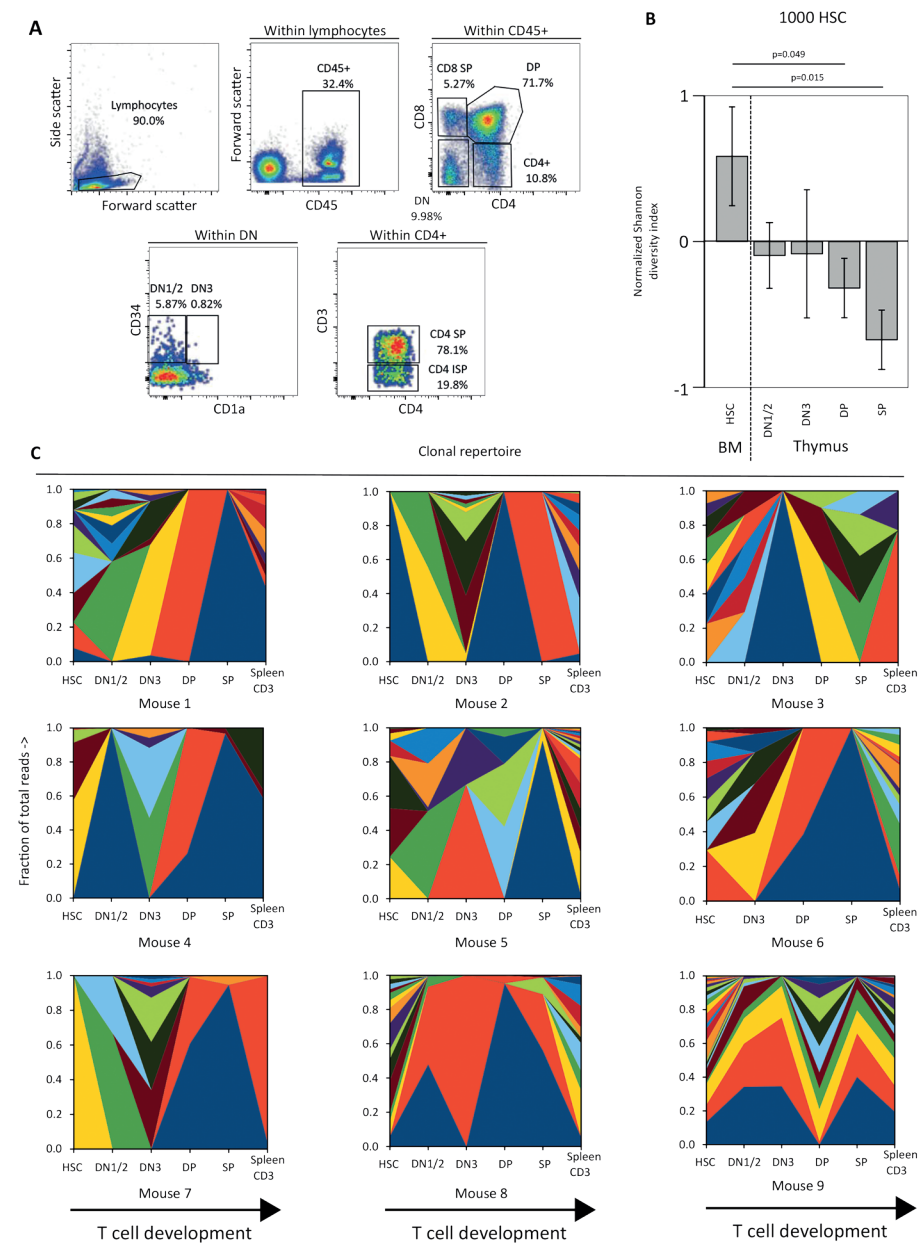
Figure 3: Clonal restriction during T cell development. A) Thymus was homogenized and cells were sorted into their developmental stages (DN1/2, DN3, DP, SP). **B)** The number of clones contributing >1% of the sample in 9 mice transplanted with barcoded HSCs or CD34+ cells were counted, and the Shannon diversity index calculated. The normalized Shannon diversity was compared between HSC in the BM and the developmental stages in the thymus. Mean normalized Shannon diversity indices for 9 mice transplanted with 1000 HSC are shown with error bars indicating SEM. Wilcoxon p-values are shown in B. **C)** Clonal repertoire, as determined by barcode analysis of sorted population in the thymus in stacked area graphs, with colors identifying the individual clones. Note that the colors are chosen for the purpose of display, which means that the same color depicts different clones in different mice.

To study thymic repopulation, various stages of human T-cell development, ranging from early double negative (DN, CD4$^-$CD8$^-$) cells to double positive (CD4$^+$CD8$^+$) and single positive mature cells (CD4$^+$ or CD8$^+$) were isolated from the thymus as described (DN1/2: CD3$^-$CD4$^-$CD8$^-$CD34$^+$CD1a$^-$, DN3: CD3$^-$CD4$^-$CD8$^-$CD34$^+$CD1a$^+$, DP: CD4$^+$CD8$^+$, SP, CD3$^+$CD8$^+$ or CD3$^+$CD4$^+$, Fig. 3A)[18]. During differentiation from polyclonal HSC to mature CD3$^+$ T cells a dramatic clonal skewing was seen in the form of reduction of the number of clones contributing more than 1% of the thymic populations. We employed the Shannon diversity index, a measure that can be used to describe biological diversity[19], to capture the frequency and abundance of barcoded clones. Using this parameter, the HSC (Fig. 3B) and high dose CD34$^+$ (Supplementary Fig. 2A, C) experiments show high diversity in BM but much lower in thymus, with clear clonal restriction at DN1/2 and subsequently a further restriction at the DN3 and DP stages. The reconstitution with the 26,000 CD34$^+$ cell dose containing lower numbers of true HSCs led to lower diversity in the BM, but still only one clone dominates at the thymic SP or DP stage (Supplementary Fig. 2B, D). Analysis of the DN3, DP and SP compartments indicated a further reduction in the number of hematopoietic clones (Fig. 3B and Supplementary Fig. 2A), while the numbers of isolated cells actually increase going from DN1/2 through DN3 to DP, which demonstrates that clonal restriction is not due to smaller thymic subpopulations investigated.

To investigate whether the restriction of clones is due to a limitation in the number of transplanted cells, we performed similar experiments with 150,000 or 26,000 CD34$^+$ cells per mouse (containing approximately 625 and approximately 108 HSC respectively[15]). While 150,000 CD34$^+$ cells are capable to generate a repopulation pattern in the thymus similar to the that observed after transplantation of 1000 purified HSC (Supplementary Fig. 2C), transplantation of 26,000 CD34$^+$ cells per mouse shows more limited clonal diversity, with most compartments consisting of a few clones (Supplementary Fig. 2D). Nevertheless, further clonal restriction during T-cell development was observed in spite of the transplantation of a 6-fold higher number of CD34$^+$ cells, or when a 10-fold higher number of phenotypically defined HSC was transplanted, suggesting that thymic clonality is primarily determined by intrathymic events rather than based on cell dose. Hence, clinically there is merit in transplanting a higher dose of CD34$^+$ cells to obtain a more diverse repertoire, yet a plateau is readily reached.

Having observed the limited number of hematological clones in the thymus, we asked the question whether this restricted number of cells would negatively influence the T-cell receptor (TCR) repertoire. At DP and SP stages a fully polyclonal pattern of *TRB* rearrangements is visible, with even further diversity in the splenic CD3$^+$ T cells (Fig. 4). From this data, we conclude that a fully diverse TCR repertoire can be generated from progeny with a high level of clonal restriction. It needs to be noted that the polyclonality in the spleen can be interpreted as the result of ongoing thymic output while the thymic analysis is more of a snapshot. Nevertheless, even at this "snapshot" the progeny of HSC clones is very small while thymic DP and SP cells have a fully diverse TCR repertoire which is further expanded in the spleen by the accumulation of cells egressing from the thymus. Because only a portion of the cells in the thymus and spleen were lentivirally transduced, the untransduced cells might contribute to this diverse repertoire, we therefore also sorted GFP$^+$ transduced cells from the spleen to

5

confirm that the TCR repertoire of the transduced cells was indeed polyclonal. This analysis demonstrated diverse repertoires in *TRD*, *TRG* and *TRB*, thereby confirming that the limited clonal repertoire of transduced cells does lead to the observed *TRB* repertoire (Supplementary Fig. 3). Our data show strong intrathymic competition between the progeny of stem cell clones. Therefore, clonality at the HSC level (hematological clonality) and a fully diverse TCR repertoire (immunological clonality) are independently regulated.
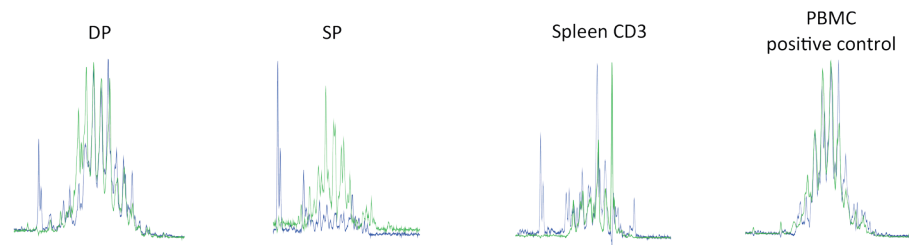

Figure 4: Separation of hematological and immunological clonality. *TRB* repertoires in DP and SP thymic subsets and sorted CD3+ splenocytes of mice transplanted with human HSC were determined. Electropherograms of two collections of primers amplifying the *TRB* locus (green and blue) show the *TRB* diversity for a representative mouse. The positive control shows PBMC of a healthy individual.

Discussion

The relationship between hematopoietic stem cells and T cells in quantitative terms previously was largely unexplored. Previous studies in mice showed that a limited number of HSC can be marked, transplanted and identified this way. Initially, such studies were performed using the unique marks that virus insertion form when they integrate into the host genome[20, 21]. From these studies several models for behavior of the hematopoietic system were postulated and mathematically modelled[22]. DNA barcoding technology allowed a much more refined insight into the composition of the blood compartments and allowed the study of aging HSC[13] and distribution of HSC clones through the different locations in the body[14] in addition to the clonal dynamics of repopulation of the bone marrow subset hierarchy after transplantation[23, 24]. The existence of myeloid, lymphoid or mixed progenitors, that had previously been observed in mice[16], was demonstrated with human cells in the NSG xenograft model[17] and while these seminal studies in the xenograft system demonstrated the dynamics of lymphoid development, they did not address T-cell development nor thymic function.

Using lentiviral cellular barcoding of purified human HSCs or CD34+ progenitor cells we here show at least 10% of the HSC clones are GFP marked in the thymus (Supplementary Fig. 5) and show considerable barcode-defined clonal restriction. How this restriction in clonal repertoire in the thymus occurs is not yet understood. It is conceivable that competition of DN cells for thymic niches (specific locations in the thymus which need to be reached for further development), fitness of the individual clone for progression in development or stochastic events drive competition between clones.

Intrathymic events that regulate TCR repertoire and the integrity and quality of thymic epithelial cells are likely an important factor. As a consequence, efforts to improve thymic reconstitution using cytokines (IL7[25],SCF, KFG[26, 27], FLT3L[28]) or hormones (GH[29], TSH[30]) and ablation of sex hormones[31] are only likely to be effective if they selectively act on the thymic microenvironment or mimic signals given by the thymic epithelial cells to developing thymocytes. Transplantation of committed T-cell progenitors together with HSCT, as shown before with mouse hematopoietic cells cultured *ex vivo* on OP9-DL1 expressing stromal support, which provide the cells with the Notch signals required to direct T-cell development[32], as well as diminishing the influence of male sex hormones known to deregulate intrathymic Notch ligand DLL4[31] may work well to improve thymic function and support diverse TCR repertoire formation. There is one interesting physiological situation in which hematopoietic reconstitution can be stimulated namely by exposure to non-inherited maternal antigens (NIMA) of the HLA-locus[33]. This phenomenon is now widely recognized in UCB transplantations and indicates that effective T-cell responses can be mounted with beneficial (e.g. graft vs leukemia) effects[34, 35]. While such exposure would theoretically lead to increased thymic output, the effect on TCR repertoire is expected to be limited, hence efforts directed at increasing overall thymic output are warranted.

Xenotransplantation of human cells in mice is a valuable approximation of the normal development of human cells. In NSG mice, the human cells develop into mature functional T cells that are responsive to immunization[10, 36], the thymus shows highly similar phenotype to normal human thymi[37]. When compared to human control samples (Supplementary Fig. 6), xenotransplanted NSG mice show lower CD3+ cell counts (Wilcoxon test, p=0.0015), but within the CD3+ cells, the percentage of CD4+ and CD8+ T cells is comparable. Furthermore, human and xenografted CD8+ T cells show similar distribution of CD45RA+ naive cells and CD45RO+ memory cells, but CD4+CD45RO+ memory T cells are present in a significantly higher proportion in the transplanted NSG mice (p=0.009), which might point to ongoing homeostatic proliferation in the CD4 compartment. Analysis of the interaction between murine thymic stroma and human T cells cells showed that T cells are capable of migrating to the site where they are expected to reside corresponding to their developmental stage in mouse thymus in response to murine Ccl25, Cxcl12 and Ccl21, all chemokines that attract T cells to the thymus[38]. Several papers have addressed the TCR repertoire in NSG mice in the presence or absence of transgenic human HLA-A2. First, Shultz *et al.*[39] demonstrated a functional EBV infection in xenografted NSG mice and compared the responses of xenografted NSG or NSG with transgenic expression of HLA-A2. No differences were observed in the frequency of naive, central memory and effector memory CD8+ T cells in the spleen nor for Granzyme A and B or Perforin expression. The only demonstrable difference between NSG and HLA-A2 expressing NSG is seen in response to HLA-A2 restricted BMLF and LMP1 proteins. Second, the issue of interaction of the xenografted cells with transgenic human HLA-A2 was elegantly addressed by Halkias *et al.*[40] where HLA-A2 transgenic NSG were compared to normal NSG after transplantation of HLA-A2 positive or negative human UCB cells. No differences were observed in repopulation and T cells in the spleen. Thus, the reported findings on T-cell development appear to be relevant for allogeneic human HSCT transplantation. However, being a xenograft model some aspects of the results should be interpreted with caution. Important T-cell subsets such as regulatory T

5

cells[40] and PLZF1^{+} innate T cells[41] which are both critical components of immune competence do not develop or function properly in NSG mice. This likely relates to the fact that MHC restriction occurs mostly on mouse epithelial cells and less frequently on human APC or via T-T interactions. Thus, clinically significant differences in the TCR repertoires of T cells selected on mouse thymus versus T cells that are selected on human thymus exist. Nevertheless, in experiments where CD34^{+} cells were transplanted into NSG mice, a survey of the IgH locus and TCR showed a comparable combinatorial diversity[42], although the screening method employed in this study (multiplexed PCR of V-J rearrangements) might not be sensitive enough to detect small differences in TCR repertoire between human and xenografted T cell samples. Moreover, in similar experiments using the same barcode library with mouse LSK hematopoietic stem/progenitor cells transplanted into congenic mice, we observed a similar thymic clonal restriction (not shown), suggesting a general applicability of the observed clonal restriction for the overall T-lymphocyte pool, with a caveat on their MHC restriction and development of specialized T-cell subpopulations.

Recent work by Rodewald and co-workers proposed cell competition as a mechanism underlying selection for cellular fitness during T-cell development[43]. This hypothesis explains the further clonal restriction at DN3, DP and SP stages that we observe in many mice. Apparently there is selection for progeny of certain HSCs clones while others are selected against. While this could be merely stochastic (neutral competition), the possibility that clonal fitness (e.g. metabolic activity, quiescence, other factors) plays a role is not unlikely given the existence of thymic stem cell clones with differential gene expression programs[43]. We therefore propose that the progeny from different HSC clones have inherently different capacity to pass through various developmental checkpoints in the thymus. Alternatively, in the experiments were barcoded CD34^{+} cells were transplanted, we cannot exclude that in some cases progenitors rather than bona fide HSCs would be the ancestors of the developing thymocytes. These progenitors are likely to have reduced fitness as well. In the experiments where phenotypically defined HSCs were transplanted, a role for such progenitors seems much less likely due to the purity of the transplanted cells. This notion is supported by the fact that in human gene therapy settings, a considerable fraction of T cells may have arisen from progenitors rather than from HSCs[44].

As a consequence, immune incompetence after HSCT is not related to the transplantation of limited numbers of HSC but to intrathymic events. While transplantation of more HSC may improve hematological reconstitution, our data suggests it will do little to improve immunological reconstitution. Thymus seeding is quickly saturated when the transplanted cell dose increases, therefore, efforts aimed at improving function of the thymic epithelium[45] most likely will be most successful in improving immunological immune reconstitution after stem cell transplantation.

Author contributions

MHB designed and performed experiments, analyzed data and wrote the manuscript.

AW, MCJAvE, ILMWT, AWL, EFdH performed experiments and discussed data.

LVB constructed the vector library. LVB, GdH, JJvR, WEF discussed data and analysis strategies. FJTS discussed data and analysis strategies and wrote the manuscript.

Disclosure of conflicts of interest

The authors have no conflicts of interest to disclose.
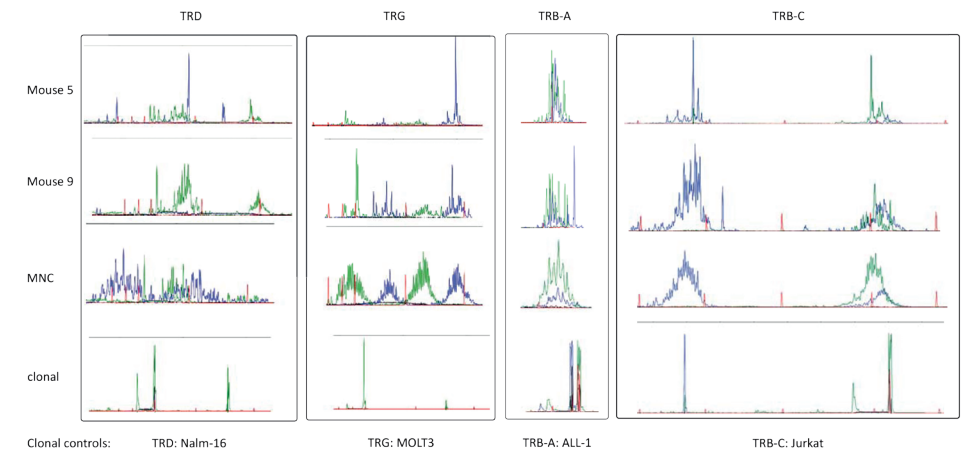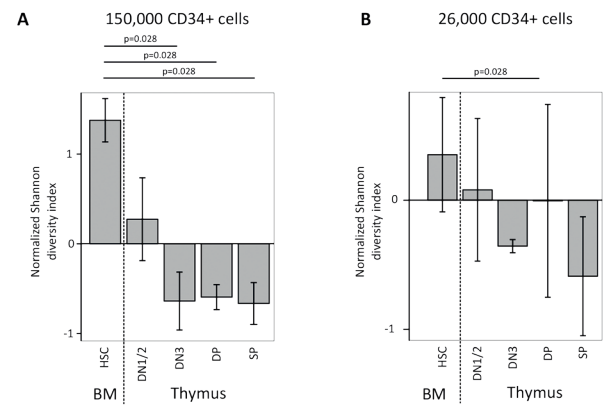
Acknowledgements

5

References

1. Szabolcs P, Cairo MS (2010) Unrelated umbilical cord blood transplantation and immune reconstitution. *Semin Hematol* 47(1):22–36.

2. Talvensaari K, et al. (2002) A broad T-cell repertoire diversity and an efficient thymic function indicate a favorable long-term immune reconstitution after cord blood stem cell transplantation. *Blood* 99(4):1458–1464.

3. Admiraal R, et al. (2015) Association between anti-thymocyte globulin exposure and CD4+ immune reconstitution in paediatric haemopoietic cell transplantation: a multicentre, retrospective pharmacodynamic cohort analysis. *Lancet Haematol* 2(5):e194–e203.

4. Wilkinson B, Owen JJ, Jenkinson EJ (1999) Factors regulating stem cell recruitment to the fetal thymus. *J Immunol Baltim Md 1950* 162(7):3873–3881.

5. Champion S, Imhof BA, Savagner P, Thiery JP (1986) The embryonic thymus produces chemotactic peptides involved in the homing of hemopoietic precursors. *Cell* 44(5):781–790.

6. Hao QL, et al. (2001) Identification of a novel, human multilymphoid progenitor in cord blood. *Blood* 97(12):3683–3690.

7. Haddad R, et al. (2004) Molecular characterization of early human T/NK and B-lymphoid progenitor cells in umbilical cord blood. *Blood* 104(13):3918–3926.

8. Kohn LA, et al. (2012) Lymphoid priming in human bone marrow begins before expression of CD10 with upregulation of L-selectin. *Nat Immunol* 13(10):963–971.

9. Weerkamp F, et al. (2006) Human thymus contains multipotent progenitors with T/B lymphoid, myeloid, and erythroid lineage potential. *Blood* 107(8):3131–3137.

10. Wiekmeijer A-S, et al. (2014) Sustained Engraftment of Cryopreserved Human Bone Marrow CD34(+) Cells in Young Adult NSG Mice. *BioResearch Open Access* 3(3):110–116.

11. Shultz LD, et al. (2005) Human lymphoid and myeloid cell development in NOD/LtSz-scid IL2R gamma null mice engrafted with mobilized human hemopoietic stem cells. *J Immunol Baltim Md 1950* 174(10):6477–6489.

12. Eapen M, et al. (2008) Outcomes after HLA-matched sibling transplantation or chemotherapy in children with acute lymphoblastic leukemia in a second remission after an isolated central nervous system relapse: a collaborative study of the Children's Oncology Group and the Center for International Blood and Marrow Transplant Research. *Leukemia* 22(2):281–286.

13. Gerrits A, et al. (2010) Cellular barcoding tool for clonal analysis in the hematopoietic system. *Blood* 115(13):2610–2618.

14. Verovskaya E, et al. (2014) Asymmetry in skeletal distribution of mouse hematopoietic stem cell clones and their equilibration by mobilizing cytokines. *J Exp Med* 211(3):487–497.

15. Notta F, et al. (2011) Isolation of single human hematopoietic stem cells capable of long-term multilineage engraftment. *Science* 333(6039):218–221.

16. Benz C, et al. (2012) Hematopoietic stem cell subtypes expand differentially during development and display distinct lymphopoietic programs. *Cell Stem Cell* 10(3):273–283.

17. Cheung AMS, et al. (2013) Analysis of the clonal growth and differentiation dynamics of primitive barcoded human cord blood cells in NSG mice. *Blood* 122(18):3129–3137.

18. Dik WA, et al. (2005) New insights on human T cell development by quantitative T cell receptor gene rearrangement studies and gene expression profiling. *J Exp Med* 201:1715–23.

19. Hill MO (1973) Diversity and Evenness: A Unifying Notation and Its Consequences. *Ecology* 54(2):427–432.

20. Schmidt M, et al. (2002) Polyclonal long-term repopulating stem cell clones in a primate model. *Blood* 100(8):2737–2743.

21. Kuramoto K, et al. (2004) The impact of low-dose busulfan on clonal dynamics in nonhuman primates. *Blood* 104(5):1273–1280.

22. Roeder I, et al. (2008) Characterization and quantification of clonal heterogeneity among hematopoietic stem cells: a model-based approach. *Blood* 112(13):4874–4883.

23. Lu R, Neff NF, Quake SR, Weissman IL (2011) Tracking single hematopoietic stem cells in vivo using high-throughput sequencing in conjunction with viral genetic barcoding. *Nat Biotechnol* 29(10):928–933.

24. Grosselin J, et al. (2013) Arrayed lentiviral barcoding for quantification analysis of hematopoietic dynamics: Arrayed Barcoding to Quantify Hematopoiesis. *STEM CELLS* 31(10):2162–2171.

25. Morrissey PJ, et al. (1991) Administration of IL-7 to mice with cyclophosphamide-induced lymphopenia accelerates lymphocyte repopulation. *J Immunol Baltim Md 1950* 146(5):1547–1552.

26. Min D, et al. (2007) Sustained thymopoiesis and improvement in functional immunity induced by exogenous KGF administration in murine models of aging. *Blood* 109(6):2529–2537.

27. Wils E-J, et al. (2012) Keratinocyte growth factor and stem cell factor to improve thymopoiesis after autologous CD34+ cell transplantation in rhesus macaques. *Biol Blood Marrow Transplant J Am Soc Blood Marrow Transplant* 18(1):55–65.

28. Fry TJ, et al. (2004) Flt3 ligand enhances thymic-dependent and thymic-independent immune reconstitution. *Blood* 104(9):2794–2800.

29. Welniak LA, Sun R, Murphy WJ (2002) The role of growth hormone in T-cell development and reconstitution. *J Leukoc Biol* 71(3):381–387.

30. van der Weerd K, et al. (2014) Thyrotropin acts as a T-cell developmental factor in mice and humans. *Thyroid Off J Am Thyroid Assoc* 24(6):1051–1061.

31. Velardi E, et al. (2014) Sex steroid blockade enhances thymopoiesis by modulating Notch signaling. *J Exp Med* 211(12):2341–2349.

32. Zakrzewski JL, et al. (2006) Adoptive transfer of T-cell precursors enhances T-cell reconstitution after allogeneic hematopoietic stem cell transplantation. *Nat Med* 12(9):1039–1047.

33. van Rood JJ, Roelen DL, Claas FHJ (2005) The effect of noninherited maternal antigens in allogeneic transplantation. *Semin Hematol* 42(2):104–111.

34. van Rood JJ, et al. (2002) Effect of tolerance to noninherited maternal antigens on the occurrence of graft-versus-host disease after bone marrow transplantation from a parent or an HLA-haploidentical sibling. *Blood* 99(5):1572–1577.

35. van Rood JJ, et al. (2009) Reexposure of cord blood to noninherited maternal HLA antigens improves transplant outcome in hematological malignancies. *Proc Natl Acad Sci U S A* 106(47):19952–19957.

36. Ishikawa F, et al. (2005) Development of functional human blood and immune systems in NOD/SCID/IL2 receptor {gamma} chain(null) mice. *Blood* 106(5):1565–1573.

5

37. Weerkamp F, et al. (2005) Age-related changes in the cellular composition of the thymus in children. *J Allergy Clin Immunol* 115(4):834–840.

38. Halkias J, et al. (2013) Opposing chemokine gradients control human thymocyte migration in situ. *J Clin Invest* 123(5):2131–2142.

39. Shultz LD, et al. (2010) Generation of functional human T-cell subsets with HLA-restricted immune responses in HLA class I expressing NOD/SCID/IL2r gamma(null) humanized mice. *Proc Natl Acad Sci U S A* 107(29):13022–13027.

40. Halkias J, et al. (2015) Conserved and divergent aspects of human T-cell development and migration in humanized mice. *Immunol Cell Biol.* doi:10.1038/icb.2015.38.

41. Lee YJ, et al. (2010) Generation of PLZF+ CD4+ T cells via MHC class II-dependent thymocyte-thymocyte interaction is a physiological process in humans. *J Exp Med* 207(1):237–246.

42. Marodon G, et al. (2009) High diversity of the immune repertoire in humanized NOD.SCID.gamma c-/- mice. *Eur J Immunol* 39(8):2136–2145.

43. Martins VC, et al. (2014) Cell competition is a tumour suppressor mechanism in the thymus. *Nature* 509(7501):465–470.

44. Fischer A, Hacein-Bey-Abina S, Cavazzana-Calvo M (2010) 20 years of gene therapy for SCID. *Nat Immunol* 11(6):457–460.

45. Tuckett AZ, et al. (2014) Image-guided intrathymic injection of multipotent stem cells supports lifelong T-cell immunity and facilitates targeted immunotherapy. *Blood* 123(18):2797–2805.

46. Csardi G, Nepusz T (2006) The igraph software package for complex network research. *InterJournal Complex Syst*:1695.

47. van Dongen JJM, et al. (2003) Design and standardization of PCR primers and protocols for detection of clonal immunoglobulin and T-cell receptor gene recombinations in suspect lymphoproliferations: report of the BIOMED-2 Concerted Action BMH4-CT98-3936. *Leukemia* 17(12):2257–231
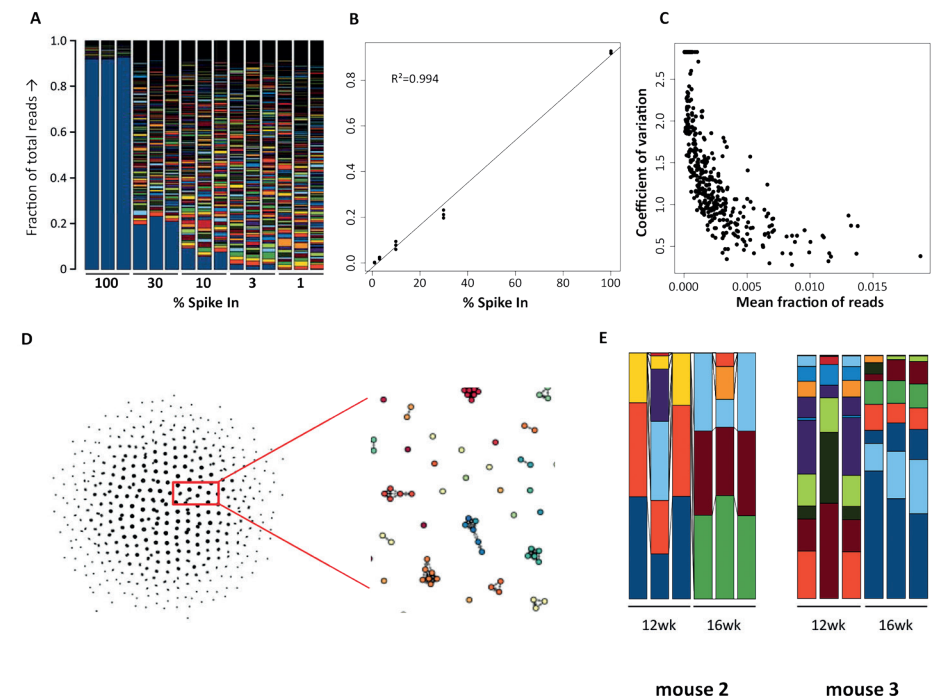
Supplementary Figure 1: Spike-in experiments to calibrate the DNA barcoding method. A plasmid sample was spiked in at equimolar ratio and diluted into a bulk barcoded sample. **A)** The bargraph shows the measured fraction of deep sequencing reads in each sample, with the lowest blue bar in the graph indicating the spiked-in plasmid. **B)** Triplicate analysis of the fraction of reads made up by the spiked-in barcode shows the least squares fitted line and the Pearson correlation coefficient. **C)** In an additional experiment, 9 repeated measures of the same sample were performed and the coefficient of variation was determined and plotted against the mean fraction of reads, showing that the precision of quantification increases with the amount of reads. **D)** A higher number of barcodes than the library complexity was retrieved from the analysis of these samples. To correct for these sequencing errors the number of dissimilar bases between all barcodes was determine and a directed acyclic graph was built for all barcodes that had less than 3 bases difference. Using this graph and an empirically determined threshold of 2 bases differences between barcodes, the reads of barcodes with <3 bases difference were combined. All barcoding data in the manuscript was processed using this procedure. **E)** Samples of PB CD19⁺ B cells were analyzed in triplicate to determine the variation of the method between samples.

5

A 150,000 CD34+ cells

B 26,000 CD34+ cells

C 150,000 CD34+ cells

D 26,000 CD34+ cells

Supplementary Figure 2: Clonal restriction during T cell development after CD34⁺ cell transplantation. Similar to the data in Fig. 2, the normalized Shannon diversity was compared between the developmental stages in the thymus **A)** of 4 mice transplanted with 150,000 CD34+ cells or **B)** 4 mice transplanted with 26,000 CD34⁺ cells. Kruskal-Wallis p-values are shown in A and B. The clonal contribution in the thymic subsets of mice transplanted with 150,000 or 26,000 barcoded human CD34⁺ cells is shown in stacked area graphs using colors to mark the individual barcoded clones in mice receiving a high (150,000 cells, **C)** or low (26,000 cells, **D)** dose of barcoded CD34⁺ cells.

Supplementary Figure 3: Hematological and immunological clonality in splenocytes. Rearrangements of *TRD*, *TRG*, and *TRB* of sorted transduced human splenic CD3⁺ cells are shown using two collections of primers to amplifying the respective loci. PBMC of a healthy individual was used a positive control and clonal rearrangements in Nalm-16 (*TRD*), MOLT3 (*TRG*), ALL-1 (*TRB-A*) and Jurkat (*TRB-C*) are shown for comparison.

5

Mouse 1

Number of clones in spleen: 39
Number of multilineage clones: 3

Mouse 5

Number of clones in spleen: 46
Number of multilineage clones: 12

Mouse 6

Number of clones in spleen: 39
Number of multilineage clones: 8

Mouse 9

Number of clones in spleen: 59
Number of multilineage clones: 21

Supplementary Figure 4: Barcoded HSC result in multilineage engraftment in NSG mice. NSG mice were transplanted with barcoded HSC and after 21 weeks, barcode content in CD19+ B cells, CD3+ T cells and CD13/CD33+ myeloid cells was determined. Ternary plots show the contribution of a clone to each lineage. Multilineage contribution is defined as contribution of a clone to each of these three lineages. The total number of clones retrieved from these spleen samples is indicated, as is the number of these clones that contribute to all three lineages.
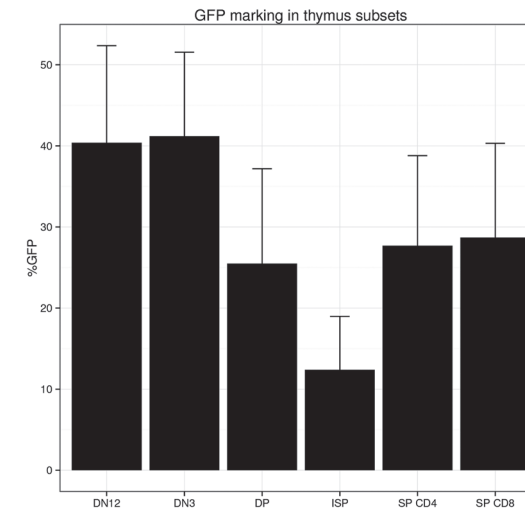
Supplementary Figure 5: GFP marking in the thymus. The percentage of GFP marking in the different thymocyte subsets after transplantation of barcoded HSC is displayed as mean + SEM (n=9).
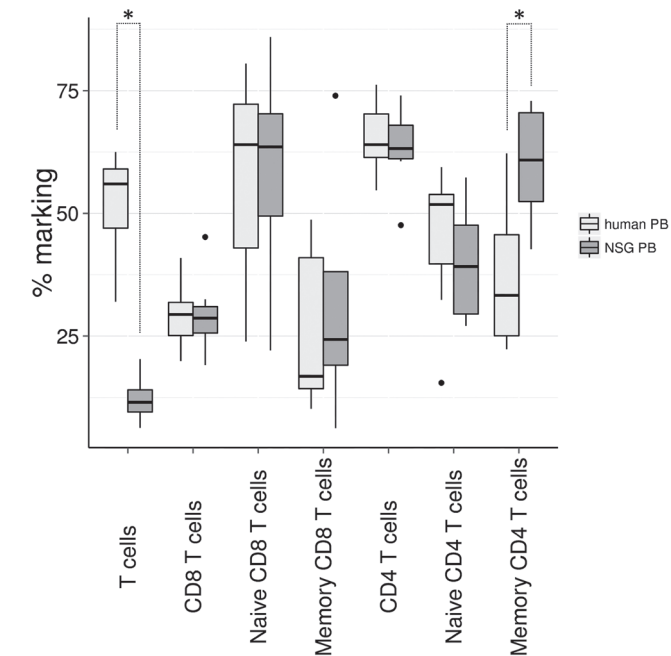
Supplementary Figure 6: Comparison of T cell subsets in human peripheral blood and xenografted NSG mice. Peripheral blood of NSG mice (n=8) transplanted with lentivirally-transduced umbilical cord blood CD34+ cells at 20 weeks post transplantation and human peripheral blood control samples (n=7, female, ages 20-52 years old) were analyzed for the expression of CD45RO and CD45RA in the CD4+ and CD8+ T cells by flow cytometry. Wilcoxon p-values smaller than 0.05 are indicated with *.

Chapter 6

Overexpression of LMO2 causes aberrant human T-cell development *in vivo* by three distinct cellular mechanisms

Anna-Sophia Wiekmeijer[1], Karin Pike-Overzet[1], Martijn H. Brugman[1], Marja C.J.A. van Eggermond[1], Martijn Cordes[1], Edwin F.E de Haas[1], Yunlei Li[2], Edwin Oole[3], Wilfred F.J. van IJcken[3], R. Maarten Egeler[4,5], Jules P. Meijerink[2], Frank J.T. Staal[1]

[1]Department of Immunohematology and Blood Transfusion, Leiden University Medical Center, Leiden, The Netherlands

[2]Department of Pediatric Oncology/Hematology, Erasmus Medical Center, Rotterdam, The Netherlands

[3]Center for Biomics, Erasmus Medical Center, Rotterdam, The Netherlands

[4]Department of Pediatrics, Leiden University Medical Center, Leiden, The Netherlands

[5]Division of Hematology/Oncology, Hospital for Sick Children/University of Toronto, Toronto, Canada

Abstract

Overexpression of *LMO2* is known to be one of the causes of T-ALL development; however the mechanisms behind its oncogenic activity are incompletely understood. *LMO2* overexpressing transgenic mouse models suggest an accumulation of immature T-cell progenitors in the thymus as main pre-leukemic event. The effects of *LMO2* overexpression on human T-cell development *in vivo*, however, are unknown. Here we report studies of a humanized mouse model transplanted with *LMO2* transduced human hematopoietic stem and progenitor cells. The effects of *LMO2* overexpression were confined to the T-cell lineage although initially multipotent cells were transduced. Three effects of *LMO2* on human T-cell development were observed: 1) a block at the DN/ISP stage, 2) an accumulation of CD4$^+$CD8$^+$ double positive CD3$^-$ cells and 3) an altered CD8/CD4 ratio with enhanced peripheral T lymphocytes. Microarray analysis of sorted DP cells overexpressing *LMO2* led to identification of an LMO2 gene set that clustered with human T-ALL patient samples of the described "Proliferative" cluster. In summary, we demonstrate previously unrecognized mechanisms by which *LMO2* alters human T-cell development *in vivo* that correlate with human T-ALL leukemogenesis.

Introduction

Animal models of leukemia have been indispensable in the study of this deadly disease. Initially, carcinogen-induced or virus-induced leukemia models were used[1,2,3], soon followed by transgenic models. As the latter are very labor-intensive to produce and can have effects outside the hematopoietic system, mosaic models in which hematopoietic stem cells (HSCs) taken from mice, manipulated *ex vivo* by retroviral transduction, and transplanted into autologous recipients, have gained much popularity. Finally, in recent years murine xenograft models have been developed to allow engraftment of primary patient samples and cell lines, as even very aggressive leukemias seldom grow in *in vitro* culture systems. With the establishment of the NSG immune deficient model[4,5], theoretically a combination of xenotransplantation and mosaic models is possible, in that human HSCs modified *in vitro* to express leukemic oncogenes, can be studied *in vivo*. Here we describe for the first time such a model, in which human CD34$^+$ stem/progenitor cells genetically modified to overexpress the *LMO2* gene were transplanted into NSG mice. The nature of this model is very suitable to gain insight into the early stages of leukemogenesis through careful dissection of cellular differentiation processes. It is less suitable for studying frank leukemia given the limited life span of humanized NSG mice[6].

Around 25 years ago, *LMO2* was discovered and shown to be frequently translocated with T-cell receptor (TCR) loci in T-cell acute lymphoblastic leukemia (T-ALL) (reviewed in[7]). In childhood T-ALL, 9% of the cases had a translocation that involved *LMO2*[8], while in 35% of T-ALL cases there is increased expression[9]. Using different conditional knockouts for *Lmo2* it was demonstrated that Lmo2 is not needed for normal T-cell development[10]. Effects of Lmo2 overexpression have been studied using different transgenic mouse models[10, 11, 12, 13]. These studies demonstrated an accumulation of CD4$^-$CD8$^-$ double negative (DN) cells within the thymus at the expense of CD4$^+$CD8$^+$ double positive (DP) cells. However, development of leukemia was heterogeneous and had a long latency, indicating that secondary mutations are needed. One of these models used the ubiquitously expressed methallothionein-1 promoter to drive the expression of *Lmo2*[13] and demonstrated that the effects of *Lmo2* overexpression were confined to the T-cell lineage.

LMO2, which is highly expressed in hematopoietic stem cells (HSC)[14], is also required in normal hematopoiesis as illustrated by the fact that knockout mice are embryonic lethal due to absence of erythrocyte development[15]. In gene therapy trials that have been conducted for X-linked SCID and Wiskott-Aldrich Syndrome (WAS), T-ALLs have occurred as the result of insertional mutagenesis, frequently leading to ectopic expression of LMO2[16, 17, 18, 19]. Integration of the viral vector in or in proximity to the *LMO2* locus caused the overexpression of this oncogene and effects were only observed within the T-cell lineage. The development of T-ALL had a relatively long latency and additional hits, e.g. in *CDKN2A*, were found in these leukemias[19]. We have shown that overexpression of LMO2, using fetal thymic organ cultures, leads to an arrest in normal development, which is not seen with the therapeutic gene in X-SCID gene therapy, the *IL2RG* gene[20, 21].

Normal T-cell development follows a developmental trajectory starting from the CD4$^-$CD8$^-$ double DN stage to the immature single positive stage (ISP), which in mice is characterized

6

by the expression of CD8 and absence of CD3[22]. In humans, however, ISP are CD4^{+} instead of CD8[+23]. From the ISP stage, the cells differentiate to the CD4^{+}CD8^{+} DP stage to become either a CD4^{+} single positive (SP) or CD8^{+} SP after positive and negative selection now expressing a functional T cell receptor (TCR)[24]. The DN compartment can be further subdivided, but for human and mouse these compartments are characterized by different markers and DN stages have been described in more detail for murine T-cell development[23, 24, 25, 26].

During normal human T-cell development LMO2 is quickly downregulated in the DN stages[21, 24]. Ectopic expression of LMO2 after this stage might therefore be able to deregulate normal thymopoiesis as a first step, eventually resulting in T-ALL. Here, we demonstrate the different effects of LMO2 overexpression on human T-cell development *in vivo* and report that differentially expressed genes are associated with the previously identified "Proliferative" cluster in human T-ALL[27].

Materials & Methods

Isolation of human CD34^{+}cells
Umbilical cord blood (UCB) was obtained from the Diaconessenhuis Hospital Leiden (Leiden, the Netherlands) after informed consent of the parents. CD34^{+} progenitors were isolated from a pool of 5 to 6 donors using the CD34 Microbead Kit (Miltenyi Biotec GmbH, Bergisch Gladbach, Germany).

Mice
NOD.Cg-*Prkdc[scid] Il2rg[tm1Wjl]*/SzJ (NSG) mice were obtained from Charles River Laboratories (Kent, United Kingdom) and bred in the animal facility at the Leiden University Medical Center. Experimental procedures were approved by the Ethical Committee on Animal Experiments of the Leiden University Medical Center. Maintenance and irradiation of mice was performed as described[28]. Female mice were used at 5-6 weeks of age. Three different experiments were performed, with in total 10 GFP transplanted mice and 12 LMO2 transplanted mice.

Flow cytometry
The following anti-human antibodies were used: CD3-PECy5 (UCHT1), CD4-APCCy7 (RPA-T4), CD7-PECy5 (M-T701), CD8-PECy7 (SK1), CD13-APC (WM15), CD16-PE (B73.1), CD19-APCCy7 (SJ25C1), CD20-PE (L27), CD33-APC (WM53), CD34-PE (8G12), CD45-V450 (HI30), CD56-PE (MY31), TCRαβ-PE (T10B9.1A-31) (all from BD Biosciences, San Jose, CA, USA). Data were acquired on a Canto II (BD Biosciences) and analyzed using FlowJo software (Treestar, Ashland, OR, USA).

Virus production and transduction
Virus of LZRS-IRES-GFP and LZRS-LMO2-IRES-GFP were produced as described[21]. Isolated CD34^{+} cells were cultured overnight in StemSpan serum-free expansion medium (StemSpan-SFEM, StemCell Technologies Inc., Vancouver, BC, Canada) in the presence of 10 ng/mL stem cell factor (SCF, a gift from Amgen, Thousand Oakes, CS, USA), 20 ng/mL recombinant human

thrombopoietin (rhTPO, R&D Systems, Abingdon, UK), 20 ng/mL recombinant mouse insulin-like growth factor 2 (rmIGF-2, R&D Systems) and 10 ng/mL recombinant human fibroblast growth factor-acidic (rhFGF-1, Peprotech, Rocky Hill, NJ, USA). Retronectin (50 μg/mL,Takara Bio Inc, Otsu, Japan) was coated on non-tissue culture treated 48-wells plates (BD Falcon, Bedford, MA, USA) o/n at 4℃. Virus (500 μL) was centrifuged onto the plate for 2 hours at 32℃ 1000xg. Supernatant was removed and $1.5*10^5$ isolated cells were added per well and transduced for 2 days.

Gene expression
RNA was isolated using the Qiagen RNeasy mini kit or micro kit according to manufacturer protocol (Qiagen). cDNA was prepared using SuperScript III and random primers (Life Technologies, Bleiswijk, The Netherlands). For qRT-PCR, the Universal Probe Library (Roche Diagnostics, Almere, The Netherlands) was used to design primer/probe combinations (except for *ABL*). Samples were run on the StepOnePlus machine (Applied Biosystems, Life Technologies, Bleiswijk, The Netherlands) using the TaqMan® Universal Master Mix II with UNG (Applied Biosystems). *ABL* was used as housekeeping gene. The following primers were used: *LMO2* Forward 5'-CGAAAGGAAGAGCCTGGAC-3' Reverse 5'-AAGTAGCGGTCCCAATGTT-3', *HES1* Forward 5'-GAAGCACCTCCGGAACCT-3' Reverse 5'-GTCACCTCGTTCATGCACTC-3', *ABL* as described before[21]. Expression was calculated relative to *ABL* and for correction of transduced cells this was divided by the fraction of transduced cells as was assessed by flow cytometry for GFP.

RNA expression analysis by microarray
Single stranded cDNA was synthesized from 1000 pg total RNA using the Ovation Pico WTA System V2 Module (NuGEN Technologies Inc, Leek, The Netherlands) in combination with the Encore Biotin Module (NuGEN Technologies Inc) according to the instructions of the manufacturer. Biotin labeling and fragmentation was performed and fragmented cDNA was hybridized onto Affymetrix Gene Atlas human U219 arrays. Microarray analysis was done in accordance with previously described guidelines[29] by the I-BFM-SG Task Force on gene expression profiling. Raw expression values were normalized using RMA[30] and the log2 expression values were compared between IRES-GFP DP cells and three LMO2-IRES-GFP samples. A gene set was created of the 136 probe sets with highest differential expression (|FC| > 0.7) corresponding to 110 genes, which was clustered using Euclidean distance Ward's method and used in a gene set enrichment analysis[31] against a dataset of human T-ALL[27] (available at http://www.ncbi.nlm.nih.goc/geo/ under accession number GSE26713). Gene expression data is available under GEO accession number: GSE79625.

LM-PCR
Ligation-mediated PCR was performed as described[32]. Fragments were cloned in pGEM-T Easy vector (Promega Benelux b.v., Leiden, The Netherlands) and sequenced using the m13 reverse primer.

Statistical analysis
Two-way ANOVA was used to test for statistical. For expression of *HES1*, a student t-test was used. A p-value smaller than 0.05 was considered significant. $*p≤0.05$, $**p≤0.01$, $***p≤0.001$, $****p≤0.0001$

Results

Transduction and overexpression of LMO2 in human CD34+ cells

Previously, it has been shown that by transplantation of CD34+ cells from either UCB[5] or human bone marrow (BM) in NSG mice a human immune system develops in these mice[28, 33]. Furthermore, T-cell developmental stages comparable to *ex vivo* human thymi were detected in the thymi obtained from transplanted NSG mice[28, 33]. We transduced the isolated CD34+ with *LMO2*-IRES-eGFP as used previously by our group for *in vitro* studies[21]. As a control, a virus without *LMO2* only containing IRES-eGFP was used (Fig. 1A). We obtained transduction efficiencies of 35% for GFP and 43% for *LMO2* in primary human CD34+ cells (Fig. 1B). The total cell sample, containing both transduced and untransduced cells, was transplanted into sublethally irradiated NSG mice two days after transduction. We on purpose chose not to sort for LMO2 expressing cells via the GFP marker, as the co-transplanted untransduced cells allow for an internal, negative control in each individually transplanted mouse. Peripheral blood was drawn every 4 weeks from these mice to monitor engraftment of human cells and lineage outgrowth (Fig. 1C). A sample of the transduced cells was expanded for an additional 6 days and then sorted based on GFP expression. The overexpression of *LMO2* was determined using qPCR and was 135 times higher in *LMO2* transduced cells as compared to the sorted GFP- cells from the same sample (Fig. 1B). No overexpression of *LMO2* was detected in GFP+ cells that were transduced with the control vector.
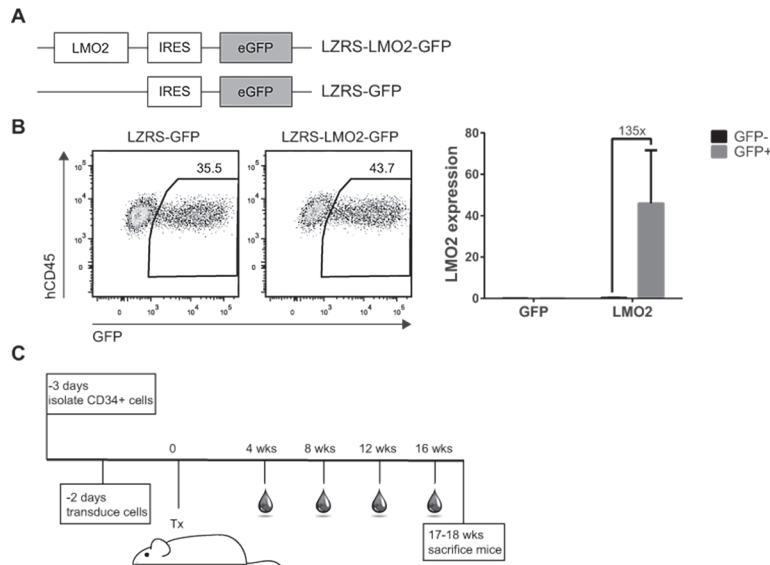

Figure 1: Overexpression of *LMO2* in CD34+ HSPCs using gammaretroviral vector. A) Schematic representation of gammaretroviral LZRS constructs that were used in this study. **B)** Transduction efficiency of both vectors in human CD34+ cells isolated from umbilical cord blood (left panel). Level of *LMO2* expression relative to *ABL* in transduced cells that were expanded for 8 days and sorted on GFP expression (mean ± sd) (right panel). **C)** Schematic representation of experimental set up.

LMO2 overexpressing cells cause increased outgrowth of T cells in humanized mice

Human engraftment reached 70% and no differences were observed between mice transplanted with GFP or *LMO2* samples, indicating that overexpression of *LMO2* does not lead to increased engraftment (Fig. 2A). Mice were sacrificed 17 to 18 weeks after transplantation. The thymus of mice that were transplanted with *LMO2* transduced CD34+ cells showed a significantly increased percentage of hCD45+ cells (Fig. 2B). However, this did not lead to an increase in absolute hCD45+ cell numbers (Fig. 2C). Transduced cells, which were detected by their expression of GFP, were more abundant in mice transplanted with *LMO2* transduced cells as compared to the GFP control mice, possibly indicating a growth advantage of *LMO2* overexpressing cells (Fig. 2D). Levels of transduced cells declined over time but surprisingly increased at 16 weeks in mice transplanted with *LMO2* transduced cells. The relative frequency of both GFP+ myeloid cells and B cells was significantly different 4 weeks after transplantation in mice transplanted with *LMO2* transduced cells (Fig. 2E,F), but the reliability of the measurement at 4 weeks might be limited by the small amount of human cells that were available for acquisition at this time point. At later time points no differences were detected for GFP+ myeloid and B cells between both groups. The frequency of GFP+ T cells in peripheral blood was significantly higher in *LMO2* overexpressing cells 16 weeks after transplantation (Fig. 2G), coinciding with the overall increase of GFP levels (Fig. 2D). In addition, we performed a different gating strategy in which we determined the frequency of different immune cell subsets within GFP- and GFP+ cells that were positive for hCD45+ (Supplementary Fig. 1A). This demonstrated that within GFP- cells of both GFP and LMO2 mice the percentages of myeloid cells, B cells and T cells were highly comparable (Supplementary Fig. 1B,D,F). Within the GFP+ cells a highly significant increase of T cells at 16 weeks after transplantation was observed in *LMO2* mice which led to a concomitant decrease in percentages of both myeloid cells and B cells (Supplementary Fig. 1C,E,G). Furthermore, the frequency of transduced cells in the thymi of humanized mice was significantly higher in mice transplanted with *LMO2* transduced CD34+ cells at the end of the experiment (Fig. 2H). When comparing the percentage of T cells within GFP- and GFP+ of both GFP and LMO2 mice, there is a significant increase of the GFP+ cells in LMO2 mice compared to the other three groups at 16 weeks (Fig. 2I). Overall, the data indicate increased outgrowth of T cells together with increased engraftment of the thymus caused by the *LMO2* overexpressing cells.

No clonal outgrowth in NSG mice transplanted with LMO2 overexpressing CD34+ cells

To check for possible clonal outgrowth of transduced cells, we performed ligation-mediated (LM)-PCR. Gel electrophoresis of vector-genome boundaries showed an oligoclonal integration pattern, which did not differ between the two groups (Fig. 3A and Supplementary Fig. 4).This indicates that outgrowth of specific clones could not be detected. The most prominent bands were excised from the gel and sequenced to determine whether integration sites were preferentially selected. No such preferential integration was observed (Supplementary Table 1). Often cells need multiple hits before they develop into leukemic cells and *NOTCH1* mutations are frequently detected in T-ALL. To determine whether *NOTCH* activation might act as a secondary hit, we determined the expression levels of *HES1*, one of the *NOTCH* target genes. Both in the thymus and the spleen no increased expression of *HES1* was observed,

6

demonstrating that Notch signaling is not increased in these mice (Fig. 3B). The expression of *HES1*, which was corrected for the percentage of transduced cells, was actually decreased in the spleens of LMO2 transplanted mice compared to GFP transplanted mice. Combining the increased frequency of T cells with the absence of clonality and lack of increased Notch signaling, we conclude that the LMO2 mice likely demonstrate a preleukemic T-ALL stage.
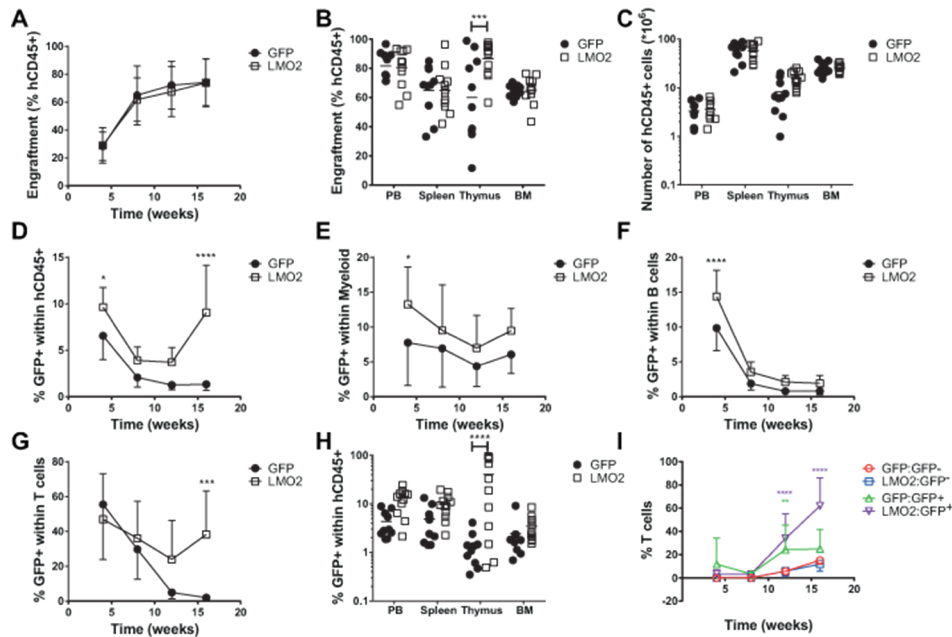
were sequential arrests in development at different immature stages of T-cell development, leading to an accumulation of cells in these stages.

Figure 3: LM-PCR shows no evidence for preferential integration. A) LM-PCR analysis of total cells from different organs 17 to 18 weeks after transplantation of GFP or *LMO2* transduced HSPCs in NSG mice. B=BM, S= spleen, T=thymus, L=100 bp ladder. **B)** Expression of *HES1* relative to *ABL* corrected for percentage GFP⁺ cells in total thymocytes (left) and spleen cells (right) (mean ± sem).

Figure 2: LMO2 enhances thymic engraftment and outgrowth of peripheral T cells. A) Engraftment was measured as the frequency of hCD45⁺ cells within live cells in peripheral blood of NSG mice transplanted with GFP or *LMO2* transduced HSPCs. **B)** Engraftment in different organs 17 to 18 weeks after transplantation and the **C)** absolute numbers of hCD45⁺ cells calculated from this. **D)** Percentage of transduced cells within total hCD45⁺ cells, **E)** myeloid cells (CD13/33⁺), **F)** B cells (CD19⁺) and **G)** T cells (CD3⁺) over time after transplantation of GFP or *LMO2* transduced HSPCs in NSG mice. **H)** Percentage of transduced cells within hCD45⁺ cells in different organs 17 to 18 weeks after transplantation. **I)** Percentage of T cells over time within hCD45⁺ GFP⁻ and GFP⁺ populations in GFP or *LMO2* transplanted mice. Green asterisks depict significance of GFP:GFP⁺ compared to GFP:GFP⁻ and LMO2:GFP⁻. Purple asterisks depict significance of LMO2:GFP⁺ compared to GFP:GFP⁻ and LMO2:GFP⁻ at 12 weeks and to all three other groups at 16 weeks. **A, D, E, F, G)** Depicted is the mean ± sd. **B, C, H)** Depicted is the mean.

Figure 4: Delayed T-cell development in *LMO2* transduced GFP⁺CD45^low cells. A) Flow cytometry plot depicting the expression of hCD45 and GFP and the gates (top) that were used for the subsequent plots depicting CD34 and CD7 (middle) and CD8 and CD4 (bottom). **B)** Distribution of GFP⁻ cells and **C)** GFP⁺CD45^low cells from thymi of mice transplanted with *LMO2* transduced HSPCs over the different stages of human T-cell development (n=2) (mean ± sem).

Overexpression of LMO2 causes delayed development in human T cell progenitors

Based on the expression of hCD45 and GFP, multiple populations could be discriminated in the thymus (Fig. 4A). In 2 out of 12 mice transplanted with LMO2 transduced cells, a GFP⁺CD45^low population was observed. This population was never observed in NSG mice transplanted with GFP alone (Supplementary Fig. 5). A fraction of *LMO2* overexpressing cells retained expression of CD34 reminiscent of highly immature cells (Fig. 4A). In addition, the percentage of CD4⁺CD8⁺ DP cells was severely reduced, while the relative abundance of both ISP and CD4⁻CD8⁻CD3⁻ triple negative (TN) was increased as compared to the untransduced cells (Fig. 4B,C). Thus, there

LMO2 overexpression results in accumulation of DP CD3⁻ cells and an altered CD8/CD4 ratio

Different levels of GFP expressing cells (named GFP⁺ and GFP⁺⁺) were present in the thymi of humanized mice. The gating strategy for GFP levels and different stages of human T-cell development are depicted in Fig. 5A. We determined the frequencies of different T-cell developmental stages within the GFP⁻, GFP⁺ and GFP⁺⁺ populations of all 10 GFP- and 12 LMO2-transplanted mice. The frequencies within the GFP⁻ cells were highly comparable

between GFP and *LMO2* transplanted mice (Fig. 5B, left panel). Within the GFP⁺ cell fraction, an increased percentage of DP CD3⁻ cells was observed in NSG mice transplanted with *LMO2* overexpressing CD34⁺ cells (Fig. 5B, middle panel). This was also observed within the GFP⁺⁺ cell fraction in which it was accompanied by a decrease in DP CD3⁺ cells (Fig. 5B, right panel). The same patterns were observed when absolute numbers were compared (Supplementary Fig. 2). These data indicate an accumulation of DP CD3⁻ cells caused by *LMO2* overexpression in human thymocytes. Furthermore, when the level of GFP increased, the ratio of CD8 over CD4 SP cells was different between GFP and *LMO2* transduced cells, which was even stronger in peripheral T cells (Fig. 5C). This indicated that overexpression of *LMO2* not only led to an accumulation of DP CD3⁻ cells but also to an altered CD8/CD4 ratio, which was sustained in the peripheral blood.
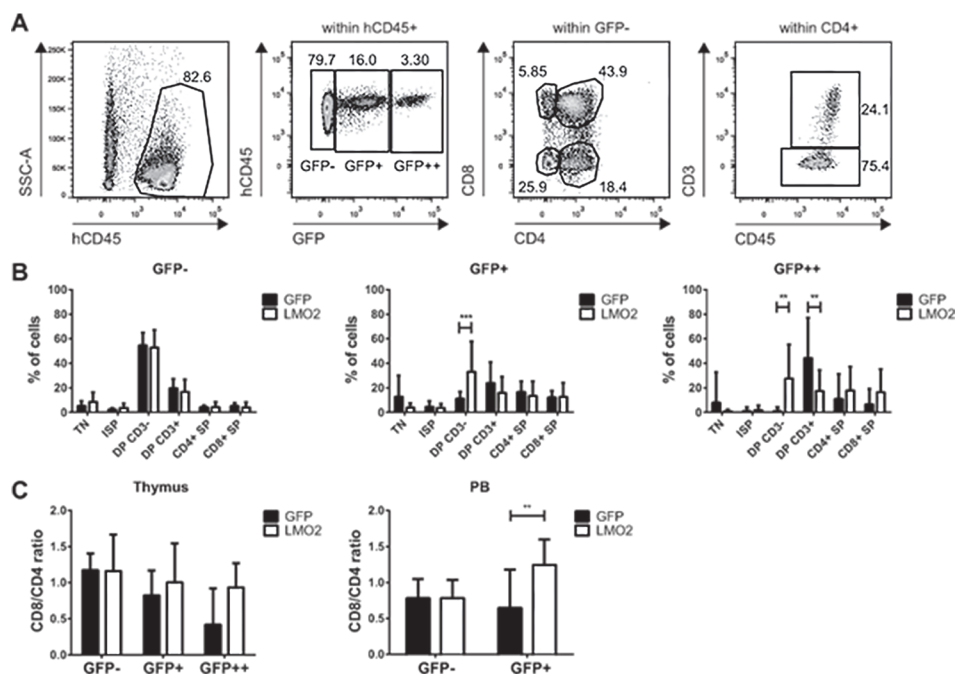
Figure 5: *LMO2* **overexpression leads to accumulation of DP CD3⁻ cells and an altered CD8/CD4 ratio.**
A) Gating strategy of flow cytometry data used for gating of different GFP levels. Depicted is an LMO2 transplanted mouse. **B)** Distribution of GFP⁻ cells (left panel), GFP⁺ cells (middle panel) and GFP⁺⁺ cells (right panel) over the different stages of human T-cell development within thymi of NSG mice 17 to 18 weeks after transplantation. **C)** Ratio of CD8/CD4 cells within the different GFP levels in mice transplanted with GFP or *LMO2* transduced HSPCs (left panel) and in peripheral blood of NSG mice 17 to 18 weeks after transplantation. **B, C)** Depicted is mean ± sd (n=10 GFP transplanted mice, n=12 LMO2 transplanted mice).

Overexpression of LMO2 increases T cells in lymphoid organs

As described, we observed an increased frequency of GFP⁺ cells within T cells of peripheral blood (Fig. 2G) and an increased percentage of T cells within GFP⁺ cells (Supplementary Fig. 1G) at 16 weeks after transplantation in the LMO2 group. Mice were sacrificed 17 to 18 weeks after transplantation and again we observed more T cells in *LMO2* transplanted mice compared to

GFP transplanted mice in PB, spleen and BM (Fig. 6A). The same was also reflected in absolute T cell numbers in PB and spleen, but not in BM (Supplementary Fig. 3A). High overexpression of *LMO2* was found in the thymus and spleen, but not in BM (Fig. 6B). The frequency of T cells was increased at the expense of B cells within the transduced cells in spleens of mice transplanted with *LMO2* overexpressing cells (Supplementary Fig. 3B). Cells that were isolated from spleens of these mice were sorted for different immune cells and here we found high overexpression of *LMO2* only in the T cells (Fig. 6C). Together, these data indicate that overexpression of *LMO2* in CD34⁺ cells leads to increased percentages of T cells in lymphoid organs and that these effects are confined to the T-cell lineage.
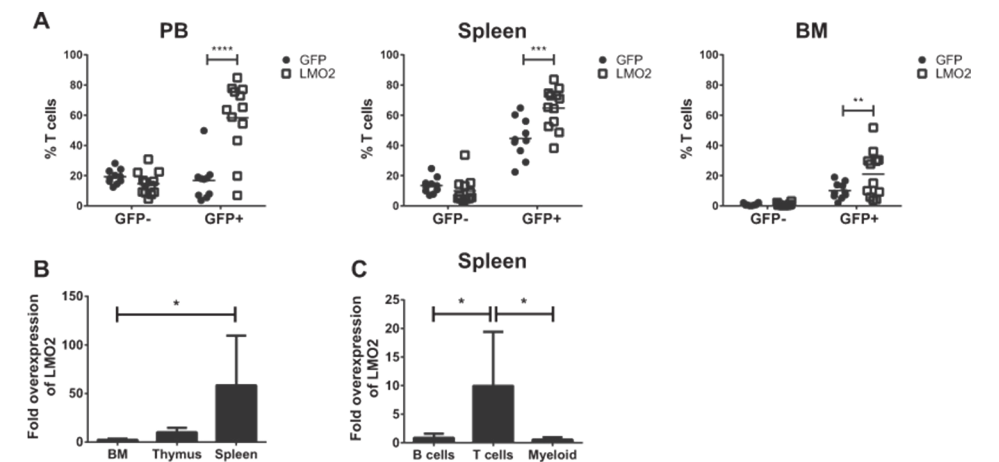
Figure 6: Increased frequency of T cells in lymphoid organs caused by *LMO2* **overexpression. A)** Percentage of T cells in GFP⁻ and GFP⁺ in peripheral blood (left panel), spleen (middle panel) and bone marrow (right panel) of mice transplanted with GFP or *LMO2* transduced HSPCs 17 to 18 weeks after transplantation. **B)** Fold overexpression of *LMO2* in LMO2 mice over GFP mice within total cells of different lymphoid organs and **C)** different cell types sorted from spleens of transplanted NSG mice. **B, C)** *LMO2* expression relative to *ABL* expression. Expression was corrected for the frequency of transduced cells in each sample. **A)** Depicted is the mean. **B, C)** Depicted is mean ± sem.

Different mechanisms underlie delayed and accelerated development as caused by LMO2 overexpression

To gain insight into the molecular mechanism underlying the effects of *LMO2* on human T cell development, we performed transcriptome analyses. We sorted the DP cells from single cell suspensions made from the thymus of transplanted NSG mice as we had observed an accumulation of DP CD3⁻ cells (for sorting strategy see Supplementary Fig. 6). The genes that were differentially expressed between *LMO2* and GFP were used as a gene set (see Supplementary Table 2 and 3) and the expression of this gene set was determined in 117 human T-ALL microarray expression sets described by Homminga *et al.*[27]. We observed clustering of our gene set of 52 upregulated genes with the described "Proliferative" and "TALLMO" signatures (Fig. 7A). Gene set enrichment analysis was subsequently performed with the 52

upregulated genes in our sorted *LMO2* DP samples. A significant negative enrichment was found with the "Immature" cluster (NOM p = 0.008) and a significant positive correlation with the "Proliferative" cluster (NOM p = 0.038) and the set of genes that was upregulated in *LMO2* mice compared to GFP mice (Fig. 7B,C). Of note, in previous transgenic mouse studies overexpressing LMO2, the retinaldehyde dehydrogenase 2 (*RALDH2*) gene was identified as prominent target gene. Nowadays, this gene is referred to as aldehyde dehydrogenase 1A (*ALDH1A2*) which is up regulated in our LMO2 experiments (~3 fold) and also found upregulated in the so-called "Proliferative" cluster of T-ALL samples. The correlation of this and other upregulated genes indicates that the effects and mechanisms that were observed in patients suffering from T-ALL is also found after transplantation of *LMO2* overexpressing cells in NSG mice.
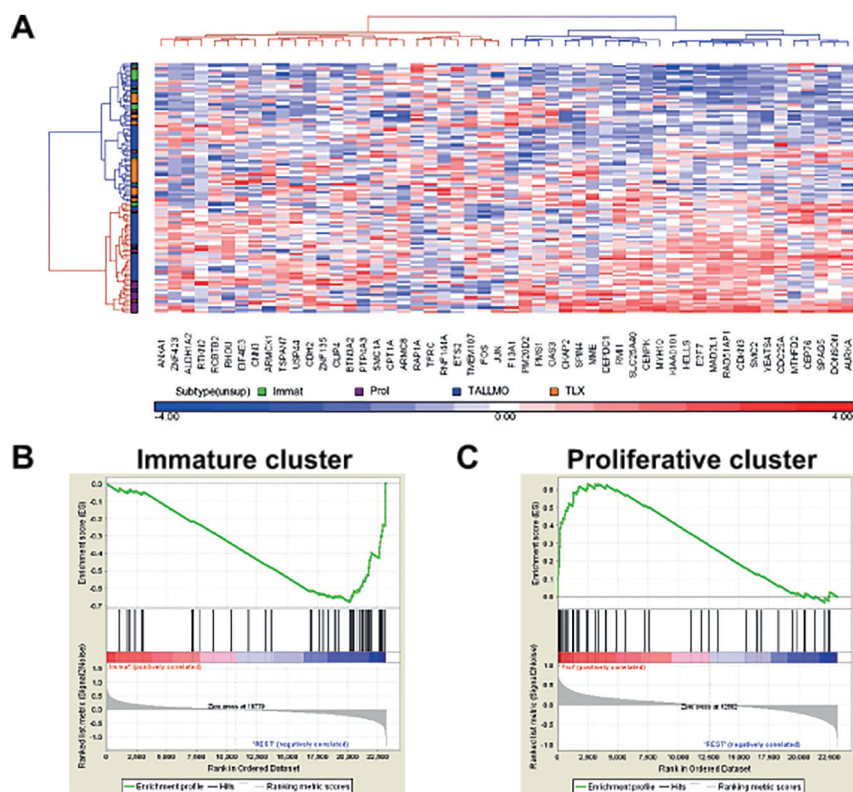
Figure 7: Correlation between significantly upregulated genes with human T-ALL samples. A) Clustering of 52 genes that were significantly upregulated in sorted DP cells from thymi of GFP and *LMO2* transplanted NSG mice with 117 human T-ALL samples, which have been described previously[27]. **B)** Gene set enrichment analysis of the 52 upregulated genes demonstrate a negative enrichment with the previously described "Immature" cluster (NES=-1.73, NOM p=0.008, FDR q=0.085) and **C)** a positive enrichment with the previously described "Proliferative" cluster (NES=1.65, NOM p=0.038, FDR q=0.085).

Discussion

Although murine and human T-cell development are largely similar, differences exist, which could have implications for the extrapolation of mechanisms found in mice to human T-ALL development. Here, we have tested the effect of *LMO2* overexpression on human T-cell development in an *in vivo* model and, to the best of our knowledge, this study shows for the first time the role of *LMO2* overexpression on human T-cell development *in vivo*. We have observed that *LMO2* overexpressing CD34^{+} cells demonstrate a preferential outgrowth of T cells after transplantation in a humanized mouse model. As corollary, in mice that express *Lmo2* under the inducible methallothionein-1 promoter there is a long latency of T-ALL development with a median of 51 weeks[13] while 50% of *CD2-Lmo2* transgenic mice develop leukemia at an age around 10 months[11]. Unfortunately, humanized NSG mice cannot be maintained for such periods as human HSCs do not provide red blood cells in these mice and due to increasing engraftment of human cells over time these mice succumb to anemia[6]. On the other hand, as the mice were sacrificed before onset of leukemia, we were able to study the mechanisms by which LMO2 alters T-cell development, independent of secondary mutations that affect the development of T-ALL in full-blown leukemia.

We observed 3 effects of *LMO2* overexpression on human T-cell development: 1) a small subset of mice displayed a delayed development with a block in the DN/ISP compartment, 2) in the majority of mice an accumulation of DP CD3^{-} cells 3) and an altered CD8/CD4 ratio. Both the accumulation of DP CD3^{-} cells and the altered CD8/CD4 ratio became more prominent with higher GFP levels and the altered CD8/CD4 ratio was also found in the peripheral blood. The delayed development of human T cells has also been shown using human/mouse fetal thymic organ cultures[21], but the other two mechanisms have not been described previously. This is inheritant to this type of *in vitro* studies in which it is difficult to study human T-cell development up to the mature stages. Such approaches also preclude finding the whole spectrum of effects caused by *LMO2* overexpression, including the accelerated development (using either fetal thymic organ cultures or the OP9-DL1 stromal cell line), demonstrating the strength of the described humanized mouse model. In both types of transgenic *Lmo2* mice, an increased DN cell frequency was found while in some mice DP cells were also present but decreased leading to T-ALL with more mature phenotypes[11, 13]. Here, we observed the increased DN frequency only in 2 out of 12 mice while the increased DP CD3^{-} frequency was ubiquitous as well as the alteration of the CD8/CD4 ratio.

Effects of *LMO2* overexpression were only observed on T-cell development although hematopoietic progenitors with multilineage developmental potential were transduced. This is concordant with data from the transgenic mouse model using the ubiquitously expressed methallothionein-1 promoter where effects were also confined to the T-cell lineage[13]. Furthermore, the insertional mutagenesis that led to T-ALL development in gene therapy trials also came from integrations resulting from transduction of human hematopoietic progenitor cells. Even though multipotent cells were transduced, cells with integration in or near *LMO2* only caused development of T-ALL and did not affect other lineages[17, 18, 19]. Patients in the

6

study by Braun *et al.*[17] that developed T-ALL, all with *LMO2* integrations, which in some cases coincided with *TAL1* integrations, had a CD4+CD8+CD3-CD7+ phenotype. We also observed an accumulation of DP cells without expression of CD3 in our humanized mice transplanted with *LMO2* overexpressing HSPCs.

It was observed that *Lmo2* increased the expression of CD4 in a murine cell line[34]. Our data also demonstrate differences in the CD8/CD4 ratio, however, here we observed fewer CD4 and more CD8 T cells. As one of the main differences between murine and human T-cell development is the phenotypic difference of the ISP stage it might be that in human T-cell development *LMO2* exerts effect on CD8 instead of CD4. This, however, needs to be further investigated.

McCormack *et al.* found that the leukemia-initiating cell (LIC) is established in the thymus of *CD2-Lmo2* transgenic mice and not in the BM[12]. This is in agreement with our data using human cells as we did not find increased frequencies of transduced cells in the BM but did in the thymus and in addition only very low overexpression of *LMO2* was found in the BM of transplanted mice. Furthermore, no preferential outgrowth of T cells was observed in *LMO2* secondary transplanted mice (data not shown), illustrating that the oncogenic event most likely occurs after thymic entry in agreement with the data published by McCormack *et al.*[12]. Using *CD2-Lmo2* mice, two different mechanisms have been described; one involving activation of *Hhex, Lyl1* and *Mycn* resulting in an ETP-ALL like pathway, the other showed upregulation of *Notch1*[35]. Here, we have described 3 effects of *LMO2* overexpression of which the delayed development that was observed in 2 of 12 mice might resemble the ETP-ALL like pathway. However, we did not find activation of the *NOTCH* signaling pathway. In mice, overexpression of *Lmo2* results in a block at immature stages of T-cell development while giving rise to T-ALL with more mature phenotypes[11, 12, 13, 35]. In humans, T-ALL with a more mature phenotype are found[27, 36] and also in patients that did develop T-ALL as result of insertional mutagenesis in or near *LMO2*[17, 18, 19, 37]. This suggests that there might be different mechanisms in human and murine T-ALL development as a consequence of *LMO2* overexpression, which might explain the differences between our data and the data obtained using transgenic *Lmo2* mice. Our data therefore provide an explanation for the more mature T-ALL subtypes in which *LMO2* overexpression is found.

The accelerated T-cell development with quicker thymic output seen in most mice overexpressing LMO2 bears significance in relation to gene therapy trials for SCID. While in the first X-linked SCID trials using now obsolete viral vectors, 5 out of 20 patients developed T-ALL as a consequence of integrations near and activation of proto-oncogenes[18, 19], most often LMO2, the same vectors in the ADA-SCID trial did not cause leukemias[38, 39]. As there normally is severe clonal restriction in the thymus[40] and X-linked SCID leads to an extreme early block in T- cell development[33] the selective pressure in X-linked SCID on T-cell progenitors is extremely high. An accelerated development caused by LMO2 may then be selected for. In ADA-SCID it is possible that non transduced progenitors benefit from ADA enzyme expressed on the surface[41] or leaking out of corrected cells thereby causing less severe selective pressure. As the exact block in human T-cell development caused by ADA deficiency is currently unknown, future studies should shed further light on this intriguing observation.

In conclusion, this is the first study to describe the role of *LMO2* overexpression on human T-cell development using an *in vivo* model. Our results suggest new mechanisms that have not been identified before in human cells but that correlate with an expression signature of human T-ALL with a proliferative phenotype. Therefore, besides arrests in normal development, accelerated development that bypasses normal checkpoints should also be considered as a mechanism for leukemogenesis.
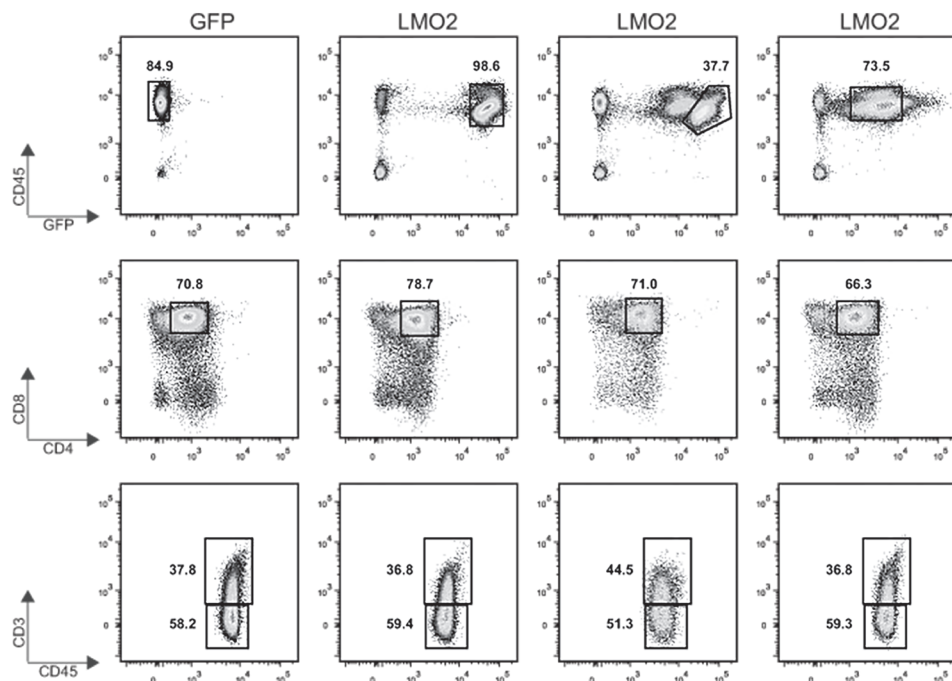
Acknowledgements

References

1. Breuer M, Slebos R, Verbeek S, van Lohuizen M, Wientjens E, Berns A. Very high frequency of lymphoma induction by a chemical carcinogen in pim-1 transgenic mice. *Nature* 1989, **340**(6228): 61-63.

2. Mattison J, Kool J, Uren AG, de Ridder J, Wessels L, Jonkers J, et al. Novel candidate cancer genes identified by a large-scale cross-species comparative oncogenomics approach. *Cancer research* 2010, **70**(3): 883-895.

3. van Lohuizen M, Verbeek S, Scheijen B, Wientjens E, van der Gulden H, Berns A. Identification of cooperating oncogenes in E mu-myc transgenic mice by provirus tagging. *Cell* 1991, **65**(5): 737-752.

4. Ishikawa F, Yasukawa M, Lyons B, Yoshida S, Miyamoto T, Yoshimoto G, et al. Development of functional human blood and immune systems in NOD/SCID/IL2 receptor {gamma} chain(null) mice. *Blood* 2005, **106**(5): 1565-1573.

5. Shultz LD, Lyons BL, Burzenski LM, Gott B, Chen X, Chaleff S, et al. Human lymphoid and myeloid cell development in NOD/LtSz-scid IL2R gamma null mice engrafted with mobilized human hemopoietic stem cells. *Journal of immunology* 2005, **174**(10): 6477-6489.

6. Shultz LD, Brehm MA, Garcia-Martinez JV, Greiner DL. Humanized mice for immune system investigation: progress, promise and challenges. *Nature reviews Immunology* 2012, **12**(11): 786-798.

7. Chambers J, Rabbitts TH. LMO2 at 25 years: a paradigm of chromosomal translocation proteins. *Open biology* 2015, **5**(6): 150062.

8. Van Vlierberghe P, van Grotel M, Beverloo HB, Lee C, Helgason T, Buijs-Gladdines J, et al. The cryptic chromosomal deletion del(11)(p12p13) as a new activation mechanism of LMO2 in pediatric T-cell acute lymphoblastic leukemia. *Blood* 2006, **108**(10): 3520-3529.

9. Ferrando AA, Herblot S, Palomero T, Hansen M, Hoang T, Fox EA, et al. Biallelic transcriptional activation of oncogenic transcription factors in T-cell acute lymphoblastic leukemia. *Blood* 2004, **103**(5): 1909-1911.

10. McCormack MP, Forster A, Drynan L, Pannell R, Rabbitts TH. The LMO2 T-cell oncogene is activated via chromosomal translocations or retroviral insertion during gene therapy but has no mandatory role in normal T-cell development. *Molecular and cellular biology* 2003, **23**(24): 9003-9013.

11. Larson RC, Lavenir I, Larson TA, Baer R, Warren AJ, Wadman I, et al. Protein dimerization between Lmo2 (Rbtn2) and Tal1 alters thymocyte development and potentiates T cell tumorigenesis in transgenic mice. *The EMBO journal* 1996, **15**(5): 1021-1027.

12. McCormack MP, Young LF, Vasudevan S, de Graaf CA, Codrington R, Rabbitts TH, et al. The Lmo2 oncogene initiates leukemia in mice by inducing thymocyte self-renewal. *Science* 2010, **327**(5967): 879-883.

13. Neale GA, Rehg JE, Goorha RM. Ectopic expression of rhombotin-2 causes selective expansion of CD4-CD8- lymphocytes in the thymus and T-cell tumors in transgenic mice. *Blood* 1995, **86**(8): 3060-3071.

14. Riddell J, Gazit R, Garrison BS, Guo G, Saadatpour A, Mandal PK, et al. Reprogramming committed murine blood cells to induced hematopoietic stem cells with defined factors. *Cell* 2014, **157**(3): 549-564.

15. Warren AJ, Colledge WH, Carlton MB, Evans MJ, Smith AJ, Rabbitts TH. The oncogenic cysteine-rich LIM domain protein rbtn2 is essential for erythroid development. *Cell* 1994, **78**(1): 45-57.

16. Avedillo Diez I, Zychlinski D, Coci EG, Galla M, Modlich U, Dewey RA, et al. Development of novel efficient SIN vectors with improved safety features for Wiskott-Aldrich syndrome stem cell based gene therapy. *Molecular pharmaceutics* 2011, **8**(5): 1525-1537.

17. Braun CJ, Boztug K, Paruzynski A, Witzel M, Schwarzer A, Rothe M, et al. Gene therapy for Wiskott-Aldrich syndrome--long-term efficacy and genotoxicity. *Science translational medicine* 2014, **6**(227): 227ra233.

18. Hacein-Bey-Abina S, Garrigue A, Wang GP, Soulier J, Lim A, Morillon E, et al. Insertional oncogenesis in 4 patients after retrovirus-mediated gene therapy of SCID-X1. *The Journal of clinical investigation* 2008, **118**(9): 3132-3142.

19. Howe SJ, Mansour MR, Schwarzwaelder K, Bartholomae C, Hubank M, Kempski H, et al. Insertional mutagenesis combined with acquired somatic mutations causes leukemogenesis following gene therapy of SCID-X1 patients. *The Journal of clinical investigation* 2008, **118**(9): 3143-3150.

20. Pike-Overzet K, de Ridder D, Weerkamp F, Baert MR, Verstegen MM, Brugman MH, et al. Gene therapy: is IL2RG oncogenic in T-cell development? *Nature* 2006, **443**(7109): E5; discussion E6-7.

21. Pike-Overzet K, de Ridder D, Weerkamp F, Baert MR, Verstegen MM, Brugman MH, et al. Ectopic retroviral expression of LMO2, but not IL2Rgamma, blocks human T-cell development from CD34+ cells: implications for leukemogenesis in gene therapy. *Leukemia* 2007, **21**(4): 754-763.

22. Rothenberg EV. Transcriptional control of early T and B cell developmental choices. *Annual review of immunology* 2014, **32**: 283-321.

23. Weerkamp F, Pike-Overzet K, Staal FJ. T-sing progenitors to commit. *Trends in immunology* 2006, **27**(3): 125-131.

24. Dik WA, Pike-Overzet K, Weerkamp F, de Ridder D, de Haas EF, Baert MR, et al. New insights on human T cell development by quantitative T cell receptor gene rearrangement studies and gene expression profiling. *The Journal of experimental medicine* 2005, **201**(11): 1715-1723.

25. Hao QL, George AA, Zhu J, Barsky L, Zielinska E, Wang X, et al. Human intrathymic lineage commitment is marked by differential CD7 expression: identification of CD7- lympho-myeloid thymic progenitors. *Blood* 2008, **111**(3): 1318-1326.

26. Ramond C, Berthault C, Burlen-Defranoux O, de Sousa AP, Guy-Grand D, Vieira P, et al. Two waves of distinct hematopoietic progenitor cells colonize the fetal thymus. *Nature immunology* 2014, **15**(1): 27-35.

27. Homminga I, Pieters R, Langerak AW, de Rooi JJ, Stubbs A, Verstegen M, et al. Integrated transcript and genome analyses reveal NKX2-1 and MEF2C as potential oncogenes in T cell acute lymphoblastic leukemia. *Cancer cell* 2011, **19**(4): 484-497.

28. Wiekmeijer AS, Pike-Overzet K, Brugman MH, Salvatori DC, Egeler RM, Bredius RG, et al. Sustained Engraftment of Cryopreserved Human Bone Marrow CD34(+) Cells in Young Adult NSG Mice. *BioResearch open access* 2014, **3**(3): 110-116.

29. Staal FJ, Cario G, Cazzaniga G, Haferlach T, Heuser M, Hofmann WK, et al. Consensus guidelines for microarray gene expression analyses in leukemia from three European leukemia networks. *Leukemia* 2006, **20**(8): 1385-1392.

30. Bolstad BM, Irizarry RA, Astrand M, Speed TP. A comparison of normalization methods for high density oligonucleotide array data based on variance and bias. *Bioinformatics* 2003, **19**(2): 185-193.

6

31. Subramanian A, Tamayo P, Mootha VK, Mukherjee S, Ebert BL, Gillette MA, *et al.* Gene set enrichment analysis: a knowledge-based approach for interpreting genome-wide expression profiles. *Proceedings of the National Academy of Sciences of the United States of America* 2005, **102**(43)**:** 15545-15550.

32. Kustikova OS, Baum C, Fehse B. Retroviral integration site analysis in hematopoietic stem cells. *Methods in molecular biology* 2008, **430:** 255-267.

33. Wiekmeijer AS, Pike-Overzet K, H IJ, Brugman MH, Wolvers-Tettero IL, Lankester AC, *et al.* Identification of checkpoints in human T-cell development using severe combined immunodeficiency stem cells. *The Journal of allergy and clinical immunology* 2016, **137**(2)**:** 517-526 e513.

34. Cleveland SM, Goodings C, Tripathi RM, Elliott N, Thompson MA, Guo Y, *et al.* LMO2 induces T-cell leukemia with epigenetic deregulation of CD4. *Experimental hematology* 2014, **42**(7)**:** 581-593 e585.

35. Smith S, Tripathi R, Goodings C, Cleveland S, Mathias E, Hardaway JA, *et al.* LIM domain only-2 (LMO2) induces T-cell leukemia by two distinct pathways. *PloS one* 2014, **9**(1)**:** e85883.

36. Nam CH, Rabbitts TH. The role of LMO2 in development and in T cell leukemia after chromosomal translocation or retroviral insertion. *Molecular therapy : the journal of the American Society of Gene Therapy* 2006, **13**(1)**:** 15-25.

37. Hacein-Bey-Abina S, Von Kalle C, Schmidt M, McCormack MP, Wulffraat N, Leboulch P, *et al.* LMO2-associated clonal T cell proliferation in two patients after gene therapy for SCID-X1. *Science* 2003, **302**(5644)**:** 415-419.

38. Aiuti A, Cattaneo F, Galimberti S, Benninghoff U, Cassani B, Callegaro L, *et al.* Gene therapy for immunodeficiency due to adenosine deaminase deficiency. *The New England journal of medicine* 2009, **360**(5)**:** 447-458.

39. Gaspar HB, Cooray S, Gilmour KC, Parsley KL, Zhang F, Adams S, *et al.* Hematopoietic stem cell gene therapy for adenosine deaminase-deficient severe combined immunodeficiency leads to long-term immunological recovery and metabolic correction. *Science translational medicine* 2011, **3**(97)**:** 97ra80.

40. Brugman MH, Wiekmeijer AS, van Eggermond M, Wolvers-Tettero I, Langerak AW, de Haas EF, *et al.* Development of a diverse human T-cell repertoire despite stringent restriction of hematopoietic clonality in the thymus. *Proceedings of the National Academy of Sciences of the United States of America* 2015, **112**(44)**:** E6020-6027.

41. Franco R, Casado V, Ciruela F, Saura C, Mallol J, Canela EI, *et al.* Cell surface adenosine deaminase: much more than an ectoenzyme. *Progress in neurobiology* 1997, **52**(4)**:** 283-294.
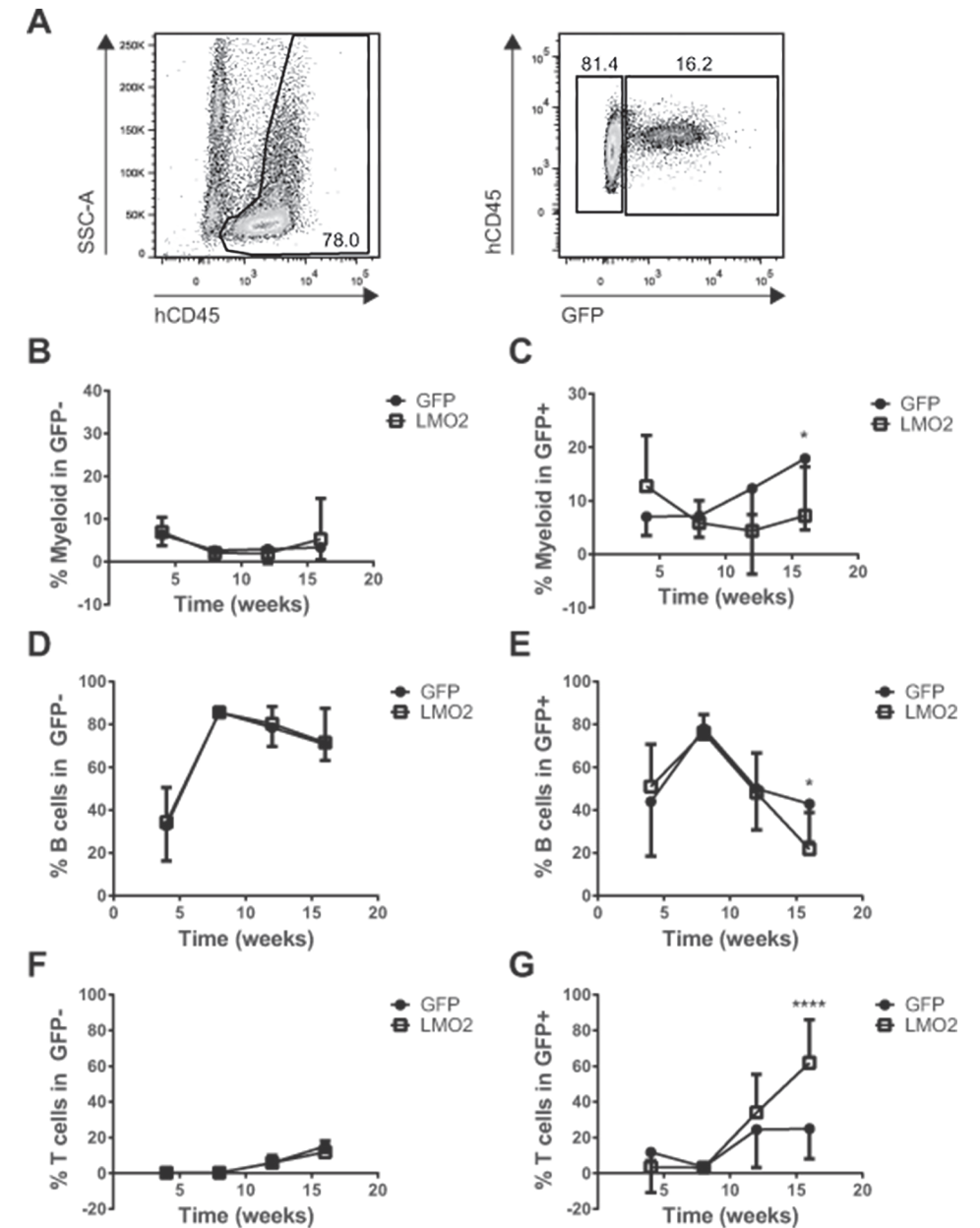
Supplementary Figure 1: Preferential outgrowth of T cells within *LMO2* transduced cells. A) Gating strategy of flow cytometry data. GFP- and GFP+ cells were defined in hCD45+ live cells within peripheral blood of transplanted NSG mice. **B)** Percentage of myeloid cells within GFP- cells and **C)** GFP+ cells. Myeloid cells were defined as CD13/33+. **D)** Percentage of B cells within GFP- cells and **E)** GFP+ cells. B cells were defined as CD19+. **F)** Percentage of T cells within GFP- cells and **G)** GFP+ cells. T cells were defined as CD3+. **B-G)** Depicted is mean ± sd.

6

Supplementary Figure 2: *LMO2* **overexpression leads to accumulation of the number of DP CD3⁻ cells.** Absolute number of cells for different stages of human T-cell development of GFP⁻ (left), GFP⁺ (middle) and GFP⁺⁺ cells (right). Gating strategy of flow cytometry data for gating of different GFP levels was performed as depicted in Fig. 2. Depicted is mean ± sd.

Supplementary Figure 3: Increased number of T cells in lymphoid organs and altered lineage distribution in spleens of mice transplanted with *LMO2* **overexpressing HSPCs. A)** Absolute number of T cells in GFP⁻ and GFP⁺ in peripheral blood (left panel), spleen (middle panel) and bone marrow (right panel) of mice transplanted with GFP or *LMO2* transduced HSPCs 17 to 18 weeks after transplantation. **B)** Percentage of cells within GFP⁻ (left) and GFP⁺ (right) cells in spleens of transplanted NSG mice. **A, B)** Depicted is the mean.

Supplementary Figure 4: LM-PCR shows no evidence for preferential integration. LM-PCR analysis of total cells from different organs 17 to 18 weeks after transplantation of GFP or *LMO2* transduced HSPCs in NSG mice. B=BM, S= spleen, T=thymus, L=100 bp ladder.

Supplementary Figure 5: GFP⁺CD45ˡᵒʷ population is not present in GFP transplanted NSG mice. Flow cytometry plot depicting the expression of hCD45 and GFP of three mice transplanted with GFP transduced HSPCs. Gating strategy is similar as described in Fig. 4.

6

Supplementary Figure 6: Sorting strategy of CD4⁺CD8⁺ DP cells for microarray analysis. hCD45⁺ single lymphocytes, either GFP⁻ or GFP⁺ were gated (top), which were then selected based on expression of CD4 and CD8 (middle). The bottom row depicts the expression of CD3 within the sorted CD4⁺CD8⁺ DP population.

Supplementary Table 1: Upregulated genes sorted by Fold change.

GFP Thymus	Arpin isoform
	Zinc finger protein 710
LMO2 BM	Phorbol-12-myristate-13-acetate-induced protein 1
LMO2 BM	Probable E3 ubiquitin-protein ligase HERC1 isoform
	Death-associated protein kinase 2
LMO2 BM	Septin-6 isoform
	Ankyrin repeat domain-containing protein SOWAHD
LMO2 BM	Actin-related protein t3
LMO2 BM	Predicted: homo sapiens tight junction protein 1 (TJP1)
LMO2 BM	RP11-143J12
LMO2 BM	DEP-domain-containing mTOR-interacting protein isoform
	Collagen alpha-1 (XIV) chain precursor

Log2 expression values were compared between IRES-GFP DP cells and three LMO2-IRES-GFP samples. Listed are the 60 probesets corresponding to 52 genes that were upregulated with highest differential expression (|FC| > 0.7).

Supplementary Table 2: Downregulated genes sorted by Fold change.

Gene name	5GFP_ GFP-DP	2LMO2_ GFP+ DP	9LMO2_ GFP++ DP	10LMO2_ GFP+ DP	Ratio (LMO2/ GFP)	Fold Change (LMO-GFP)
RAP1A	4,733	11,396	10,526	8,382	2,134	5,368
ALDH1A2	3,854	7,246	6,969	6,849	1,822	3,167
F13A1	3,366	7,294	6,475	5,826	1,941	3,166
OAS3	4,629	7,507	8,248	7,477	1,673	3,115
AURKA	4,632	7,599	7,207	8,299	1,663	3,070
ALDH1A2	4,364	7,541	7,442	6,747	1,660	2,879
FOS	2,732	2,776	6,450	7,249	2,010	2,760
TSPAN7	5,124	8,024	7,693	7,802	1,530	2,716
ALDH1A2	5,134	8,171	8,055	7,230	1,523	2,684
RMI1	3,329	5,590	5,590	6,424	1,762	2,538
RCBTB2	5,397	7,557	7,600	8,561	1,465	2,509
CDC25A	3,873	5,479	6,281	7,196	1,632	2,446
CDH2	4,426	5,992	7,189	7,141	1,530	2,348
PTP4A3	4,149	5,585	6,273	7,469	1,553	2,293
E2F7	3,330	5,316	4,958	6,343	1,663	2,209
PM20D2	3,787	5,187	6,362	6,418	1,581	2,202
JUN	2,991	3,874	6,408	5,238	1,730	2,183
ZNF423	3,700	5,876	6,875	4,808	1,582	2,153
USP44	4,086	6,140	6,310	6,267	1,527	2,153
TMEM107	3,619	5,322	6,156	5,754	1,587	2,125
CEP76	3,727	6,506	5,126	5,910	1,569	2,120
EIF4E3	4,878	7,002	7,050	6,937	1,434	2,118
CKAP2	4,333	6,618	6,048	6,346	1,463	2,005
SPIN4	3,554	5,374	5,748	5,491	1,558	1,984
CNN3	3,128	4,043	4,339	6,955	1,634	1,984
HELLS	3,096	4,498	4,875	5,624	1,615	1,903
YEATS4	4,031	5,891	5,634	6,148	1,461	1,860
CPT1A	3,659	6,345	4,763	5,439	1,507	1,857
MME	4,404	6,197	6,346	6,143	1,414	1,825
TFRC	3,832	5,173	5,706	6,086	1,476	1,824
SLC25A40	2,986	4,745	4,688	4,985	1,609	1,820
RHOU	3,763	5,001	5,563	6,112	1,477	1,795
RAD51AP1	3,251	4,410	5,071	5,636	1,550	1,787
RMI1	4,171	5,624	5,624	6,578	1,425	1,771
MYH10	3,260	4,621	5,778	4,621	1,536	1,747
PMS1	4,113	5,432	6,190	5,878	1,418	1,720
KIAA0101	3,182	4,203	4,203	6,282	1,539	1,714

6

EIF4E3	4,033	5,756	5,575	5,878	1,422	1,703
MAD2L1	3,108	4,597	5,038	4,781	1,546	1,697
CENPK	2,855	3,860	4,214	5,443	1,578	1,651
DEPDC1	3,442	4,662	5,043	5,574	1,479	1,650
OAS3	3,112	4,177	4,994	5,097	1,528	1,643
RAD51AP1	2,818	3,958	4,096	5,215	1,569	1,604
ANXA1	3,292	4,045	5,811	4,794	1,483	1,591
CDKN3	3,544	5,106	4,587	5,647	1,443	1,569
MTHFD2	2,894	3,899	4,229	5,229	1,538	1,558
BTN3A2	2,982	4,599	3,608	5,404	1,522	1,555
DONSON	3,352	5,170	4,619	4,908	1,462	1,547
ARMC8	3,453	4,409	4,259	6,293	1,444	1,535
SPAG5	3,541	4,811	4,773	5,486	1,418	1,482
RNF144A	2,769	3,472	4,310	4,765	1,511	1,414
TSPAN7	3,132	4,416	3,995	5,180	1,447	1,399
CLIP4	3,103	3,677	4,555	5,141	1,437	1,355
ETS2	3,067	3,698	4,197	5,314	1,436	1,336
ZNF135	3,089	3,095	2,819	7,198	1,415	1,282
RTKN2	2,553	3,706	3,952	3,734	1,487	1,245
ANXA1	2,662	3,194	4,800	3,617	1,454	1,209
SMC2	2,562	3,055	3,307	4,769	1,448	1,149
SMC1A	2,755	3,281	3,628	4,794	1,416	1,146
ARMCX1	2,551	3,265	3,273	4,407	1,430	1,097

Log2 expression values were compared between IRES-GFP DP cells and three LMO2-IRES-GFP samples. Listed are the 65 probesets corresponding to 58 genes that were upregulated with highest differential expression (|FC| > 0.7).

Supplementary Table 3: Relates to Figure 7. Downregulated genes sorted by Fold Change.

Gene name	5GFP_ GFP-DP	2LMO2_ GFP+ DP	9LMO2_ GFP++ DP	10LMO2_ GFP+ DP	Ratio (LMO2/ GFP)	Fold Change (LMO-GFP)
C2CD4B	6,854	3,241	3,255	3,241	0,474	-3,608
IFT172	6,676	3,265	3,371	3,038	0,483	-3,451
BAZ1A	9,462	6,129	6,190	5,951	0,644	-3,372
TMEM181	6,141	2,930	2,915	2,896	0,474	-3,227
BLMH	7,471	4,329	4,044	4,605	0,579	-3,146
H1F0	7,436	4,565	2,819	5,872	0,594	-3,017
REXO2	7,541	5,117	4,842	3,645	0,601	-3,007
ITM2C	6,142	3,450	3,211	2,898	0,519	-2,956
RASSF6	7,458	3,882	4,656	5,089	0,609	-2,915
TNKS	6,511	3,734	3,734	3,576	0,565	-2,829
REXO2	7,224	4,871	4,520	3,856	0,611	-2,808
REXO2	6,388	3,935	3,802	3,110	0,566	-2,772
H1F0	8,257	5,200	5,339	6,237	0,677	-2,665
SOCS4	7,965	5,084	5,427	5,427	0,667	-2,652
CALN1	6,617	3,907	3,368	4,843	0,610	-2,577
SNX16	7,421	5,327	4,228	5,327	0,668	-2,460
NRDE2	6,848	4,743	4,375	4,056	0,641	-2,457
THEMIS2	6,380	4,099	4,099	3,805	0,627	-2,379
MRPL15	7,558	5,355	5,475	4,766	0,688	-2,359
ENPP2	6,485	3,110	5,352	4,059	0,644	-2,311
LHFPL2	6,590	4,686	4,127	4,176	0,657	-2,260
ZNF418	5,272	2,753	3,169	3,177	0,575	-2,239
CENPC	6,351	3,790	4,273	4,273	0,648	-2,239
MTSS1	5,737	3,577	3,564	3,449	0,615	-2,207
TIAM1	6,613	4,764	4,862	3,851	0,679	-2,120
DMXL2	6,355	4,065	4,494	4,170	0,668	-2,112
CREB1	6,668	5,609	4,854	3,263	0,686	-2,093
CCDC112	5,859	3,925	3,469	3,928	0,644	-2,085
CCDC112	6,092	4,212	3,930	3,914	0,660	-2,073
C11orf54	6,328	4,564	4,342	3,913	0,675	-2,054
TMEM155	6,581	4,226	3,747	5,621	0,688	-2,050
RDH10	5,618	3,495	3,541	3,689	0,636	-2,043
CPLX1	5,008	2,969	2,915	3,146	0,601	-1,999
SYK	6,608	4,669	4,669	4,522	0,699	-1,988
AKNA	5,859	4,198	3,995	3,428	0,661	-1,985
COQ10B	5,409	3,719	3,170	3,390	0,634	-1,982
EIF2AK3	4,838	2,954	2,922	2,773	0,596	-1,955

DOCK1	6,059	4,077	3,969	4,365	0,683	-1,922
DPPA4	5,150	3,005	3,450	3,286	0,630	-1,903
ITCH	5,862	4,088	3,829	4,063	0,681	-1,868
DUSP18	5,780	4,071	4,158	3,511	0,677	-1,866
DOCK1	4,584	2,760	2,730	2,701	0,596	-1,854
CCDC107	6,065	5,888	3,338	3,481	0,698	-1,829
CALN1	5,542	3,735	3,350	4,174	0,677	-1,789
GNE	5,749	3,726	3,932	4,253	0,691	-1,779
LMO7	5,038	3,299	3,326	3,154	0,647	-1,778
MAN1A1	5,541	3,692	3,888	3,932	0,693	-1,703
CCNT1	5,526	3,995	4,067	3,422	0,693	-1,698
LOC100506797	4,791	3,007	3,470	3,026	0,661	-1,623
SH3RF1	4,585	3,094	3,042	2,925	0,659	-1,565
ENPEP	4,782	3,176	3,277	3,277	0,678	-1,538
SMAD1	5,140	3,588	2,995	4,260	0,703	-1,526
GP1BA	4,800	3,432	3,310	3,089	0,683	-1,523
PLEKHA1	4,516	2,577	3,597	2,892	0,669	-1,494
CIDECP	4,714	3,254	3,287	3,134	0,684	-1,489
WSB1	4,912	4,250	3,390	2,676	0,700	-1,473
MRPS11	4,883	3,510	3,649	3,146	0,703	-1,448
NDUFS2	4,843	3,631	3,399	3,206	0,705	-1,431
TMEM181	4,665	3,347	3,347	3,014	0,694	-1,429
RRAGD	4,356	3,046	2,986	2,782	0,674	-1,418
GALK2	4,650	3,450	3,054	3,250	0,699	-1,399
SUFU	4,342	3,017	2,980	2,875	0,681	-1,385
TRAK1	4,627	3,098	3,423	3,219	0,702	-1,380
BCAR3	4,489	3,037	3,137	3,205	0,696	-1,363
CNN2	4,192	3,095	3,067	2,414	0,682	-1,334

6

Chapter 7

General Discussion

The hematopoietic stem cell (HSC) maintains all the different cells present in our blood during our life by a delicate and balanced process of both self-renewal and differentiation. These processes are controlled by intricate networks of many signaling pathways regulating the different lineage choices. Most of the cells from the different cell lineages develop within the bone marrow (BM) except for T cells that need another specialized environment, which is provided by the thymus[1]. In mice, T-cell development has been studied extensively and in depth due to availability of transgenic mice, which enables studying the effects of genes on T-cell development. In addition, different *ex vivo* and *in vitro* assays exist to study development of T cells, such as gene expression studies of subsets, fetal thymic organ cultures (FTOC) and cocultures on different OP9 stromal cell lines to study kinetics and differentiation potential of precursor populations. For studies on human T-cell development researchers were only able to use these last assays as transplantation assays that supported human T-cell development were not available. With the development of humanized mouse models these assays have become available as now it is possible to transplant human precursor populations in severely immunodeficient mice that do allow for development of human lymphoid cells[2-4].

In this thesis, one of these immunodeficient mouse strains has been used to study different aspects of human T-cell development in an *in vivo* setting. Using these mice with an optimized transplantation protocol provided new insights in human T-cell development, thereby demonstrating the localization of several developmental checkpoints. Furthermore, this approach was used together with whole exome sequencing to determine the gene causative for a form of atypical severe combined immunodeficiency (SCID) and the precise developmental arrest. By overexpression of *LMO2* in HSPCs, it was demonstrated how *LMO2* can cause aberrant human T-cell development.

Humanized mouse models

Transgenic mouse models have been proven very useful in studies on hematopoiesis, as the effects of overexpression and absence of genes can be studied and more insight into underlying mechanisms can be obtained. Many of the obtained data can be extrapolated to humans, however, for T-cell development there are also many differences, as observed for mouse models of SCID compared to patient phenotypes. This disease, which is characterized by a deficiency of functional T cells, can be caused by mutations in several genes as described in **chapter 1**. The mouse model for RAG1-SCID mirrors the human situation in peripheral blood as both patients and mice show a deficiency in both T cells in B cells[5]. On the other hand, *Il7ra* knockout mice suffer from a deficiency in B cells besides their T-cell deficiency[6], while this is not observed in IL7RA-SCID patients[7]. This illustrates that some genes have comparable function in both humans and mice while other genes might have additional functions in one of the species.

The development of humanized mouse models[2-4] has allowed for studies on human hematopoiesis[8]. In **chapter 2** it was demonstrated that with a short culture a robust engraftment was obtained using one of these mouse models, the NOD/Scid-Il2rg^{-/-} (NSG), with outgrowth of different cell lineages. Both T cells and B cells that did develop were functional and secondary transplantations were performed, which demonstrated that the hematopoietic stem cells (HSCs) were not exhausted. Most importantly, the optimized protocol did allow for transplantation of HSPCs obtained from cryopreserved human bone marrow (BM). The level of engraftment of BM-derived HSPCs was lower as compared to mice transplanted with cord blood-derived HSPCs but both lineage development and relative abundance of different cell types was highly comparable. This made it possible to perform studies on arrests in development for different types of SCID as described in **chapter 3** and **chapter 4**.

One drawback of humanized mouse models is the xenograft setting; what effect does this have on selection of T-cell progenitors and to what extent are cytokines cross-reactive? T-cell progenitors undergo both positive and negative selection in the thymus whereby binding to MHC is crucial. Most probable, the progenitors will be selected on murine MHC as expressed by the thymic epithelial cells but also on human MHC, which is expressed on dendritic cells and B cells that did develop from transplanted HSPCs and have migrated to the thymus[9]. This is illustrated by the finding that both murine MHC restricted[4] and human MHC restricted responses have been detected in humanized mice[2, 4, 10]. In addition, the same populations were found both in thymi from engrafted NSG mice as in *ex vivo* human thymi as described in **chapter 2**. By studying the migrational patterns of thymocytes on slices of murine and human thymus it was demonstrated that these patterns were not altered when human thymocytes were put on murine thymic stroma and that migration was induced by the same chemokines in both species[11]. Collectively, these results demonstrate interspecies crosstalk and suggest no large abnormalities in thymocyte selection in this xenograft setting. In addition, it was demonstrated in **chapter 3** that the relative frequencies of different stages of B-cell precursor populations in the BM of transplanted NSG mice is highly comparable to the corresponding *ex vivo* BM aspirate of the donor. This further validates the use of this model for studies on human lymphopoiesis.

Different adaptations have been made to the NSG mouse model that, depending on the research question, might lower interspecies burdens. Human leukocyte antigen (HLA)-A2 transgenic NSG mice have been generated[12] and they have been compared side by side with NSG mice[9]. No differences in conventional human T-cell development were observed between the two strains and this was not different from fetal and postnatal human thymi[9]. In addition, we have detected a normal polyclonal TCR repertoire in humanized NSG mice (see **chapter 3**), thereby demonstrating that MHC differences did not lead to development of a skewed repertoire of the TCR. However, it was found that in both normal NSG mice and HLA-A2[+] NSG mice transplanted with human hematopoietic stem and progenitor cells (HSPCs) there were differences in FOXP3^{+} thymocytes when compared to human thymi, probably caused by lack of cytokine crosstalk[9].

It has also been suggested that there is restricted crosstalk in cytokines needed for myeloid development, such as M-CSF. To overcome this, the MITRG and MISTRG mouse strains have been developed[13]; both are *Rag2^{-/-}Il2rg^{-/-}* mice that are knock-ins for the human alleles of M-CSF, IL-3/GM-CSF and TPO and the MISTRG mice are also transgenic for the human SIRPα gene.

7

SIRPα recognizes CD47, which is expressed on hematopoietic cells, and this interaction reduces phagocytosis of the transplanted human cells[14]. Both mouse strains better support the development of human myeloid cell subsets and NK cells and functionality[13]. Although NSG mice are severely immunodeficient, a sublethal dose of irradiation is needed for efficient engraftment of human HSPCs. Irradiation causes the release of free radicals and cytokines, which might have effect on the fitness of the HSPCs that will be transplanted thereafter. To circumvent this problem, NSG mice carrying a mutation in their Kit receptor have been created[15]. The ligand of this receptor is stem cell factor (SCF) a cytokine needed for stem cell self-renewal. The murine stem cells in the NSG-Kit^{-/-} mouse are unfit as their receptor cannot respond to SCF and therefore they will be outcompeted upon transplantation of other HSPCs. Therefore, irradiation prior to transplantation is not needed in these mice, which allows for better studies on HSC capacities and clonality as demonstrated by an increased SCID repopulating cell (SRC) frequency in these mice (also called NSGW41) when compared to normal NSG that were irradiated prior to transplantation[15]. Strikingly, these NSGW41 had higher engraftment of human cells in their peripheral blood when transplanting limiting cell numbers and demonstrated better outgrowth of myeloid cells compared to NSG mice. It would be interesting to study the addition of human genes for cytokines, as in the MITRG and MISTRG mouse strains, in the NSGW41 strain on development of different cell lineages, their subsets and functionality.

Checkpoints in human T-cell development

Much of the knowledge on T-cell development stems from murine studies as previously human T-cell development could only be studied *ex vivo* or *in vitro*. This has changed with the development of the different humanized mouse models. However, murine T-cell development remains better characterized with the description of markers for many subpopulations, especially of the early double negative (DN) compartment in the thymus[16]. Human and murine T-cell development are comparable with respect to the following; the most immature populations are in de CD4^{-}CD8^{-} DN compartment, immature single positive (ISP) cells develop into CD4^{+}CD8^{+} double positive (DP), which after selection become either CD4^{+} or CD8^{+} single positive (SP)[17]. However, ISP are CD8^{+}CD3^{-} in mice while CD4^{+}CD3^{-} in humans and the markers described to characterize the murine DN compartment are not applicable to human T-cell progenitors[18]. This, combined with the fact that the phenotype in transgenic mice is not always comparable to the phenotype observed in patients, illustrates that there are also many interspecies differences and not all murine data can be extrapolated to human T-cell development.

The data described in **chapter 3** demonstrates that mutations in genes causative for SCID, such as IL7RA and IL2RG, show a phenotype different from their corresponding mouse mutants. When HSPCs from either IL7RA- or IL2RG-SCID were transplanted in NSG mice a very early block in T-cell development was observed, probably caused by an immediate need of signaling through these receptors after thymic entry. Also in normal thymopoiesis a restriction in the

number of hematopoietic clones was observed between HSCs sorted from BM and DN1/2 cells sorted from thymi of NSG mice transplanted with barcoded HSCs (see **chapter 5**). This might be correlated with cytokine driven expansion of a limited number of clones directly after seeding of the thymus. It has indeed been suggested that IL-7 and SCF have both a proliferative and survival effect on early thymocytes[19, 20]. Both in Il7r^{-/-} and Il2rg^{-/-} mice the defect in survival of early thymocytes could be rescued by expression of the anti-apoptosis Bcl2 protein[21, 22]. It is unknown whether in human T-cell development IL-2 and IL-7 play the same role, however, in **chapter 3**, we show an early block in T-cell development for both IL2RG- and IL7RA-SCID. Using TREC analysis it was demonstrated that DN cells have a high proliferative history[23]. Combined with the clonal restriction in these same stages as described in **chapter 5** this might suggest that also in human T-cell development there is expansion of a limited number of hematopoietic clones, which could be driven by IL-2 and IL-7.

In human T-cell development the point of β-selection has been ascribed to different stages; the immature single positive (ISP)[24-26] or the DN3 stage[17]. Transplantation of Artemis-SCID HSPCs in the NSG mouse model demonstrated that the initiation of *TRB* rearrangement might be earlier than previously described (**chapter 3**), namely at the CD7^{+}CD5^{+}CD1a^{-} DN stage. The number of hematopoietic clones was also decreased between the DN1/2 and DN3 stage, in which DN3 was characterized by expression of CD1a (**chapter 5**). It remains difficult to determine the precise stage of β-selection as the DN compartment of human T-cell progenitors is not characterized in detail and different markers are being used. Based on above described data, a model of human T-cell developmental stages is herewith proposed (Fig. 1) that indicates the checkpoints that we described.
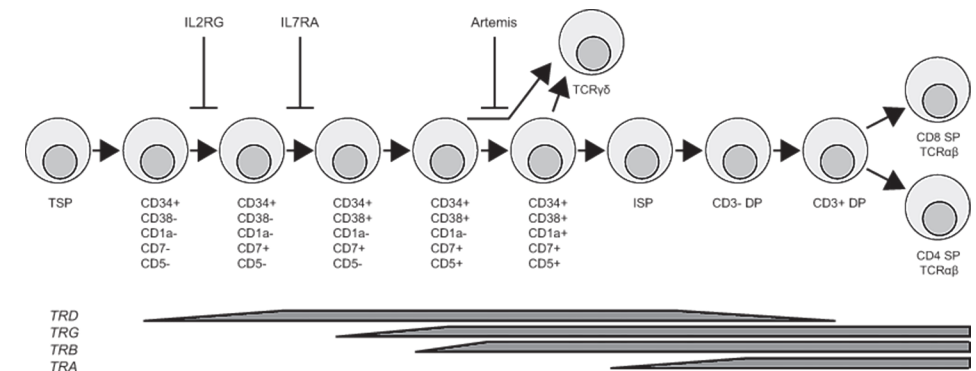

Figure 1: Proposed model of human T-cell development. Model based on data described in chapter 3 and literature indicating the arrests in human T-cell development for different types of SCID. Indicated are the stages of rearrangement of T cell receptor (TR) loci and markers to identify different stages in the CD4^{-}CD8^{-} double negative (DN) compartment. TSP; thymus seeding progenitor, ISP; immature single positive, DP; double positive (CD4^{+}CD8^{+}), SP; single positive.

In this thesis, we demonstrated the arrests in T-cell development for SCID caused by mutations in 3 different genes, for which patients were selected with a null mutation (i.e. no residual activity of the mutated protein). Many patients exist that do have residual activity of the protein

depending on the type of mutation. These patients often present with an atypical form of SCID, such as Omenn syndrome. Omen syndrome is most often caused by hypomorphic mutations in *RAG1*[27] or *RAG2*[28] but has, for instance, also been described for *CORO1A* mutations[29]. It was even demonstrated that similar mutations in *RAG1* can lead to a diverse clinical presentation probably caused by differences in endogenous antigenic challenge and environmental factors[30]. Furthermore, upon transplantation of HSPCs from a RAG2-SCID patient in the described NSG mouse model, it was observed that there was indeed a deficiency in both T cells and B cells in the peripheral blood as in the patient. However, in the thymus there was development until the CD3⁻CD4⁺CD8⁺ double positive (DP) with rearrangement of *TRD*, *TRG* and *TRB* (unpublished data). This demonstrates that even the patients that phenotypically present as a null mutant, might still have residual activity and therefore not be a molecular null mutant. In **chapter 3** it was already demonstrated that a hypomorphic IL2RG-SCID indeed is different from the null mutant after transplantation in the NSG mouse. Therefore, it would be interesting to study patients with different mutations in the same gene in the humanized NSG model to obtain more insights into the functional effects of various mutations on T-cell development.

Identification of new types of SCID

In addition to studying hypomorphic patients, the described NSG model can also be used to study patients suspected of SCID with atypical presentation. This will enable the exclusion of niche factors and determine whether the presumed defect is intrinsic to the hematopoietic cells. Using this approach it was determined that a girl with an atypical presentation of SCID indeed suffered from T⁻B⁺NK⁺-SCID and that the arrest in T-cell development was at the DP to single positive (SP) transition (see **chapter 4**). Although disease characteristics of SCID with unknown genetic cause can be studied using this murine model, unfortunately, the duration of this type of experiments is too long to aid in diagnosis in this type of patients.

Whole exome sequencing (WES) of the patient and both parents was performed to search for the underlying genetic defect after exclusion of known SCID-causing genes by Sanger sequencing. Previously, WES of a patient and her parents has led to the discovery of a mutation in CARD11, which was thereby inactivated, and led to the development of SCID[31]. Casanova *et al.*, have postulated guidelines for studies on genetic causes for primary immunodeficiencies[32]. Primary immunodeficiency is a group of inherited rare diseases and therefore studies on disease causing genetic aberrations often rely on single patients. Thereby, it is more difficult to determine the affected gene in a single patient as compared to other types of diseases where more patients are available. As the analysis is more difficult in these case studies, the candidate gene needs to be validated in different assays. This can be done by cellular assays or animal models. However, most of the genes that are causative in inborn errors of immunity have been discovered in single patients[32]. Only after publication of the study that identifies the first patient, other patients can be screened for the same gene as not often these patients would present in the same center. In **chapter 4** we have identified a heterozygous *de novo* mutation in *VPS4B* using WES in a SCID patient with atypical presentation. By transplanting patient derived

CD34⁺ cells in the NSG mouse model, an arrest in T-cell development was demonstrated at the DP stage, which led to a T-cell deficiency in peripheral blood. We hypothesize that the identified mutation translates into a dominant negative form of VPS4B protein that might affect TCR signaling. However, confirmation by functional experiments is still needed. The results described in **chapter 4** potentially link a new gene to the development of T⁻B⁺NK⁺-SCID.

Newborn screening

Newborn screening for SCID is implemented in many states in the USA and more countries might follow. In the Netherlands, the "Gezondheidsraad" (Health Council) has advised the Minister of Health to implement SCID, amongst other diseases, in the newborn screening[33]. This will be performed by TREC analysis on Guthrie card dried blood spots, which will detect T cell lymphopenia[34]. If tested positive, the patient will be referred for testing of the underlying defect. There already exists a fraction of SCID patients for whom the underlying genetic defect remains unknown, ranging from 7 to 33% of SCID patients[35-39], and when included in newborn screening the incidence of SCID might increase and thereby also the number of SCID patients with unknown cause. Using WES analysis of the SCID patient and both parents new genes can be identified. Combined with a gene therapy approach, the patient cells could be transplanted in NSG mice to confirm the causative effect of the gene and determine the stage of arrest(s) in lymphoid development in mice transplanted with untransduced HSPCs. Other patients that are suspected to suffer from SCID from the newborn screening could then also be screened for these newly identified genes. Newborn screening will lower the age of diagnosis for more SCID patients and this might benefit their outcomes after transplantation as it has been demonstrated that the survival after hematopoietic stem cell transplantation (HSCT) before the age of 3.5 months is higher[40]. In France, it has been calculated that transplantation before 3.5 months of age will be cost-effective[41].

T-ALL development in gene therapy trials by insertional mutagenesis

HSCT provides a cure for SCID; however survival is worse when a matched donor is not available[42]. Gene therapy might be an alternative and for many types of SCID, there are studies either in a clinical trial[43, 44] or in a preclinical phase[45-48]. Initial clinical trials for X-linked SCID (caused by mutations in *IL2RG*) and ADA-SCID have shown to be successful, but unfortunately 5 out of 20 IL2RG-SCID patients treated with gene therapy developed T-ALL caused by insertional mutagenesis (see **chapter 1**). Development of T-ALL caused by insertional mutagenesis was also found in 6 out of 10 treated patients in a gene therapy trial for Wiskott-Aldrich Syndrome (WAS), which is also a primary immunodeficiency, using a same type of vector as the initial trials for X-linked SCID and ADA-SCID[49]. Trials initiated thereafter made use of newly developed and safer SIN-lentiviral or SIN-gammaretroviral vectors and up to now no leukemias have been observed in treated patients[50-52].

What remains striking is that ADA-SCID patients did not develop T-ALL after gene therapy while similar gammaretroviral vectors have been used as in the other trials in which expression of the transgene was driven by the long terminal repeat (LTR)[53-56]. The T-ALLs that developed in the X-linked SCID trials and the WAS trial all had an integration in or nearby *LMO2*, a gene frequently upregulated in T-ALL[49, 55, 56]. LMO2 is normally highly expressed in HSCs and is downregulated early in human T-cell development[57]. In the ADA-SCID trials these integrations were also found in cells from peripheral blood of treated patients but no leukemia development was observed[58]. It remains a question why T-ALL did not develop in the ADA-SCID trials. The most likely answer is the difference in disease background[44].

SCID disease background

In **chapter 3** the stages of arrest in development were studied for different types of SCID including X-linked SCID and ADA-SCID. For X-linked SCID, caused by a mutation in *IL2RG*, a very early arrest just after seeding of the thymus was observed. It has been reported by Kohn *et al.* that in these patients there is no aberrancy in prethymic commitment and that effects of *IL2RG* deficiency will most likely be present in the thymus and not in the thymus seeding progenitor (TSP)[59]. For ADA-SCID no phenotype could be observed after transplantation in the NSG mouse model, most likely caused by complementation of murine ADA as this enzyme is also secreted. Therefore it remains elusive where the arrest in human T-cell development is in ADA-SCID patients. Joachims *et al.* have mimicked this by inhibition of ADA in human cells in FTOC and have observed a gradual decrease of populations during development most severely affecting the more mature populations[60]. However, the data obtained from transplantation of ADA-SCID derived HSPCs in NSG mice does demonstrate that in a gene therapy setting the transduced cells might have a bystander effect of the non-transduced cells thereby decreasing the selective pressure. For X-linked SCID the block in development is very early; at a normally high proliferative stage. The cells that were transduced with the correct version of *IL2RG* will have a highly selective advantage, as the block is alleviated, and undergo rapid expansion. When LMO2 expression is not downregulated due to insertional mutagenesis, this will give additional proliferative advantage during T-cell development. It was indeed observed in **chapter 6** that overexpression of *LMO2* in HSPCs, which were transplanted in NSG mice, gives rise to accelerated human T-cell development leading to higher frequencies of T cells in peripheral lymphoid organs together with an altered CD8/CD4 ratio. In addition, a delay in development was observed in some but not all mice confirming previous data obtained from *in vitro* studies[57]. Together with an accumulation of CD3- DP cells this study indicates three different mechanisms by which *LMO2* overexpression affects human T-cell development.

WAS patients do have low T-cell numbers in their peripheral blood, which have reduced functionality, and it is thought that this decrease is caused by diminished thymic output[61]. As WAS protein (WASP) deficiency affects migrational properties[62], it might be that the arrest in T-cell development is leaky and caused by the lowered capacity to migrate through the thymus during development. It would be of interest to determine the stage of arrest in human T-cell

development for WAS patients. Knowledge on the stage of arrest might provide more insights into the mechanisms of ectopic expression of LMO2 on T-ALL development in these patients and whether this is comparable to the mechanisms in X-linked SCID.

In a gene therapy trial for X-linked chronic granulomatous disease (X-CGD), using a gammaretroviral vector driving expression of the transgene by the LTR, insertional mutagenesis in *EVI1* resulted in the development of myelodysplasia. X-CGD can be caused by a mutation in *GP91phox* that affects the phagocytic capacity of neutrophils. These cells belong to the myeloid lineage and therefore myeloid cells that are transduced with the correct version of *GP91phox* will most probably have a selective advantage over their non-transduced counterparts. In WAS, all lineages are affected and in the above described gene therapy trials for WAS patients did develop both T-ALL and acute myeloid leukemia (AML) due to insertional mutagenesis. Leukemia of B cells and/or NK cells has not been observed in the gene therapy trial for WAS. Also in the X-linked SCID trials, in which beside the T cells also the NK cells are affected by IL2RG deficiency, leukemia in NK cells was not observed. It could be that the selective advantage for B cells and NK cells over untransduced cells is not as great as for T cells and myeloid cells whereby they experience less selective pressure leading to lower changes for development of clonal outgrowth of B cells and NK cells.

Assessment of genotoxicity of preclinical viral vectors

As leukemia development by insertional mutagenesis was not observed in preclinical models, new screening methods for genotoxicity have been developed. The *in vitro* immortalization (IVIM) assay screens for clonal outgrowth of transduced lineage-negative murine BM cells using a limiting dilution assay[63]. Using this assay, different designs of vectors can be screened in a preclinical stage to determine their genotoxicity in a relatively short period. However, it is a myeloid skewed assay and thereby it is unknown how accurate the predictions will be for development of T-ALL due to the stringent selective pressure during T-cell development, which might be different from the limiting dilution used in this assay. A different assay makes use of lineage-negative BM cells of tumor-prone *Cdkn2a-/-* mice that are then transduced with different designs of viral vectors and transplanted in wildtype mice[64]. The advantage of this model is the *in vivo* readout by tumor development, although the selective advantage over uncorrected cells, as present in a gene therapy setting, is not there. Both assays make use of murine BM-derived cells, but as indicated, differences exist between human and murine lymphoid development. In **chapter 6** it was demonstrated that the humanized NSG model can be used to study the effects of LMO2 overexpression in human cells. The same model might be used to study insertional mutagenesis in human cells. Experiments to assess genotoxicity of viral vectors in NSG mice have been performed by transplanting CD34+ cells that were transduced by an LTR-driven gammaretroviral vector in these mice[65]. Presence of dominant clones was observed in transplanted NSG mice, however, no tumor development was observed as was in the *Cdkn2a-/-* mouse model. It was speculated that longer duration (more than 6 months) of experiments would be needed or secondary transplantations to observe

insertional mutagenesis caused leukemias. In conclusion, there is currently no accurate model to determine genotoxicity of integrating viral vectors in human cells in a preclinical setting that will be predictive for the clinical setting, at least for lymphoid leukemias.

Up to now, insertional mutagenesis in gene therapy trials has only been observed when gammaretroviral constructs driving expression of the transgene from the viral LTR were used. During preclinical testing in mouse models insertional mutagenesis leading to development of T-ALL has not been observed. As described in **chapter 1**, clinical trials for primary immunodeficiencies are currently based on using selfinactivating (SIN) vectors that drive expression of the transgene from in internal promoter thereby decreasing enhancer activities on nearby genes. Recently, alpharetroviral vectors have been demonstrated to be successful in correcting X-linked chronic granulatomous disease (CGD) in preclinical models[66]. These vectors have a more safe integration profile than both gammaretroviral and lentiviral vectors, which lowers the chance of insertional mutagenesis[67]. However, viral vectors need integration in the host genome for stable expression and this remains random whereby the chance of insertional mutagenesis will always remain.

Targeted strategies for gene correction

Correcting the genetic defect itself instead of expressing a correct version of the affected gene would allow for physiological expression and normal regulation of the gene without the need for random integration of a viral vector. This strategy is being tested by many different labs using different technologies. Genovese *et al.*, have used zinc finger nucleases (ZFNs), which generate a site-specific double strand break (DSB) in the DNA together with an integrase-defective lentiviral vector (IDLV) encoding a gene targeting construct for *IL2RG*[68]. Hereby, they corrected the IL2RG mutation in HSCs from an X-linked SCID patient and after transplantation in NSG mice there was restored development of both T cells and NK cells. Another approach makes use of patient-derived induced pluripotent stem cells (iPSCs) combined with transcription activator-like effector nucleases (TALENs) to correct the mutation in *IL2RG*[69]. *In vitro* it was shown that corrected cells could differentiate into both T cells and NK cells while the uncorrected cells could not. The advantage of these types of approaches is the site-specific correction thereby circumventing the chance for insertional mutagenesis. However, the number of cells that can be specifically targeted by these strategies at this moment remains low as compared to viral transduction, which is used currently in gene therapy clinical trials. Another repair approach utilizes the CRISPR/Cas9 system in which guide RNAs target the Cas9 endonucleases to the gene of interest, which is mutated, to generate DSBs[70]. When the correct version of the gene is introduced as well, this can be used as template to repair the DSB by homologous recombination thereby correcting the mutation. This has not been used for SCID yet, but proof of principle has been obtained by correcting a mutation in *CFTR*, which can cause cystic fibrosis, in organoid cultures and thereby restoring functionality[71]. The CRISPR/Cas9 system is easier to adapt for different targets, by changing the sequence of the guide RNA, and results in comparable or higher targeting efficiencies than ZFNs or TALENs and therefore is a promising

tool for future site-specific gene therapy[72]. However, to obtain enough cells for transplantation into patients after site-specific gene correction, even higher targeting efficiencies or better stem cell expansion protocols will be needed.

Future perspectives

Knowledge on human T-cell development lags behind that of murine T-cell development. Using humanized mouse models, the role of genes on human T-cell development can now be studied in an *in vivo* setting by transplantation of human null mutants and other patient samples, which will provide new insights. As SCID is a rare disease, the availability of human SCID derived HSPCs is limited. Potentially, this could be circumvented by exploiting the CRISPR/Cas9 system to induce DSBs in genes of interest in cord blood-derived $CD34^+$ cells. Repair of these DSBs can occur via non-homologous end-joining (NHEJ), leaving insertion/deletion (indel) mutations that can lead to frameshift mutations and premature stopcodons[73]. Introduction of the targeting sequence together with Cas9 and a reporter gene can be performed by lentiviral transduction[74]. In addition, the function of genes that are known to be important in murine T-cell development and of which the role in human T-cell development is unknown, such as *TCF7* deficiency[75], could be tested using this system. Screening for knockouts is easy when the targeted gene normally results in a protein expressed on the cell surface. These HSPCs could then be sorted after transduction and transplanted in immunodeficient mice. The most preferable model could be the NSGW41; these mice do not need to be irradiated, which could otherwise also affect transplanted HSPCs. As described, without irradiation a better estimation of repopulation capacity can be made. When the targeted gene does not result in a surface-expressed protein, clones would have to be grown to be screened on DNA level. Currently, there are no protocols available that would allow for this expansion while maintaining repopulating capacity of HSPCs.

Furthermore, the above described NSGW41 will be very useful for better characterization of the "true" long-term repopulating (LT)-HSC. The $Lin^-CD34^+CD38^-CD90^+CD45RA^-CD49f^+$ have a LT-HSC frequency of 1 in 10.5 cells[8]. In mice the expression of c-Kit is used for characterization of the HSC compartment. Currently, there is also indication that expression of this receptor on human HSC would confer more potent repopulation activity[15]. Another marker used for isolation of more primitive HSPCs is CD133 of which the expression is, in contrast to CD38, less influenced during culture[76]. Sorting of different fractions of the hematopoietic progenitor compartment and transplantation into non-irradiated NSGW41 mice might help in the search for the "true" LT-HSC and more differentiated progenitors and their developmental potential, which might result in a more defined human hematopoietic developmental hierarchy. As transplantation of single cells remains challenging, barcoding technology[77] (and **chapter 5**) could be used to determine whether progenitors give multi-lineage output or are more restricted. More insights towards the phenotype of human multipotent progenitors and their lineage offspring would be of great interest as also here differences remain between mice and man[78]. As described above, Dick and coworkers have performed many studies on the identification of the human LT-HSC and their multipotent offspring. As the T-cell potential was not studied in their *in vivo* experiments, it remains difficult to determine presence of common progenitors for different lymphoid lineages and when this potential diverges.

7

An impracticality of the existing data on human T-cell development is the different antibodies that have been used by different labs when studying human T-cell development. Combining these antibody panels would allow for integration and better comparison of existing datasets. However, antibody panels for flow cytometry are limited to a maximum of 17 antibodies per panel[79]. Therefore, integration of data would only be able if multiple panels would be designed, which will need to have substantial overlap to be able to compare data from different tubes. Recently, a new technology has been developed combining flow cytometry with mass spectrometry, which is called cytometry by time-of-flight (CyTOF)[80, 81]. Instead of labelling antibodies with a fluorochrome, they are labelled with rare earth metal isotopes. As there is no spectral overlap, compensation of signals is not needed and currently more than 40 parameters can be measured simultaneously which in the future might extend up to 100 parameters[82]. This technique would allow for the inclusion of most of the markers used by different research groups, in order to generate a comprehensive overview of human T-cell development. Especially, more insight in the DN compartment would be very useful to better stage arrests in development for different types of SCID and to better define ETP-ALL, a type of T-ALL of very immature phenotype with poor prognosis[83]. Potential new populations of progenitors could then be sorted with their defining markers using regular flow cytometry and their developmental potential could be studied using the OP9-DL1 coculture system[84]. Furthermore, these sorted populations could be used for expression analysis and analysis of rearrangement of TCR loci, as has been performed previously for the known populations of human T-cell development[17]. Together this might provide more insights into signaling networks regulating TCR rearrangements and may provide targets for treatment of ETP-ALL. Insights in the earliest progenitor within the human thymus might provide insights towards the phenotype of the elusive human thymus seeding progenitor, for which many phenotypes have been proposed so far[85-88].

References

1. Rothenberg, E.V. Transcriptional control of early T and B cell developmental choices. *Annu Rev Immunol* 2014, **32**: 283-321.

2. Ishikawa, F., *et al.* Development of functional human blood and immune systems in NOD/SCID/IL2 receptor {gamma} chain(null) mice. *Blood* 2005, **106**(5): 1565-1573.

3. Shultz, L.D., *et al.* Human lymphoid and myeloid cell development in NOD/LtSz-scid IL2R gamma null mice engrafted with mobilized human hemopoietic stem cells. *J Immunol* 2005, **174**(10): 6477-6489.

4. Traggiai, E., *et al.* Development of a human adaptive immune system in cord blood cell-transplanted mice. *Science* 2004, **304**(5667): 104-107.

5. Mombaerts, P., *et al.* RAG-1-deficient mice have no mature B and T lymphocytes. *Cell* 1992, **68**(5): 869-877.

6. Peschon, J.J., *et al.* Early lymphocyte expansion is severely impaired in interleukin 7 receptor-deficient mice. *J Exp Med* 1994, **180**(5): 1955-1960.

7. Puel, A., Ziegler, S.F., Buckley, R.H., Leonard, W.J. Defective IL7R expression in T(-)B(+)NK(+) severe combined immunodeficiency. *Nat Genet* 1998, **20**(4): 394-397.

8. Notta, F., *et al.* Isolation of single human hematopoietic stem cells capable of long-term multilineage engraftment. *Science* 2011, **333**(6039): 218-221.

9. Halkias, J., *et al.* Conserved and divergent aspects of human T-cell development and migration in humanized mice. *Immunol Cell Biol* 2015.

10. Marodon, G., *et al.* High diversity of the immune repertoire in humanized NOD.SCID.gamma c-/- mice. *Eur J Immunol* 2009, **39**(8): 2136-2145.

11. Halkias, J., *et al.* Opposing chemokine gradients control human thymocyte migration in situ. *J Clin Invest* 2013, **123**(5): 2131-2142.

12. Shultz, L.D., *et al.* Generation of functional human T-cell subsets with HLA-restricted immune responses in HLA class I expressing NOD/SCID/IL2r gamma(null) humanized mice. *Proc Natl Acad Sci U S A* 2010, **107**(29): 13022-13027.

13. Rongvaux, A., *et al.* Development and function of human innate immune cells in a humanized mouse model. *Nat Biotechnol* 2014, **32**(4): 364-372.

14. Takenaka, K., *et al.* Polymorphism in Sirpa modulates engraftment of human hematopoietic stem cells. *Nat Immunol* 2007, **8**(12): 1313-1323.

15. Cosgun, K.N., *et al.* Kit regulates HSC engraftment across the human-mouse species barrier. *Cell Stem Cell* 2014, **15**(2): 227-238.

16. Ramond, C., *et al.* Two waves of distinct hematopoietic progenitor cells colonize the fetal thymus. *Nat Immunol* 2014, **15**(1): 27-35.

17. Dik, W.A., *et al.* New insights on human T cell development by quantitative T cell receptor gene rearrangement studies and gene expression profiling. *J Exp Med* 2005, **201**(11): 1715-1723.

18. Weerkamp, F., Pike-Overzet, K., Staal, F.J. T-sing progenitors to commit. *Trends Immunol* 2006, **27**(3): 125-131.

19. Petrie, H.T., Zuniga-Pflucker, J.C. Zoned out: functional mapping of stromal signaling microenvironments in the thymus. *Annu Rev Immunol* 2007, **25**: 649-679.

7

20. Wang, H., Pierce, L.J., Spangrude, G.J. Distinct roles of IL-7 and stem cell factor in the OP9-DL1 T-cell differentiation culture system. *Exp Hematol* 2006, **34**(12): 1730-1740.

21. Kondo, M., Akashi, K., Domen, J., Sugamura, K., Weissman, I.L. Bcl-2 rescues T lymphopoiesis, but not B or NK cell development, in common gamma chain-deficient mice. *Immunity* 1997, **7**(1): 155-162.

22. Maraskovsky, E., *et al.* Bcl-2 can rescue T lymphocyte development in interleukin-7 receptor-deficient mice but not in mutant rag-1-/- mice. *Cell* 1997, **89**(7): 1011-1019.

23. van der Weerd, K., *et al.* Combined TCRG and TCRA TREC analysis reveals increased peripheral T-lymphocyte but constant intra-thymic proliferative history upon ageing. *Mol Immunol* 2013, **53**(3): 302-312.

24. Blom, B., Spits, H. Development of human lymphoid cells. *Annu Rev Immunol* 2006, **24**: 287-320.

25. Soulier, J., *et al.* HOXA genes are included in genetic and biologic networks defining human acute T-cell leukemia (T-ALL). *Blood* 2005, **106**(1): 274-286.

26. Taghon, T., *et al.* Notch signaling is required for proliferation but not for differentiation at a well-defined beta-selection checkpoint during human T-cell development. *Blood* 2009, **113**(14): 3254-3263.

27. Lee, Y.N., *et al.* A systematic analysis of recombination activity and genotype-phenotype correlation in human recombination-activating gene 1 deficiency. *J Allergy Clin Immunol* 2014, **133**(4): 1099-1108.

28. Chou, J., *et al.* A novel homozygous mutation in recombination activating gene 2 in 2 relatives with different clinical phenotypes: Omenn syndrome and hyper-IgM syndrome. *J Allergy Clin Immunol* 2012, **130**(6): 1414-1416.

29. Moshous, D., *et al.* Whole-exome sequencing identifies Coronin-1A deficiency in 3 siblings with immunodeficiency and EBV-associated B-cell lymphoproliferation. *J Allergy Clin Immunol* 2013, **131**(6): 1594-1603.

30. IJspeert, H., *et al.* Similar recombination-activating gene (RAG) mutations result in similar immunobiological effects but in different clinical phenotypes. *J Allergy Clin Immunol* 2014, **133**(4): 1124-1133.

31. Greil, J., *et al.* Whole-exome sequencing links caspase recruitment domain 11 (CARD11) inactivation to severe combined immunodeficiency. *J Allergy Clin Immunol* 2013, **131**(5): 1376-1383 e1373.

32. Casanova, J.L., Conley, M.E., Seligman, S.J., Abel, L., Notarangelo, L.D. Guidelines for genetic studies in single patients: lessons from primary immunodeficiencies. *J Exp Med* 2014, **211**(11): 2137-2149.

33. Gezondheidsraad. *Neonatale screening: nieuwe aanbevelingen*, vol. 2015/08. Gezondheidsraad: Den Haag, 2015.

34. Puck, J.M. Laboratory technology for population-based screening for severe combined immunodeficiency in neonates: the winner is T-cell receptor excision circles. *J Allergy Clin Immunol* 2012, **129**(3): 607-616.

35. Alsmadi, O., *et al.* Molecular analysis of T-B-NK+ severe combined immunodeficiency and Omenn syndrome cases in Saudi Arabia. *BMC Med Genet* 2009, **10**: 116.

36. Gaspar, H.B., *et al.* How I treat severe combined immunodeficiency. *Blood* 2013, **122**(23): 3749-3758.

37. Kwan, A., *et al.* Newborn screening for severe combined immunodeficiency and T-cell lymphopenia in California: results of the first 2 years. *J Allergy Clin Immunol* 2013, **132**(1): 140-150.

38. Pasic, S., *et al.* Severe combined immunodeficiency in Serbia and Montenegro between years 1986 and 2010: a single-center experience. *J Clin Immunol* 2014, **34**(3): 304-308.

39. Yu, G.P., *et al.* Genotype, phenotype, and outcomes of nine patients with T-B+NK+ SCID. *Pediatr Transplant* 2011, **15**(7): 733-741.

40. Pai, S.Y., *et al.* Transplantation outcomes for severe combined immunodeficiency, 2000-2009. *N Engl J Med* 2014, **371**(5): 434-446.

41. Clement, M.C., *et al.* Systematic neonatal screening for severe combined immunodeficiency and severe T-cell lymphopenia: Analysis of cost-effectiveness based on French real field data. *J Allergy Clin Immunol* 2015.

42. Gennery, A.R., *et al.* Transplantation of hematopoietic stem cells and long-term survival for primary immunodeficiencies in Europe: entering a new century, do we do better? *J Allergy Clin Immunol* 2010, **126**(3): 602-610 e601-611.

43. Persons, D.A. Lentiviral vector gene therapy: effective and safe? *Mol Ther* 2010, **18**(5): 861-862.

44. Persons, D.A., Baum, C. Solving the problem of gamma-retroviral vectors containing long terminal repeats. *Mol Ther* 2011, **19**(2): 229-231.

45. Carbonaro, D.A., *et al.* Preclinical demonstration of lentiviral vector-mediated correction of immunological and metabolic abnormalities in models of adenosine deaminase deficiency. *Mol Ther* 2014, **22**(3): 607-622.

46. Pike-Overzet, K., *et al.* Correction of murine Rag1 deficiency by self-inactivating lentiviral vector-mediated gene transfer. *Leukemia* 2011, **25**(9): 1471-1483.

47. Thornhill, S.I., *et al.* Self-inactivating gammaretroviral vectors for gene therapy of X-linked severe combined immunodeficiency. *Mol Ther* 2008, **16**(3): 590-598.

48. van Til, N.P., *et al.* Correction of murine Rag2 severe combined immunodeficiency by lentiviral gene therapy using a codon-optimized RAG2 therapeutic transgene. *Mol Ther* 2012, **20**(10): 1968-1980.

49. Braun, C.J., *et al.* Gene therapy for Wiskott-Aldrich syndrome--long-term efficacy and genotoxicity. *Sci Transl Med* 2014, **6**(227): 227ra233.

50. Aiuti, A., *et al.* Lentiviral hematopoietic stem cell gene therapy in patients with Wiskott-Aldrich syndrome. *Science* 2013, **341**(6148): 1233151.

51. Hacein-Bey-Abina, S., *et al.* A modified gamma-retrovirus vector for X-linked severe combined immunodeficiency. *N Engl J Med* 2014, **371**(15): 1407-1417.

52. Hacein-Bey Abina, S., *et al.* Outcomes following gene therapy in patients with severe Wiskott-Aldrich syndrome. *JAMA* 2015, **313**(15): 1550-1563.

53. Aiuti, A., *et al.* Gene therapy for immunodeficiency due to adenosine deaminase deficiency. *N Engl J Med* 2009, **360**(5): 447-458.

54. Gaspar, H.B., *et al.* Hematopoietic stem cell gene therapy for adenosine deaminase-deficient severe combined immunodeficiency leads to long-term immunological recovery and metabolic correction. *Sci Transl Med* 2011, **3**(97): 97ra80.

55. Hacein-Bey-Abina, S., *et al.* Insertional oncogenesis in 4 patients after retrovirus-mediated gene therapy of SCID-X1. *J Clin Invest* 2008, **118**(9): 3132-3142.

56. Howe, S.J., *et al.* Insertional mutagenesis combined with acquired somatic mutations causes leukemogenesis following gene therapy of SCID-X1 patients. *J Clin Invest* 2008, **118**(9): 3143-3150.

57. Pike-Overzet, K., *et al.* Ectopic retroviral expression of LMO2, but not IL2Rgamma, blocks human T-cell development from CD34+ cells: implications for leukemogenesis in gene therapy. *Leukemia* 2007, **21**(4): 754-763.

7

58. Candotti, F., *et al.* Gene therapy for adenosine deaminase-deficient severe combined immune deficiency: clinical comparison of retroviral vectors and treatment plans. *Blood* 2012, **120**(18): 3635-3646.

59. Kohn, L.A., *et al.* Human lymphoid development in the absence of common gamma-chain receptor signaling. *J Immunol* 2014, **192**(11): 5050-5058.

60. Joachims, M.L., *et al.* Restoration of adenosine deaminase-deficient human thymocyte development in vitro by inhibition of deoxynucleoside kinases. *J Immunol* 2008, **181**(11): 8153-8161.

61. Park, J.Y., *et al.* Early deficit of lymphocytes in Wiskott-Aldrich syndrome: possible role of WASP in human lymphocyte maturation. *Clin Exp Immunol* 2004, **136**(1): 104-110.

62. Ochs, H.D., Thrasher, A.J. The Wiskott-Aldrich syndrome. *J Allergy Clin Immunol* 2006, **117**(4): 725-738; quiz 739.

63. Modlich, U., *et al.* Cell-culture assays reveal the importance of retroviral vector design for insertional genotoxicity. *Blood* 2006, **108**(8): 2545-2553.

64. Montini, E., *et al.* Hematopoietic stem cell gene transfer in a tumor-prone mouse model uncovers low genotoxicity of lentiviral vector integration. *Nat Biotechnol* 2006, **24**(6): 687-696.

65. Haemmerle, R., *et al.* Clonal Dominance With Retroviral Vector Insertions Near the ANGPT1 and ANGPT2 Genes in a Human Xenotransplant Mouse Model. *Mol Ther Nucleic Acids* 2014, **3**: e200.

66. Kaufmann, K.B., *et al.* Alpharetroviral vector-mediated gene therapy for X-CGD: functional correction and lack of aberrant splicing. *Mol Ther* 2013, **21**(3): 648-661.

67. Suerth, J.D., *et al.* Alpharetroviral self-inactivating vectors: long-term transgene expression in murine hematopoietic cells and low genotoxicity. *Mol Ther* 2012, **20**(5): 1022-1032.

68. Genovese, P., *et al.* Targeted genome editing in human repopulating haematopoietic stem cells. *Nature* 2014, **510**(7504): 235-240.

69. Menon, T., *et al.* Lymphoid Regeneration from Gene-Corrected SCID-X1 Subject-Derived iPSCs. *Cell Stem Cell* 2015, **16**(4): 367-372.

70. Jinek, M., *et al.* A programmable dual-RNA-guided DNA endonuclease in adaptive bacterial immunity. *Science* 2012, **337**(6096): 816-821.

71. Schwank, G., *et al.* Functional repair of CFTR by CRISPR/Cas9 in intestinal stem cell organoids of cystic fibrosis patients. *Cell Stem Cell* 2013, **13**(6): 653-658.

72. Doudna, J.A., Charpentier, E. Genome editing. The new frontier of genome engineering with CRISPR-Cas9. *Science* 2014, **346**(6213): 1258096.

73. Ran, F.A., *et al.* Genome engineering using the CRISPR-Cas9 system. *Nat Protoc* 2013, **8**(11): 2281-2308.

74. Kabadi, A.M., Ousterout, D.G., Hilton, I.B., Gersbach, C.A. Multiplex CRISPR/Cas9-based genome engineering from a single lentiviral vector. *Nucleic Acids Res* 2014, **42**(19): e147.

75. Tiemessen, M.M., *et al.* The nuclear effector of Wnt-signaling, Tcf1, functions as a T-cell-specific tumor suppressor for development of lymphomas. *PLoS Biol* 2012, **10**(11): e1001430.

76. Drake, A.C., *et al.* Human CD34+ CD133+ hematopoietic stem cells cultured with growth factors including Angptl5 efficiently engraft adult NOD-SCID Il2rgamma-/- (NSG) mice. *PLoS One* 2011, **6**(4): e18382.

77. Gerrits, A., *et al.* Cellular barcoding tool for clonal analysis in the hematopoietic system. *Blood* 2010, **115**(13): 2610-2618.

78. Doulatov, S., Notta, F., Laurenti, E., Dick, J.E. Hematopoiesis: a human perspective. *Cell Stem Cell* 2012, **10**(2): 120-136.

79. Chattopadhyay, P.K., *et al.* Quantum dot semiconductor nanocrystals for immunophenotyping by polychromatic flow cytometry. *Nat Med* 2006, **12**(8): 972-977.

80. Bandura, D.R., *et al.* Mass cytometry: technique for real time single cell multitarget immunoassay based on inductively coupled plasma time-of-flight mass spectrometry. *Anal Chem* 2009, **81**(16): 6813-6822.

81. Bendall, S.C., *et al.* Single-cell mass cytometry of differential immune and drug responses across a human hematopoietic continuum. *Science* 2011, **332**(6030): 687-696.

82. Bendall, S.C., Nolan, G.P., Roederer, M., Chattopadhyay, P.K. A deep profiler's guide to cytometry. *Trends Immunol* 2012, **33**(7): 323-332.

83. Coustan-Smith, E., *et al.* Early T-cell precursor leukaemia: a subtype of very high-risk acute lymphoblastic leukaemia. *Lancet Oncol* 2009, **10**(2): 147-156.

84. Awong, G., *et al.* Characterization in vitro and engraftment potential in vivo of human progenitor T cells generated from hematopoietic stem cells. *Blood* 2009, **114**(5): 972-982.

85. Haddad, R., *et al.* Molecular characterization of early human T/NK and B-lymphoid progenitor cells in umbilical cord blood. *Blood* 2004, **104**(13): 3918-3926.

86. Haddad, R., *et al.* Dynamics of thymus-colonizing cells during human development. *Immunity* 2006, **24**(2): 217-230.

87. Kohn, L.A., *et al.* Lymphoid priming in human bone marrow begins before expression of CD10 with upregulation of L-selectin. *Nat Immunol* 2012, **13**(10): 963-971.

88. Six, E.M., *et al.* A human postnatal lymphoid progenitor capable of circulating and seeding the thymus. *J Exp Med* 2007, **204**(13): 3085-3093.

7

Chapter 8

English summary

A single hematopoietic stem cell (HSC) can make up all the different cells of the immune system. Most of the different cell lineages of the immune system develop in the bone marrow. T cells, however, develop in the thymus where a specialized environment is present. Within the thymus, the T-cell progenitors are selected; T cells that do not recognize antigens and autoreactive T cells are deleted. T cells are needed to fight virus infections, provide help to B cells during bacterial infections and can also be reactive towards tumors.

A multipotent progenitor migrates from the bone marrow, via the bloodstream, to the thymus. After engraftment in the tissue, this progenitor will start to proliferate and develop towards more mature cell types. Once committed to the T-cell lineage, it will start to rearrange different parts in the DNA, T-cell receptor loci that can form a T-cell receptor. This rearrangement provides the great diversity that is present within the T-cell receptors expressed on mature T cells to ensure recognition of many different antigens of, for instance, pathogens.

T-cell development follows a defined path during which the thymus seeding cell will proliferate and differentiate. Most of the knowledge of this development stems from studies performed in mice. The availability of many transgenic mouse strains makes it possible to study the influence of signaling pathways on the development of T cells. Knowledge on the development of human T cells is mainly derived from descriptive studies in which *ex vivo* human thymus material is studied by cellular phenotyping and gene expression analysis or *in vitro* assays as described in **chapter 1**.

There are different diseases in which patients suffer from abnormal T-cell development from which insights can be gained into the pathways regulating human T-cell development. Such diseases include on the one hand Severe Combined Immunodeficiency (SCID), in which there is a block in T-cell development leading to absence of functional T cells, and on the other hand T-cell acute lymphoblastic leukemia (T-ALL) where patients suffer from an accelerated malignant growth of T cells. As it is difficult to study the mechanisms behind both these forms of pathological T-cell development, an optimized *in vivo* model for the study of human T-cell development has been developed that is described in **chapter 2**. As the NOD/Scid-Il2rg$^{-/-}$ (NSG) mice are severely immunodeficient, caused by the absence of NK cells, B cells and T cells, they allow the engraftment of human cells. A short culture of isolated human hematopoietic stem and progenitor cells (HSPCs) allows for possibility of genetically modifying these HSPCs while maintaining robust engraftment of human cells and the development of a human immune system in this mouse. The B cells and T cells that develop within in these mice are able to mount an immune response to an endogenous antigen demonstrating their functionality. The HSCs present in the transplant do engraft in the bone marrow of the mouse and are able to self-renew as illustrated by the fact that bone marrow from primary recipients can fully engraft secondary recipients. In addition, the optimized protocol also leads to good engraftment of HSPCs obtained from human bone marrow and development of the different lymphoid cell types. Together with the finding that thymi from mice engrafted with human hematopoietic cells show comparable human T-cell development to *ex vivo* analyzed human thymus biopsies opened the possibility to study patient material from biobanks.

8

This idea has been exploited in **chapter 3** to study the stages of arrest in human T-cell development for different types of SCID. As from most of the SCID patients no thymic biopsies are taken, the T-cell developmental blocks have remained elusive. Previously, extrapolations have been made from knockout mice. However, it was found that the blocks in human T-cell development for different types of SCID reside at earlier stages then anticipated from these models illustrating the differences between human and murine T-cell development. From the obtained data, a model was proposed that shows and early need for cytokine-driven proliferation directly after seeding of the thymus by progenitors. In addition, the point of β-selection could be attributed to an earlier stage then previously described as demonstrated by the block in development observed for Artemis-SCID. As this study illustrated the power of the model in detecting developmental arrests in development of human lymphoid cells, HSPCs from a patient with atypical presentation of SCID were transplanted in these immunodeficient mice. In **chapter 4** the results of this study are described that confirmed that the patient indeed suffered from T$^-$B$^+$NK$^+$-SCID. The arrest in development was found to reside in the CD4$^+$CD8$^+$ double positive stage. As none of the known SCID-causing genes contained a genetic aberration, whole exome sequencing of the patient and both parents was performed leading to the detection of a heterozygous *de novo* mutation in *VPS4B* in this patient. This gene has not been previously associated with SCID.

Chapter 5 described the severe restriction of hematopoietic clones during human T-cell development demonstrating two restriction points. Despite the severe hematopoietic clonal restriction this limited number of clones can still make up a very diverse polyclonal T-cell receptor repertoire, which is needed to fight different pathogens that are encountered on a daily basis.

In contrast to **chapter 3 and 4**, in which gene deficiencies were studied, the effect of overexpression of *LMO2*, a known oncogene in T-ALL, on human T-cell development was studied. *LMO2* was overexpressed in human HSPCs isolated from umbilical cord blood and these cells were transplanted in the severe immunodeficient NSG mice as described in **chapter 6**. In gene therapy trials for immunodeficiencies, T-ALL did develop in several patients due to insertional mutagenesis. Often the insertion of the therapeutic vector was in or near *LMO2* and resulted in overexpression of this gene causing the development of T-ALL in some patients. Transgenic mouse models for *Lmo2* demonstrated blocks in immature T-cell progenitors and the development of leukemia with a long latency. Using the humanized NSG mouse model, it was demonstrated that *LMO2* overexpression causes aberrant human T-cell development by three different mechanisms; the delayed development as also observed in transgenic mice and *in vitro* assays, an accumulation of CD4$^+$CD8$^+$ double positive cells and accelerated development leading to a higher frequency of mature T cells.

Altogether, this thesis describes novel insights in human T-cell development by transplanting human HSPCs in severe immunodeficient NSG mice. Thereby a model is provided that can further aid both in fundamental studies and can be used for optimization of gene therapy approaches and stem cell expansion protocols. Furthermore, it illustrates (see **chapter 7**) the need for more in depth understanding of human T-cell development, which could help further improve T-cell reconstitution after transplantation in patients and might aid in the diagnosis and future treatment of patients with T-ALL.

8

Nederlandse samenvatting

Een enkele hematopoietische stamcel (HSC) kan door middel van zelfvernieuwing en differentiatie zorgen voor alle verschillende celtypen van het afweersysteem. De meeste van de verschillende typen afweercellen ontwikkelen zich in het beenmerg. Behalve de T-cellen, die hebben een gespecialiseerde omgeving nodig. Deze omgeving vinden zij in de thymus. De thymus is beter bekend als de zwezerik, een orgaan boven het hart dat kleiner wordt vanaf de puberteit. In dit orgaan worden de voorlopers van volwassen T-cellen opgeleid en geselecteerd. Cellen die geen antigenen herkennen of cellen die antigenen van het eigen lichaam herkennen worden daar verwijderd. Als dit niet gebeurt, dan zou dit leiden tot een sterk verhoogde incidentie van auto-immuunziekten, bijvoorbeeld diabetes. Tijdens ons leven hebben we T-cellen nodig om ons te beschermen tegen virusinfecties. Daarnaast helpen ze B-cellen om bacteriële infecties te voorkomen én kan hun respons gericht zijn tegen tumoren.

Een multipotente voorlopercel migreert vanuit het beenmerg, via de bloedsomloop, naar de thymus. Nadat hij daar aankomt, start de voorlopercel met delen (proliferatie) en ontwikkelt hij zich tot een meer volwassen celtype. Daarbij verliest hij geleidelijk zijn multipotentie. Door middel van verschillende signaleringen kunnen er verschillende ontwikkelpaden actief worden in de cel. Als de cel zich ontwikkelt tot een volwassen T-cel, herschikt hij verschillende stukken in het DNA die coderen voor de T-cel receptor. Deze receptor is nodig om antigenen te herkennen. Antigenen zijn stukjes eiwit die worden gepresenteerd door andere cellen aan de T-cel. Door het DNA dat codeert voor de T-cel receptor te herschikken, kan de grote diversiteit worden gegenereerd die nodig is om de vele verschillende antigenen van bijvoorbeeld virussen en bacteriën te kunnen herkennen. Dat zorgt dan weer voor een optimaal functionerend afweersysteem.

Nadat de multipotente voorlopercel is aangekomen in de thymus, begint hij zich te delen en te ontwikkelen (differentiatie) via verschillende stadia. De meeste kennis over deze differentiatie is afkomstig uit studies met muismodellen. Doordat er veel verschillende transgene muismodellen beschikbaar zijn, is het mogelijk om de rol van verschillende signaleringsroutes gedurende de T-cel ontwikkeling te bestuderen. De meerderheid van onze kennis over de ontwikkeling van T-cellen bij de mens komt uit beschrijvende studies. Hierbij wordt menselijk thymusweefsel bestudeerd. Dat gebeurt aan de hand van analyse van de aanwezigheid van verschillende celtypen en ontwikkelingsstadia en de expressie van genen in de verschillende celtypen. Deze studies en data afkomstig van proeven met cellen in kweekbakjes, worden beschreven in **hoofdstuk 1** van dit proefschrift.

Als we ziektes met problemen in de T-cel ontwikkeling bestuderen, zouden we meer inzicht kunnen krijgen in de ontwikkeling van deze T-cellen en de signaleringsroutes die een rol in spelen gedurende deze ontwikkeling. Dit soort ziektes zijn onder andere Severe Combined Immunodeficiency (SCID) en T-cel acute lymfoblastische leukemie (T-ALL). SCID is een ernstige aangeboren afwijking waarbij er geen functionele T-cellen aanwezig zijn in het bloed. Meestal wordt de diagnose in het eerste levensjaar gesteld. Onder andere doordat een kind veel infecties heeft en achterblijft in de groei. Momenteel zijn er zestien genen bekend die

8

SCID kunnen veroorzaken. Een mutatie in één van deze genen kan leiden tot een blokkade in de ontwikkeling van T-cellen. Wat kan leiden tot een T-cel deficiëntie. T-ALL is een vorm van leukemie waarbij er een kwaadaardige wildgroei is van T-cellen. Het is lastig om de mechanismes die aan deze twee vormen van pathologische T-cel ontwikkeling ten grondslag liggen te onderzoeken bij de mens. Dat komt doordat er geen biopten van de thymus worden genomen bij deze patiënten.

In **hoofdstuk 2** wordt een geoptimaliseerd gehumaniseerd muismodel beschreven dat gebruikt kan worden voor het *in vivo* bestuderen van T-cel ontwikkeling van menselijke cellen. Daarbij wordt gebruik gemaakt van een muis met een sterk verzwakt immuunsysteem: de NOD/Scid-Il2rg$^{-/-}$ (NSG) muis. Deze muis heeft geen NK-cellen, B-cellen en T-cellen; celtypen die cruciaal zijn in een afweerreactie. Daardoor is dit type muis een goede ontvanger van menselijke cellen. In een gewone muis worden menselijke cellen afgestoten omdat de muis deze als indringer ziet. De NSG-muis doet dat niet omdat hij verschillende typen immuuncellen mist. Hierdoor is het mogelijk om de NSG muis te transplanteren met humane hematopoïetische stam- en progenitorcellen (HSPC) zonder dat deze worden afgestoten. HSPC bestaan uit bloedstamcellen - de HSC - en multipotente voorlopercellen. Al deze cellen zijn te herkennen aan de expressie van CD34 op het celoppervlak. De HSPC werden geïsoleerd uit navelstrengbloed en werden kort gekweekt in het lab. Deze korte kweek maakt genetische modificatie mogelijk. Een ander voordeel van een korte kweek is dat de HSPC hun stamceleigenschappen behouden. Genetische modificatie is toegepast in **hoofdstuk 5 en 6** van dit proefschrift.

De data in **hoofdstuk 2** laat zien dat de kort gekweekte HSPC, na transplantatie in de NSG-muis, migreren naar het beenmerg en kunnen differentiëren in cellen van het menselijk immuunsysteem. De humane B- en T-cellen die zich in de muis ontwikkelen, zijn ook functioneel aangezien zij een afweerrespons laten zien tegen een lichaamsvreemd antigeen. Eén van de eigenschappen van een HSC is zelfvernieuwing. Deze capaciteit kan bepaald worden door het beenmerg van de ontvangende muis te isoleren en vervolgens te transplanteren in een andere muis. Daar moet zich dan weer een immuunsysteem ontwikkelen. Ook in het geoptimaliseerde model was het mogelijk om het beenmerg – dat humane HSC bevat – te transplanteren in een tweede muis. Dit toont aan dat de HSC niet verloren gaan of uitgeput raken. Ook was het mogelijk om, naast navelstrengbloed, HSPC te isoleren uit humaan beenmerg en te transplanteren in de NSG-muis. Daardoor is het mogelijk om patiëntmateriaal uit bio-banken in dit model te bestuderen. Dat kan omdat de thymus uit NSG-muizen getransplanteerd met humane cellen er erg vergelijkbaar uit ziet met humaan thymusmateriaal. En omdat het met het geoptimaliseerde protocol mogelijk is om HSPC uit menselijk beenmerg te transplanteren.

Patiëntmateriaal afkomstig uit een bio-bank is gebruikt in **hoofdstuk 3** om de blokkades in T-celontwikkeling voor verschillende typen SCID te onderzoeken. Bij de meeste SCID-patiënten worden geen biopten van de thymus genomen. Daardoor is niet bekend waar de blokkades in T-celontwikkeling precies liggen. Door muizen te bestuderen die hetzelfde gen missen, weten we in welk stadium de blokkades liggen in deze muizen. Maar het is lastig deze data te extrapoleren naar de mens. De data in **hoofdstuk 3** laat zien dat de blokkades in een vroeger stadium liggen dan voorspeld vanuit de muismodellen. Dit laat duidelijk de

verschillen in T-celontwikkeling zien tussen de muis en de mens. Met de verkregen data is een model opgesteld voor humane T-celontwikkeling. Dit model laat zien dat direct nadat een multipotente voorloper cel aankomt in de thymus deze gaat prolifereren onder invloed van cytokines (groeifactoren). Ook laat het model zien dat het punt van β-selectie – een belangrijk selectiepunt in T-cel ontwikkeling – in een eerder stadium plaats vindt dan eerder beschreven. Dit kon worden afgeleid uit het stadium waarin T-cel ontwikkeling blokkeert bij Artemis-SCID.

De hierboven beschreven studie laat duidelijk de kracht van het geoptimaliseerde gehumaniseerde muismodel zien bij het ontdekken van blokkades in T-cel ontwikkeling. In **hoofdstuk 4** wordt een patiënt beschreven met een atypische klinische presentatie van SCID. Door HSPC van deze patiënt in het muismodel te transplanteren, kon worden bevestigd dat deze patiënt inderdaad een T$^-$B$^+$NK$^+$-SCID patiënt was. De blokkade in de T-celontwikkeling lag in het CD4$^+$CD8$^+$ dubbel positieve stadium; het stadium waarin de T-cel selectie ondergaat via de T-cel receptor. Omdat in geen van de genen die geassocieerd zijn met SCID een mutatie kon worden ontdekt, is de genetische code van de exonen van alle genen van zowel de patiënt als beide ouders bepaald. Exonen zijn stukken DNA die coderen voor eiwitten en daarom zou een mutatie in deze gebieden kunnen leiden tot een eiwitverandering. Deze analyse leidde tot de detectie van een nieuwe mutatie in VPS4B in deze patiënt. Dit gen werd voorheen nog niet geassocieerd met SCID.

Hoofdstuk 5 beschrijft de beperking van het aantal hematopoïetische klonen gedurende humane T-cel ontwikkeling. Door introductie van een unieke barcode in HSPC en transplantatie in NSG-muizen, kan het aantal klonen per ontwikkelingsstadium worden bestudeerd. Ondanks de sterke afname van het aantal hematopoïetische klonen, ontstaat er wel een polyklonaal repertoire van verschillende T-cel receptoren. Dit laat zien dat een enkele hematopoïetische kloon kan uitgroeien in meerdere T-cel klonen. Een grote verscheidenheid aan T-cel klonen is nodig om een goede afweerrespons te kunnen maken tegen de verschillende ziekteverwekkers die wij dagelijks tegenkomen.

In tegenstelling tot **hoofdstuk 3 en 4**, waarin gendeficiënties zijn onderzocht, is in **hoofdstuk 6** het effect van een te hoge expressie van het *LMO2*-gen onderzocht op humane T-cel ontwikkeling. *LMO2* is een oncogen dat vaak tot verhoogde expressie komt in T-ALL. Ook in klinische trials voor gentherapie voor immuundeficiënties ontwikkelden een aantal patiënten T-ALL als gevolg van insertionele mutagenese. Vaak was de insertie van de therapeutische vector in het DNA in de buurt van het *LMO2*-gen. Dat kwam daardoor tot verhoogde expressie en dat kan leiden tot T-ALL. Transgene muismodellen voor *Lmo2* laten een blokkade in T-celontwikkeling zien in een vroeg stadium. Verder laten deze muismodellen zien dat de muizen leukemie ontwikkelen als zij ongeveer één jaar oud zijn. Het effect van LMO2 op humane T-celontwikkeling werd onderzocht door *LMO2* tot overexpressie te brengen in humane HSPC. Deze HSPC waren geïsoleerd uit navelstrengbloed en vervolgens getransplanteerd in het gehumaniseerde muismodel. Deze transplantatie toonde aan dat LMO2 via drie verschillende mechanismen kan zorgen voor deregulatie van humane T-celontwikkeling; een vertraagde

8

ontwikkeling zoals ook geobserveerd in transgene muizen en in kweekbakjes, een accumulatie van CD4$^+$CD8$^+$ dubbel positieve cellen en een versnelde ontwikkeling die resulteerde in een verhoogde frequentie van T-cellen in het bloed.

Kort samengevat beschrijft dit proefschrift nieuwe inzichten in humane T-cel ontwikkeling door middel van transplantatie van humane HSPC in muizen met een sterk verzwakt immuunsysteem. Het geoptimaliseerde gehumaniseerde muismodel kan verder worden gebruikt in fundamentele studies naar de ontwikkeling van T-cellen en voor optimalisatie van strategieën voor gentherapie en stamcelexpansie protocollen. Verder illustreert het (zie **hoofdstuk 7**) de noodzaak voor een beter begrip van en meer inzicht in humane T-cel ontwikkeling. Dit kan helpen om de uitgroei van T-cellen na stamceltransplantatie te verbeteren. Daarnaast kan het helpen bij de diagnose en toekomstige behandeling van patiënten met T-ALL.

8

Dankwoord

Dan nu eindelijk het gedeelte van mijn proefschrift dat waarschijnlijk het meeste gelezen zal worden: het dankwoord. Dit proefschrift is niet zonder hulp en steun tot stand gekomen en daarom wil ik graag een aantal mensen bedanken.

Allereerst, wil ik Frank en Karin bedanken. Ik kan me ons eerste gesprek nog herinneren; het enthousiasme en de passie waarmee jullie over het betreffende onderzoek spraken heeft me aangestoken. De afgelopen jaren heb ik veel geleerd door onze discussies over de data en de interpretatie er van.

Graag wil ik Frits, Adrian en Mirjam bedanken voor het doornemen van dit proefschrift. Mirjam, heel erg bedankt voor het beschikbaar stellen van de kostbare SCID samples. De samenwerking heeft vele mooie resultaten opgeleverd.

Ook waren er samenwerkingen met vele anderen en jullie wil ik dan ook graag bedanken. Arjan en Robbert, Martijn, Ton en Ingrid, Hanna, Gijs en Wibowo, Daniela, Erdogan, Yunlei en Jules, Renske en Jasper en de medewerkers van de afdeling Verloskunde van het Diakonessenhuis Leiden. Door jullie samples en/of hulp bij analyses is dit proefschrift mede tot stand gekomen.

Natuurlijk kan ik niet de collega's en oud-collega's vergeten van het Staal lab, Fibbe lab en Stamcellab. Voor de gezelligheid op het lab, hulp bij experimenten, goede gesprekken, werkdiscussies, labuitjes en koffiepauzes op de brug. Collega's van de IHB en natuurlijk van de FeCo; bedankt voor de gezelligheid bij afdelingsuitjes, retraites en natuurlijk de borrels.

Ook buiten het lab zijn er vele mensen die ik wil bedanken want er is meer dan onderzoek in het leven. Dames van FOXX, vrienden van The Gang, Sanne, Claire, Manon, Theo, Lizzy, Max, Anita, Stephan, Ella, Stef, Robert en mam bedankt voor alle afleiding, steun, en interesse.

Dan mijn paranimfen; Willemien en mijn moeder. Van dichtbij hebben jullie de ups en down meegemaakt en deze met mij gevierd of me gesteund. Bedankt dat jullie op deze voor mij belangrijke dag aan mijn zijde willen staan.

Last but not least, Marc. Ook jij hebt van dichtbij dit hele promotietraject meegemaakt en hebt geluisterd, gevierd en kritische vragen gesteld. Samen slaan we ons overal door heen, over een paar maanden beginnen we aan een nieuw groot avontuur, maar samen met jou weet ik zeker dat dit heel mooi gaat worden!

Bedankt!

Curriculum Vitae

Anna-Sophia Wiekmeijer werd geboren op 3 januari 1986 te Haarlem. In 2004 behaalde zij haar VWO diploma aan het Atheneum College Hageveld te Heemstede. In datzelfde jaar begon zij haar studie Biomedische Wetenschappen aan de Universiteit Leiden en het Leids Universitair Medisch Centrum (LUMC). In 2007 behaalde zij haar Bachelor diploma en twee jaar later, in 2009, haar Master diploma in de afstudeerrichting Research. Tijdens haar Masterstudie was zij lid van de jaarvertegenwoordiging van de Masterstudenten en het uitvoerend orgaan van de studie Biomedische Wetenschappen (2007-2008). Gedurende haar studie liep zij stage bij prof. dr. S.H. van der Burg op de afdeling Klinische Oncologie van het LUMC tijdens haar Bachelor en tijdens de Master eerst bij prof. dr. E.R. de Kloet op de afdeling Medische Farmacologie van het Leiden Amsterdam Center for Drug research (LACDR)/LUMC en daarna bij prof. dr. T.N.M. Schumacher op de afdeling Immunologie van het Nederlands Kanker Instituut (NKI).

In januari 2010 startte zij met haar promotieonderzoek op de afdeling Immunohematologie en Bloedtransfusie van het LUMC bij prof. dr. F.J.T. Staal en dr. K. Pike-Overzet. Hieruit is dit proefschrift voortgekomen. Momenteel is zij postdoctoraal onderzoeker in de groep van prof. dr. W.E. Fibbe op dezelfde afdeling en doet zij onderzoek naar de heterogeniteit van mesenchymale stromale cellen (MSC) en hun effecten op het immuunsysteem.

8

List of publications

Wiekmeijer AS, Pike-Overzet K, Brugman MH, van Eggermond MC, Cordes M, de Haas EF, *et al.* Overexpression of LMO2 causes aberrant human T-Cell development in vivo by three potentially distinct cellular mechanisms. *Experimental hematology* 2016.

Staal FJ, Wiekmeijer AS, Brugman MH, Pike-Overzet K. The functional relationship between hematopoietic stem cells and developing T lymphocytes. *Annals of the New York Academy of Sciences* 2016, **1370**(1): 36-44.

Wiekmeijer AS, Pike-Overzet K, H IJ, Brugman MH, Wolvers-Tettero IL, Lankester AC, *et al.* Identification of checkpoints in human T-cell development using severe combined immunodeficiency stem cells. *The Journal of allergy and clinical immunology* 2016, **137**(2): 517-526 e513.

Schmitz F, Kooy-Winkelaar Y, Wiekmeijer AS, Brugman MH, Mearin ML, Mulder C, *et al.* The composition and differentiation potential of the duodenal intraepithelial innate lymphocyte compartment is altered in coeliac disease. *Gut* 2016, **65**: 1269-1278.

Brugman MH, Wiekmeijer AS, van Eggermond M, Wolvers-Tettero I, Langerak AW, de Haas EF, *et al.* Development of a diverse human T-cell repertoire despite stringent restriction of hematopoietic clonality in the thymus. *Proceedings of the National Academy of Sciences of the United States of America* 2015, **112**(44): E6020-6027.

Wiekmeijer AS, Pike-Overzet K, Brugman MH, Salvatori DC, Egeler RM, Bredius RG, *et al.* Sustained Engraftment of Cryopreserved Human Bone Marrow CD34(+) Cells in Young Adult NSG Mice. *BioResearch open access* 2014, **3**(3): 110-116.

Homminga I, Pieters R, Langerak AW, de Rooi JJ, Stubbs A, Verstegen M, *et al.* Integrated transcript and genome analyses reveal NKX2-1 and MEF2C as potential oncogenes in T cell acute lymphoblastic leukemia. *Cancer cell* 2011, **19**(4): 484-497.

8